



**UNIVERSIDADE ESTADUAL DE CAMPINAS
INSTITUTO DE GEOCIÊNCIAS**

MANIMALA MUNISWAMY

***TITLE: TECTONIC SETTING AND STRUCTURAL CONTROLS ON KIMBERLITE
MAGMATISM IN BRAZIL***

***AMBIENTE TECTÔNICO E CONTROLES ESTRUTURAIS DO MAGMATISMO
KIMBERLÍTICO NO BRASIL.***

CAMPINAS

2015

NÚMERO: 525/2015

MANIMALA MUNISWAMY

***“TITLE: TECTONIC SETTING AND STRUCTURAL CONTROLS ON KIMBERLITE
MAGMATISM IN BRAZIL”***

***AMBIENTE TECTÔNICO E CONTROLES ESTRUTURAIIS DO MAGMATISMO
KIMBERLÍTICO NO BRASIL.***

**DOCTORATE THESIS PRESENTED TO THE INSTITUTE OF
GEOSCIENCES OF THE UNIVERSITY OF CAMPINAS TO
OBTAIN Ph.D. GRADE IN SCIENCES IN AREA GEOLOGY
AND NATURAL RESOURCES**

**TESE APRESENTADA AO INSTITUTO DE GEOCIÊNCIAS
DA UNIVERSIDADE ESTADUAL DE CAMPINAS PARA
OBTENÇÃO DO TÍTULO DE DOUTORA EM GEOCIÊNCIAS
NA ÁREA DE GEOLOGIA E RECURSOS NATURAIS**

SUPERVISOR/ ORIENTADOR: PROF. DR. ELSON PAIVA DE OLIVEIRA

**ESTE EXEMPLAR CORRESPONDE À VERSÃO FINAL
DA TESE DEFENDIDA PELA ALUNA MANIMAL MUNISWAMY
E ORIENTADO PELO PROF. DR. ELSON PAIVA DE OLIVEIRA**

CAMPINAS

2015

Agência(s) de fomento e nº(s) de processo(s): CNPq, 190304/2010-3

Ficha catalográfica
Universidade Estadual de Campinas
Biblioteca do Instituto de Geociências
Márcia A. Schenfel Baena - CRB 8/3655

M925t Muniswamy, Manimala, 1980-
Tectonic setting and structural controls on kimberlite magmatism in Brazil /
Manimala Muniswamy. – Campinas, SP : [s.n.], 2015.

Orientador: Elson Paiva de Oliveira.
Tese (doutorado) – Universidade Estadual de Campinas, Instituto de
Geociências.

1. Kimberlito. 2. Tectonica (Geologia). 3. Geologia estrutural. I. Oliveira,
Elson Paiva de. II. Universidade Estadual de Campinas. Instituto de
Geociências. III. Título.

Informações para Biblioteca Digital

Título em outro idioma: Ambiente tectônico e controles estruturais do magmatismo
kimberlítico no Brasil

Palavras-chave em inglês:

Kimberlite

Tectonic (Geology)

Structural Geology

Área de concentração: Geologia e Recursos Naturais

Titulação: Doutora em Geociências

Banca examinadora:

Elson Paiva de Oliveira [Orientador]

Emilson Pereira Leite

Ricardo Kalikowski Weska

Darcy Pedro Svizzero

José Paulo Donatti Filho

Data de defesa: 28-08-2015

Programa de Pós-Graduação: Geociências



UNIVERSIDADE ESTADUAL DE CAMPINAS
INSTITUTO DE GEOCIÊNCIAS
PÓS-GRADUAÇÃO EM GEOCIÊNCIAS NA
ÀREA DE GEOLOGIA E RECURSOS NATURAIS

AUTORA: Manimala Muniswamy

Tectonic Setting and Structural Controls on Kimberlite Magmatism in Brazil

ORIENTADOR: Prof. Dr. Elson Paiva de Oliveira

Aprovada em: 28 / 08 / 2015

EXAMINADORES:

Prof. Dr. Elson Paiva de Oliveira - Presidente

Prof. Dr. Emilson Pereira Leite

Prof. Dr. Ricardo Kalikowski Weska

Prof. Dr. Darcy Pedro Svizzero

Dr. José Paulo Donatti Filho

A Ata de Defesa assinada pelos membros da Comissão Examinadora, consta no processo de vida acadêmica do aluno.

Campinas, 28 de agosto de 2015.

Dedication

“I dedicate this thesis to my husband Ganesh Nanjarajiah, for all the motivation has given me to complete this PhD and being a pillar of Support”

*“Whatever be the apparent diversity of things it is wisdom,
to analyse and perceive the basic truth of the matter”. Tirukural Couplet No 355.*

Acknowledgements

This thesis would not have been possible without the guidance and help of several individuals who in one way or another contributed and extended their valuable assistance in the preparation and completion of this study. First and foremost, my utmost gratitude to my supervisor Dr. Elson Paiva Oliveira who guided me throughout this study with his expertise and knowledge whilst allowing me the room to work in my own way. He has been a keen critic for my work and has improved my scientific acumen by doing so.

This project is funded by CNPq-TWAS full time postgraduate fellowship grant no 3240240127 and Process No: 190304/2010-3, from TWAS/CNPq. CNPq-TWAS is the Brazilian scientific and technological council for research and TWAS is The Academy of Sciences for developing world council. These two organisations have facilitated the funding for this PhD research work. The financial support from these councils has facilitated my passion of becoming a Doctorate in Geosciences. I greatly acknowledge this funding and assistance to make me realize my passion in research.

My special thanks to Dr. Simon Richard for designing the initial project and assisting me all through the research. A special thanks to Chris Smith for providing me all the reading materials which were not in my access and encouragements. Prof. Emilson has been helping me with the Geophysics part of my research. A special thanks for his guidance and for upgrading my knowledge on Geophysics. Prof. Ricardo Weska has been a great inspiration and has provided me with special kimberlite samples. His help is remarkable and is greatly acknowledged. He has helped me to understand Amazonian craton better than what has been learnt from literature.

My heart felt thanks to Dr. Araujo Debora, for putting me in contact with the right people to get samples and information. Alan Kobussen and Paul Agnew from Rio Tinto provided me with the samples without which the geochemistry part of the work would not have been possible. I specially thank Rio Tinto and the team members for helping me with samples, other field and technical help. The financial assistance for field accommodation from Rio Tinto came in as a boon for my work. Valdir Silveira, helped me with geological data for Brazil. I acknowledge my thanks to him.

Alexandre Lisban Lake, from CPRM, helped me to get the geophysics aeromagnetic data and I am very much thankful to him. CPRM, as an organisation helping researchers provided with the aeromagnetic data of this research project. I acknowledge their support and help for this. Felix Nannini, research scholar from USP, helped me for the sample from Extra-Amazonian region. I acknowledge his help with special thanks. Prof. Darcy Pedro's insightful thoughts on Brazilian kimberlites gave me new dimension in my research. I thank him for sharing his knowledge. Venkatasubramanyam from Rio Tinto India and Mr. Sojen from Debeers extended their helping hand with kimberlite stratigraphy, geophysics and geology in general. My special thanks to both of them. Prof. Jacinta Enzweiler has improved my knowledge on Geochemistry and been an inspiration. A special thanks to her. Maria Aparecida Vendemiatto and Margaette both helped me in analysing the geochemistry samples.

A special thanks to Miss.Fernanda from Cuiaba for helping me while sample collection and stay. My study room mates Gustavo, Marco, Delinardo, Daneilo and Mauricio made my stay at university very pleasant and helped me in my understanding about Brazilian geology better. My very special thanks to all of them for making me comfortable at the university stay.

My special thanks to my mother-in-law, Mrs. Pushpa for taking care of my daughter during my last year of research. Special thanks to Rosangela madam and Racheal for helping me in all my personal needs in a foreign land. My Brazilian friends Linduara, Adriana, Michelle, Pricilla, Mrs. Renata, Prof. Asit Choudary, Mariana, Flavia and many more have helped me a lot. My heart felt thanks to all of them. Finally, I would like to thank my parents, sister and other family members specially my daughter *Khushi Ganesh* for being cheerful without my presence with her. I specially thank my dad Mr. K. Muniswamy for his motivation during my low times.

Author's Declaration

I declare that the work in this dissertation was carried out in accordance with the requirements of the University's Regulations and Code of Practice for Research Degree Programmes and that it has not been submitted for any other academic award. Except where indicated by specific reference in the text, the work is the candidate's own work. Work done in collaboration with, or with the assistance of, others, is indicated as such. Any views expressed in the dissertation are those of the author.

Contents

| Description | Page number |
|---|--------------------|
| Chapter 1 Aim - Tectonic Setting and Structural Controls on Kimberlite Magmatism in Brazil | 18-19 |
| Chapter 2 Introduction | 21-25 |
| Chapter 3 Study Area and Field work | 26-27 |
| Chapter 4 Kimberlite Review. | 28-34 |
| Chapter 5 Geological Framework of Brazil. | 35-39 |
| Chapter 6 Role of Brazilian plate in Global Plate tectonics. | 40-44 |
| Chapter 7 Corridor-125 and its Kimberlites | 45-50 |
| Chapter 8 Structural Framework of Corridor-125 with mapped structures. | 51-55 |
| Chapter 9 Geophysical Characterization of Brazilian Structures and kimberlite along Corridor-125 | 56-91 |
| Chapter 10 Revised Structural Framework of Corridor-125 by the integration of mapped and aeromagnetic structures. | 92-93 |
| Chapter 11 Geochemistry of Brazilian Kimberlites Analysed. | 94-107 |
| Chapter 12 Plate Tectonic Reconstructions | 108-120 |
| Chapter 13 Discussion and Conclusions | 121-127 |
| References | 128-143 |

APPENDIX

Contents of Figures

Chapter 2: Introduction

Fig.1a: Global distribution of kimberlites on present day plate positions.

Fig.1b: Global distribution of kimberlites with reconstructed plate positions to 130 Ma.

Fig.2: Global Lithospheric provinces (Archons, Protons and Tectons) with kimberlite distribution. The colour of dots for kimberlite location corresponds to the diamond content of the kimberlite as shown on map after Ekstrand et al, 1995 and Janse, 2007.

Chapter3: Study Area and Field Work.

Fig.3: Sample Location map with structural provinces background.

Chapter 4: Kimberlite Review

Fig. 4: Kimberlite pipe morphology and facies.

Chapter 5: Geological Framework of Brazil

Fig.5: Structural Provinces of Brazil with cities capitals.

Fig.6: Igneous provinces of Brazil from CPRM database 2004 with respect to Corridor-125.

Chapter 6: Role of Brazilian plate in Global Plate tectonics

Fig.7: South American plate with tectonic boundary type.

Chapter 7: Corridor-125 and its Kimberlites (Occurrence, Clusters and Age)

Fig.8: Oceanic extension of Continental Corridor-125 lineament in the Brazilian plate with global EMagV2 background.

Fig.9: Brazilian Kimberlite age map.

Fig.10: Kimberlite Clusters along Corridor-125 with structural provinces background. The region in yellow corresponds to Paleozoic basins.

Table.1: Kimberlite Age from literature.

Chapter 8: Structural Framework of Corridor-125 with mapped structures.

Fig.11: Structural Framework of Corridor-12 with Tectonic province background. The black dots represent kimberlites, black lines represent structures. Blue line is the Giga Transbrasiliano lineament.

Chapter 9: Geophysical Characterization of Brazilian Structures and kimberlite along Corridor-125

Fig.12: Aeromagnetic projects location map. The region in sky blue is the project 1009, the region in bright green is the project 1068, the region in blue dark blue is project 1043 and the region in red is the project 1017. Back ground regions represent structural provinces.

Fig.13: 1017_Total magnetic intensity anomaly Map with lineaments, alkaline intrusives (Catalao I and II).The magnetic intensity are in nT.

Fig.14: 1009 Total magnetic intensity anomaly Map with magnetic lineaments, alkaline intrusive and kimberlites. The magnetic intensity are in nT.

Fig. 15: Amazonian region Total magnetic intensity anomaly map with kimberlite, mafic intrusions, lineaments. The magnetic intensity is in nT units.

Fig.16(a): Extra-Amazonian region Total Intensity map filtered to 100m upward continuation.

Fig.16(b): Amazonian region TMI with 500m upward continuation.

Fig.17: Extra-Amazonian and Amazonian Region Reduced to pole map.

Fig.18: Amazonian Region Reduced to pole map.

Fig.19a: Extra-Amazonian Region Amplitude of Analytical Signal map.

Fig.19b: Extra-Amazonian and Amazonian Region Amplitude of Analytical Signal map.

Fig.20: Amazonian Region Amplitude of Analytical Signal map with lineaments, alkaline intrusions and kimberlites.

Fig.21: Amazonian Region Amplitude of Upward Continuation map with lineaments, mafic intrusions, kimberlite and other structures.

Fig.22: Extra-Amazonian Euler Structural Index-1 Solutions with TMI Map background. Black dots represents Euler Structural index-1 solutions.

Fig.23: Extra-Amazonian Euler Structural Index-2 Solutions with Depth range.

Fig.24: Amazonian Euler Structural Index-1 Solutions with TMI background. Black dots represents Euler Structural index-1 solutions.

Fig.25: Amazonian Euler Structural Index-2 Solutions and kimberlite as Red Big circles represent kimberlites.

Fig.26: Linear Structural Elements of Amazon region with Amplitude of Analytical Signal background and black open circles represent kimberlites studied.

Fig.27: Linear Structural Elements of Extra-Amazon region with Analytical signal map background and blue open circles represent kimberlites studied.

Fig.28: Amazonian Kimberlite Analytical signal signatures geophysically tested.

Fig.29: Extra-Amazonian known Kimberlites studied for modelling by integrated Analytical signal, Euler solution index-2 and Keating Coefficient.

Fig.30: Extra-Amazonian Keating Coefficient Anomaly pick plot with known kimberlites.The Keating Coefficient Anomaly is represented by blue circle and known kimberlites are represented by white circles.

Fig.31: Amazonian Kimberlite Analytical signal signatures geophysically tested.

Fig.32: Amazonian region Keating Coefficient Anomaly pick plot with known kimberlites. The Keating Coefficient Anomaly is represented by blue circle and known kimberlites are represented by white circles.

Chapter 10: Revised Structural Framework of Corridor-125 by the integration of mapped and geophysical structures.

Fig.33: Revised Structural Frame work of Corridor-125 with dyke swarms, kimberlites, magnetic and mapped structures.

Chapter 11: Geochemistry of Samples Analysed

Table.2: Major Elements geochemical analysis results with crustal index values.

Table.3: Trace Element results from ICP-MS geochemical analysis.

Fig.34: Graph to distinguish the samples into fresh or altered kimberlites with Al₂O₃ Vs SiO₂. The uncontaminated kimberlite region after Mitchell, 1986.

Fig.35: Major element TiO₂ Vs K₂O plot. The Kimberlite type areas pertaining to group I, II, Transition type and lamproites from Becker and le Roex, (2006); Becker, (2007) and Jaques, (1984).

Fig 36: Major element SiO₂ Vs Nb/La plot. The Kimberlite type areas pertaining to group I, II, Transition type and lamproites from Becker and le Roex, (2006); Becker, (2007); Jaques,(1984).

Fig.37: Major element SiO₂ Vs Pb plot. The Kimberlite type areas pertaining to group I, II, Transition type and lamproites from Becker and le Roex, (2006); Becker, (2007); Jaques, (1984).

Fig.38: Major element SiO₂ Vs Th/Nb plot. The Kimberlite type areas pertaining to group I, II and Transition type and lamproites from Becker and le Roex, (2006); Becker, (2007); Jaques,(1984).

Fig.39: Chondrite normalized REE Pattern graph for analysed samples and South African trend (Data from Becker and Le Roex 2006 and Becker at al., 2007).

Fig.40: Primitive mantle normalized multielement graph (Mc Donough and Sun 1995) of South African Group I, Group II and transitional group kimberlites (Data from Becker and Le Roex 2006 and Becker at al., 2007).

Fig.41: Primitive mantle normalized multielement graph for analysed samples after Mc Donough and Sun 1995.

Chapter 12: Plate Tectonic Reconstructions

Fig.42: Diagrammatic representation of Euler pole and plate rotation relationship.

Fig.43: An example of triple junction with African, Arabian and Somalian plates are currently rifting.

Fig.44: 300 Ma reconstructions with Brazilian plate in pink boundary. African plate with multiple blocks and Laurentian plate in green. The position of the corridor-125 is also marked.

Fig.45: 225 Ma to 170 Ma reconstruction of Brazilian plate.

Fig.46: 130 Ma Reconstruction of Brazilian plate with progressing rift between Laurentian and Brazilian plate.

Fig.47: 126 Ma Reconstruction of Brazilian plate with South Atlantic rift initiation at the southern tip of the South American (Brazilian plate).

Fig.48: 110 Ma Reconstruction of Brazilian plate with progressing South Atlantic rift. Tristan Cunha hotspot is seen on the newly developing oceanic part of the Brazilian plate well below Corridor-125.

Fig.49: 75 Ma Reconstruction of Brazilian plate with progressing South Atlantic rift. Trinidad Martin Vaz (TMV) hotspot is seen under the corridor-125 of the Brazilian plate. This hotspot moves away from the corridor-125 after 75 Ma further north and finally reaches the oceanic crust on the east coast of Brazil.

Fig.50: Present day position of Brazilian plate and east coast hotspot locations.

Fig.51: TMV Paleo-track over Brazilian plate with respect to Corridor-125 from gplates for the present day position of Brazilian plate.

Chapter 13: Discussion on the role of Hotspot Trinidad-Martin Vaz (TMV) in kimberlite emplacement.

Fig. 52: *Georeferenced TMV hotspot trail up to 300Ma with respect to Corridor-125 and kimberlite occurrences.*

Publication: Tectonic and Structural Controls on Phanerozoic-Cretaceous Kimberlite Emplacement along Corridor-125, Brazil - A Review

Fig.1: Corridors-125 and Kimberlite occurrence in Brazil. 1. Northern-Amazon Region, 2. Southern Amazon Craton, 3. São Francisco Craton, 4. Brasilia Belt, 5. Ribeira Belt, 6. Borborema province, 7. Parana Basin, 8. Parecis Basin, 9. Parnaiba Basin. Pink stars are kimberlite and related rock. The boundary enclosed in red is the location of Corridor-125.

Fig.2: Kimberlite Clusters along Corridor-125 with Structural provinces background.

Fig.3: Simplified Brazil Map with Structural provinces after Almeida, 1981.

Fig.4: Oceanic extension of Continental Corridor-125 lineament in the South American plate with EMagV2 background and GSFML fracture zones and Mid-Atlantic ridge.

Fig.5: Structural Framework of Corridor-12 with Tectonic province background. The black dots represent kimberlites, black lines represent structures. Blue line is the Giga Transbrasilino lineament.

Fig.6: Extra-Amazonian kimberlite clusters and associated structural lineaments with structural provinces background. Pink open circles represent kimberlite and related rocks.

Fig.7: Amazonian region kimberlite clusters and associated structural lineaments. Pink open circles represent kimberlite and related rocks.

Fig.8: Brazilian Kimberlite age map (Data source from literature).

Fig.9 (a and b): TMV hotspot Trail along the Corridor-125 with kimberlite occurrences.

Table.1: Brazilian kimberlite ages from literature.

Graph.1: A plot of Brazilian plate velocity magnitude in cm/year Vs time in Ma.

Graph.2: A plot of Brazilian plate Azimuth as angular velocity Vs time in Ma.

RESUMO

Em escala global o alojamento de kimberlitos é controlado por estruturas translitosféricas pré-existentes ou recém formadas por tectonica de placas conhecidas como Lineamentos continentais. Esses lineamentos são formados durante a reorganização de placas antes da formação de riftes oceânicos e estendem-se para o rifte oceânico e falhas transformantes em desenvolvimento antes da deriva. Finalmente as placas derivam. Deste modo, há uma ligação genética entre lineamentos continentais translitosféricos, seus equivalentes em falhas transformantes oceânicas e o alojamento de kimberlitos. O Corredor 125 no Brasil é um desses lineamentos continentais translitosféricos que hospedam kimberlitos e outras rochas máfico-ultramáficas. O alinhamento de rochas máficas e ultramáficas nas partes amazônica e extra-amazônica do Corredor 125 é apenas uma coincidência. A parte extra-amazônica do corredor foi formada inicialmente há 1.8 Ga e foi reativada várias vezes desde então como evidenciado por diferentes grupos de idades de diques máficos, agrupamentos de kimberlitos e de outras rochas máficas ao longo de todo o seu comprimento e largura. A ativação estrutural mais antiga na parte amazônica do corredor ocorreu há 1.8 Ga. Os kimberlitos ao longo do Corredor 125 formam picos de idades entre 226 e 268 Ma, 120 e 122 Ma, 80 e 94 Ma e em 74 Ma. A reconstrução tectônica da placa sul-americana revela que a trajetória da trilha do hotspot Trindade-Martim Vaz não coincide com o Corredor 125 e que não há nenhuma progressão aparente na idade de kimberlitos ao longo do corredor. Diferente de sugestões anteriores, a trilha do hotspot Trindade-Martim Vaz como possível fonte de alojamento do magma kimberlítico é descartada. Ao contrário, o alojamento de kimberlitos esteve relacionado provavelmente à reorganização do supercontinente Pangea (kimberlitos de 226-268 Ma), incipiente abertura do Oceano Atlântico de 120 a 122 Ma quando o movimento da placa sul-americana foi caracterizado por zig-zags, e a última fase de intrusão de kimberlitos entre 80 e 94 Ma e há aproximadamente 74 Ma quando houve o segundo aumento na velocidade da placa. Os períodos de tempo desprovidos de kimberlitos são estágios quando a placa sul-americana esteve estável ou experimentando velocidade e direção de movimento regular.

ABSTRACT

On a global scale kimberlite emplacement is controlled by pre-existing/newly formed translithospheric structures known as Continental Lineaments due to plate tectonics. These translithospheric continental lineaments are formed during plate-reorganisation prior to oceanic rift formation. Further these lineaments extend onto the newly developing oceanic rift and transform fractures prior to the drift. Finally the plates drift apart. Hence, there is a genetic link between continental translithospheric lineaments, its oceanic transform fracture counterparts and associated kimberlite emplacement. Corridor-125 in Brazil is one such continental translithospheric lineaments, which host kimberlites and other mafic/ultramafic rocks. This Amazonian part and Extra-Amazonian part of the corridor is a coincidental alignment along with its associated mafic and ultramafic magmatism. The Extra-Amazonian part of this corridor was formed initially about 1.8 Ga and has been reactivated several times as evidenced by different age group of mafic dyke swarm, kimberlite clusters and other mafic rocks along its entire length and width. The oldest known structural activation on the Amazonian part of the corridor is 1.8 Ga. The kimberlite age along Corridor-125 is found to peak at 226 to 268 Ma, 120 to 122 Ma, 80 to 94 Ma and 74 Ma. Plate tectonic reconstruction of South American plate reveals the path of Trinidad-Martin Vaz (TMV) hotspot trail does not coincide with the Corridor and there is no apparent kimberlite age progression along Corridor-125. Unlike previous suggestions, the role of TMV as possible source for kimberlite emplacement is ruled out. The kimberlite emplacement is rather related to Pangea supercontinent plate re-organization (226-268 Ma kimberlites); incipient South Atlantic rifting from 120 to 122 Ma when the South American plate movement was characterized by cusps and jogs; and the last phase of kimberlite emplacement from 80 to 94 and 74 Ma is due to the second phase of increased plate velocity. The quiescent periods devoid of kimberlites are stages when the South American plate was stable or experiencing a smooth plate velocity and direction.

Chapter 1

Tectonic Setting and Structural Controls on Kimberlite Magmatism in Brazil

Aim

The aim of the research is to test the hypothesis that kimberlite/lamproite emplacement are controlled by structural corridors which are formed or reactivated during the early stages of supercontinent deformation like rifting, subduction etc.

Kimberlite emplacement in time and space are intrinsically related to particular stages in the life cycle of supercontinents and its associated translithospheric structures (Jelsma et al., 2009). The periods devoid of kimberlite magmatism corresponds to times of supercontinent stabilization where plate motions are smooth (Jelsma et al., 2009).

The kimberlites of Brazil are aligned in well-defined corridors or fields. The kimberlites are associated with sub-vertical lithosphere-scale fracture zones (DeBoorder, 1982, Fitton et al., 1986). These structurally defined corridors are a characteristic of kimberlites and associated alkaline intrusives around the world. One such example being the Azimuth-125 lineament (named after the compass direction of the alignment – Crough et al., 1980) in Brazil which is the continuation and mirror image of Angola-DRC lineament/LucapaGraben (Marsh 1973). Few other examples are, the alignment of kimberlites from Kimberley to Pretoria and beyond in South Africa (Jelsma et al., 2004, 2009), Olenek-DaldynAlakit-MaloBotyobinsky in Siberia (Kushev et al., 1992).

Often, there is a progression in kimberlite age, variation in composition of magmas, diamond content of kimberlites along these corridors/lineaments. There is age progression observed in Brazil (Crough et al, 1980). The Brazilian lineament encompasses rocks from carbonatite to kamaflagite to lamproite to kimberlites. Marsh (1973) related the linear zones of alkaline intrusives (carbonatites and kimberlites) in Angola and SW Africa to the on-land extension of oceanic transform fracture zones, however, this interpretation is somewhat ambiguous as the oldest age of oceanic crust and the associated seafloor fractures is around 160 Ma yet kimberlite emplacement predates the formation of these fracture zones by several

tens of millions of years. Accordingly, it is suggested that displacement at the transforms resulted in reactivation of old continental structures.

Hence, the project is aimed at testing the above hypothesis by studying structural setting, geophysical characterization, geochemistry and geological setting of selected kimberlites from Brazil. This research aims at answering a global-scale question -where and when are kimberlites emplaced, and what are the tectonic controls on kimberlite magmatism. The methodologies and ideas generated will have implications for kimberlite exploration on a global scale.

Structure of thesis

To arrive at the aim of the research, the following objectives are considered:

1. Introduction and Kimberlite Review
2. Study Area and Fieldwork for sample collection.
3. Geological Framework of Brazil.
4. Global Tectonic events and Role of Brazilian plate (Tectonic events including periods of major plate reorganisations, continental breakup, subduction and hotspot positions).
5. Brazilian Kimberlites (Clusters, Age and Mapped Structural framework).
6. Aeromagnetic Characterization of Brazilian platform.
 - a. Aeromagnetic investigation of the Structural features associated with Kimberlite emplacements.
 - b. Aeromagnetic Signatures of kimberlite bodies.
6. Geochemistry of Brazilian kimberlites and their significance to the nature of mantle source region.
7. Revised Structural Framework of Corridor-125 by the integration of mapped and Aeromagnetic structures.
8. Plate Tectonic Reconstruction of Brazilian plate
 - a. Brazilian kimberlite association with hotspot paleo-track.
 - b. Brazilian kimberlite association with South Atlantic Rift along eastern border of Brazilian plate.
 - c. Brazilian kimberlite association with Pacific Plate subduction along the western border of the Brazilian plate.
9. Discussion and Conclusions.
 - a. Structural Trend controlling the kimberlites along Corrido-125
 - b. Aeromagnetic signatures of corridor-125 kimberlites
 - c. Geochemical nature of corridor-125
 - d. Tectonic trigger induced Petrogenetic model for Corridor-125 kimberlites.
 - e. Final Reconstruction of Brazilian plate from present day to Permo-Triassic times.
10. Future Research.

Chapter 2

Introduction

Brazilian kimberlite occurrences along the Corridor-125, its structural controls and tectonic settings are evaluated using the geological, aeromagnetic and geochemical data in this research. The aim of the research is to test the hypothesis that kimberlite/lamproite emplacement are controlled by structural corridors which are formed or reactivated during the early stages of supercontinent deformation like rifting, subduction etc. Thus, the results from this research investigation lead to the better understanding of global scale plate tectonic events its genetic link to the regional scale structures and magmatism particularly kimberlite magmatism.

Global distribution pattern of kimberlite and their association along rifted margins forms the basis for this hypothesis. Kimberlites are distributed on every continent worldwide (except Antarctica) as shown in Fig.1a. In present-day plate tectonic framework, the synchronicity of eruption on different continents appears to be unrelated. But upon reconstructing the plates back in time reveals geometry in kimberlite distribution (Fig.1b) being centered around regions of rifting but also exhibit intercontinental switching of magmatism. Geometry in the distribution pattern is due to structural corridors on a global scale.

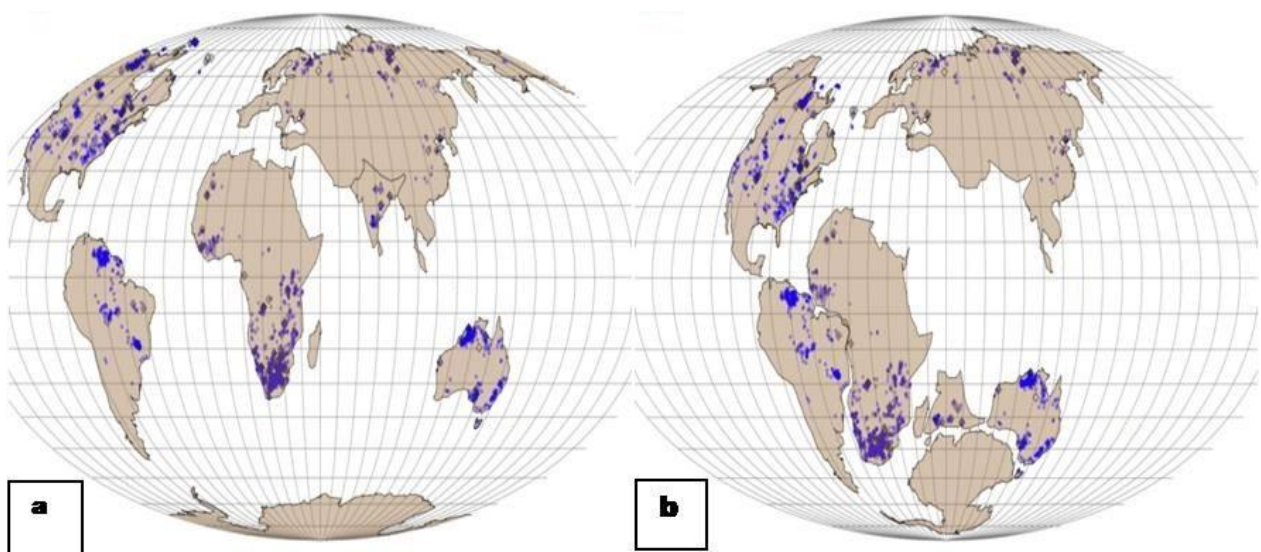


Fig.1a: Global distribution of kimberlites on present day plate positions. **Fig.1b:** Global distribution of kimberlites with reconstructed plate positions to 130 Ma

Dawson (1989) and Janse and Sheahan(1995) have shown that kimberlites occur only on Archons, i.e. cratonic regions underlain by Archean basement, whereas lamproites occur on some Protons, i.e. Proterozoic mobile belts adjacent to Archons. These are termed as lithospheric provinces (Fig.2). The specific preferential occurrence of kimberlites within ancient Archean and Precambrian terranes older than 1.5 Ga (Clifford's Rule") has direct relationship with the diamond stability field (Clifford, 1966). The necessary P-T conditions of diamond stability are provided by thick, old lithospheric mantle roots. Because of the low paleogeothermal gradients these lithospheric mantle roots typically lie under ancient continental nuclei (Archean and Proterozoic craton).

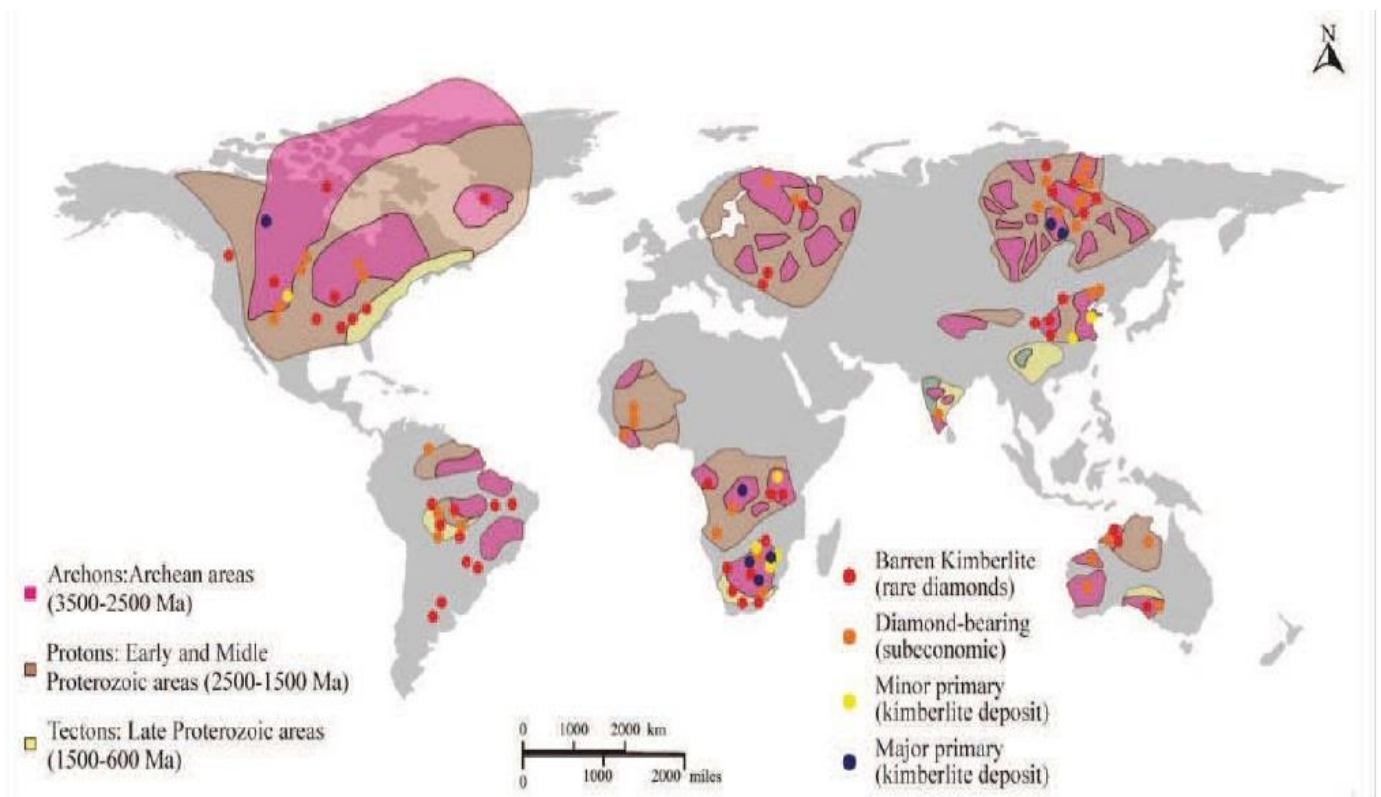


Fig. 2: Global Lithospheric provinces (Archons, Protons and Tectons) with kimberlite distribution. The colour of dots for kimberlite location corresponds to the diamond content of the kimberlites as shown on map after Ekstrand et al, 1995 and Janse, 2007.

Structural corridors are lineament or set of lineaments. These lineaments are zones of weakness or structural displacements in the crust, which can be mapped or indirectly inferred by the presence of magmatic rocks aligned in a straight or slightly curving manner when the younger geological and tectonic processes often mask its presence underneath (Hobbs et al, 1976). The length of lineament varies considerably and is typically measured in tens or

hundreds of kilometers. The lineaments that are up to 100km are termed as mega-lineament where as those that are longer than 100km are termed as giga-lineament.

Kimberlite magmatism is episodic along the structural corridors. Thus, there is often grouping of kimberlites in one area termed as clusters. Further, this clustering repeats on a subregional scale on the craton and forms fields. On regional scale, these kimberlite fields are oriented along translithospheric lineaments acting as structural controls. This regional scale orientation of kimberlites is known as corridors. It is also observed that, kimberlite emplacement in time and space is related to global plate tectonics and its associated translithospheric structural controls (White et al., 1995; Barnett et al., 2013; Jelsma et al., 2009). These translithospheric structures are the regional structural controls for kimberlite emplacement (Sykes, 1978). The structures contained within the corridors are repeatedly reactivated (White et al., 1995) thereby forming the pathways for kimberlite magmas with different age groups. On subregional scale kimberlites are preferentially emplaced at the tips and shoulders of rifts, major preexisting dyke swarms, structural bends, step-overs, and fault intersections (Jelsma et al., 2004; Gladdkov et al. 2005). Within structural corridors the brittle structures of the crust form the local structural controls for kimberlite emplacement. Thus, structural controls are seen on varying scales.

Kimberlite emplacements are found to peak with respect to specific time. As examples on the African plate kimberlite episodicity is observed at five major time periods

- 85-95 Ma-(Davis, 1977; Smith et al., 1985; Le Roex et al., 2003; Wu et al., 2010)
- 120 Ma- (Smith et al., 1985; Phillips et al., 1998).
- 235 Ma- (Kinny et al., 1989)
- 510-530 Ma-(Phillips et al., 1998)
- 1200 Ma- (Smith et al., 1985)

On the North American plate, kimberlites have been emplaced over a period of approximately 1 billion years with several peaks. Among them, around 80% of all known North American kimberlites are younger than about 200 Ma (Heaman et al., 2004). The time periods are as follows:

- 50-60 Ma (Lockhart et al., 2004),
- 70-80 Ma (Aravanis, 1999)
- 95-103 Ma (Zonneveld et al., 2004)
- 150-160 Ma (Heaman and Kjarsgaard, 2000)
- 170-180 Ma (Kong et al., 1999; Heaman and Kjarsgaard, 2000)

The continental structures control the position of transforms in the newly developing younger ocean (Lister et al, 1986). Thus, there exists a genetic link between the oceanic transforms and the continental Lineaments. Due to complex overprinting of the younger tectonic events post dating the plate rifting at global and local scales, there is masking of the older continental lineaments where as the ocean floor is tectonically less disturbed in nature. As a result they retain the structural signatures i.e. transform fractures signatures on the ocean floor and is much easily observed in comparison to landward counterparts. The orientations of the present day oceanic and continental lineament may be different because of the change in Euler pole dynamics after the oceanic crust started to form. A single plate could have played part of different supercontinent life cycle and thus the continental lineaments are associated with more than one set of ocean floor lineaments. In such a case, the most recent ocean floor signatures are much easier to associate with the continental lineaments while the older ones are masked by younger events. At times the relationship between older continental lineaments with its respective oceanic transforms becomes impossible to demonstrate. Kimberlite magma emplacement pathways are interpreted to be reactivated pre-existing lineaments or newly created ones due to the dynamics of plate tectonic events at different stages of supercontinent life cycle (DeWit, 2007; Moore et al, 2008; Jelsma et al, 2009). Thus, the kimberlite emplacement, continental lineaments and the oceanic transforms are all genetically related. There are several periods of kimberlite emplacement worldwide associated with plate tectonic events. It is possible to establish the link between the kimberlites and the lineaments and their associated plate tectonic events. The complexity lies in associating the older events. This is particularly true with respect to the association of older than Mesozoic kimberlites. On the other hand it is much easily accomplished with younger kimberlites.

Continental and Oceanic Lineament Genetic Link

The Continental lineaments manifest themselves as faults and fractures, which forms the pathway for kimberlite magma migration and emplacement. The process continues and the weakness extends on to the newly forming mid-ocean ridges and transforms in the oceanic crust. There are discrete batches of kimberlite magma emplacement on the continents at different stages of continental plate movement. The process continues during and after the rifting of the plates characterized by cusps and jogs. One way of finding the link with the kimberlite emplacement and rifting is by looking at the oceanic transforms with its corresponding continental lineaments.

In summary, this research aims at evaluating the proposed genetic link between continental lineaments with the oceanic lineaments, episodicity in kimberlite magmatism, reactivation of structural lineaments, plate tectonic events associated, types of kimberlites based on geochemistry and geophysical nature of kimberlites on the Brazilian platform. Petrogenetic modeling and Plate tectonic reconstruction will be the final results of this research work.

Chapter 3

Study Area and Field work carried

The NW-SE trending Lineament-125 or Azimuth-125 of Brazil (Crough et al 1980, Bizzi, 1995; Bizzi et al, 1995a, 1995b; Gibson et al., 1995; Carlson et al., 2007) is the study area. This lineament runs from Rio de Janeiro in São Paulo state to Porto Velho in Rondonia state. Along the entire length and width of the lineament kimberlite and other alkaline rocks are seen. In fact, this is not just a lineament, instead it is a zone made up of several lineaments majority of which are trending in NW-SE direction. Interpretation of geophysical aeromagnetic map reveals, this lineament is made up of several parallel to subparallel lineaments in NW-SE trend and also cross cut by NE-SW trending Transbrasiliano Lineament (TBL). Hence, this zone of multiple lineaments associated with kimberlites is termed as Corridor-125. Corridor-125 with its plethora of exotic mantle-derived rocks is an excellent platform to understand the kimberlite magmatism, its structural and tectonic controls.

Field work for the Sample Collection

Samples were collected along Corridor-125 from the states of Minas Gerais, Rondonia and Mato Grosso. The sample type from Rondonia and Mato Grosso are drill core samples; the samples from Minas Gerais are outcrop samples. Moderate to high intensity weathering is common in Brazilian samples. Due care is taken to select the least weathered sample for geochemical analysis. In spite of this careful selecting, the samples from Rondonia and Mato Grosso were all weathered ones. The Minas Gerais sample showed least weathering and was almost fresh hard rock sample. Names of the samples are Collier-01, Collier-04, Juina-23, Cosmos-01, Tumeliero-13, Forca and Indaia.

Sample location is shown on the map in fig.3 with the names of the kimberlites sampled. The Collier-01, 04, Juina-23 and Cosmos-01 are all from Rondonia and Mato Grosso states. The Indaia and Forca are from Minas Gerais state.

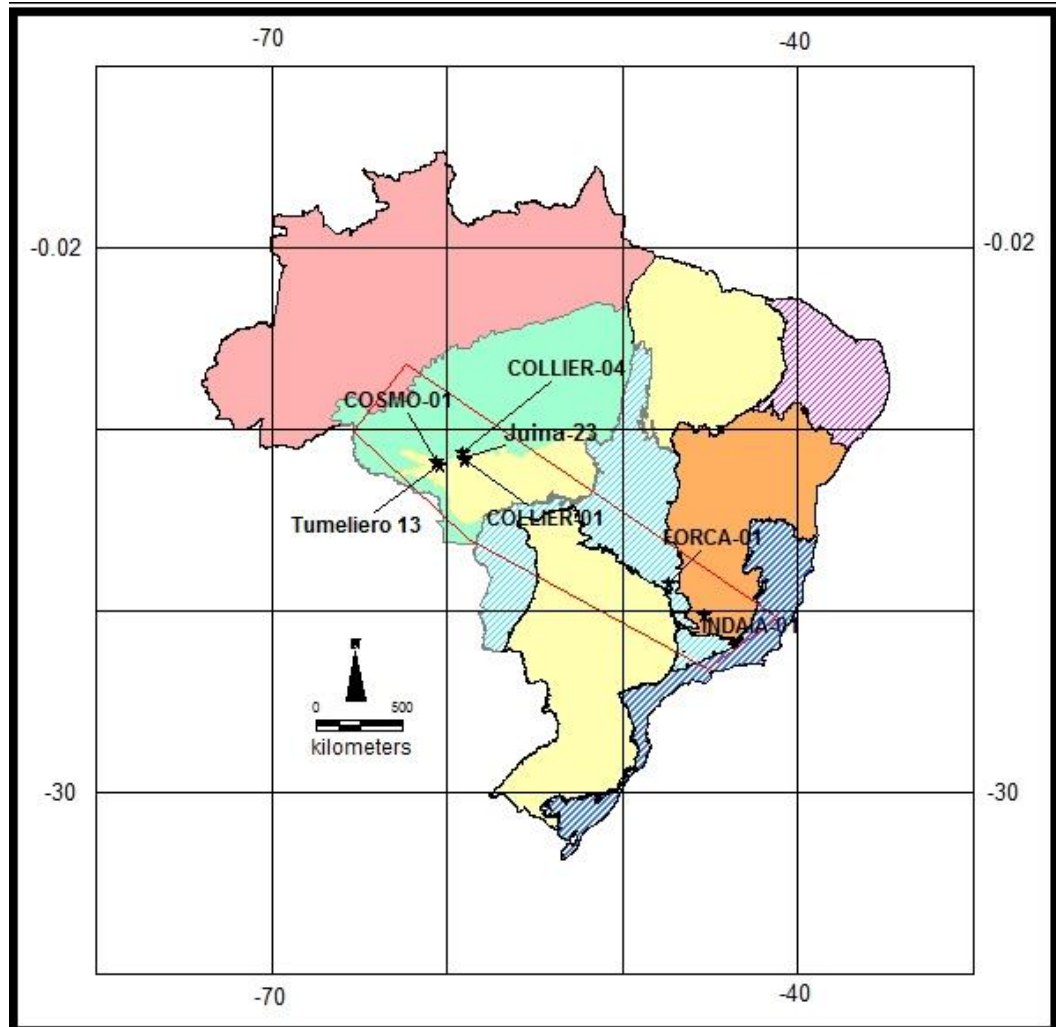


Fig.3: Sample Location map with structural provinces background.

Chapter 4

Kimberlite Review

The term kimberlite was proposed in the year 1987 by Prof. Henry Carvil Lewis with the description as porphyritic mica-bearing peridotitic volcanic breccia (Lewis, 1987; 1988). Later, this term has been used worldwide. Kimberlites are ultrapotassic, volatile-rich rocks with extremely enriched incompatible element signatures. They originate at depths greater than 200 km below the surface of the Earth, below thick, cool Archean craton roots (Mitchell, 1986). As kimberlite magma rise towards the surface, they entrain fragments of the mantle through which they pass. Hence, they are hybrid in nature and these mantle fragments provide "windows" nature of the mantle below. The cool peridotitic roots of Archean cratons have been identified as the source region for diamonds recovered from kimberlites and lamproites (Mitchell, 1986). The presence of mantle derived diamonds in kimberlites makes it more interesting from economic point of view. The revised definition from older definitions of kimberlite is given by Mitchell (1986)

“Kimberlites are a clan of volatile-rich (dominantly CO₂) potassic ultrabasic rocks. Commonly, they exhibit a distinctive inequigranular texture resulting from the presence of macrocrysts (and in some instances megacrysts) set in a fine grained matrix. The megacryst/macrocryst consists of rounded anhedral crystals of magnesian ilmenite, Cr-poor titanite, pyrope, olivine, Cr-poor clinopyroxene, phlogopite, enstatite, Ti-poor chromite. Olivine is the dominant member of the macrocryst assemblage. The matrix minerals include: second generation euhedral primary olivine and/or phlogopite, together with perovskite, spinel (titaniferous magnesian aluminous chromite titanite chromite, members of the magnesian ulvospinel-ulvospinel-magnetite series), diopside (Al- and Ti-poor), monticellite, apatite, calcite, and primary late stage serpentine (commonly Fe rich). Some kimberlites contain late stage poikilitic euhedral phlogopites. Nickeliferous sulfides and rutile are common accessory minerals. The replacement of early-formed olivine, phlogopite, monticellite and apatite by deuteric serpentine and calcite is common. Evolved members of the clan may be devoid of, or poor in, macrocrysts and composed essentially of calcite, serpentine, and magnetite, together with minor phlogopite, apatite, and perovskite.”

Kimberlite pipe morphology

Kimberlite intrusions are typically conical in shape (Fig.4) and are referred to as pipes due to their appearance (Mitchell, 1986). Some kimberlites can be of champagne glass shaped. The kimberlite pipes with conical-shape are taken as standard for classification and understanding. They are made up of different zones with each zone having its own texture and mineralogy. Clement & Skinner (1985) classified kimberlite pipes into three facies namely crater, diatreme and hypabyssal from surface to bottom of the pipe based on their intrusion characteristics. Crater facies is composed of volcanoclastic material. The diatreme facies is steep sided and the lower most hypabyssal facies is irregular and complex with it dykes and sills. This simple classification has been revised based on the nature of texture being either volcanoclastic or coherent by Scott Smith et al., 2013.

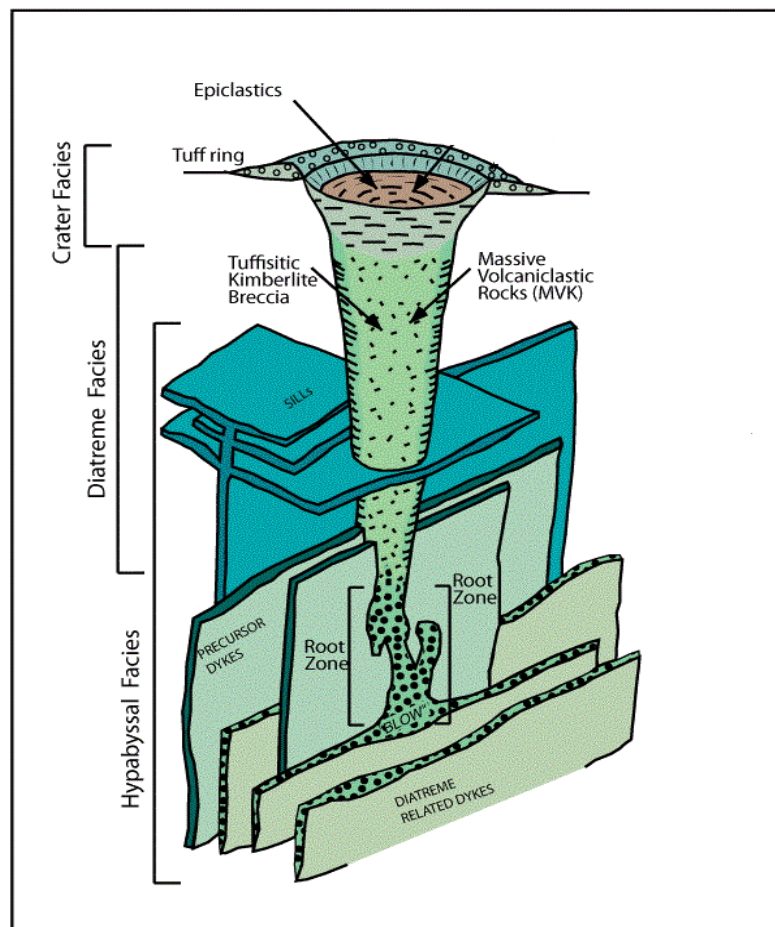


Fig. 4: Diagrammatic representation of typical Kimberlite pipe morphology source---Mitchell, (1986).

Kimberlite classification

Currently three groups of kimberlites have been identified, Group I kimberlites, Group II kimberlites and Transitional Group kimberlites. The Group I and II classification was given by Smith (1983) based on isotopic affinities (Sr-Nd-Pb isotopic signatures). Later Mitchell (1995) proposed the term orangeite for group II kimberlites. The orangeite or Group II kimberlites are rare and restricted in its occurrence and are found in South Africa, India and Finland. The Transitional Group kimberlites are the rarest compared to other types of kimberlites with very limited occurrences and studies carried out (Beard et al., 2000; Kaminsky et al., 2004; Becker et al., 2007; Donatti-Filho et al., 2013b). These transitional type kimberlites show mixed signatures from group I and Group II. In Brazil, kimberlites along Corridor-125 are of three types Group I (Concordo-2), Transitional Group (Tres Ranchos) and Lamproites (Juina).

Mineralogy of kimberlites

The mineralogy of kimberlites is complicated as they are hybrid in nature containing minerals varying from upper mantle to upper crustal conditions. The presence of numerous xenoliths, megacryst suits and secondary alteration complicates the generalization about kimberlite mineralogy. In spite of this, the rock exhibits distinct inequigranular texture with xenoliths and groundmass.

Xenoliths: The xenoliths can be of mantle origin or country rock fragments. Mantle xenoliths made up of varying proportions of (i) peridotites, (ii) eclogites and (iii) metasomatised nodules including glimmerites, MARID (mica, amphibole, rutile, ilmenite, and diopside) suite xenoliths (Dawson and Smith, 1977; Dawson, 1980) are found in kimberlites. The type and proportions of xenoliths vary from one kimberlite to another. They normally constitute 2% in volume to that of the total kimberlite (Dawson, 1980) but can be as high as 50% volume (Cox et al., 1973). Country rock fragment also varies in amount, type and size between different kimberlites and within the same kimberlite pipe. Within a kimberlite pipe the country rock fragment size, shape and distribution can give important information about the emplacement process and reworking of material within a kimberlite pipe (Schmincke, 1984).

Megacrysts and Macrocrysts: Smaller fragments bigger than 1cm mineral fragments or minerals found embedded in kimberlites are termed as Megacrysts and macrocrysts. This is a non genetic term and includes olivine, garnet, clinopyroxene, orthopyroxene, phlogopite, ilmenite and zircon. Olivine is the most abundant mineral phase in group I compared to group II kimberlites. In case of Transitional group kimberlites the olivine content is in between group I and II kimberlites. It is difficult to distinguish between the phenocrystal and xenocrystal olivine as their compositions overlap. The group II kimberlites contain phlogopite as abundant mineral phase. It occurs as macrocrysts, microphenocrysts, and groundmass and can make up 50% of the mineral assemblage. In comparison, phlogopite from transitional kimberlites falls between Group I and Group II values.

Diamonds also forms part of xenocryst phase and they are sampled randomly by an ascending kimberlite (Boyd and Gurney, 1986; Stachel and Harris, 2008). In most cases diamonds have been dated as a lot earlier than the age of the kimberlite that brought it to the surface (Evans and Harris, 1989; Bulanova, 1995; Pearson and Shirey, 1999). Temperature and pressure required for the formation of diamonds is found to be between 4-6 GPa (150-200 km depth) and 1000-1200⁰Ctemperature (Bulanova, 1995; Stachel et al., 2005; Stachel and Harris, 2008).

Groundmass: Skinner and Clement (1979); Clement and Skinner (1985) defined the groundmass as the relicts after removing all of the foreign material and macrocrysts and includes monticellite, serpentine, phlogopite, calcite, diopside, apatite, spinel and perovskite. Kimberlites groundmass is susceptible to syn- and post-emplacement alterations due to primary and secondary minerals and accordingly, it complicates the geochemistry of groundmass. In most kimberlites the groundmass is dominated by second generation serpentine, calcite and microliticdiopside.

Geochemistry of Kimberlites

The major- and trace-element geochemical of kimberlites are hindered by the ubiquitous presence ofcrustal, xenolithic and xenocrystic material. The measured values indicate the total resultant geochemistry due to primary magma, xenocrysts, phenocrysts and their alteration products.

Major element concentration range will be, low in SiO₂ (25–30 wt. %), low in Al₂O₃ (usually <3 wt. %), very low in Na₂O (usually < 1 wt. %), high MgO (20–38 %), high CaO (5–14%), moderate FeO (6–16%), low TiO₂ (< 4%), and low K₂O (<2), although K₂O levels can reach 7% in Group II kimberlites due to the increased phlogopite content (Mitchell, 1986; Mitchell, 1995). Group II kimberlites may also contain slightly higher SiO₂ and lower contents of MgO than their Group I.

Group I, Group II and transitional kimberlites are all highly enriched in LREE with respect to HREE, which is a reaction of a very low degree of partial melting of the source (Le Roex et al., 2003; Becker and Le Roex, 2006). In general, the ratio of LREE to HREE (La/Yb, normalised to chondritic mantle abundances) ranges from 80 to 200 (Mitchell, 1986). Trace element pattern provides guide to distinguish between Group I and Group II kimberlites. Group I kimberlites have lower Ba/Nb (<12), Th/Nb (<1.1) and La/Nb (<1.1) and higher Ce/Pb (>22) ratios, whereas Group II kimberlites show enrichment in Pb, Rb, Ba, and LREE and also contain Cr and Nb depletions with respect to Group I kimberlites. With the exception of few trace element range spanning the entire range (for example Ni), Transitional kimberlite major and trace element characteristics tend to fall between those of Group I and Group II kimberlites (Becker et al., 2007).

Some of group I kimberlites trace element ratios (such as Ce/Pb, Nb/U, La/Nb, Ba/Nb, Th/Nb) are also diagnostic of ocean island basalts (Smith, 1983). At the same time it has characteristics (refractory Mg numbers, Ni content) similar to subcontinental lithospheric mantle (Le Roex et al., 2003; Becker and Le Roex, 2006). This complicates ascertaining of these kimberlite sources to simple convecting asthenospheric source.

Source region of kimberlite magma

Source of kimberlite magma is argumentative with number of sources proposed including the convecting upper mantle, the sub-continental lithospheric mantle, the lower mantle and the core/mantle boundary (Smith, 1983; Ringwood et al., 1992; Tainton and McKenzie, 1994; Nowell et al., 2004; Becker and Le Roex, 2006; Paton et al., 2009; Tappe et al., 2011; Tappe et al., 2012; Guarino et al., 2013; Tappe et al., 2013).

General agreement of source region has been assigned to Group II kimberlite genesis. Their extremely enriched isotopic range, distinctive REE pattern, and refractory element concentration ranges (High Mg number and Ni, low Al₂O₃ and HREE). These characteristics will be achieved by a source that has undergone extreme metasomatic enrichment and subsequently been isolated from the convecting mantle for a substantial period of time. The SCLM that has undergone ancient (>1 Ga) metasomatic enrichment via melts derived from the asthenospheric mantle fulfils these requirements (Tainton and Mckenzie, 1994, Becker and Le Roex, 2006). Interpreting Group II Kimberlite source region is more complicated. A SCLM source has been proposed by several authors (Tainton and McKenzie, 1994; Le Roex, 2003; Harris et al., 2004 and Becker and Le Roex, 2006).

Two-stage melting model was proposed by Tainton and Mckenzie (1994) to accommodate the diversity observed in geochemistry of Group I kimberlites. Initially, the SCLM kimberlite source must have been strongly depleted by ~20% melting in the garnet stability field in order to account for the characteristic low HREE abundances. This depleted source is subsequently enriched by the infiltration of sub-lithospheric source, small scale metasomatic melts. Interaction with this small-scale melt would increase concentrations of highly incompatible elements to a greater degree than the less incompatible HREE. Finally, with the removal of a very low melt fraction (0.4 – 0.3%) within the garnet stability field kimberlite magma is generated, thereby concentrating the LREE and producing a melt with trace element concentrations that is observed.

Becker and Le Roex (2006) propose a similar method of formation, with a strong relationship between Group I kimberlites and OIB (Sr/Nd isotope ratios, along with Ce/Pb, Nb/U, La/Nb, Ba/Nb, and Th/Nb elemental ratios) they suggest the enrichment process must have been achieved by OIB related fluids. Becker and Le Roex (2006) also emphasized that, in order to explain the bulk earth Sr and Nd isotope ratios, kimberlite magmatism must have occurred soon after the metasomatic enrichment event.

Presence of ultra-deep source diamond inclusion phases (majoritic garnet, magnesio-wüstite, and ferropericlase present in diamonds) in Group I kimberlites has been a hindrance to the SCLM source theory. Ringwood et al. (1992) argue that a SCLM source cannot adequately explain these observations. These phases being stable at depths of >400km, these diamonds should have originated from such deep sources and thereby the magma entrapping

these diamonds. Hence, they proposed that these kimberlites originate from within the transition zone (400-650km depth). They proposed a two-stage melting model similar to that of Tainton and McKenzie (1994), where asthenospheric charzburgite has been metasomatically enriched by small degree partial melts originating from subducted oceanic crust situated at boundary layer depth. This model invokes partial melting of ancient subducted crustal deep asthenospheric levels, forming “melt pools” which subsequently rise and congregate at sublithospheric depths. The congregation of these asthenospheric melt pools homogenises the melt, explaining the isotopic signatures observed, whilst also increasing the pressure on the overlying SCLM, resulting in fracturing and kimberlite emplacement.

The origin of transitional kimberlites is least documented in kimberlite literature. As a preliminary proposal, a magma mixing through a single plumbing system theory is proposed by Becker et al, 2007. Few other authors have proposed transitional kimberlites are sourced from the base of the SCLM, where asthenospheric fluids/melts have interacted with the SCLM and subsequently melted (Beard et al., 2000; Donatti-Filho et al., 2013b). A SCLM source has been suggested for Brazilian transitional kimberlites in order to accommodate their isotopic and incompatible trace element signatures (Gibson et al., 1995; Donatti-Filho et al., 2013b; Guarino et al., 2013); and the problematic presence of high pressure inclusions (e.g. Collier 4, Bulanova et al., 2010) in many Brazilian diamonds are not thought to represent the source of the kimberlites (Bulanova et al., 2010; Walter, 2011).

Chapter 5

Geological Framework of Brazil

Geological Framework and Structural Trends

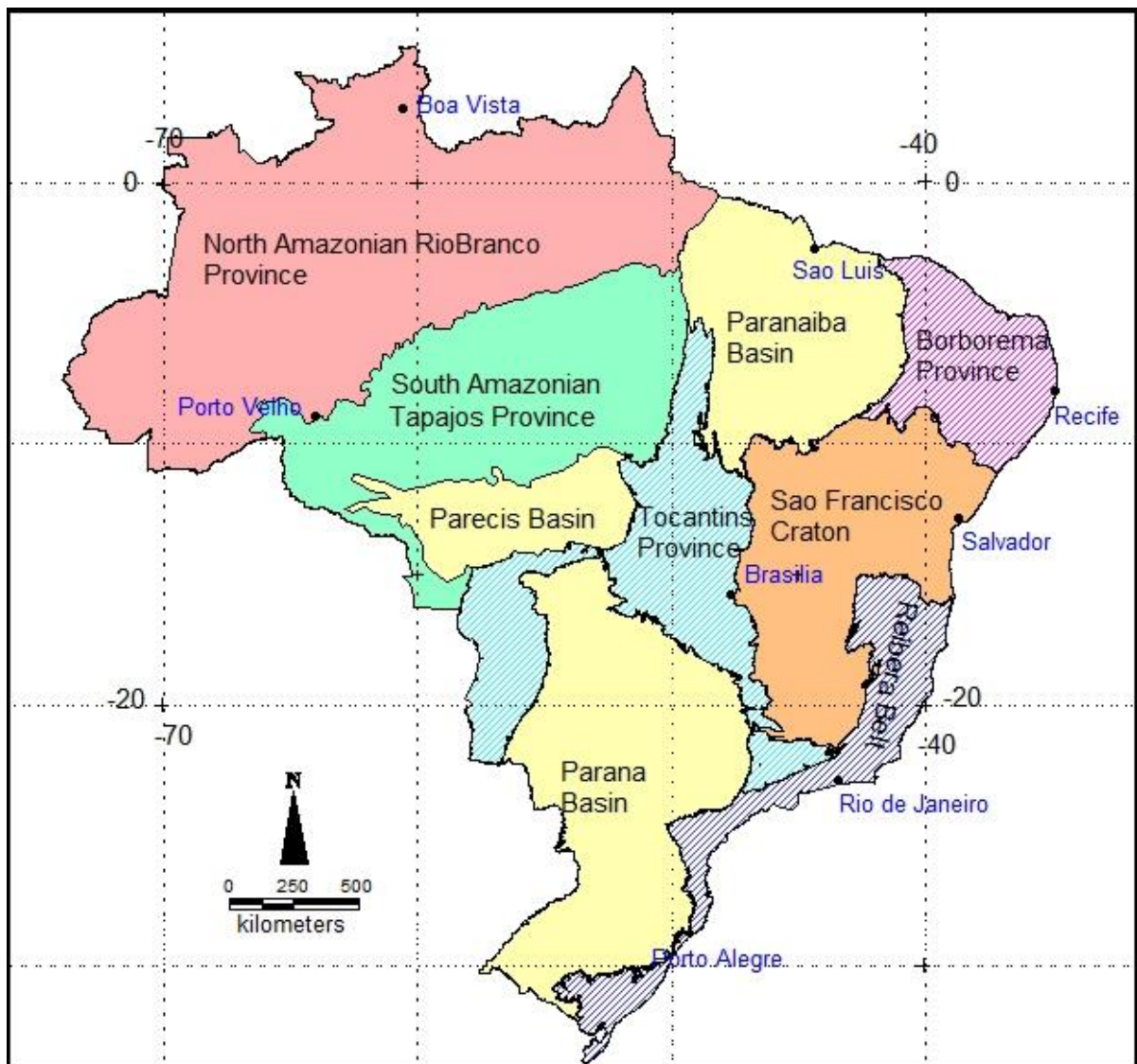


Fig. 5: Structural Provinces of Brazil with major cities modified After Almeida et al, (1981) and CPRM Database.

Brazilian platform is made up of Amazon, São Francisco, Rio de la Plata, São Luiz and Paranapanema cratons surrounded by Neoproterozoic fold belts and Paleo- to Mesoproterozoic domains with fold belts separating the cratonic fragments (Fig.5). Major part of the cratonic regions are covered by intracratonic Palaeozoic rift basins namely Parecis,

Parana, Parnaíba, Amazonas, Alto Tapajós and Solimões basins (Fig.5). Transbrasiliano lineament is a shear zone that runs from the NE of the country to the SW and further down into Argentina. The east coast of the country is a rift margin due to South Atlantic opening. To the north, the country is bound by equatorial rift margin. The Western margin is bounded by Andes orogeny which is the result of Nazca plate subduction.

Prior to the amalgamation of various tectonic blocks of Brazil, it was proposed that Clymene Ocean existed between the São Francisco and Amazonian Craton (Cordani et al, 2013). The Clymene ocean closure and final amalgamation of tectonic blocks -São Francisco, Paranapanema, Rio de la Plata and Amazon cratons of Brazil took place during Brasiliano cycle around 650 to 600 Ma (Cordani et al, 2013; Almeida, 1978). Neves et al, 2014 have considered the Amazon cratonic region along with the thrust and fold belts of Paraguay-Araguaia belt as one tectonic unit and the region west of it as another unit. Accordingly, in this current study, this broad classification of Amazonian and Extra-Amazonian regions aids in better understanding of the geotectonic evolution with respect to kimberlite magmatism.

Due to the collision of Amazon craton with São Francisco craton east verging thrust and nappes developed on the Extra-Amazonian region. Major east verging nappes are Araxa nappe, Passos, Guaxupe and Socorro nappes. In the Central Brazilian region in between the Amazon craton, Paranapanema craton and São Francisco craton Tocantins fold belt is found. Brasilia belt is the fold belt of Tocantins province along Corridor-125 and its associated kimberlites are found intruding this fold belt.

The Amazon craton is an accreted landmass of several mobile belts with successive younging from east to west. This craton is divided into two cratonic blocks by Amazonas basin- The Rio Branco craton and the Guapore Craton. The Guapore craton is synonymously referred to as Brazilian Amazon craton and the Rio Branco with Guyanian Amazon craton. With the same convention of Amazon craton refers to Guapore craton in our study. The structural province classification calls this Guapore craton as Tapajós province. The central basement rock forms the nucleus of this accreted landmass with age greater than 2.3 Ga (Tassinari and Macambira, 1999) and subsequently cratonized during 1.7 Ga (Almeida et al, 1981). Six provinces are recognised from the NE to SW of Amazonian region. The corridor-125 is represented by Rio Negro-Juruena mobile belt which is further divided into three tectonostratigraphic units namely Roosevelt, Jamari and Nova Brasilândia belts and

Rondonian-Sanignacio province (Tassinari et al, 1996). Further south of Brazil in Paraguay the mobile belt province is termed as Sunsas mobile belt province is seen. Scattered pieces of this mobile belt rocks are also seen in patches in SW Rondonia state.

Nova Brasilandia belt (E-W trending) formed in an intracratonic rift setting with the proto-ocean opening and closure. This oceanic opening was during Grenville time during which there was extensive orogenic in Laurentia. The suture zone from Nova Brasilandia belt up to southwest Paraguay thrust zone is a mega structure called Guapore suture zone (WNW-ENE trending) which resulted due to Mesoproterozoic suturing of Paraguay block and Amazonian craton (Hartmann, 2012). The area between Guapore suture zone and the Paraguay block is characterized by NW frontal thrusts and NE lineaments due crustal shortening along E-W direction (Rizzotto et al, 2013). Few ophiolites have been found and has been dated from this Guapore suture zone (Rizzotto et al, 2013) proving the fact that there was proto-ocean prior to suturing.

The Parecis basin is a rift-sag basin found to the east of Guapore suture zone. The Rodinian breakup and continental rift extension resulted in weak zones which during Palaeozoic times evolved into Parecis basin. This rift system was further filled by sag deposits due to thermal subsidence. The thermal subsidence is accomplished due to cessation of rift along with compression stresses from Andean region. The NW trending Pimenta Bueno and E-W trending Colorado rifts are associated with this basin.

North of Nova Brasilandia belt, the basement rock is overprinted by Jiparana shear zone of Grenville age. Jiparana shear zone consists of two trends- NNW and EW ductile deformation. (Tohver et al, 2005). Jiparana shear zone ductile deformation is interpreted as structures formed due to the collision of Laurentia with Amazonian craton (Tohver et al, 2005).

The Guapore basin is situated from the southwest margin of Brazil up to southeast boundary of Parecis basin. This basin architecture and the basement structures are poorly known due to cover sediments. From the neotectonic framework, the structural trends are NW-SE due to compression in E-W direction, NE-SW transtensional and transpressive N-S lineaments (SouzaFilho et al. 1990) due block rotation and translation of South American plate.

The kimberlite occurrence in Extra-Amazonian basement is not clearly known as it is situated at the marginal zone where two cratons have collided and amalgamated. These two cratons involved are São Francisco craton and the Paranapanema craton, which is now covered by Parana basin sediment cover. The São Francisco craton basement rocks are slightly older than the Amazonian basement and the oldest age known is around 3.1 Ga (Almeida et al, 1981). This basement was cratonized during subsequent tectonic event around 1.7 Ga (Almeida et al, 1981). It is interpreted that the kimberlite occurrences in the Extra-Amazonian region south of São Francisco craton is intruded into the São Francisco cratonic basement from the gravity geophysics data (Pereira et al, 2005).

Geological Framework of Corridor-125

Main geological units along Corridor-125 are the NE-trending Neoproterozoic (Brasiliano/Pan-African) Ribeira Orogen in the Southeast, São Francisco craton basement, NE-trending Neoproterozoic Brasilia Orogen, Phanerozoic Parana basin, NE-trending Neoproterozoic Paraguai-Araguaia Orogen followed by Amazonian craton basement (NW-trending Mesoproterozoic Rondonian and Sunsas orogens) and Phanerozoic Parecis Basin. The NE-trending Transbrasiliano lineament cuts across Corridor-125. On the western side of Transbrasiliano lineament there occurs the Amazonian craton and on the eastern side the Extra-Amazonian region.

The main structural features and geological units that characterize Corridor-125 are NW-trending Proterozoic mafic dyke swarms (Pará de Minas dyke swarm) in the Extra-Amazonian region and the NW-trending Serra Formosa and Rio Guaporé arches in the Phanerozoic Parecis Basin and its basement, Amazonian craton. In between the latter two arches another major structural feature is the Pimenta Bueno graben in the Parecis basin. In the Extra-Amazonian region the Pará de Minas dyke swarm continues, without significant deformation, beneath the Brasilia orogen up to the Transbrasiliano Lineament as seen on aeromagnetic maps to be shown in a later section. Other lineaments at high to moderate angle to Corridor-125 are common and in several places the intersections with Corridor-125 are sites of kimberlite clustering.

Mafic and ultramafic magmatism along Corridor-125

Along corridor-125, there are several alkaline rocks clustered in distinct provinces (fig.6). They are Juina, Poxoreu, Batovi, Alto Paranaíba igneous provinces. It is quite interesting to see that all these igneous provinces are also associated with kimberlite occurrences. Next to the east coast of Brazil with continuation from corridor-125, there are two more igneous provinces – Abrolhos and Trindade igneous provinces. Basalts, Kamafugites and carbonatites are also found within the corridor-125 along with the igneous province.

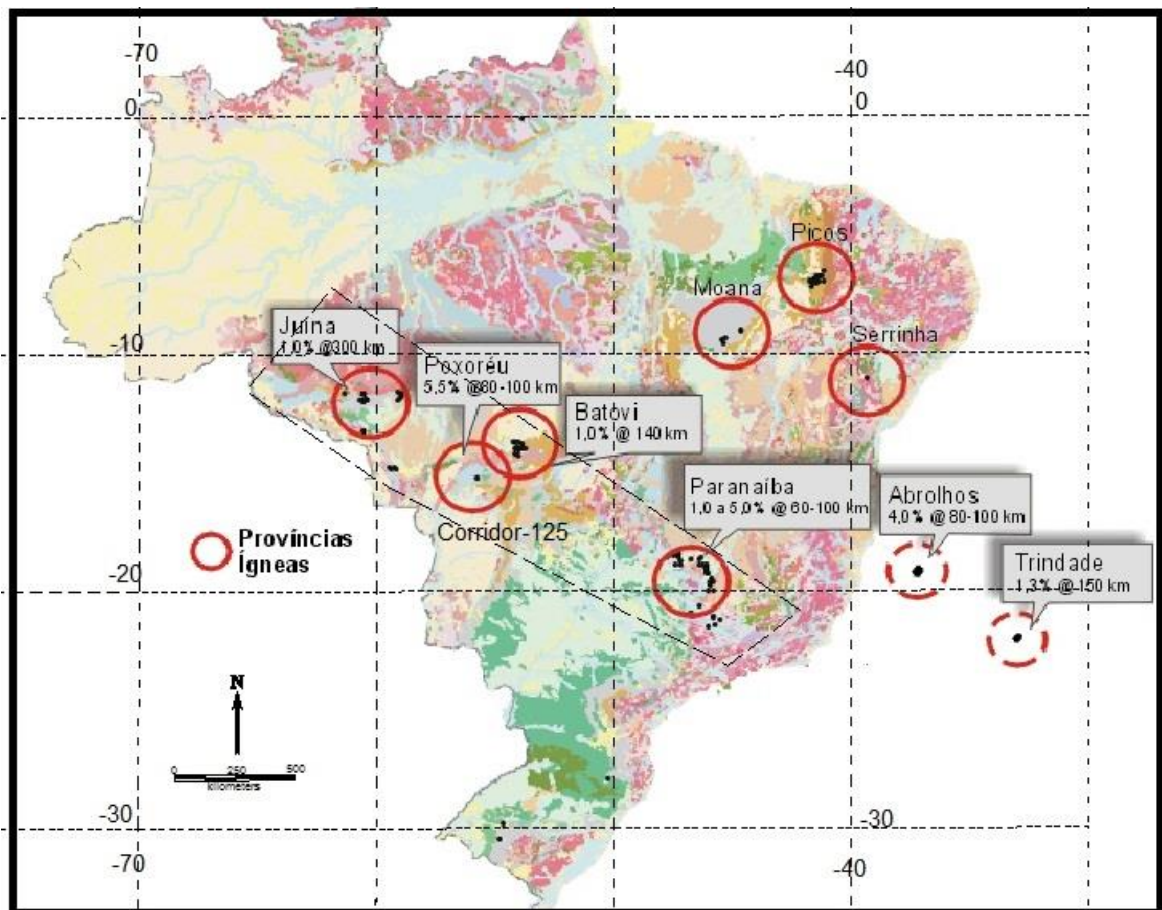


Fig. 6: Igneous Provinces of Brazil from CPRM Database, 2004 with respect to Corridor-125

Chapter 6

Role of Brazilian plate in Global Plate tectonics

Introduction

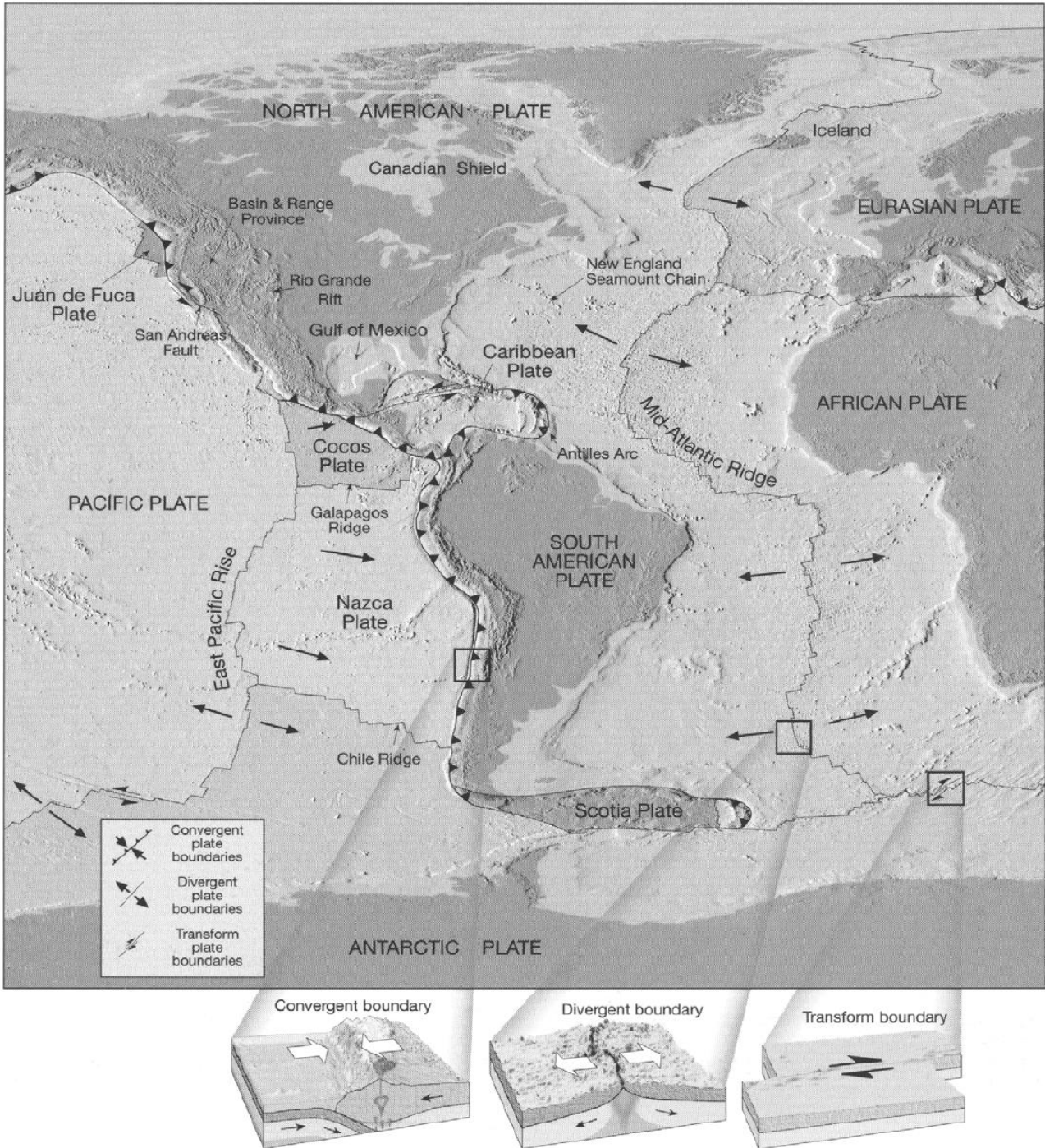


Fig. 7: South American plate with tectonic boundary type.

The present day configuration of continents and ocean is the result of rearrangement of various blocks that make up the continents and ocean. These blocks are termed as Tectonic plates. Each tectonic plate is made up of thinner oceanic and thicker continental parts. The vertical limits of the plate go up to lithospheric depths. These plates are dynamic and are in continuous motions, which are not recognizable easily due to its slow rate. This movement of lithospheric plates or Tectonic plates is the basis of Plate tectonics which was first observed and proposed theoretically in 1960s by Alfred Wegener based on continental drift theory. Further, it has evolved into the concept of today's Plate Tectonics.

Currently, there are eight major plates and many minor ones. South American plate is one such major tectonic plate. This plate consists of the continental part and the South Atlantic part as the oceanic part. As mentioned earlier, the movement of tectonic plates rearranges the plates into different configuration, this is known as supercontinent. To precisely explain supercontinents, it is the amalgamation of several or all plates together at a particular time at a particular position on the globe. Plate boundaries play an important role in plate tectonics. Hence, understanding the type of plate boundary and the processes involved marks the key to the concept of plate tectonics.

Supercontinent formations are accomplished by three types of boundary types: transform convergence /subduction and divergence/ rifting of two or more plates. The transform boundary is conservative plate boundary; the divergent boundary is constructive and the convergent boundary is destructive in nature. The plate boundaries involved in the above movements are of the type continental-continent lithosphere, continent-oceanic lithosphere and oceanic-oceanic lithosphere. In plate tectonics the landmass is always conserved. The loss of landmass at subduction is compensated by the production of new oceanic crust at the midoceanic rifts.

The supercontinent formation and breakup are episodic, giving rise to the idea of a supercontinent cycle (Nance et al., 1986). A supercontinent life cycle consists of rifting and breaks up of one supercontinent, followed by a stage of reassembly in which dispersed plates collide to form a new supercontinent. Here most or all plates in different configurations from the older supercontinent (Hartnady, 1991). The assembly process generally takes much longer

than fragmentation, and often overlaps in time with the initial phases of rifting that mark the beginning of a new supercontinent dispersal phase. The supercontinental cycles provide a record of the processes controlling the formation and distribution of continental crust throughout the Earth's history by means of magmatism and orogeny associated with it. It also influences isotopic and elemental geochemical cycles, climatic distributions and changing environments which affect the evolution of organisms.

Brazilian plate is an accretion of various minor blocks forming part of South American plate. South American plate is made up of main Brazilian plate, Salado subplate consisting of Salado and Colorado basins. Throughout this thesis, Brazilian plate is synonymously used with South American plate. As we are focusing on corridor-125, which is within the Brazilian plate all the reconstruction and interpretation is carried out with respect to Brazilian plate. Brazil has been part of many supercontinent lifecycle though not in the same framework of continental mass.

Major supercontinents

The existence of older than 1.3 Ga supercontinents is likely but their configurations are not understood very well and not documented. Rodinia is the well documented supercontinent in which Brazilian plate formed a major part though not in the exact shape, size and position as today. This supercontinent timing is interpreted at 1.3-1.0 Ga. It fragmented at 750-600 Ma paving way for the next supercontinent assembly. This break up followed by rearrangement of plates led to the formation of Gondwana supercontinent. In fact, the rearrangement continued up to 550 Ma with further rearrangements. Note worthy rearrangement of our interest in this period is the collision and assembly of the São Francisco craton in Brazil and the Congocraton in Africa occurred in the Early Proterozoic. Paleomagnetic and paleoclimatic data indicate that during the early Palaeozoic most continents remained at low, equatorial latitudes (Scotese, 1984; Jurdy et al., 1995). The Pacific/Nazca plate is subducting from Cambrian up to today under the South American plate forming the subduction zone. The result of this subduction is the Andean orogen on the Western margin of South American plate.

Further rearrangement of the tectonic plates occurred resulting in Pangea Supercontinent around 300Ma. Pangea was composed of Laurentia (North America- Eurasia) and Gondwana (India, Africa-South America and Antarctica-Australia) surrounded by Tethys in the east and Pacific ocean in the west. Around 280 to 225 Ma Pangea drifted apart along south of North America and North of South America giving rise to Central Atlantic Ocean. This Permo-Triassic rifting was followed by cretaceous South Atlantic rifting and opening up of South Atlantic Ocean at 120 Ma. Thus Africa and South America separated and reached the present day configurations.

The driving forces guiding the plate motions has been a subject of debate from long times. There are many hypotheses concerning the driving forces for plate tectonics. To name some of them are

- Mantle Convection theory: Mechanical boundary exists below the Earth's hard crust in the form of lithosphere and asthenosphere. These two layers of the Earth are contrastingly different with respect to density and heat flow or temperature. The lithosphere is cooler than the asthenosphere. Due to this temperature gradient, convection current develops serving as the driving force moving the plates above them.
- Fixed hotspot theory: Based on the location of hotspots close to midoceanic ridges and seamount volcanic age progression, it is proposed that hotspots serve as the driving force which moves the plates above them when they rise from deeper mantle to higher. Here the rising mantle plume provides the necessary heat and material in the form of igneous activity for the melting and rifting of the plates.

All these theories explain the processes involved around the plate boundaries ie horizontal tectonics. The theories does not provide satisfactory reasoning for the intraplate magmatism which is found associated with plate tectonics especially kimberlite magmatism. Several attempts (Hastings & Sharp, 1979; Morgan, 1983; Le Roex, 1986; Skinner, 1989; Skinner et al., 2004; O'Neill et al., 2005) have been made to show the genetic link with the hotspots and kimberlite emplacements. One such example is the North American kimberlite magmatism age progression associated with fixed hotspotpaleo-track over a moving plate (Heaman et al, 2004). But the age progression and hotspot paleo-track is not consistent on all continents and occurrences.

Tectonic elements of Brazilian plate at present day configuration

The Brazilian/South American plate (Fig.7) is bounded to the west by Subducting Pacific plate (Nazca plate with reference to Brazilian corridor-125). The eastward motion of Pacific plate has been active from 300 Ma up to present resulting in steep subduction and slab roll over. The subducted slab is restricted to Brazilian plate and there is no evidence for its continuation below African plate. The east coast of Brazil is bounded by rift margin. This rift margin is a result of Cretaceous opening of South Atlantic Ocean around 130 to 120 Ma. To the north, Brazil is bounded by a rift margin. This northern rift margin is the result of Triassic rifting between Laurentia and South American plates. Brazilian oceanic plate boundary is represented by the Mid-Atlantic ridge.

Chapter 7

Corridor-125 and its Kimberlites (Occurrence, Clusters and Age)

Corridor-125, A Regional Scale Structural Lineament

Brazilian kimberlites are preferentially oriented along major lineaments (Fig.1) namely, Az-125, Transbrasiliano Lineament (TBL), Blumenau lineament, Rio Alonzo Lineament, Rio Grande Arch and Amazonas basin Lineaments. Of these lineaments, Azimuth-125, referred to as Corridor-125 in this research, hosts the maximum number of discoveries thereby indicating a fundamental structural control on their emplacement. Key is to understand the interplay between the structural and plate tectonic controls and the timing and location of kimberlite emplacement along Corridor-125.

Corridor-125 is composed of several mega- and giga-lineaments and trends NW-SE from Rio de Janeiro to Porto Velho (Fig.1). The total length of the corridor is around 2700 km and its width of 500km is estimated with the kimberlite occurrence bordered by the dyke swarms. The width of the boundary is chosen arbitrarily just outside the kimberlite occurrence area to get a picture of the geology, structure and geophysical signatures of the host rocks and its structures during study. Later this region will be checked for any signatures on geophysical aeromagnetic data to precisely delineate the corridor boundary.

Continental Scale Lineament Analysis

The genetic link between the oceanic transform fractures and Corridor-125 is studied by using “Global seafloor fabric and magnetic lineation (GSFML) database by Matthews et al., (2011) and Wessel et al., (2014). The transform fractures signatures from GSFML are used in GIS platform. These fracture zones are plotted against the Earth Magnetic Anomaly Grid Version.2 (EMagV2 by Maus et al, 2009) data to trace back the fracture zones up to the Brazilian Eastern board. This result is further overlain by the global oceanic age isochron and bathymetric data. By doing so, we further refined the trace back toward higher preciseness. Once, the data trace was achieved up to the border, the total field aeromagnetic

map which is reduced to IGRF, 1km square grid from the CPRM (Brazilian Geological survey) was utilized to identify the continental expression of the lineament.

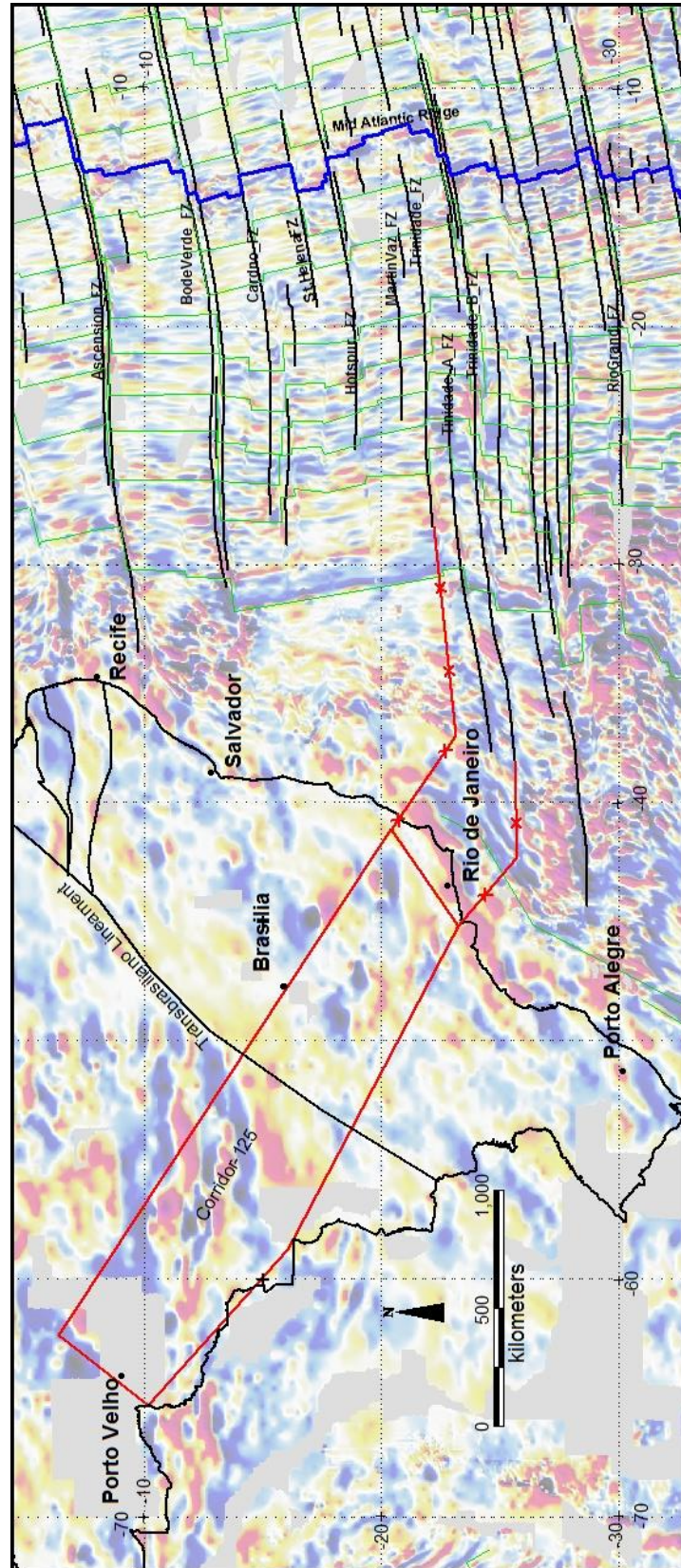


Fig.8: Oceanic extension of Continental Corridor-125 lineament in the Brazilian plate with global EMagV2 background and GSFML fracture zones and Mid Atlantic ridge.

The opening up of South Atlantic has a genetic link with the corridor-125 and the kimberlite occurrences along this corridor. With initiation of South Atlantic rift at 140Ma, it manifested in the oceanic extension of the continental lineaments of South American plate. Corridor-125, Transbrasiliano lineaments are the examples of such oceanic extension associated with South Atlantic rift. This link can be traced back with the help of Earth Magnetic Anomaly Grid data as shown in fig.8. The major oceanic fractures that are associated with the landward counterpart along Corridor-125 are Trindade fracture zone, Trindade_A fracture zone and Trindade_B fracture zone.

Kimberlite Clusters along Corridor-125

The kimberlite occurrences along Corridor-125 can be broadly classified into the following clusters (Fig.9):

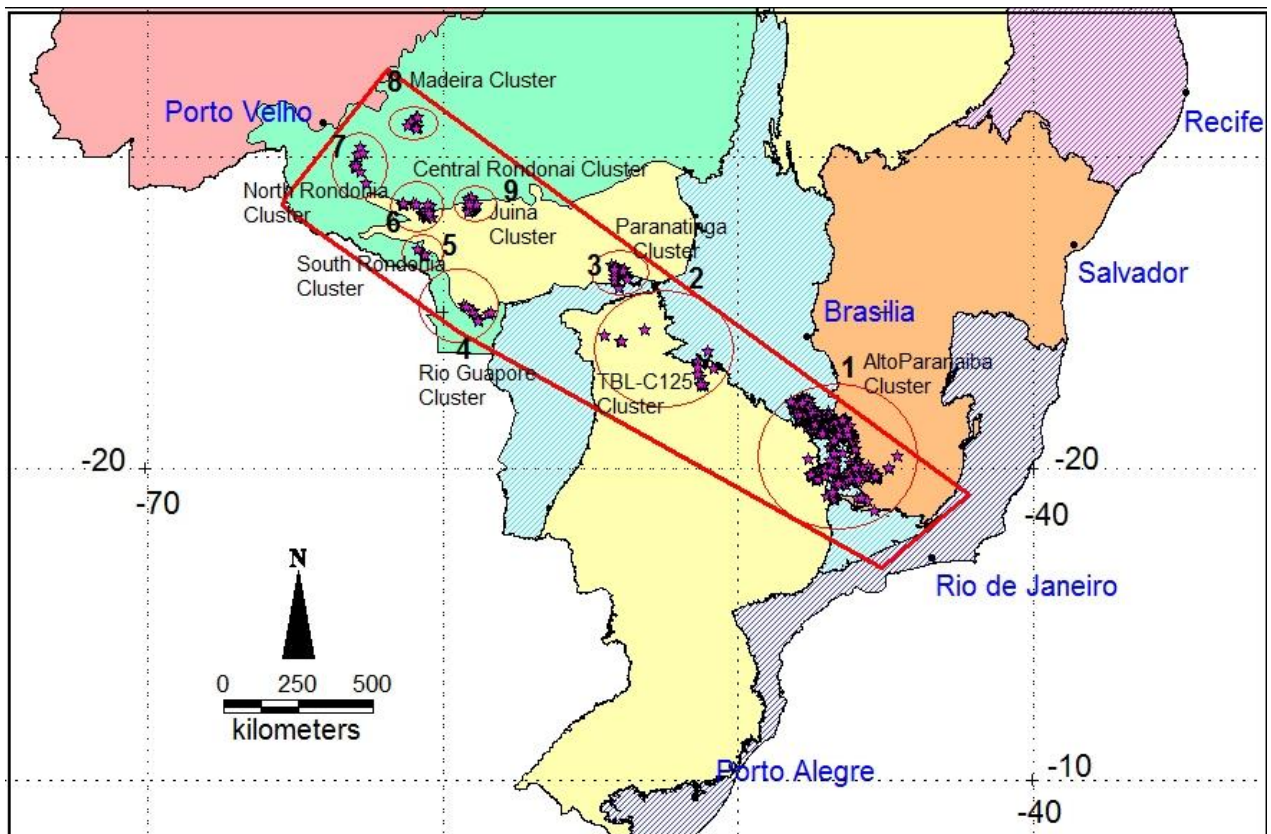


Fig.9: Kimberlite Clusters along Corridor-125 with structural provinces background. The region in yellow corresponds to Paleozoic basins.

1. Alto Paranaíba cluster;
2. TBL-C-125 Right cluster
4. TBL-C125 Left cluster
3. Upper Paraguay cluster (Rio Guapore and Paranatinga clusters),
4. South Rondonian cluster,
5. Central Rondonian cluster,
6. North Rondonian cluster,
7. Madeira cluster,
8. Juina cluster.

Alto Paranaíba Cluster is found in the state of Minas Gerais and Goiás forming a good cluster. The Transbrasiliano cluster is divided into two subclusters as left and right clusters since they are found on either side of Transbrasiliano lineament along corridor-125. The Transbrasiliano clusters are found in the state of Mato Grosso. The Upper Paraguay cluster is again subdivided into Rio Guapore and Paranatinga clusters. They are found in the state of Mato Grosso. The North, South and Central Rondonian clusters are found in Rondonia state. The Madeira and Juina clusters are found in the state of Mato Grosso.

Structurally, AltoParanaíba and Transbrasiliano right kimberlite clusters are associated with Tocantins tectonic province to the base of São Francisco craton and at the margin of the Parana sedimentary basin. Transbrasiliano left kimberlite cluster is associated periphery of Parana Sedimentary basin. The Paranatinga cluster is associated with Amazonian craton basement and Tocantins structural province. The Rio Guapore cluster is associated with Upper Paraguay thrust zone and Tapajos tectonic province. Juina cluster is associated with Parecis basin and Tapajos tectonic province. The North, South and Central Rondonian clusters are associated with Tapajos Tectonic province.

Brazilian Kimberlite Age and Episodicity

The Brazilian kimberlite age clusters (Fig.10) are of six major peaks with intermittent quiescent periods. Four of these periods of kimberlite peaks are associated with Corridor-125. There are two known Proterozoic kimberlites in Brazil, namely the Salvador kimberlite, which are dated as 1150 Ma (Watkins et al, 2009; Dewit, 2010) and the Brauna kimberlites, which are dated at 642 Ma (Donatti-Filho et al., 2013). All other kimberlites are Permo-Triassic in age. The Proterozoic kimberlites are absent along corridor-125. Permo-Triassic

and Cretaceous kimberlite clusters are found along the corridor-125 and are grouped into the following clusters and listed below:

1. 226-268 Ma
2. 120-122 Ma
3. 80-94 Ma
4. 74 Ma

| SI_N o | Name_Unit | Age in Ma | Method_Dating | Year_Dating/Ref |
|-----------|-----------------|--------------|--|---|
| 1 | Collier 04 | 93 | U/Pb on Zircon | Heaman et al 1998 |
| 2 | Batovi 07 | 120 | U/Pb on Zircon | Heaman et al 1998 |
| 3 | P-01 | 120 | U/Pb on Zircon | Heaman et al 1998 |
| 4 | Brauna 03 | 678 | U/Pb on Zircon, Perovskite | J P Donatti-Filho et al. 2013 |
| 5 | Brauna 07 | 641 | U/Pb on Zircon, Perovskite | J P Donatti-Filho et al. 2013 |
| 6 | Canastra 01 | 120 | K/Ar on Phlogophite | Pereira & Fuck, 2005 |
| 7 | Pandrea-01 | 93 | U/Pb on Zircon | P. Andrezza et al, 2008 |
| 8 | Pandrea-06 | 93 | U/Pb on Zircon | P. Andrezza et al, 2008 |
| 9 | Pandrea-07 | 93 | U/Pb on Zircon | P. Andrezza et al, 2008 |
| 10 | Tres Ranchos 04 | 81 | U/Pb on Perovskite, Rb/Sr on Phogophite | Bizzi, 1995; Felgate, 2014 |
| 11 | Tres Ranchos 78 | 87 | Rb/Sr on Phlogophite | Felgate, 2014 |
| 12 | Tres Ranchos 27 | 82 | U/Pb on Perovskite | Felgate, 2014 |
| 13 | Tres Ranchos 14 | 87 | U/Pb on Perovskite | V. Guariano et al, 2013 |
| 14 | Carolina | 232 | Rb/Sr on Phlogophite | Hunt et al, 2009 |
| 15 | Cosmos 01 | 226 | Rb/Sr on Phlogophite | R. Creaser, 2006; Masum and Smith 2008 |
| 16 | Cosmos 03 | 240 | Rb/Sr on Phlogophite | Felgate, 2014 |
| 17 | Concordo 01 | 267 | U/Pb on Perovskite | Felgate, 2014 |
| 18 | Jacare 01 | 242 | U/Pb on Perovskite | Felgate, 2014 |
| 19 | Perdizes 02 | 88 | Rb/Sr on Phlogophite | Felgate, 2014 |
| 20 | Perdizes 04 | 94 | U/Pb on Perovskite | Felgate, 2014 |
| 21 | Limpeza 18 | 80 | U/Pb on Perovskite | Felgate, 2014 |
| 22 | Limeira 01 | 91 | U/Pb on Perovskite | V. Guariano et al, 2013 |
| 23 | Pantano 01 | 84 | U/Pb on Perovskite | V. Guariano et al, 2013 |
| 24 | Pantano 02 | 82 | U/Pb on Perovskite | V. Guariano et al, 2013 |
| 25 | Lemes | 84 | U/Pb on Perovskite | V. Guariano et al, 2013 |
| 26 | Indiana 01 | 80 | U/Pb on Perovskite | V. Guariano et al, 2013 |
| 27 | Esperanca | 76 | K/Ar on Mica (80 Ma) | Davis 1977 |
| 28 | Pepper 13 | 237 | U-Pb on Perovskite | Masum et al, 2008 |
| 29 | Poco Verde | 85 | Rb/Sr on Phlogophite | Felgate, 2014 |
| 30 | Santa Rosa 04 | 83 | Rb/Sr on Mica, Rb/Sr on Phogophite | Rogério S. Pereira &Reinhardt. A. Fuck, 2005; Felgate, 2014 |
| 31 | Successo 08 | 74 | Rb/Sr on Phlogophite | Felgate, 2014 |
| 32 | X270 | 89 | U/Pb on Perovskite | Heaman, 2002 |
| 33 | Botavi-09 | 122 | U/Pb on Zircon | Davis 1977 |
| 34 | Salvador 01 | 1150 | Rb/Sr on Phlogophite | Williamson and Pereira 1991, Dewit, 2010. |

Table.1: Brazilian Kimberlite Age and method of dating.

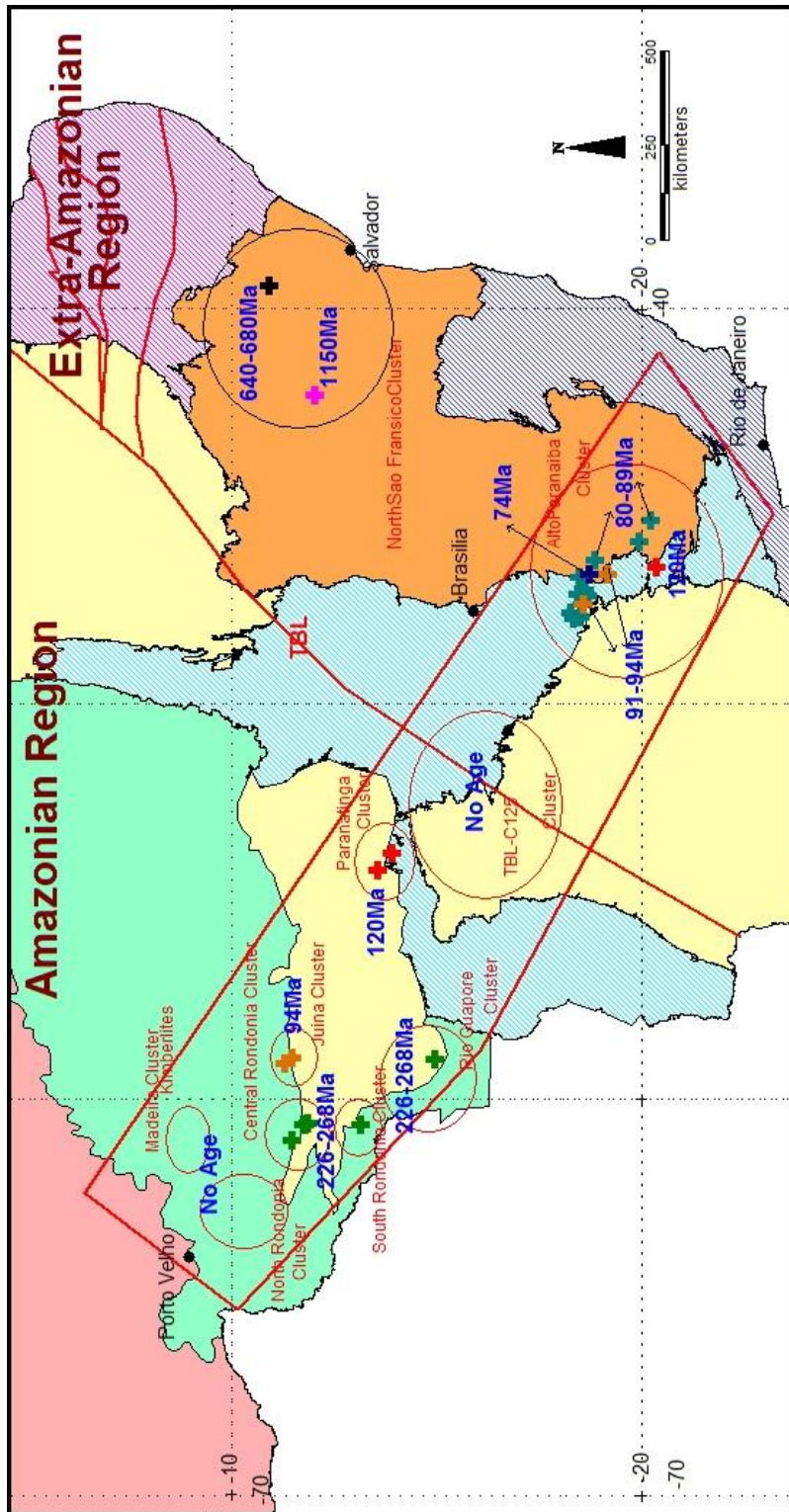


Fig 10:
Brazilian Kimberlite age
map with structural
provinces background.

Chapter 8

Structural Framework of Corridor-125 with mapped structures

A compilation from the available geological, aeromagnetic, and lineament maps of Brazil (CPRM, 2004 etc.) has resulted in the identification of several mega-and giga-lineament systems along corridor-125 (Fig.11) that has favored the kimberlite emplacement while other are not. The oldest structural activity is derived from the age of the oldest known dyke swarm dating back to 1.8Ga. After which this corridor has been subjected to several reactivations and these reactivations are expressed as different age group mafic and ultramafic rocks along its entire length. The Amazonian and Extra-Amazonian craton structural frameworks are dealt separately.

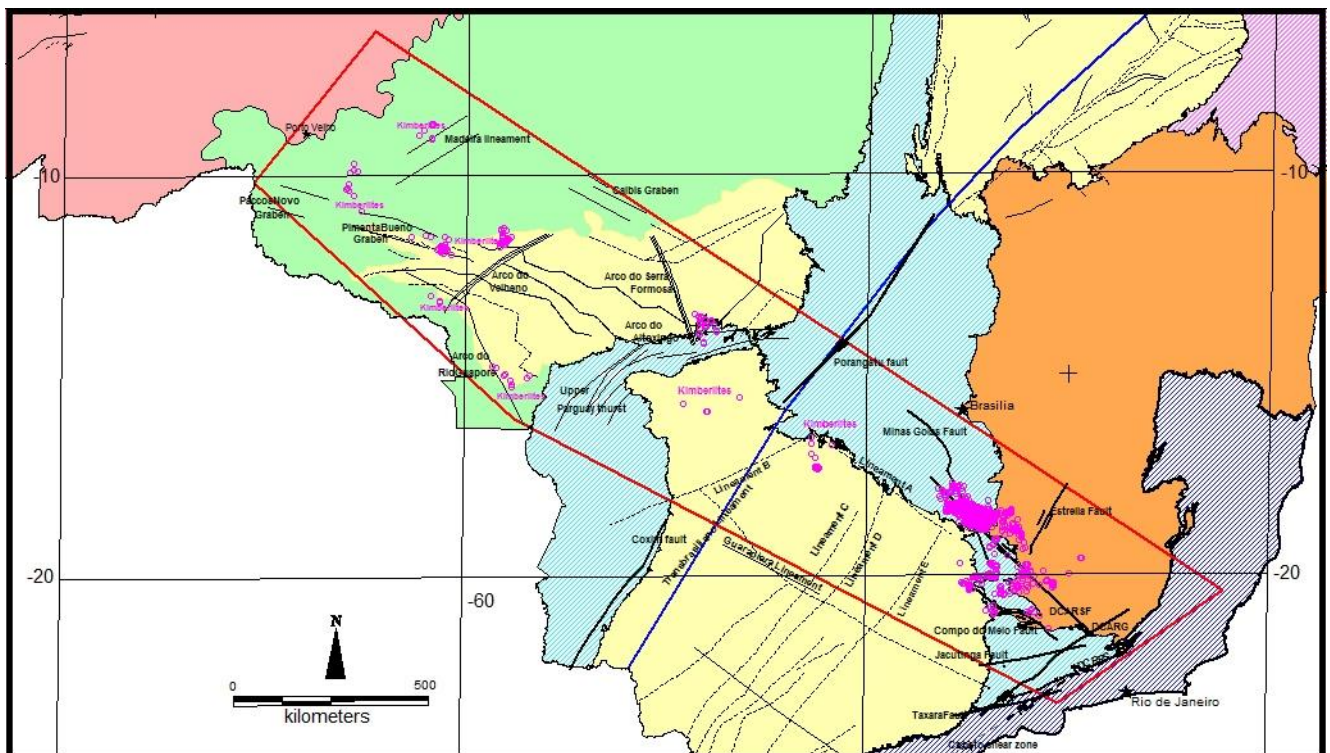


Fig.11: Structural Framework of Corridor-125 with Tectonic province background. The pink circles represent kimberlites, black lines represent structures. Blue line is the Giga Transbrasilino lineament.

General structural framework of the Extra-Amazonian craton consists of numerous NW-SE trending parallel to subparallel lineaments running from SE end, which are cross cut by NE-SW structures. The NW-SE subparallel lineaments sometimes are modified due to prevailing local tectonic regime where nappes and thrusts are seen as surface expression. The southeastern most part of the corridor is characterized by the coast parallel lineaments, which are also parallel to the corresponding orogens. TBL is the most magnificent NE-SW trending lineament cross cutting the corridor-125.

The TBL intersection with Corridor-125 has favored two major kimberlite clusters. The lateral branching at the SW end of the TBL has also favored two kimberlite clusters. These two sets of kimberlite occurrences on either sides of TBL are referred to as Western TBL-C-125 and Easter TBL_C-125 clusters. On the southeastern end of the Corridor-125, there are no kimberlite occurrences (SE-Ribera belt); adjacent to it, the AltoParanaiba arch is associated with the biggest kimberlite clustering in numbers.

This clustering of kimberlites is referred to as Alto Paranaiba cluster, which gives detailed information for the understanding of the lineament, kimberlite occurrences, age clustering etc. Alto Paranaiba cluster of kimberlites are associated with a network of NW lineaments intersecting with NE and NNW lineaments. The most significant ones are named as below:

DCARSF:

NW trending Upper Rio São Francisco Crustal discontinuity is a major continental lineament situated at the center of the corridor width. It forms one of the major kimberlite favoring lineaments in the Alto Paranaiba region. This lineament is associated with parallel to subparallel dyke swarms in the southeastern region. There are several magnetic signatures running parallel to these dyke swarms from the SE São Francisco cratonic region up to TBL. Though we have Brasilia belt as the geomorphic feature bordering São Francisco craton, the magnetic signature lineaments running all along the length of the corridor-125 up to TBL is a good evidence of thin-skinned tectonics and a proof for intact basement. Hence, the Brazilian kimberlites are found in the mobile belts does not deviate from Clifford's rule.

Compo de Meio lineament starts as a NW lineament and has a characteristic bending around the São Francisco cratonic southern boundary. There are kimberlites clustering around this lineament. Beyond this lineament there is a non-kimberlite occurrence zone. Hence, it is taken as lower boundary of the corridor-125

Minas-Goiás system: This megalineament is roughly NE trending forms part of the structures that hosts kimberlites of Alto Paranaíba Cluster.

Lineament A: this is another major megalineament (location in Fig.4), which starts at the Northwestern end of the DCARF almost subparallel to it and runs further NW and probably extends up to the Transbrasiliano Lineament. Its extension up to TBL is seen as intermittent minor linear mag signatures. This lineament hosts the next cluster of kimberlites, which is separated from the AltoParanaíba cluster by a non-kimberlite zone.

Estrela Fault: trends NE-SW and is a reverse strike-slip fault (Allaoua Saadi et al, 2002). It also forms part of the most influential lineaments of Alto Paranaíba kimberlite cluster.

NE-SW subparallel set of lineaments: There is a set of 3 sub parallel lineaments (C, D and E), which cut the corridor just after the Alto Paranaíba cluster of kimberlites and end at the A-lineament. These lineaments are not associated with kimberlite occurrence. There are dyke swarms occurring all along the lineament especially in the portion of Corridor-125.

Upper Paraguai Thrust: This thrust zone is found at the suture zone between Amazonian and Extra-Amazonian region. It forms the western margin of the Paraguai-Tocantins Marginal Suture zone.

Porangatu Fault Zone: This fault is also situated in the Paraguai-Tocantins Suture zone. It is a dextral fault (Allaoua Saadi et al, 2002) with no kimberlite occurrence along this fault but clustering is found to the left and right of this thrust zone.

WSW-ENE trending B-lineaments: Next to the Southern end NE-SW cluster lineament there is a lineament named B-Lineament. It intersects with the lineament A and forms the loci for the new cluster of kimberlites.

Kimberlite barren lineaments in Extra Amazonian Region

Lancinha-Cubatão-Além Paraíba Fault: This fault system trending NE-SW is found to the Southeastern end of the Corridor-125. It is a strike-slip fault found more associated with South Atlantic extension and there is no evidence of kimberlite.

Rio Paraíba DoSul Crustal discontinuity (DCRPS): It is also at the Southern end of the corridor with dextral and vertical sense of (Allaoua Saadi et al, 2002). No kimberlite is associated with this lineament.

Jacutinga Fault: trends WSW-ENE fault is found towards SE portion of the Corridor-125. This fault is not associated with any kimberlite occurrence.

General structural framework of the Amazonian craton: consists of NNW, NW, NE and E-W trend, which has favored one cluster of Kimberlites in this craton. The grabens, horst and rifts associated with Parecis basin forms the major loci of kimberlite emplacement. A detailed account on the grabens, horst and lineaments are listed below:

- Pimenta Bueno Graben,
- Madiera lineament.
- Arcs, Horsts, Flexutures and structural bends

- a. **Madeira Lineament:** This Lineament trends NE and forms an important structural control for Kimberlites north of PimentaBuneno.
- b. **Arco do Rio Guapore Lineament:** This lineament forms the lower boundary at the northwestern side of the Corridor-125. It is the suture zone between the Paraguay block and the Amazon craton. This lineament shows concavity towards the Paraguay block. It consists of two clusters of kimberlites; one on the northern portion of the lineament and one on the southern portion.
- c. **Arco Do Alto Xingu lineament:** is also one of the important structures trending NE and hosting Paranatinga kimberlites at the intersection of Arco do Serra Formosa which trends NNW. The kimberlites are seen only to the southeast of the Arco do Serra Formosa. Along with this, the paranatinga kimberlites are found in Southeastern end of Pimenta Bueno graben, brasnorte high, and in the SW-Xingu Graben.
- d. The Juina kimberlite cluster is found in the Parecis basin horst region.

The Paccas Novo graben, Colorado graben and Caibis graben found in Amazonian craton do not host any kimberlites. The Amazonian kimberlites are mainly associated with rifts, arcs, horst and graben associated with Paleozoic Parecis basin structural reactivation as we notice the NW Pimenta Bueno graben kimberlites are emplaced at 232 to 242 Ma whereas the SE end of the Pimenta Bueno graben kimberlites (Paranatinga kimberlites) were emplaced at 120 Ma. The Juina (95 Ma) kimberlites are found on the horst structures of the Parecis basin border. The Arco do Rio Guapore found to the SW border of the Parecis basin hosts kimberlites with emplacement age of 267.8 Ma (Concordo-1). In nutshell the structural reactivation of Parecis basin from 267.8 Ma to 95 Ma have resulted in the different kimberlite clusters. NW of Parecis basin the kimberlites are emplaced where there are NE-SW flexures. The last group of kimberlites is associated with NE trending Madeira lineament.

Chapter 9

Aeromagnetic Characterization of Brazilian Structures and kimberlite along Corridor-125

The aeromagnetic survey has been a distinguished geophysical survey method due to its rapid rate of coverage and low cost per unit area explored. The main purpose of magnetic survey is to detect rocks or minerals possessing unusual magnetic properties that reveal themselves by causing disturbances or anomalies in the intensity of the earth's magnetic field. Airborne geophysical surveying is the process of measuring the variation of different physical or geochemical parameters of the earth such as distribution of magnetic minerals, density, electric conductivity and radioactive element concentration. Aeromagnetic survey maps the variation of the geomagnetic field, which occurs due to the changes in the percentage of magnetite in the rock and reflects the variations in the distribution and type of magnetic minerals below the earth surface and measure variations in basement susceptibility. Local variations occur where the basement complex is close to the surface and where concentration of ferromagnetic minerals exists.

Key functions of aeromagnetic survey and interpretation is to quantitatively map the magnetic basement structures beneath sedimentary cover. Depth to source interpretation of magnetic field data provides important information on study area architecture for exploration and for mapping areas where the mineralization is at a depth suitable for economic exploitation. Apart from this, aeromagnetic survey and interpretation is handy tool in determining the structural framework of the area which is hidden by cover sediments, thrusts and other geotectonic elements. All methods used to estimate depth to magnetic source benefit from discrete, isolated source bodies of appropriate shape and moderate to strong magnetization. The process of determining the location and depth of a source from gridded potential field data begins with the construction of a function from the data such that the function peaks over the source. Examples of such functions is the analytic signal amplitude (ASA) The objective of most magnetic field survey is to produce images for qualitative geological interpretation and gridding is often optimized to reduce noise in the images of Total Magnetic Intensity (TMI) or its enhancement, such as the ASA. Image processing of the grids enhances details and provides maps that facilitate interpretation by even non-specialist.

Aeromagnetic method being a faster economical and versatile geophysical tool may help reveal both large and small scale features, including differences in basement type, magnetic intrusion, volcanic rocks, basement surface and fault structures.

Kimberlite rocks have characteristic conical or carrot shape or champagne glass shaped vertical bodies and are termed as pipes. The magnetic signatures of kimberlite pipes are due to its contrasting magnetic properties with that of the background country rock into which they have been intruded.

Several geophysical methods are utilized to characterize or generate targets for the kimberlite pipes such as the magnetic method (Sarma et al., 1999; Keating and Sailhac, 2004), electro- magnetic (Smith et al., 1996), and gravity method (Vasanthi and Mallick, 2005) during regional exploration for kimberlites worldwide. The magnetic method is widely utilized to characterize the kimberlites where a conical geometry with steeply dipping walls and diminishing diameter with depth (Skinner, 1986) forms the basis of the study. Kimberlite pipes are moderately to strongly magnetized, with susceptibilities in the range from 1 to 80×10^{-3} units SI (Power et al., 2004). Variation in the observed magnetic response arises due to weathering, chemistry and content of magnetic minerals, depth, erosion level, and remnant magnetization, as well as the orientation and intensity of the inducing field. The conductivity of a kimberlite is also variable because it depends upon porosity, chemical composition, depth, weathering, alteration, and contrast with background.

The Kimberlite pipe signature from an air-borne survey in low magnetic latitudes may be complex (Keating and Sailhac, 2004) as is the case with Brazil. In high magnetic latitudes, the anomaly signatures are circular. At equator, the signatures become negative. To overcome the complex magnetic signatures of kimberlite pipes in low-latitude regions, several enhancement techniques, such as gradient (vertical, horizontal) and analytic signal, are used (Cowan et al., 2000). These techniques can rectify and produce expected circular signature of a kimberlite pipe.

This research work is aimed at evaluating and determining the basement structures controlling the kimberlite emplacement and its corresponding geodynamic events along corridor-125. Based on the geodynamic evolution, two geological domains (Amazonian and

Extra-Amazonian Regions) were identified and evaluated from the geophysical data with its corresponding assemblages of contrasting rock types, as well as different regional structures identified in this study. These domains are interpreted to be markedly separated by thrusts. A digitized aeromagnetic data of covering major part of Extra-Amazonian and small part of Amazonian region from CPRM, the Geological Survey of Brazil, airborne geophysical series (1000) were employed to determine the locations of Kimberlites and to interpret the structural framework.

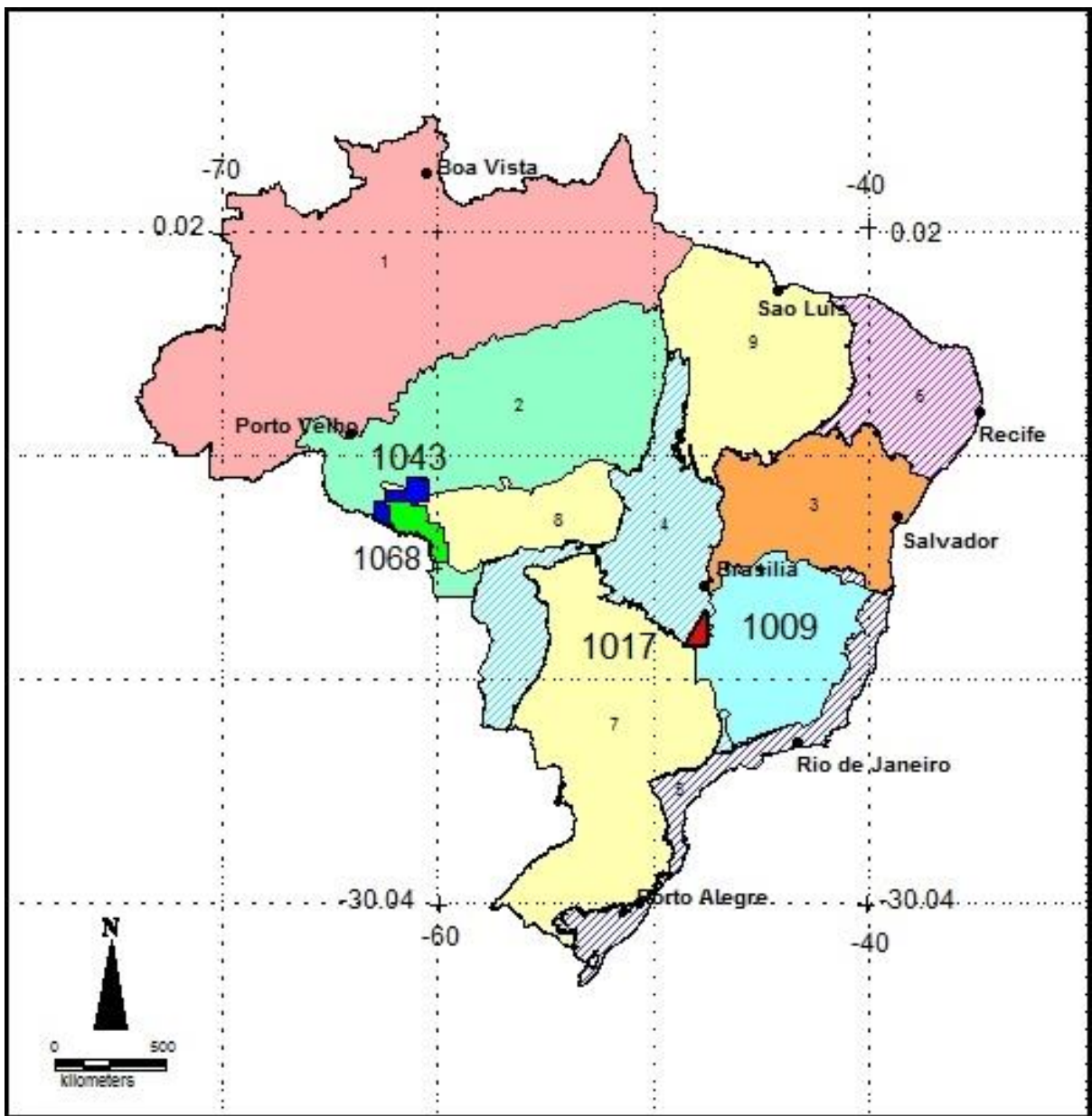


Fig.12: Aeromagnetic projects location map. The region in sky blue is the project 1009, the region in bright green is the project 1068, the region in blue dark blue is project 1043 and the region in red is the project 1017. Background regions represent structural provinces.

Aeromagnetic Data:

Aeromagnetic data for four projects were obtained from CPRM spread out into two regions of the corridor-125 as shown in Fig.12. These projects are named as

- Serra dos Parecis aeromagnetic project-1043 of Amazonian Region,
- Southeast Rondonia aeromagnetic project-1068 of Amazonian Region,
- APIP aeromagnetic project-1017 of Extra-Amazonian Region and
- CGBA aeromagnetic Project-1009 of Extra-Amazonian Region.

The data used in the present work from Extra-Amazonian region is based on results of aeromagnetic surveys carried out in the study area. The earliest of these, known as Project 1009, refer to surveys carried out during 1971 and 1972 as part of Geophysical agreement between Brazil and Germany. The Proton precision magnetometer Model L-803 with a bird sensor hung by a cord around 25m in length to the Aerocommander aircraft was utilized for the aeromagnetic survey. The results of this survey, acquired initially in analog form, were later digitized by Paterson, Grant & Watson Ltd. (PGW) and Western Mining Company (WMC). These digital data sets, made available for academic research by Company of Mineral Resources Research (CPRM), were acquired for purposes of the present work. The nominal flight height for data acquisition was 150m and spacing of flight lines was 2 km. The preferred direction of survey lines of this project was East-west. In the pre-processing stage, necessary corrections and merging were carried out.

The Data from project-1017 was surveyed using proton precision magnetometer Model G-803 with the sensor mounted at the tip of the tail as stinger to Aerocommander 680F aircraft. The digitized data in the form of xyz format with nominal flight of 150m and line spacing of 2km apart; survey line direction NE-SW was acquired from CPRM for interpretation and analysis in this work. This data was later unified with GIS platform for final interpretation after processing separately.

The data from Amazonian region is based on results of aeromagnetic surveys carried out in the study under the name Project 1043 and 1068, refer to surveys carried out during 1979 (project 1043) and 2006 (project 1068) as part of Geophysical Surveying Program of Brazil. The results were digitally collected data sets, made available for academic research by Company of Mineral Resources Research (CPRM).

For the project 1043, Proton precision magnetometer, Model G -803 with a sensor mounted on the tip of the tail as stinger to the Islander aircraft PT- KNE whose average speed of operation was 220 km / h +/- 10 % was used to carry out the survey.

In case of Project-1068, two aircrafts with magnetometers were utilized namely,

- a. The PR-PRS Aircraft was fitted with optically pumped cesium-vapor magnetometer model G-822-A, with a resolution of 0.001 nT and operating range of between 20,000 to 100,000 nT. It was mounted at the tip of the tail of the aircraft as stinger type. The received signal passes through a preamplifier located in the cone base tail of the aircraft and sent to the compensator integrated system to other data RMS acquisition system / DGR33 PDAS 1000. Readings of gross magnetic field and offset are made every 0.1 seconds, which is equivalent to the speed 280 km / h of the aircraft, approximately 7.8 meters on the ground;
- b. E-FZN Aircraft was fitted with Scintrexcesium-vapor magnetometer model CS-2, with 0.001 nT resolution and operating range of between 20000-100000 nT. It was mounted on the tip of the tail of the aircraft- stinger type. It received signal via preamplifier located at the base of the tail cone of the aircraft and sent to the system acquisition / aeromagnetic compensation contained in FASDAS system. Readings of gross and offset magnetic field are made every 0.1 seconds, which is equivalent to the speed of 280 km / h of the aircraft, approximately 7.8 meters on the ground.

The nominal flight height for data acquisition was 150m and spacing of flight lines was 2 km. The preferred direction of survey lines of this project was North-South. These data sets were processed separately and the results were studied separately.

Geological Context of the Study Area

The Corridor-125, Brazil is situated between 10 degrees and 20 degrees in the Southern Hemisphere which corresponds to low magnetic latitude. Hence, the magnetic signatures of the kimberlites are affected by typical low-magnetic latitude characteristics.

Accordingly, due care is taken by incorporating necessary enhancement techniques in the interpretation of the data.

The Extra-Amazonian region forms part of the paranapanema and São Francisco craton. The paranapanema craton is currently represented by the Parana basin margin in the study area. The APIP project study area comprises thrust zone as a result of collision of the two cratons and further tectonically reactivated into Brasiliano mobile belt. The Easter boundary of the Brazil is result of extensional tectonics due to rifting from South Africa around 120 Ma. This area consists of basement rocks of Archean age outcrop mainly in the southern and southeastern parts. Isolated blocks have also been identified in the northwestern parts. Most of the remaining area is covered by metamorphic complexes of Proterozoic age. Phanerozoic sediment cover occurs over Southern part of the study area. A characteristic feature of this province is the presence of a significant number of alkaline magmatic intrusions of Cretaceous to Tertiary period.

Seismic studies have shown that the crustal thickness is around 40km (Assumpção et al, 2004) in São Francisco craton and 32 to 42 km in Brasilia belt and adjacent areas. The Ribeira belt to the southeast is estimated to have a crustal thickness of 37km (Assumpção et al, 2004).

The projects 1043 and 1068 forms part of the Amazonian region of the study area. The Amazon region along Corridor-125 is an amalgamation of various blocks with suture zone (Guapore Suture at south western boundary), Parecis rift basin, Nova Brasilândia tectonic belt and thrust zone (Upper Paraguay thrust). Further, western boundary of the South American platform has been affected by the Nazca plate subduction. Accordingly there are different sets of geophysical lineaments characteristics, some expressing themselves on the surface geology and others masked by younger sediment cover. An investigation of these geophysical projects throws insight into different lineaments and its control on kimberlite occurrences. Amazon region has very few outcrops of Archean basement rocks and majority of the region is covered by Phanerozoic to recent sediment cover. A characteristic feature of this province is the presence of a significant number of alkaline magmatic intrusions of Permo-Triassic and Cretaceous period. Kimberlites are also part of this Permo-Triassic magmatism.

Data Processing Techniques

The bulk of aeromagnetic data processing in the present work was carried out using the computer software package Geosoft Oasis Montaj version 8.4.1. Built-in facilities of this package allowed homogenization of the database and elaboration of maps, making use of standard procedures of interpolation, gridding, and plotting methods. The package was also used for setting geographic coordinates, which in the present work are referenced to as the datum WGS84 and its corresponding UTM zones.

The next step in data processing has been removal of the International Geomagnetic Reference Field (IGRF) from the records of the total field. This has been an important part of data processing in view of the significant time differences in data acquisition and the large area extent of the surveys. The built-in IGRF reference fields corresponding to the year of data collection, available in the software package Geosoft Oasis Montaj utilized. The removal of the field originating in the core of the Earth and the external variations occurring mainly in the ionosphere and the sun allows derivation of the field of crustal origin. This crustal field was corrected for *heading* and incorporated into an ensemble of corrected data sets. Filters were then applied to correct directional trends. In addition, leveling and microleveling corrections were carried out to eliminate distortions of flight lines. The results obtained at this stage were used in deriving the map of the Total intensity magnetic field of the study area.

Interpretation of the Results

Further analysis and interpretation is carried out by the following techniques namely upward continuation, Analytical Signal, Reduced to Magnetic pole, Euler Deconvolution techniques and keating coefficient for each of these four projects separately.

Euler Deconvolution Technique: employed in this work has the objective of extracting information about the depths of magnetic sources. The result is independent of the direction and inclination of the main magnetic field and the orientation of the magnetic sources. Thus, the method is relatively insensitive to small-scale distortions of the field. A total magnetic anomaly (T) without correction of regional values produced by a set of three-dimensional sources satisfies the homogeneous field equation of Euler:

$$(x - x_0) \frac{\partial T}{\partial x} + (y - y_0) \frac{\partial T}{\partial y} + (z - z_0) \frac{\partial T}{\partial z} = N (B - T)$$

Where x_0 , y_0 , and z_0 are the initial coordinate positions of the anomalous source, B is the regional magnetic field and N is the structural index (Reid et al, 1990).

In the practice the variations in the degree of homogeneity of the field are associated with a set of structural indices, which specifies the type of magnetic source. According to Thompson (1982) a structural index of zero represents contact between different types of rocks, while index of 1 represents linear features such as faults and dykes. Also, the structural indices 2 and 3 are indicative of cylindrical and spherical structures, respectively.

The results obtained indicating the depths of sources are plotted in a map by using the kriging interpolation method, with a specified grid size. Any differences or similarities are indications that the systematic differences/similarities in the depths of magnetic sources arise from mechanisms related to the thermal regime of the crust.

Analytic Signal technique: used in interpretation of aeromagnetic data is basically the magnitude of the second derivative in the three directions of the magnetic field. For a vertical cylinder, the shape of analytical signal is independent of field orientation and remanence and always results in a compact, almost circular anomaly (Nabighian, 1972). In practice, the analytical signal is regarded as the best tool for locating the edges of bodies that have magnetic contrast. When applied to the residual field magnetic anomaly the responses highlight the surface boundaries of geological bodies with contrasts in magnetic properties relative to the surrounding rocks. Hsu, 2002, suggests use of second and even higher order derivative to better highlight the bodies. However, higher orders enhance the noise leading to unrealistic solutions, especially when dealing with low quality data sets.

Therefore, two advantages exist in using the analytic signal to identify magnetic anomalies from kimberlite pipes: first, it is independent of remanence; second, as it will be shown, it performs well at low magnetic latitudes. Such a compact circular or nearly circular anomaly is known as bull's eye anomaly.

Reduction to Magnetic Pole technique: In this method, the magnetic anomaly is transformed to its signature at the magnetic pole with vertical magnetic inclination. The magnetic anomaly becomes independent of the direction of the original field. This method transforms the magnetic field of the observed anomaly to its probable result of vertical field inclination measured at magnetic pole (Nabighian et al., 2005). This transformation converts the bipolar anomalies to monopole ones. However, in the presence of remanent magnetization the processing is not clear conversion to monopole anomalies (Shurbet et al, 1976; Schnetzler and Taylor, 1984; Roest and Pilkington, 1993) especially when the field of remanent magnetism is different from the current regional magnetic field.

Once, the interpretations are carried out individually for the projects. For easy visualization and analysis, Grid knitting-Suture Technique was used for the Extra-Amazonian region data. This method enables the joining of two separate fabrics turning them into a single mesh. In this technique, the meshes are joined one by one until all five loops form a single fabric end. This is transformed into a database using the Sample Grid procedure, which is also a function of Oasis Montaj™, version 8.4.1. Proper homogenization was not achieved by Grid knitting-Suture technique for the Amazonian Region Data and hence, were overlaid on each other in GIS platform for better visualization and analysis.

RESULT AND DISCUSSION

Discussion -Anomalous/Total Magnetic Intensity Field Map

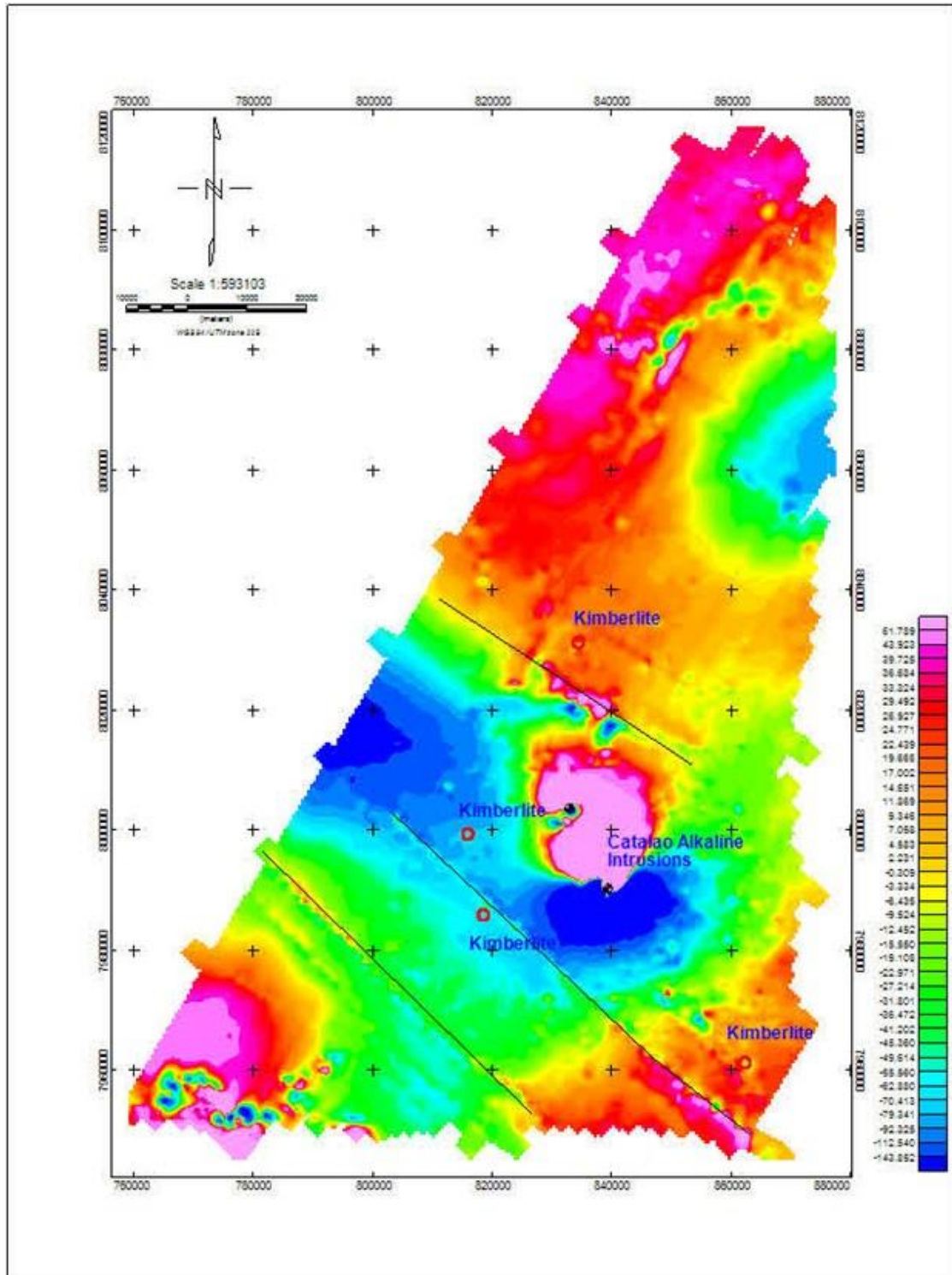


Fig.13: 1017_Total magnetic intensity anomaly Map with lineaments, alkaline intrusives (Catalao I and II). The magnetic intensity are in nT.

1017 Project: TMI map (Fig.13) shows central region with dipole magnetic anomalies due to alkaline intrusions present in the area. The kimberlites are found intruded around this central alkaline region. But no significant clear anomaly is seen on this map. The magnetic signature of the larger diameter alkaline intrusion masks the kimberlite occurrence. Another major characteristic feature noticed is the weathering zone of the alkaline intrusive. These alkaline intrusives are Catalão I and Catalão II. Lack of clear kimberlite signature is also attenuated due to the fact that this study area is in low-latitude region. Structural elements of the region visible are few (three) NW-SE trending magnetic lineaments with linear magnetic signatures.

Project 1009 Total Intensity magnetic Anomaly Map (Fig.14)

This project consists of numerous normal magnetic dipoles spread throughout. Majority of them are due to alkaline intrusives of the region and few of them due to granitoid bodies. The structural elements of the region visible are the NW-SE magnetic lineaments in the south-central region and, NS to NE to NNE in the north and eastern region. The NW-SE magnetic lineaments are the corridor-125 lineaments with magnetic signatures in the Brasilia belt region. The NS to NE to NNE trending lineaments of the northern and eastern region corresponds to Ribeira belt structures. High magnetic anomaly marked as black triangle with no. 5 (Fig. 14) in the south-east is due to the iron-formations. There are few slightly elongated dipoles corresponding with known kimberlites with less clarity to individual pipes. The co-existence of the small diameter kimberlite pipes in comparison to large diameter alkaline intrusions in this area masks clarity in the kimberlite along with low latitude problem. Multiple intrusions, co-existing alkaline intrusion and high weathering are probably the main reasons for the less clarity of the kimberlite signature anomalies.

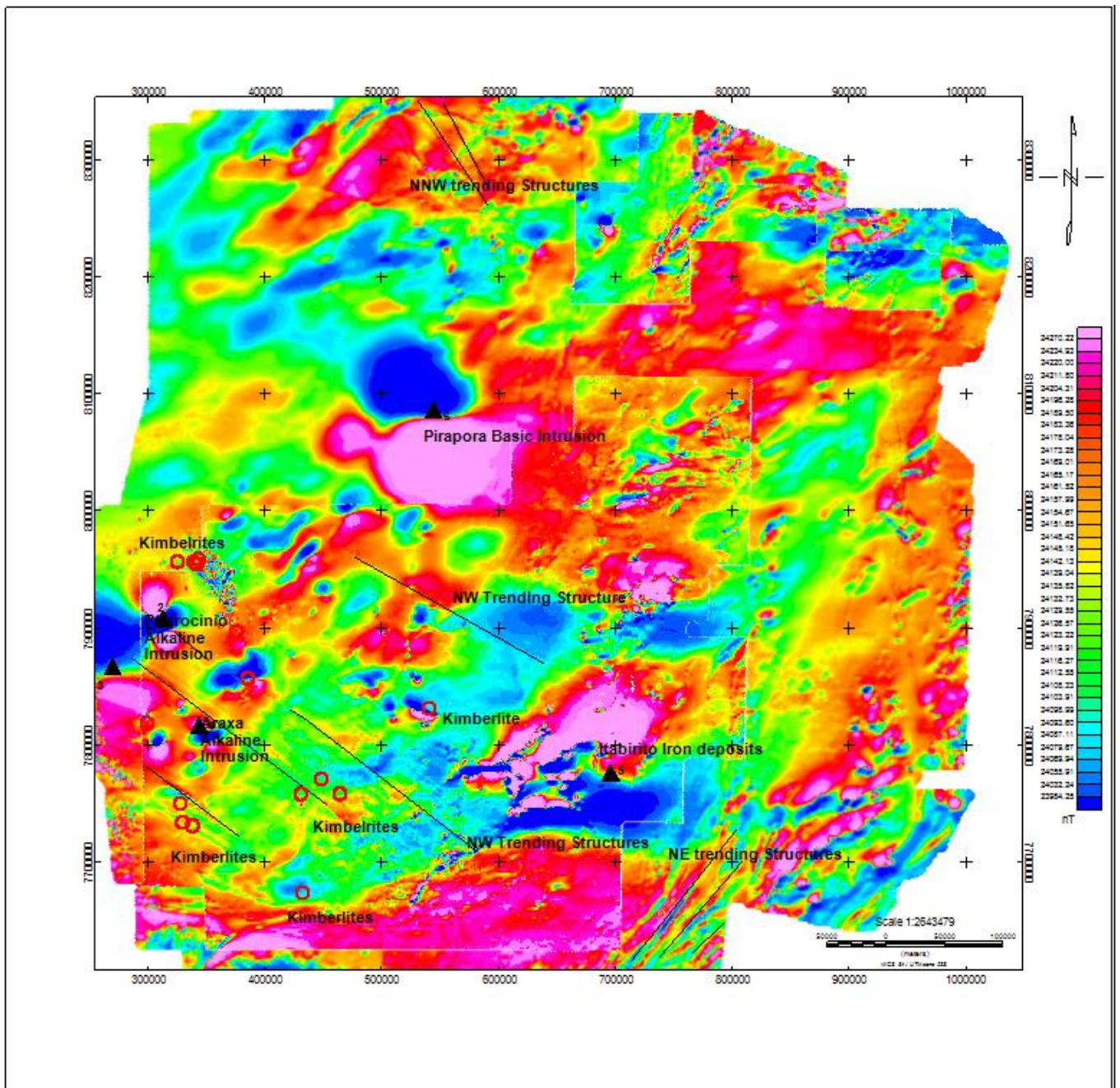


Fig.14: 1009 Total magnetic intensity anomaly Map with magnetic lineaments, alkaline intrusive and kimberlites. The magnetic intensity in nT.

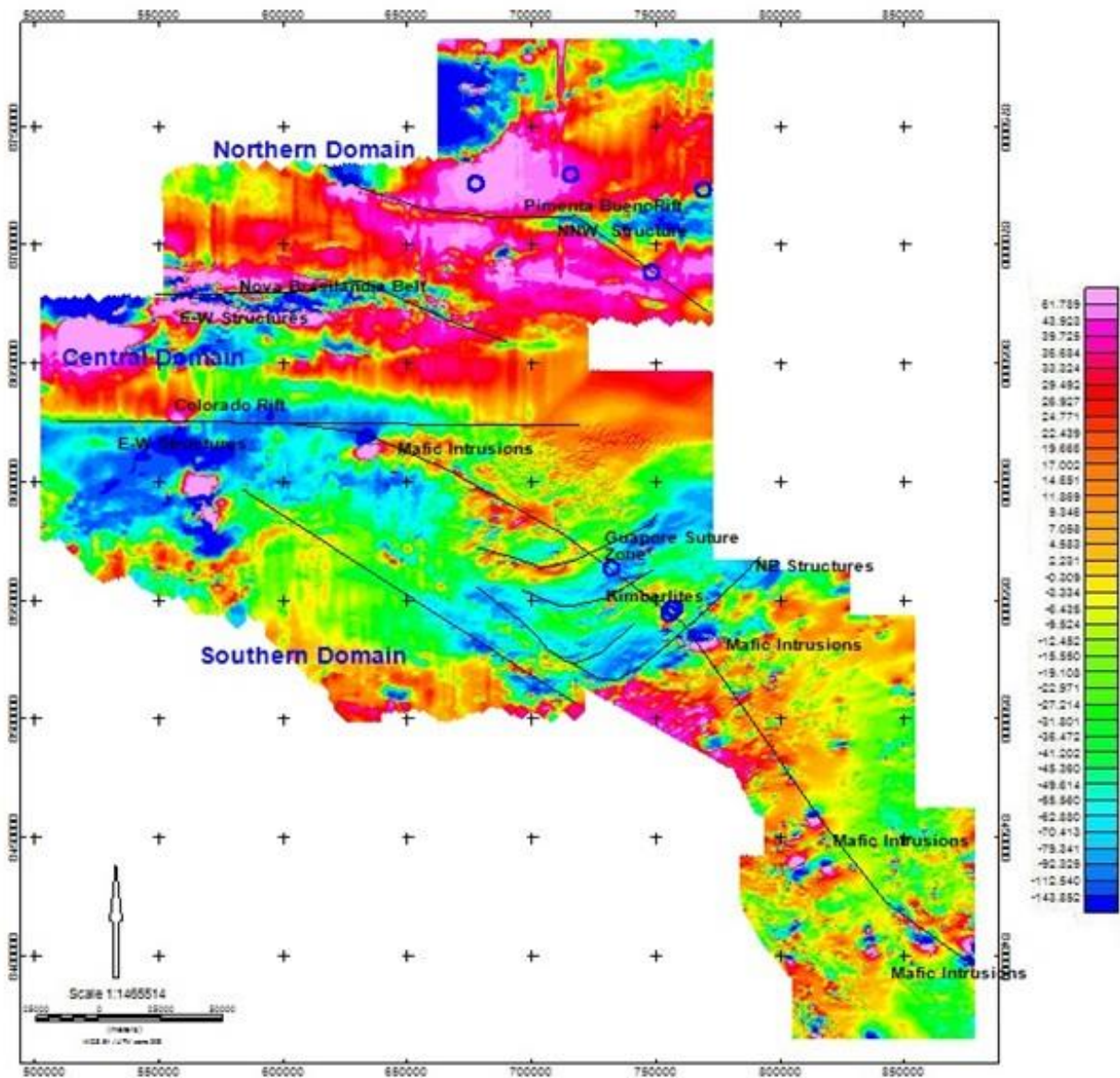


Fig. 15: Amazonian region Total magnetic intensity anomaly map with kimberlite, mafic intrusions, lineaments. The magnetic intensity is in nT units.

The Amazonian region aeromagnetic TMI map (Fig.15): reveals three domains. North of Nova Brasilândia belt region is termed as the northern domain; the region south of Nova Brasilândia up to Colorado rift is the central domain and the region to the southeast of Nova Brasilândia is the Southern domain. The northern domain is characterised by NW Pimenta Bueno rift, high intensity magnetic signatures. The central domain is characterized by E-W trending lineament (e.g. Nova Brasilândia belt, Colorado rift) etc. This domain is also characterized by high magnetic intensity signatures. Few dipole magnetic signatures are seen

along the Guapore suture zone, in Nova Brasilândia belt. Kimberlite dipole signatures are not seen. The characteristic structural features of the central domain are the thrust and NE trending lineaments. The NW trending lineaments (2 in number) to the western margin is also another significant lineament group. These two groups of lineaments along with the thrust zone structure are not seen on the ground which is covered by sediments.

The southern domain is characterized by magnetically quite zone in comparison to the other two zones in terms of structural thrusting high intensity magnetic signatures. Numerous magnetic dipoles corresponding to alkaline and granitoid intrusions are seen along NNW-SSE structure parallel to Guapore suture zone on the western margin of the region.

Discussion -Upward Continuation map

Upward continuation (Fig.16a, 16b and 21) has enhanced the alkaline intrusions with bottom of the depth being deeper and also enhances the magnetic lineaments implying its deeper origin.

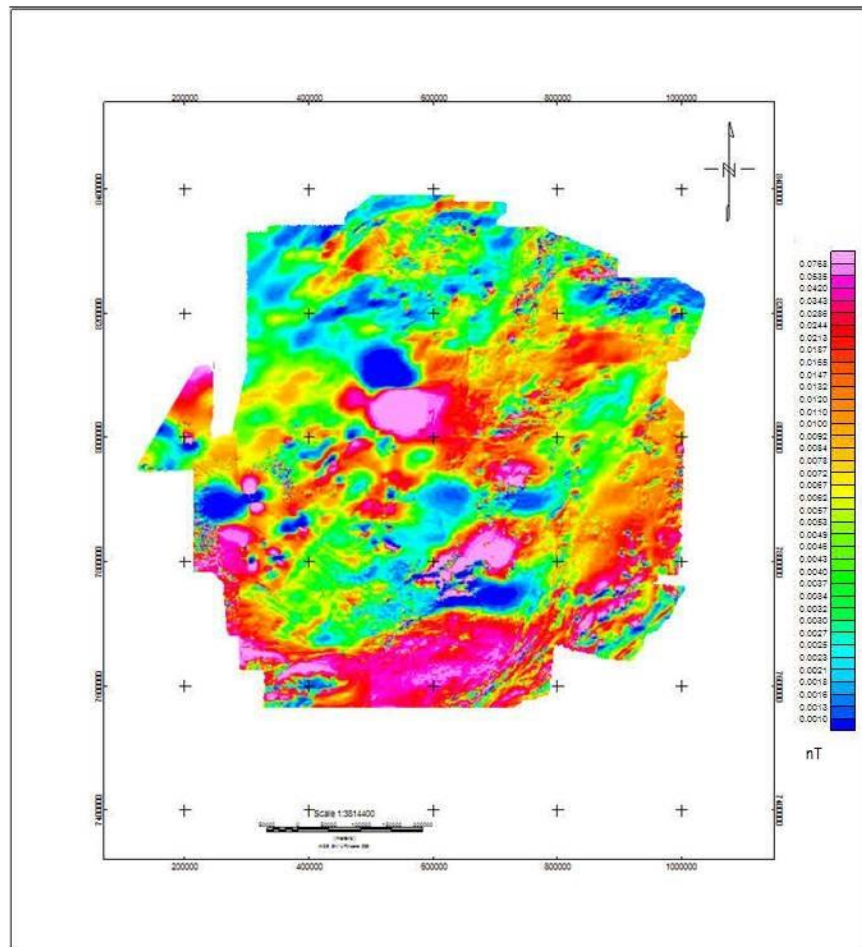


Fig.16 (a): Extra-Amazonian region Total Intensity map filtered to 100m upward continuation

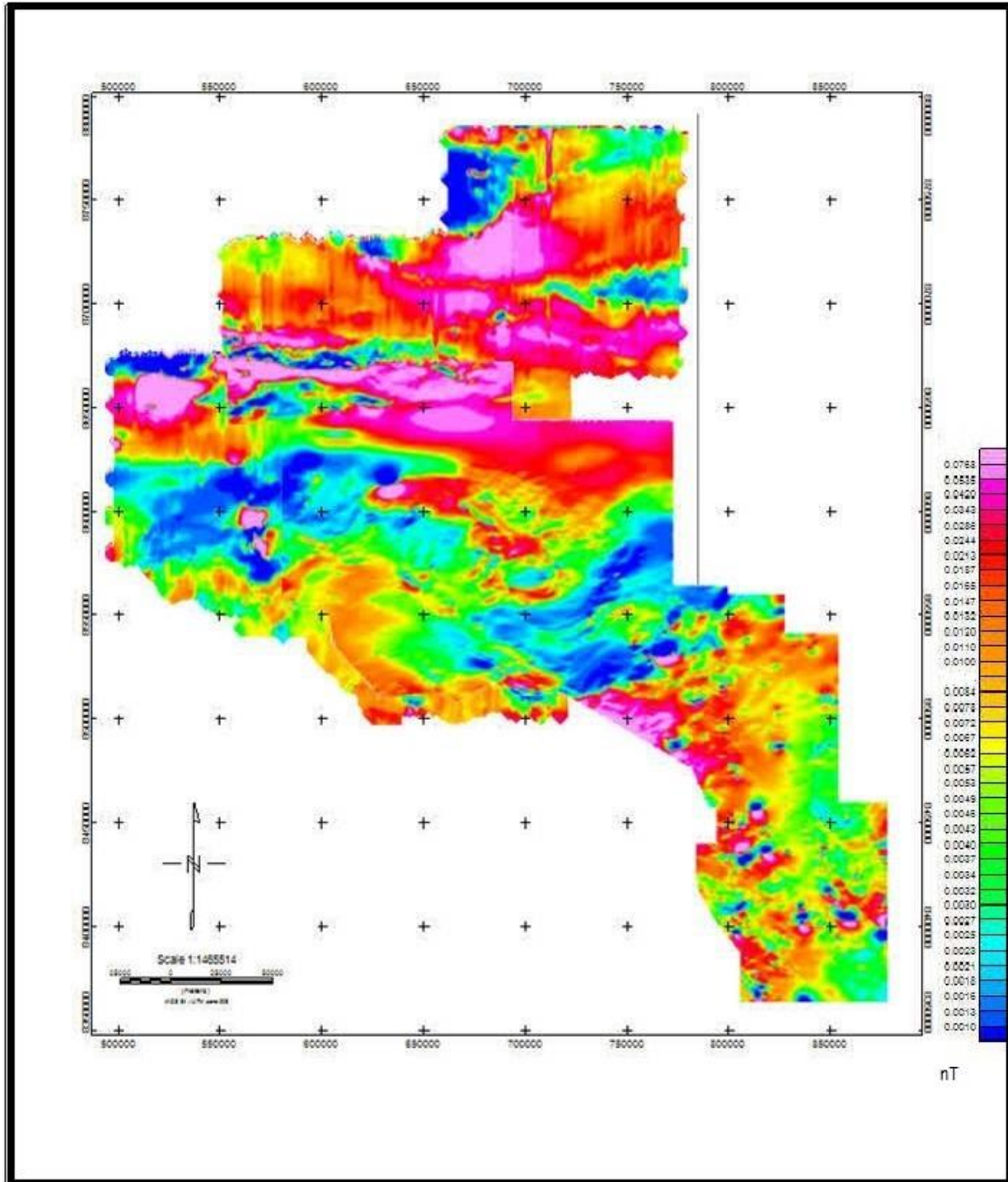


Fig.16 (b): Amazonian region TMI with 500m upward continuation.

On 1068 and 1043 project maps shallow depth magnetic anomalies of mafic and ultramafic intrusions are enhanced along with the linear structural elements corresponding to thrust and crustal shortening seen on the TMI maps. Kimberlite signatures are not clearly identifiable.

Discussion -Reduced to Pole Map

In this map from 1017 and 1009 projects (Fig.17), most of the anomalies seen in the TMI map are transformed to monopoles while few anomalies show distortions and there is no clear visible dipole or monopole. This is especially true with some kimberlite signatures. In the absence of the regional magnetic field the magnetic dipoles would transform into monopoles. The observed non-transformation implies that the presence of remanent magnetisation of the magnetic bodies whose paleomagnetic field direction is different from the current direction of the magnetic field.

The Amazonian region reduced to pole map (Fig. 18) also shows distorted signatures rather than dipoles or monopoles that are seen on TMI map. This implies the presence of remanent magnetization with different direction of magnetic field than the current magnetic field direction.

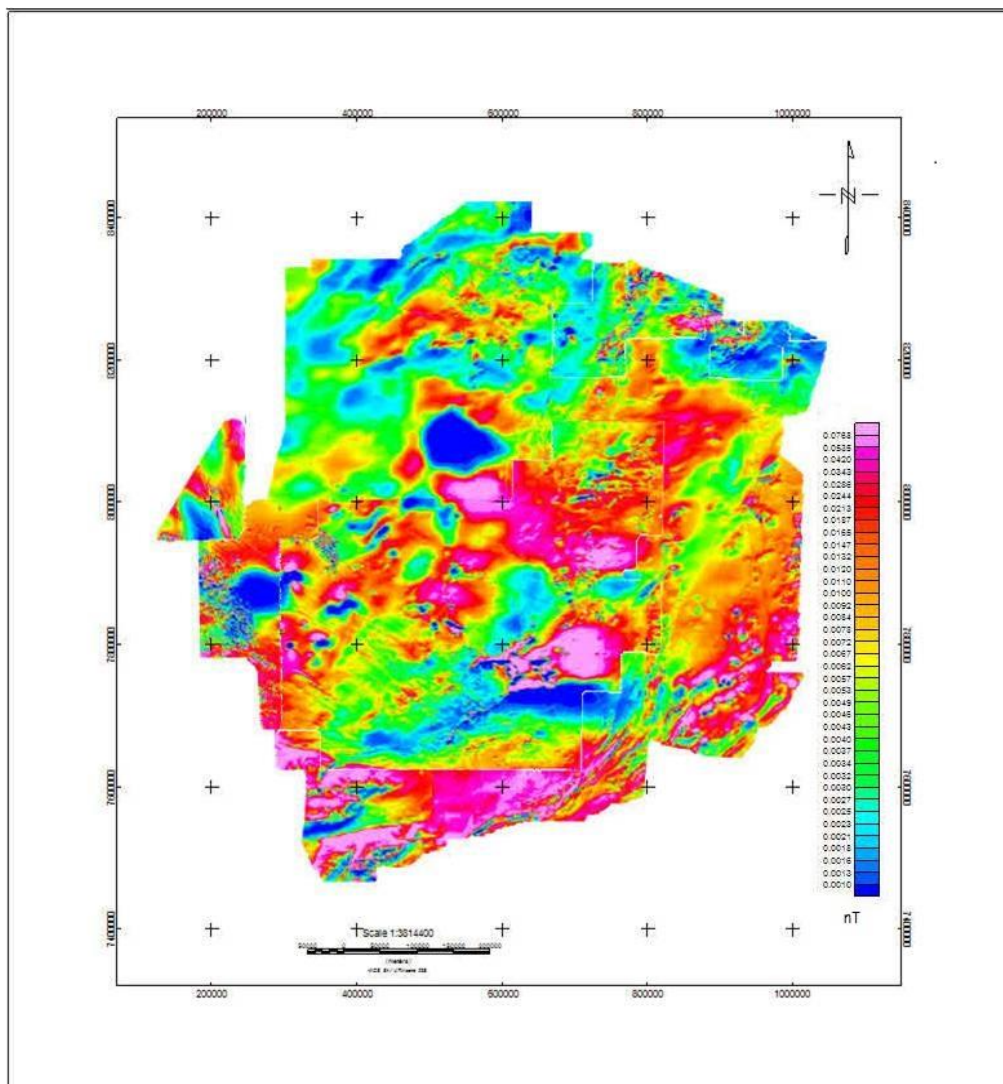


Fig.17: Extra-Amazonian and Amazonian Region Reduced to pole map.

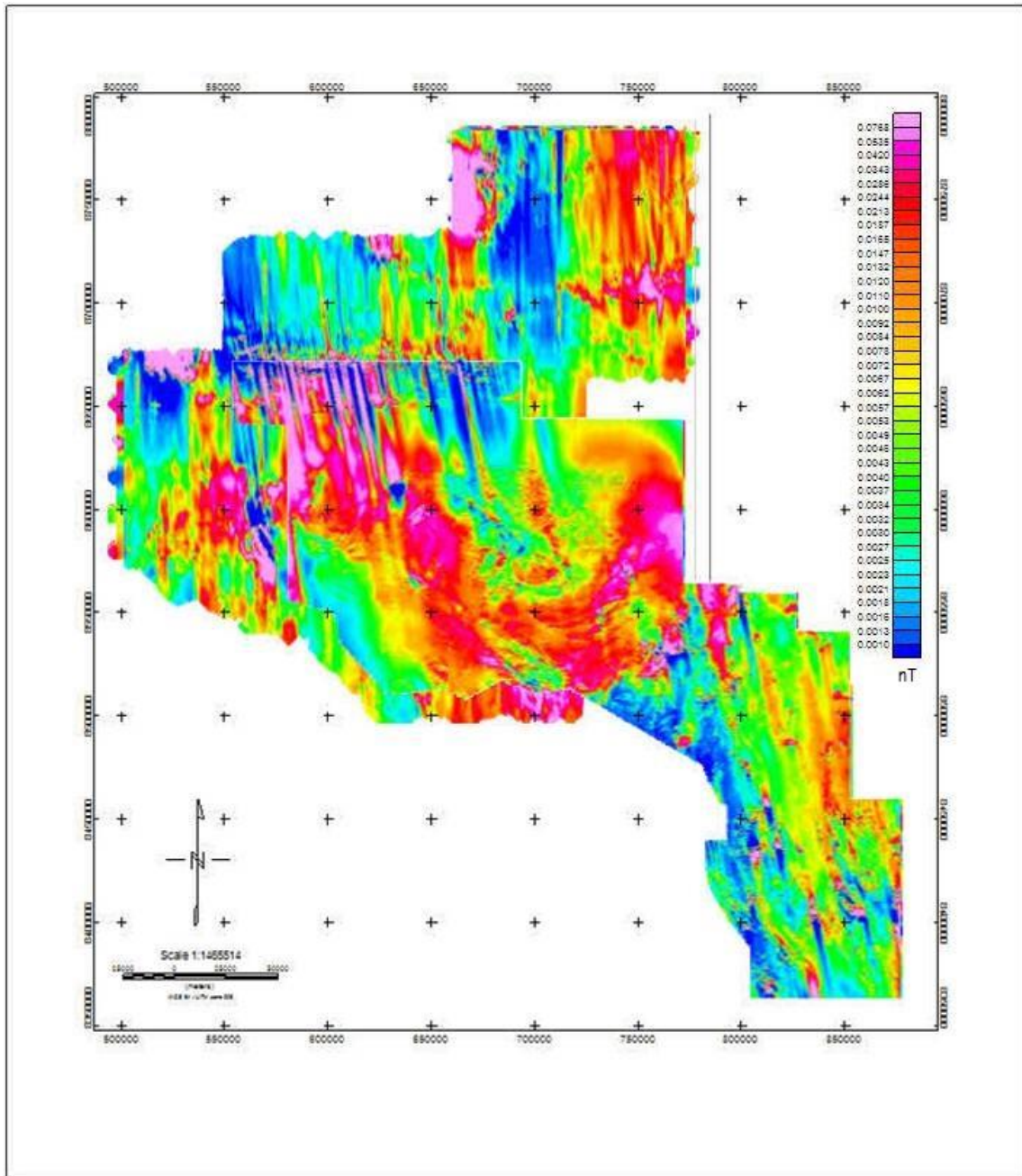


Fig.18: Amazonian Region Reduced to pole map.

Discussion -Analytical Signal Map

The ASA map (Fig19 a, 19b and 20) from projects-1017, 1009, 1043 and 1068 show circular and oval anomalies over mapped alkaline intrusions and even on the few kimberlite pipes. The lineaments seen on the TMI map is more clearly identifiable. New lineaments which not visible on TMI are also seen trending subparallel to the magnetic lineaments seen on the TMI map.

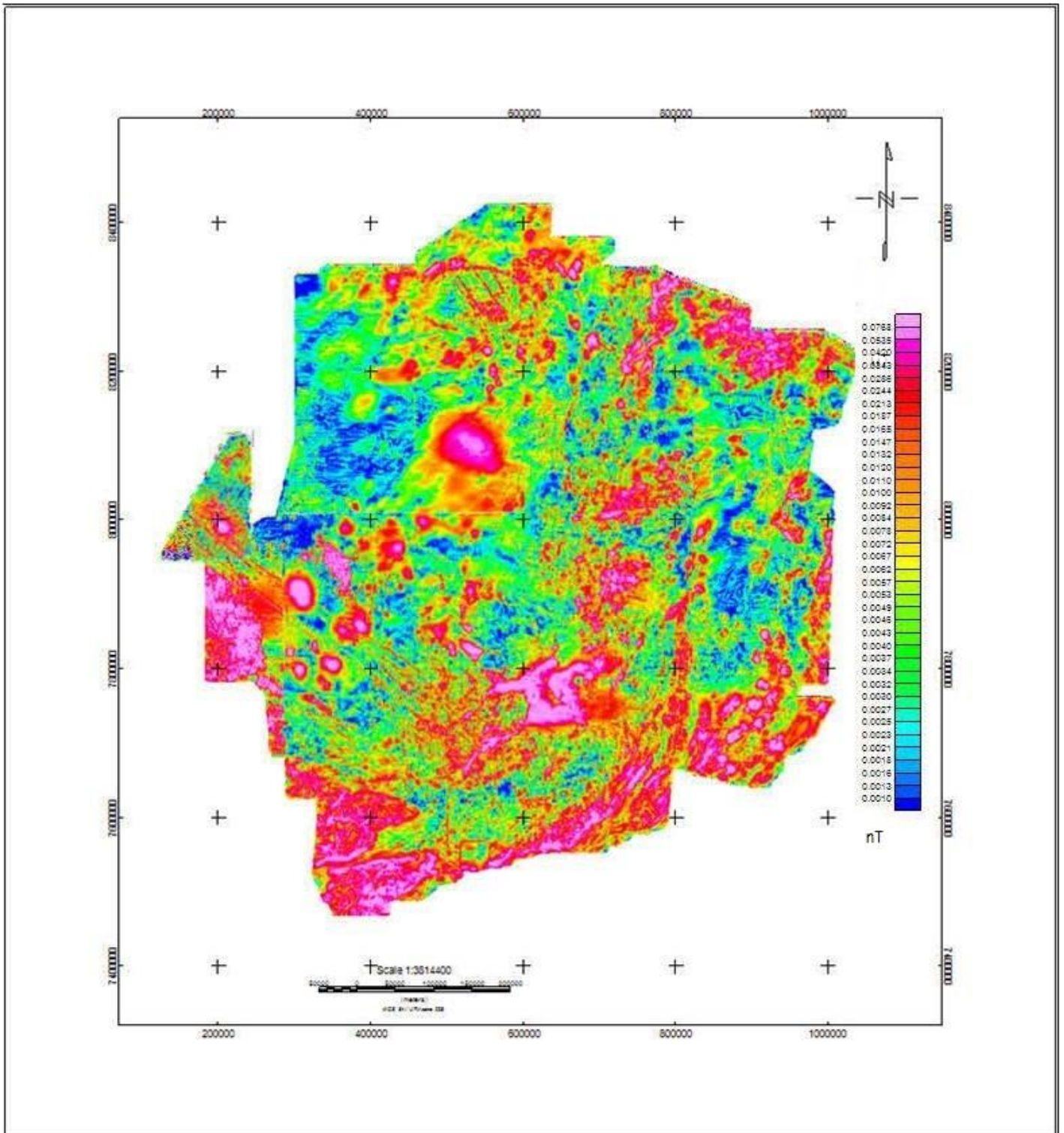


Fig.19a: Extra-Amazonian Region Amplitude of Analytical Signal map.

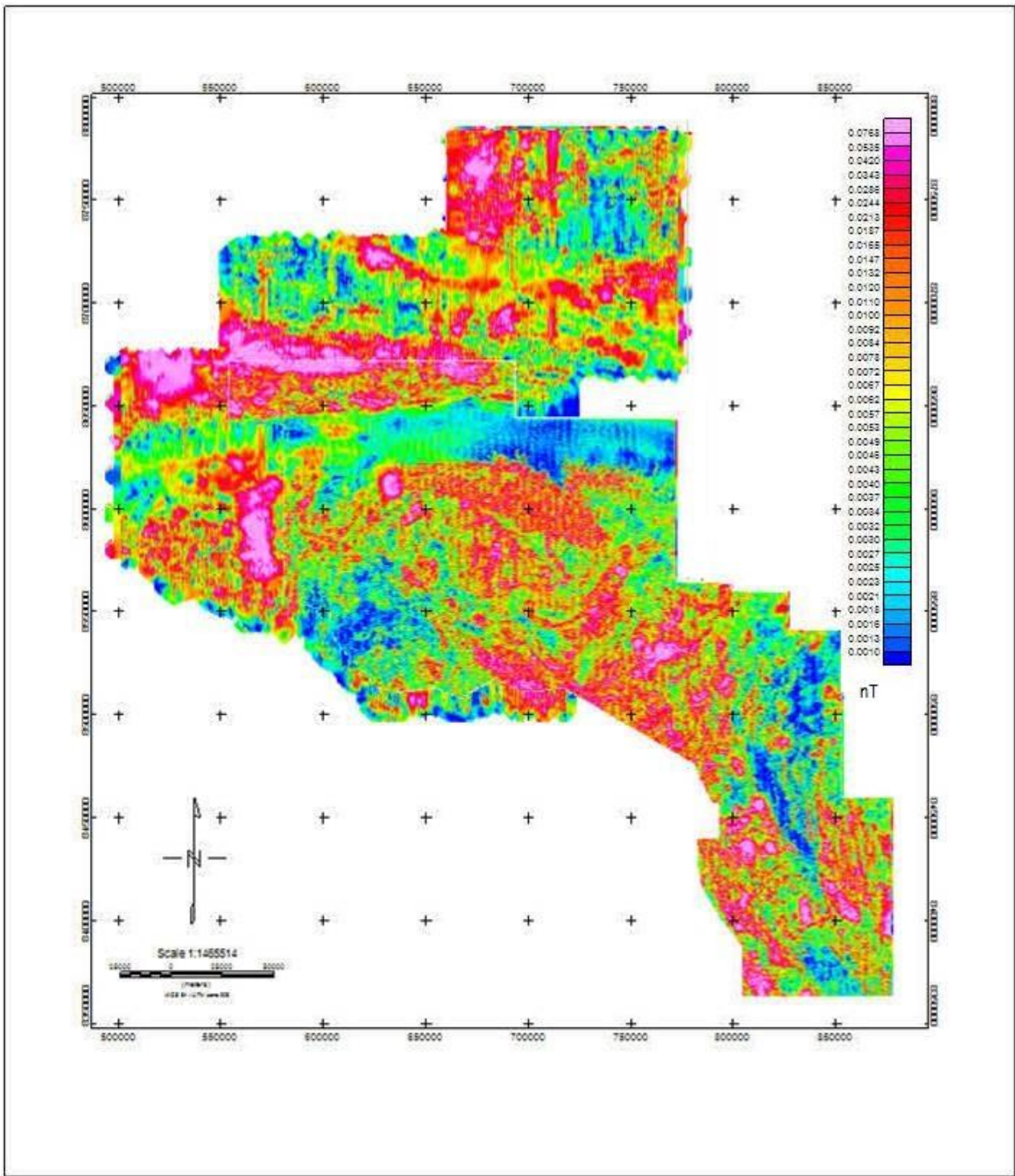


Fig.19b: Extra-Amazonian and Amazonian Region Amplitude of Analytical Signal map.

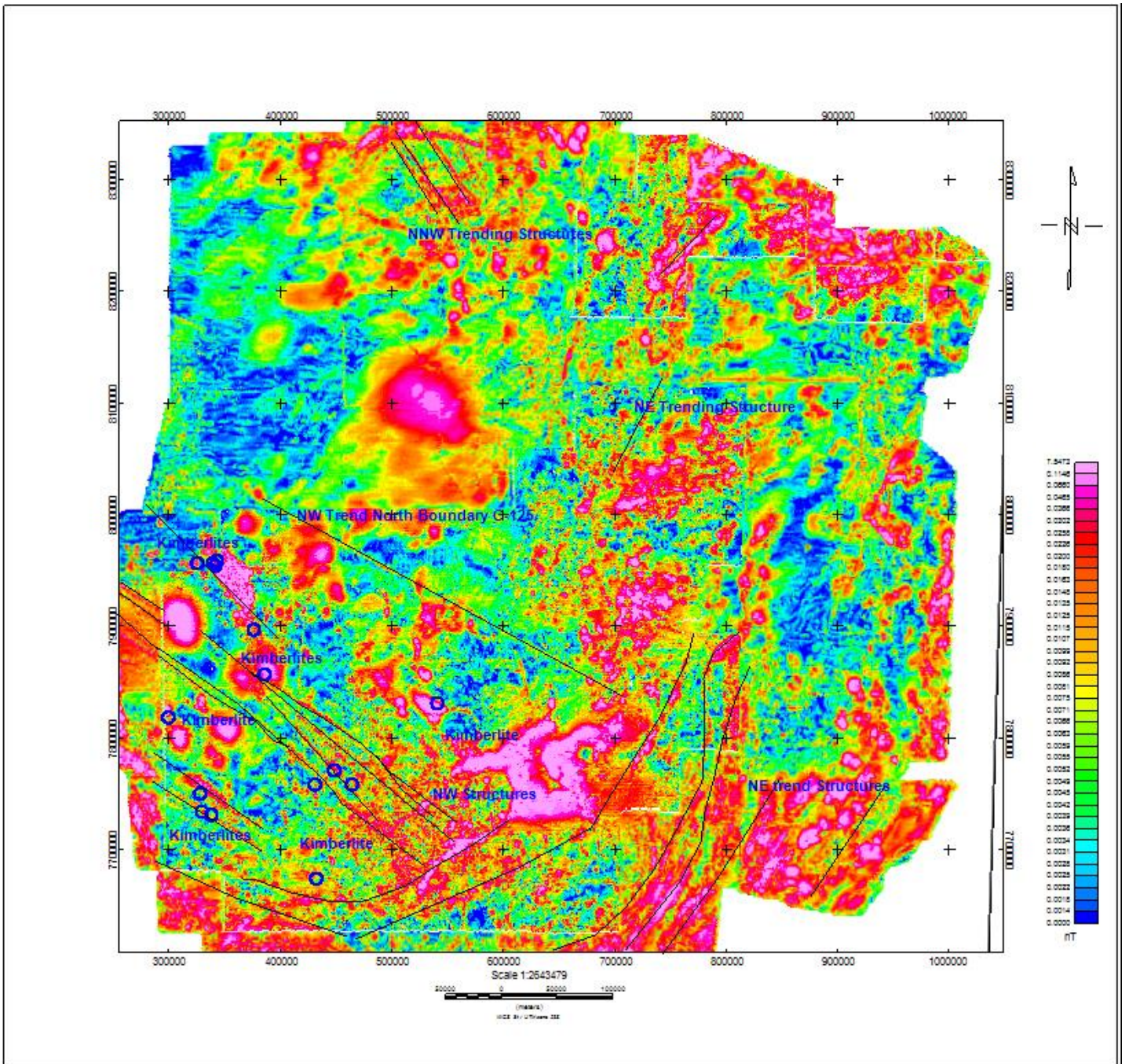


Fig.20: Amazonian Region Amplitude of Analytical Signal map with lineaments, alkaline intrusions and kimberlites.

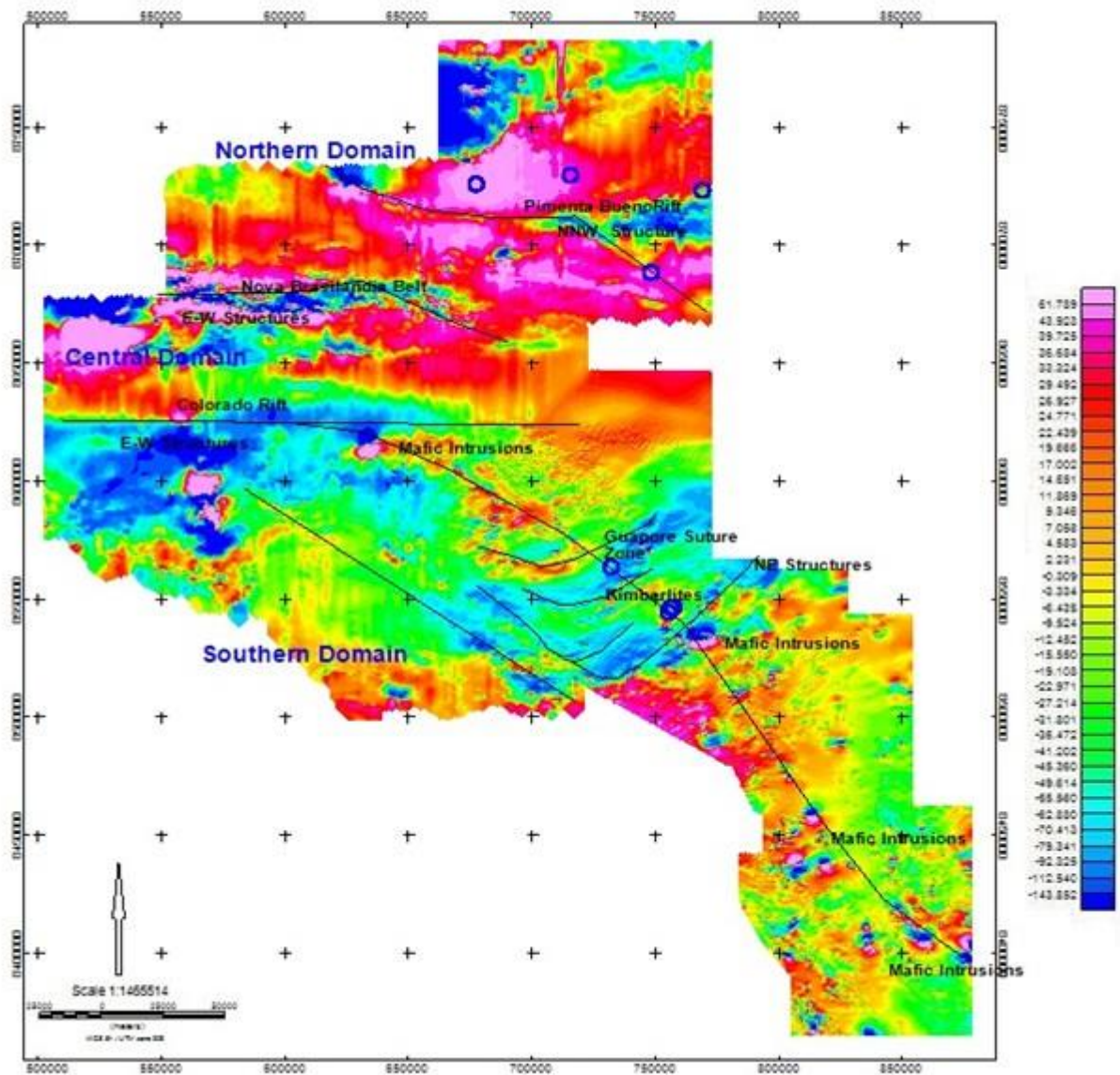


Fig.21: Amazonian Region Amplitude of Upward Continuation map with lineaments, mafic intrusions, kimberlite and other structures.

The Northern boundary of the Corridor-125 on Extra-Amazonian region is demarcated very well by a NW-SE trending magnetic low lineament beyond which there is a non-kimberlite zone. The subparallel NW-SE lineaments are also absent beyond this northern boundary. There are many circular and oval anomalies on this map where no known kimberlites or other alkaline rocks are known. These are probably new circular anomaly bodies for further follow-up. Further analysis if ASA map is correlated with Euler solution index-2 to find potential kimberlite/alkaline body in the region.

Discussion - Euler Deconvolution Map Structural Indices.

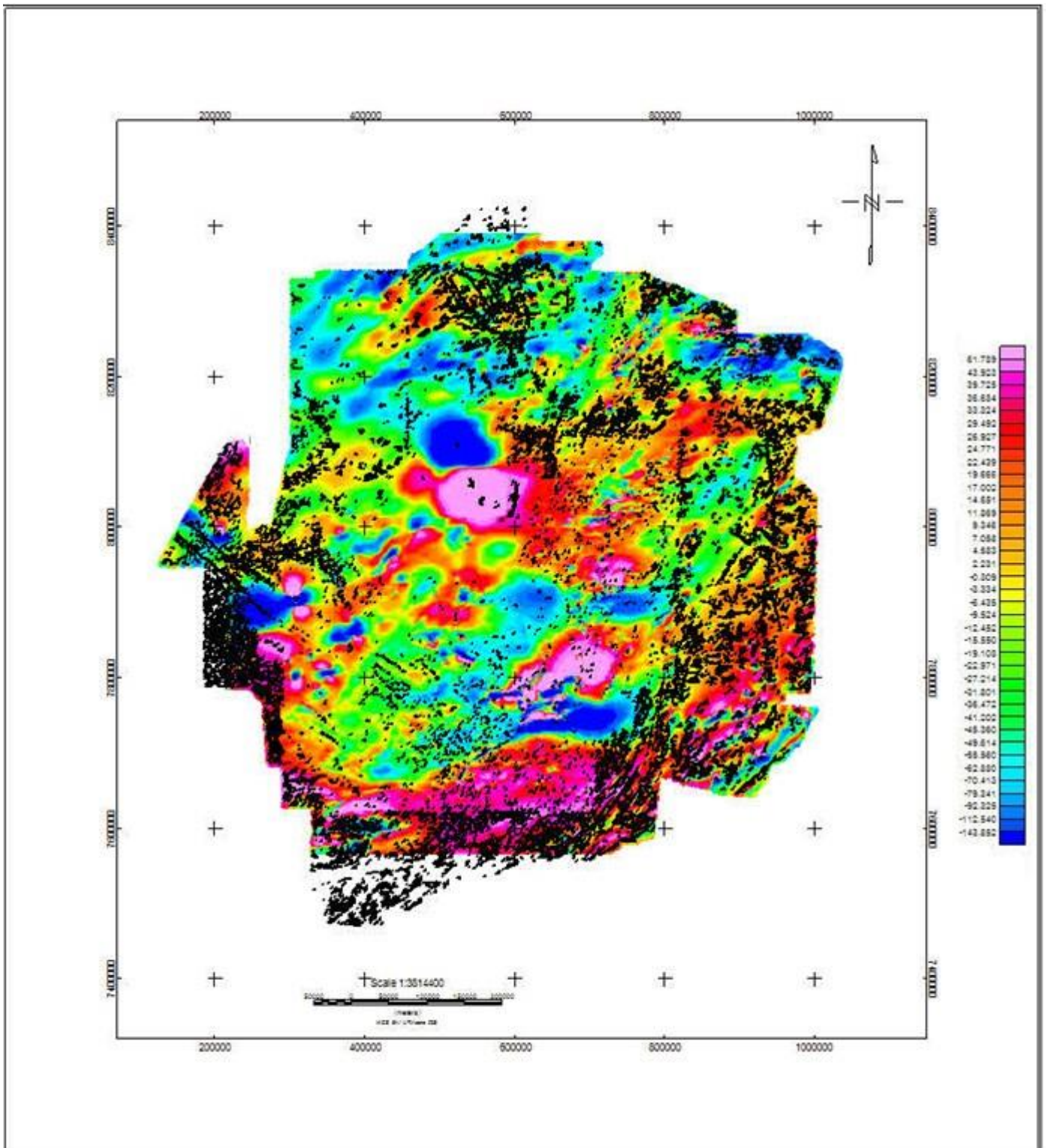


Fig.22: Extra-Amazonian Euler Structural Index-1 Solutions with TMI Map background.

Black dots represent Euler Structural index-1 solutions.

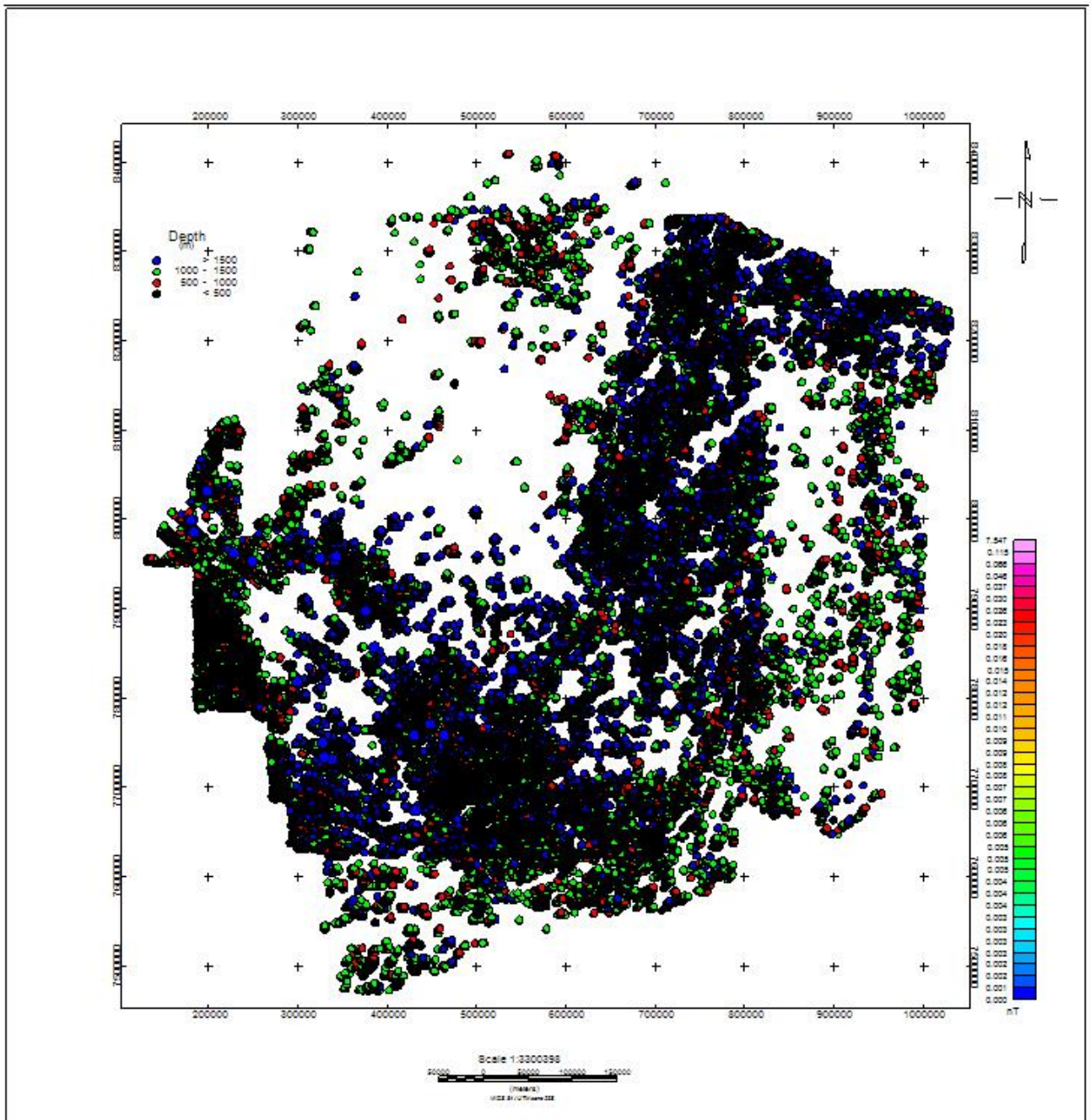


Fig.23: *Extra-Amazonian Euler Structural Index-2 Solutions with Depth range.*

Map corresponding to Euler structural index for magnetics generated shows, significant correlation with the magnetic dipole anomalies, linear structures. The Structural index-2 (Fig.23) representing pipes/ cylinders corresponds very well with few known kimberlites, most of the known alkaline intrusions of the region in Extra-Amazonian Region. Possible new kimberlite targets are also seen with correlating analytical signal and Euler SI-2. The SI-1 (Fig.22) representing linear features correspond well with the basement structures of the region which is not mapped.

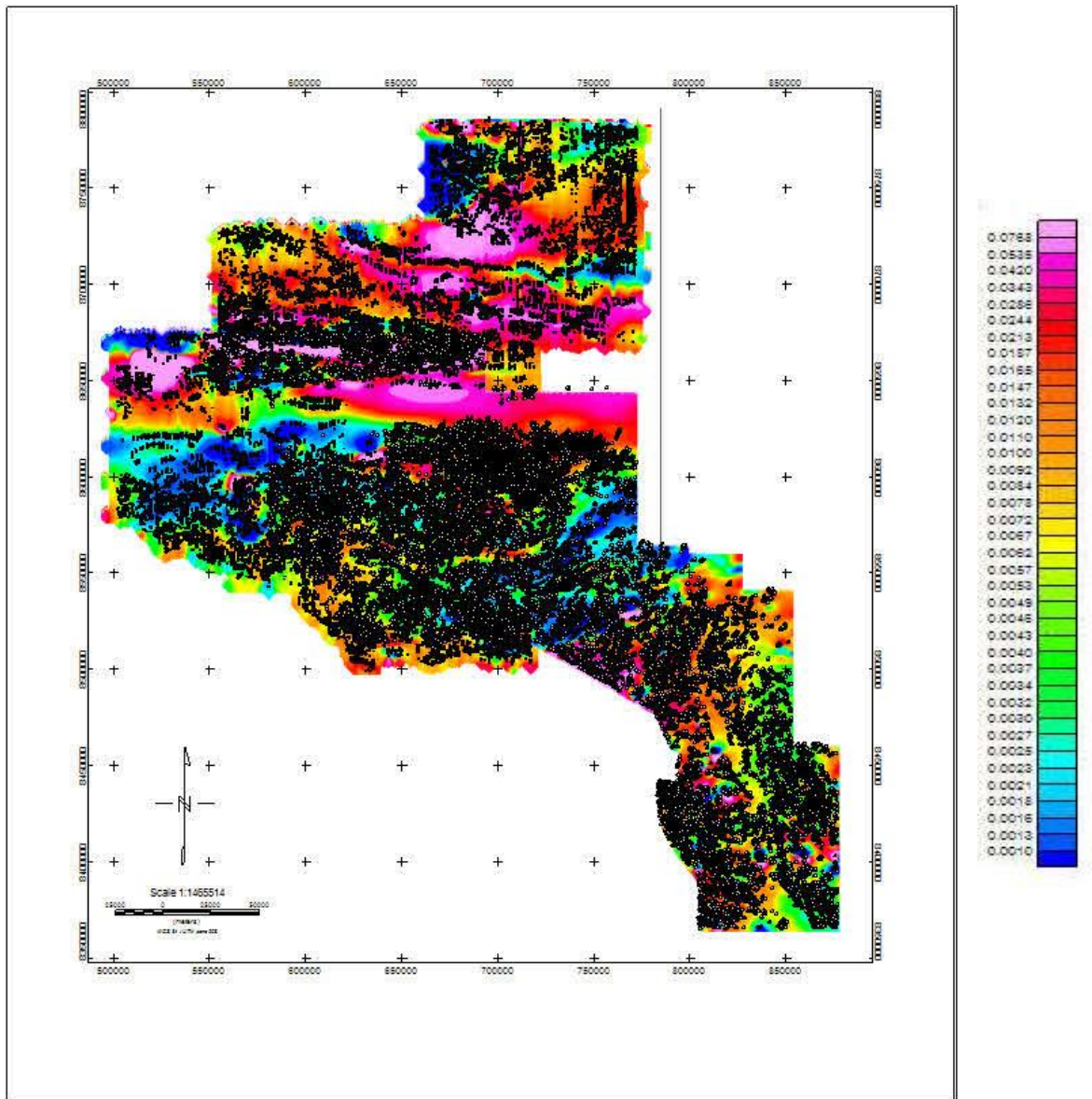


Fig. 24: Amazonian Euler Structural Index-1 Solutions with TMI background. Black dots represent Euler Structural index-1 solutions.

The presence of these features is a clue for the basement intact situation which could be termed as thin skin tectonics. This Brasilia belt region is characterized by E-W nappes and thrust. These structures are not seen on the basement structures when upward continuation filter is used. This proves the fact that the region has been subjected to thin skin tectonics. Hence, we find numerous diamondiferous kimberlites in this region which are characteristic of cratonic basement region.

The structures to the north corridor-125(Extra-Amazonian region) are NNW, NE, NS to NNE trending; here as the Corridor-125 is characterized by majority of the lineaments with NW-SE trend. The region above Corridor-125 north boundary is less infested with structural lineaments and SI-2 solutions from Euler Deconvolution. This region is represented by São Francisco craton basement which has not been affected by NW-SE structures.

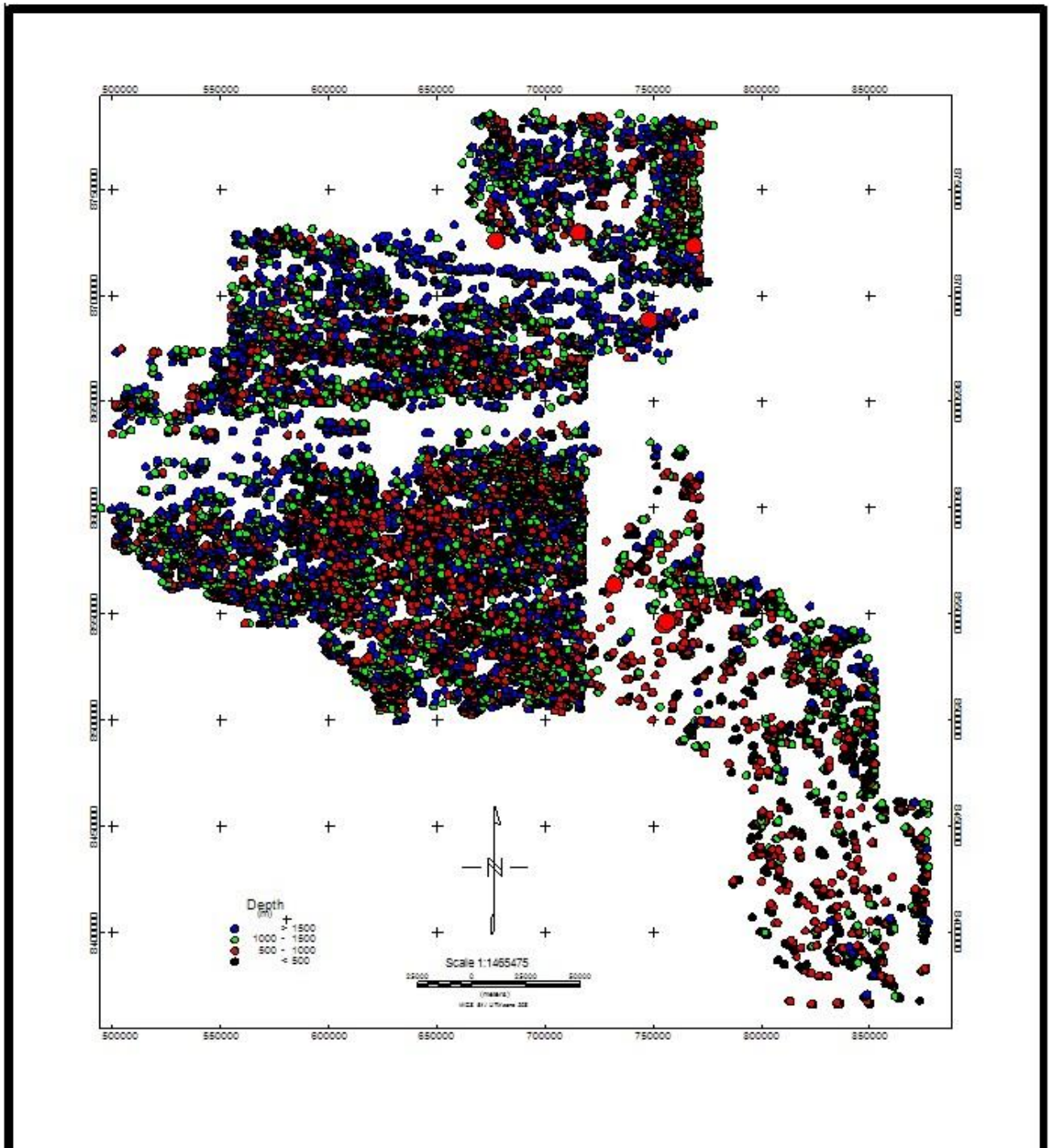


Fig.25: Amazonian Euler Structural Index-2 Solutions and kimberlite as Red Big circles represent kimberlites.

On the Amazon region, the Euler Structural index-1 (Fig.24) representing the linear features, dykes and sills are significant as majority of this region is covered by phanerozoic to recent sediments. The observed structures are NW-SE magnetic low lineaments on the western margin, NE-SW magnetic lineaments and N-S Nappes/thrust at the central region and of the study area. The southern region is devoid of major nappes but NW-SE and NE-SW lineaments are seen. Other features of significance the NNW-SSE Guapore suture zone on the western region; E-W trending Nova Brasilandia belt, Colorado rift and NW trending Pimenta Bueno rift in the northern region of the study area. Structural index-2 (Fig.25) corresponding to cylinders is found in good correlation to granitoid intrusions, alkaline intrusions and kimberlites.

Geophysics Interpretation related to Structural lineaments

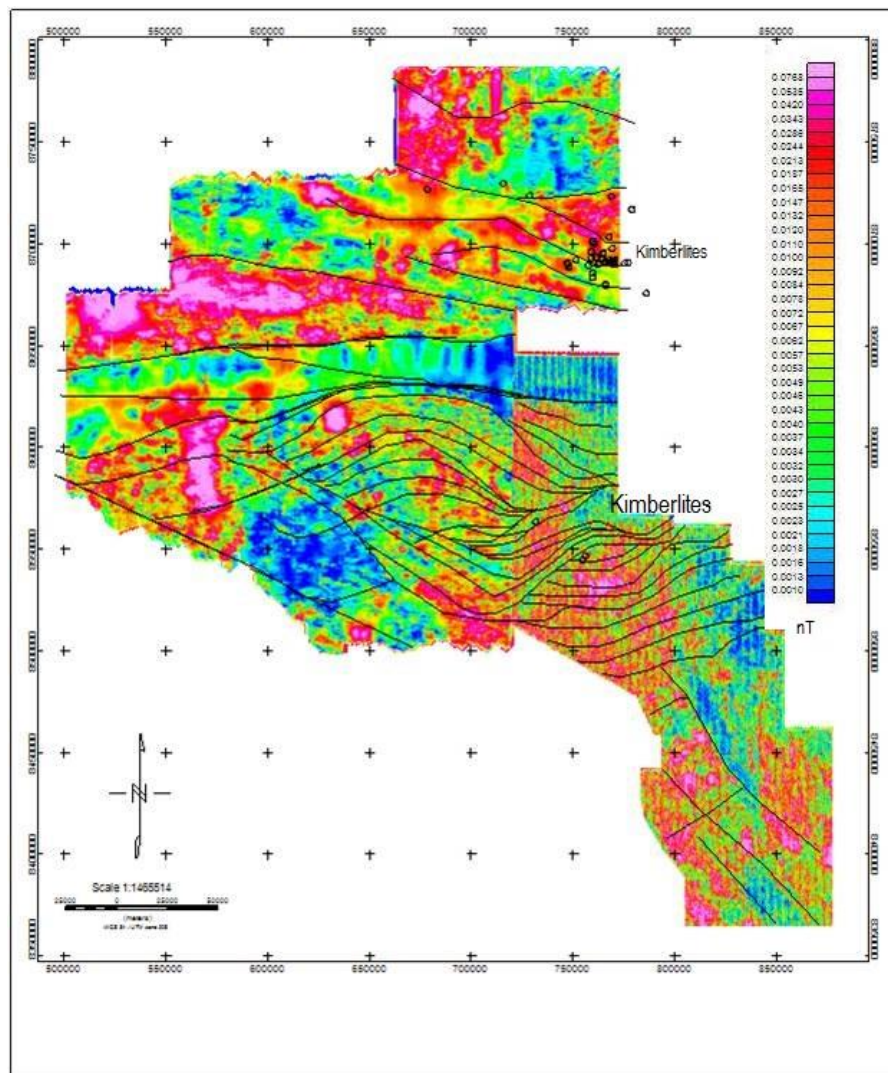


Fig.26: Linear Structural Elements of Amazon region with Amplitude of Analytical Signal background and black open circles represent kimberlites studied.

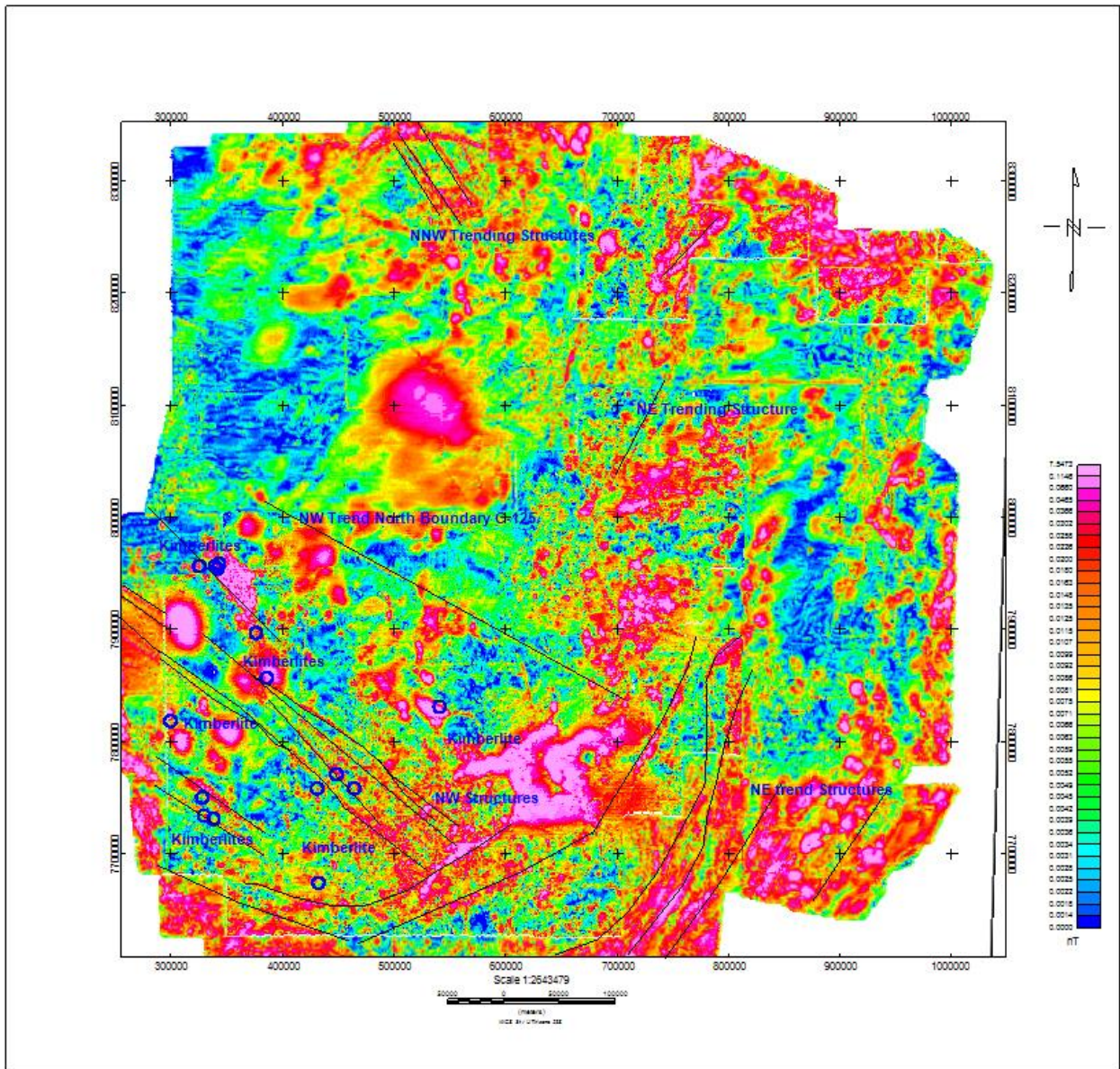


Fig.27: Linear Structural Elements of Extra-Amazon region with Analytical signal map background and blue open circles represent kimberlites studied.

The aeromagnetic data processing from Corridor-125 and its results has thrown significant new trends in the structural and magmatic rock configuration of the region. The magnetic characters of the alkaline, kimberlitic and country rock types are also very well distinguished and understood with respect to the regional dynamics. The Corridor-125 basement structures are not mapped clearly owing to its lack of signatures on ground and satellite imageries. This study delineates the width and length of the lineament and its nature with respect to basement structures, kimberlite and other alkaline rock intrusions. The result

challenges the continuity of the corridor-125 from East coast of the country on to the Amazonian craton. The northern boundary of the lineament has been clearly identified and delineated from the Aeromag data on the Extra-Amazonian region (Fig.26 and 27).

The revised extent of the corridor-125 is it starts from east coast of the country and runs up to Upper Paraguay thrust. There are no signatures of this lineament extending on to Amazonian craton. Instead, the basement structural configuration on the Amazonian craton is influenced by 1.4Ga collision of Paraguay block with Amazonian craton and Brasiliano collision of São Francisco-Paranapanema cratons. These collisions have resulted in subduction zones, suture zones, thrusting and folding of the Amazonian region boundary. Within the cratonic region, it has resulted crustal shortening, thrusting and rift zones. Guapore suture zone is the result of amalgamation between Amazonian craton and Paraguay block. Upper Paraguay-Araguaia thrust is the suture zone between the Amazonian and Extra-Amazonian block. Jiparan shear (North of the geophysics study area) zone has been interpreted as Grenville age (Tohver et al, 2005) Jiparan shear zone is associated with NS nappes in the northern part of the Rondonia state, which host another set of kimberlites along corridor-125.

As a concluding remark, the Amazonian region is characterised by different set of lineaments (Fig.26 and 27), mafic and other rock units which has undergone basement reworking prior and during Grenville times with the formation of structural lineaments seen in the aeromagnetic data. These lineaments has been controlling the kimberlite emplacement during Permo-Triassic and cretaceous periods rather than as part of corridor-125 extension. During both the periods of kimberlite emplacements, plate reorganisation and structural reactivations has triggered kimberlite magmatism and hence, these kimberlites are geochemically different from each other. The Extra-Amazonian region has undergone thin skin tectonic reworking where the basement is intact with NW-SE lineaments (Fig.27) along the kimberlite occurrence area. This lineament has been structurally controlling the kimberlite and related rocks of cretaceous age due to reactivation during South Atlantic rifting. The thrust and nappes seen as surface geomorphic expression has been due to the Brasilia belt evolution from Brasiliano times during which the Transbrasiliano lineament NE-SW was also formed.

Aeromagnetic characterization of Corridor-125 kimberlites

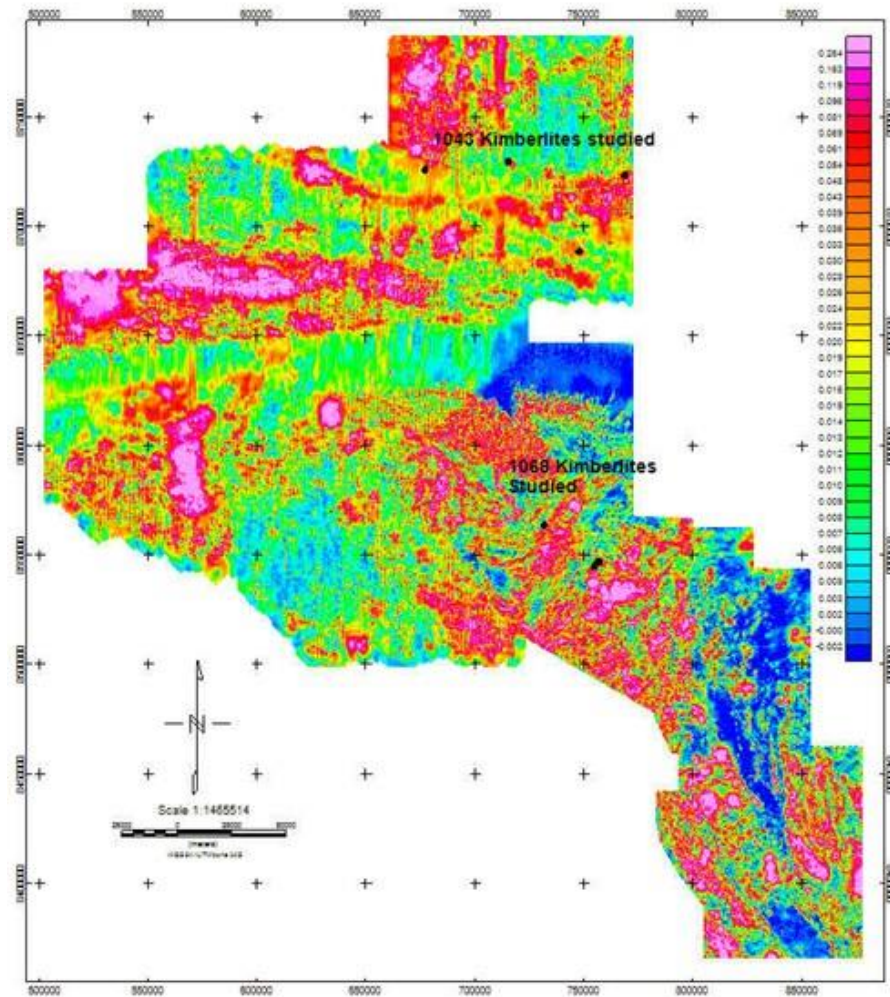


Fig.28: Amazonian Kimberlite Analytical signal signatures geophysically tested.

The kimberlite signature recognition is achieved by integrating analytical signal and Euler structural indexing technique for cylinders and pipes. Many of the known kimberlites show good correlation with circular or oval analytical signal anomalies (Fig.28, 29, 30 and 31) overlapping with good cluster of structural index-2 on them. But many kimberlites especially multiple intrusions of the same kimberlite are not correlated properly which could be due to regional coverage nature of the data with large line spacing and or low-latitude nature of the study area. With more high resolution data acquisition by decreasing the line spacing a better correlation could be achieved for all kimberlites of small diameter and multiple intrusions in Brazil.

The kimberlites from 1068 Project in the central domain of Amazonian region show complex analytical signal anomaly. Further refining could be achieved by ground magnetics survey and its interpretation. The results from this study also signify the fact that aeromagnetic results are not a stand along tool in kimberlite recognition. But as an added tool it will be one of the best tools to identify kimberlites.

Keating Coefficient for Potential Kimberlite body

Keating Coefficient method is a simple pattern recognition technique to identify magnetic anomalies of modelled kimberlite signature with prior knowledge of the known kimberlite spatial data and dimension. In this method approximate value of kimberlite radius, depth to the top of the kimberlite body and an appropriate threshold for the survey region. With the inclination and declination already determined, a model pipe grid is generated and run over the Total magnetic field grid as a moving window. Each grid node is correlated with the model grid to look for any vertically dipping cylindrical body which is the representative of kimberlite pipe. During correlation, the grid retains the value greater than the threshold specified. The final anomaly coefficient data gives the location depth and magnetic nature of the potential kimberlite. Further, the potential kimberlite body signature recognition is achieved by integrating analytical signal, Euler structural indexing technique for cylinders and pipes and Keating coefficient anomaly picks. Some of the known kimberlites show good correlation with circular or oval analytical signal anomalies overlapping with good cluster of structural index-2 on them. But many kimberlites especially multiple intrusions of the same kimberlite are not correlated properly which could be due to regional coverage nature of the data with large line spacing and or low-latitude nature of the study area. With more high resolution data acquisition by decreasing the line spacing a better correlation could be achieved for all kimberlites of small diameter and multiple intrusions in Brazil.

Extra-Amazonian Region Kimberlite keating coefficient picks tested with the selected known kimberlites are correlated with the Analytical signal (Fig. 29 and 30) and Euler Structural Index-2. This integrated approach works very well with tight clustering of SI-2 over Analytic signal circular anomalies and keating coefficient potential anomaly. The drawback in this method is observed where the basement is too deep as or the kimberlite multiple intrusion or when the kimberlite is associated with other large diameter alkaline intrusions. Last but not the least, highly deformed regions with numerous subparallel magnetic

high lineaments also masks the kimberlite signatures. Extra-Amazonian Region Kimberlite modelling with Keating Coefficient shows good correlation with the known tested known kimberlites and Keating coefficient anomaly picks with a depth of overburden 50m.

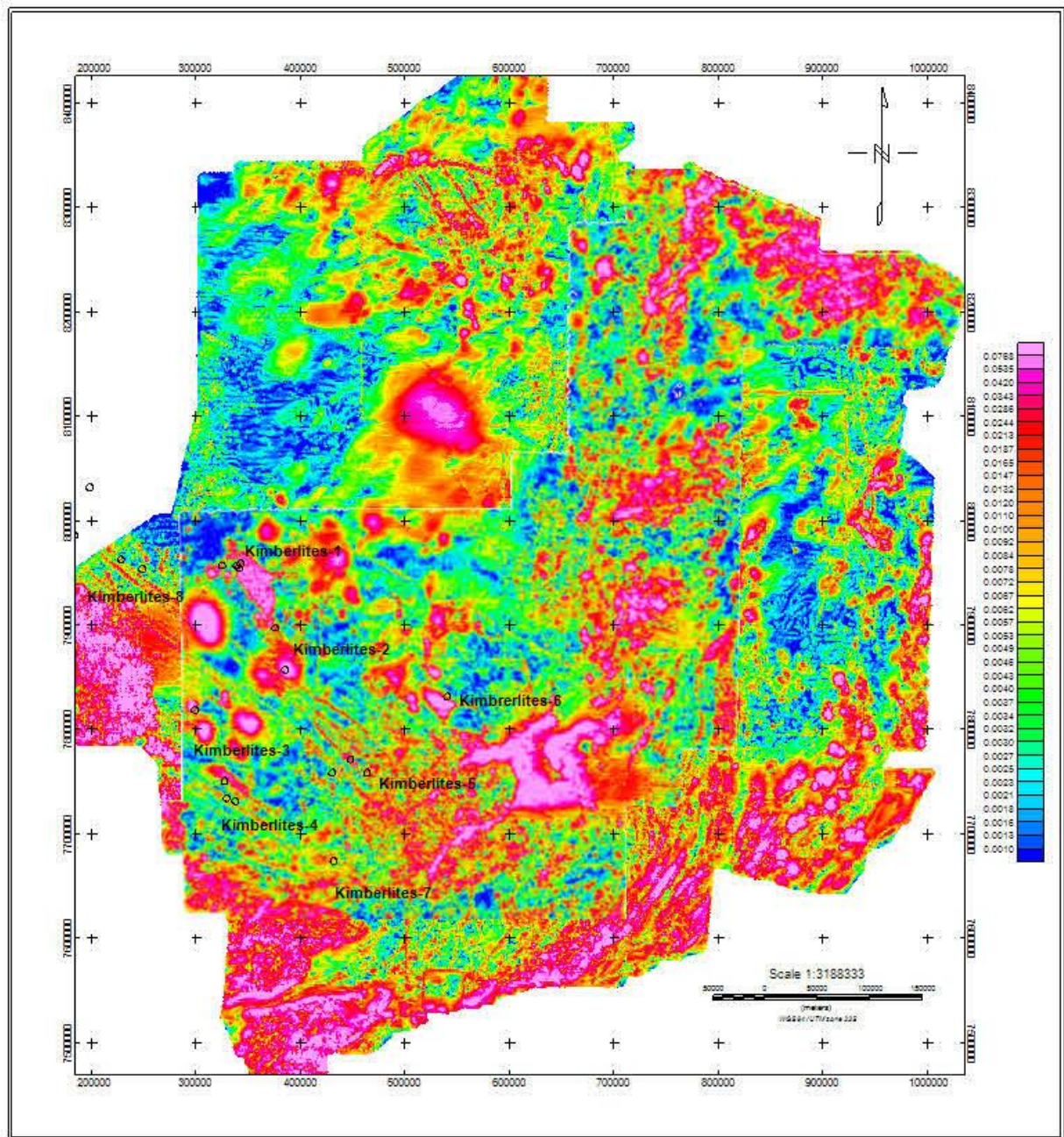


Fig. 29: Extra-Amazonian known Kimberlites studied for modelling by integrated Analytical signal, Euler solution index-2 and Keating Coefficient.

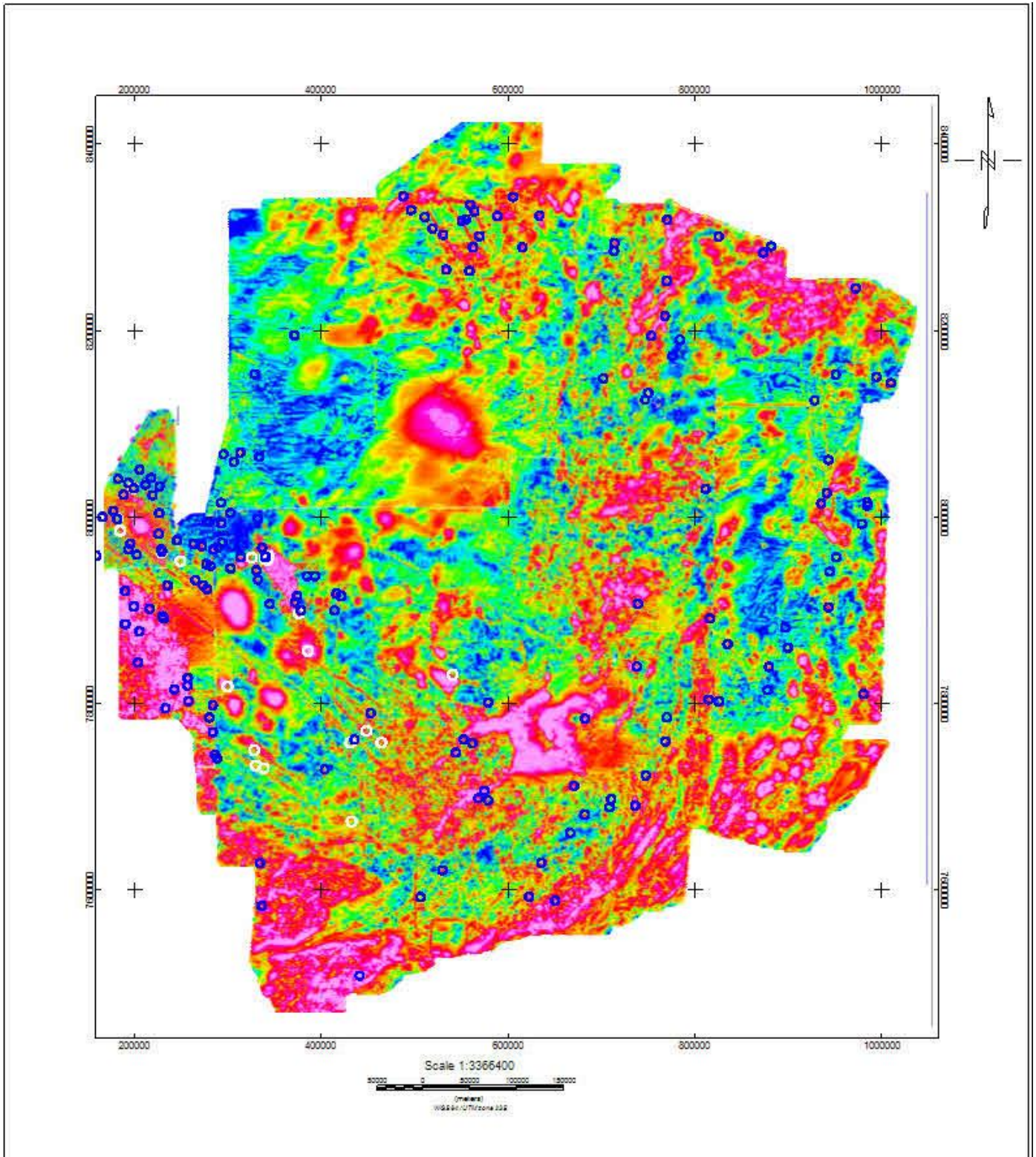


Fig. 30: Extra-Amazonian Keating Coefficient Anomaly pick plot with known kimberlites. The Keating Coefficient Anomaly is represented by blue circle and known kimberlites are represented by white circles.

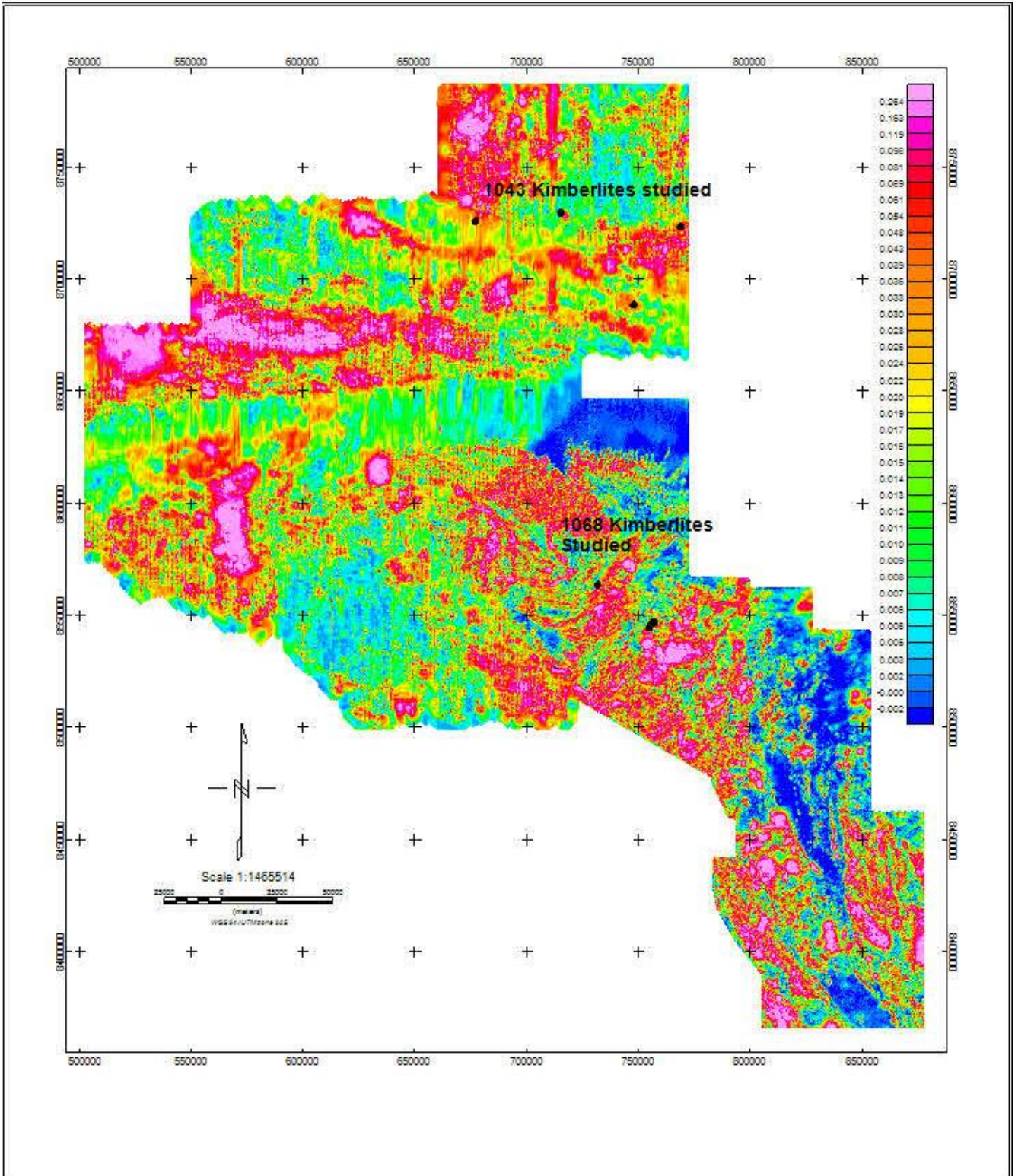


Fig.31: Amazonian Kimberlite Analytical signal signatures geophysically tested.

Amazonian Region Kimberlite Signature: Combined Analytic signal signatures, Euler SI-2 and Keating coefficient anomaly picks (Fig. 31 and 32) has identified shallow depth kimberlite bodies. The deeper source kimberlites found in the graben region of Pimenta

Bueno are not identified by this method. There are more shallow depth anomalies which needs ground checking for potential kimberlite pipes. Being one of the best low latitude region with numerous kimberlite bodies, the magnetic data is tested to arrive at the best possible methods and techniques by which the kimberlite bodies can be magnetically modelled and identified. The Northern Domain consists of shallow and slightly deeper depth to top of the kimberlite bodies. Pimenta Bueno kimberlites are deeper seated than the North Rondonia cluster kimberlites. The Southern Domain host comparatively shallow depth kimberlites which are covered by neotectonic sediments. There are interesting shallow depth source potential kimberlite anomalies which needs ground checking.

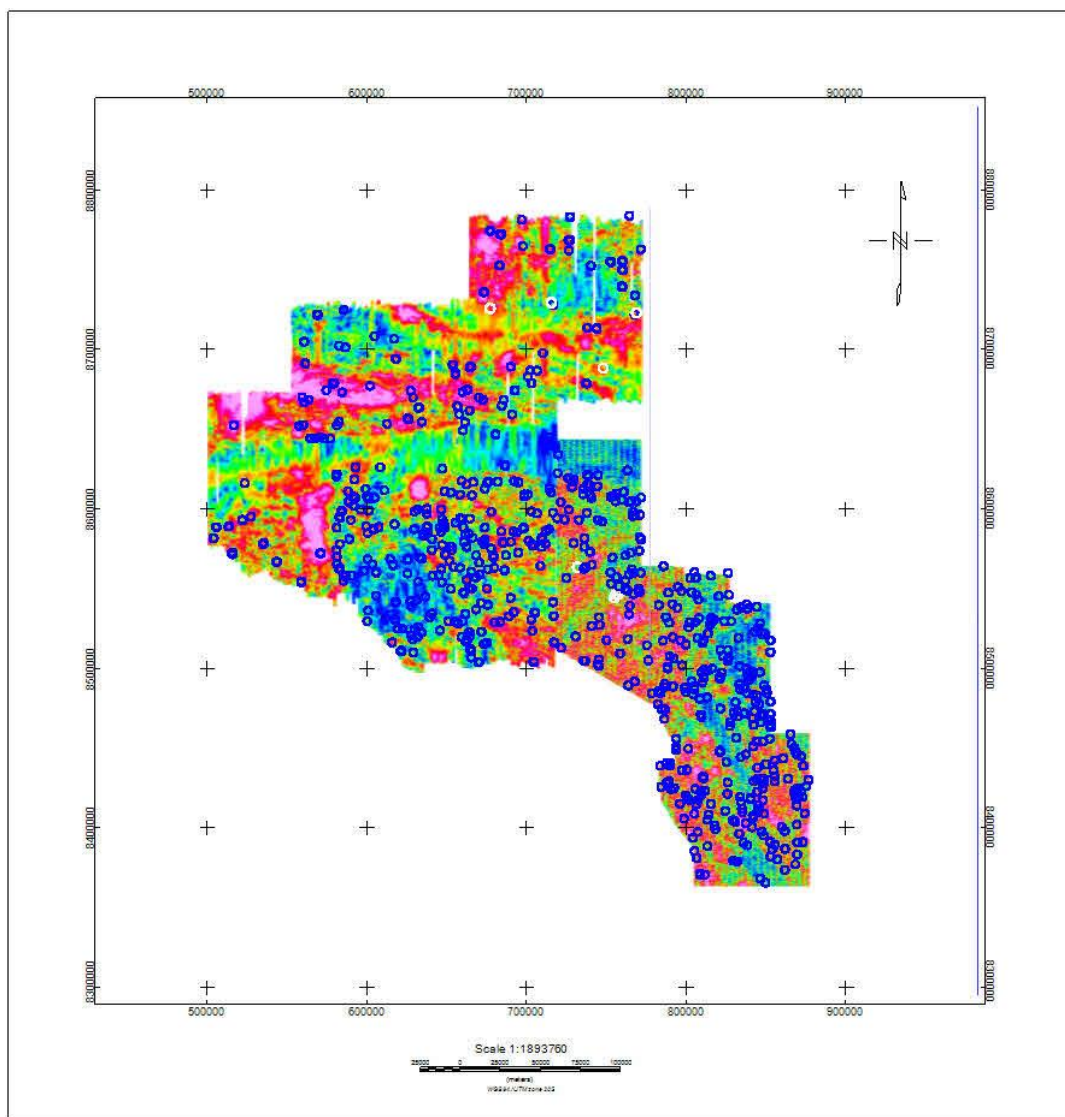


Fig. 32: Amazonian region Keating Coefficient Anomaly pick plot with known kimberlites. The Keating Coefficient Anomaly is represented by blue circle and known kimberlites are represented by white circles.

Chapter 10

Revised Structural Framework of Corridor-125 by the integration of mapped structures and magnetic structures.

In this section, the mapped structures from all available sources like CPRM database, USGS Quaternary lineament map mapping project for Brazil, Megalineament map of Brazil etc., are integrated with the geophysically picked lineaments which have found to be associated with the kimberlite occurrences. The result of this integration is presented in the fig. 33, as revised structural framework for corridor-125. It is interesting to see the basement structures that are hidden below the sedimentary cover in Brazil pops up and shows link to older tectonic events and have been reactivated during subsequent tectonic activities. Reactivation during Kimberlite emplacement is an evidence for this observation where in the basement structural trend associated with older than Brasiliano time is reactivated around Cretaceous and Permo-Triassic times.

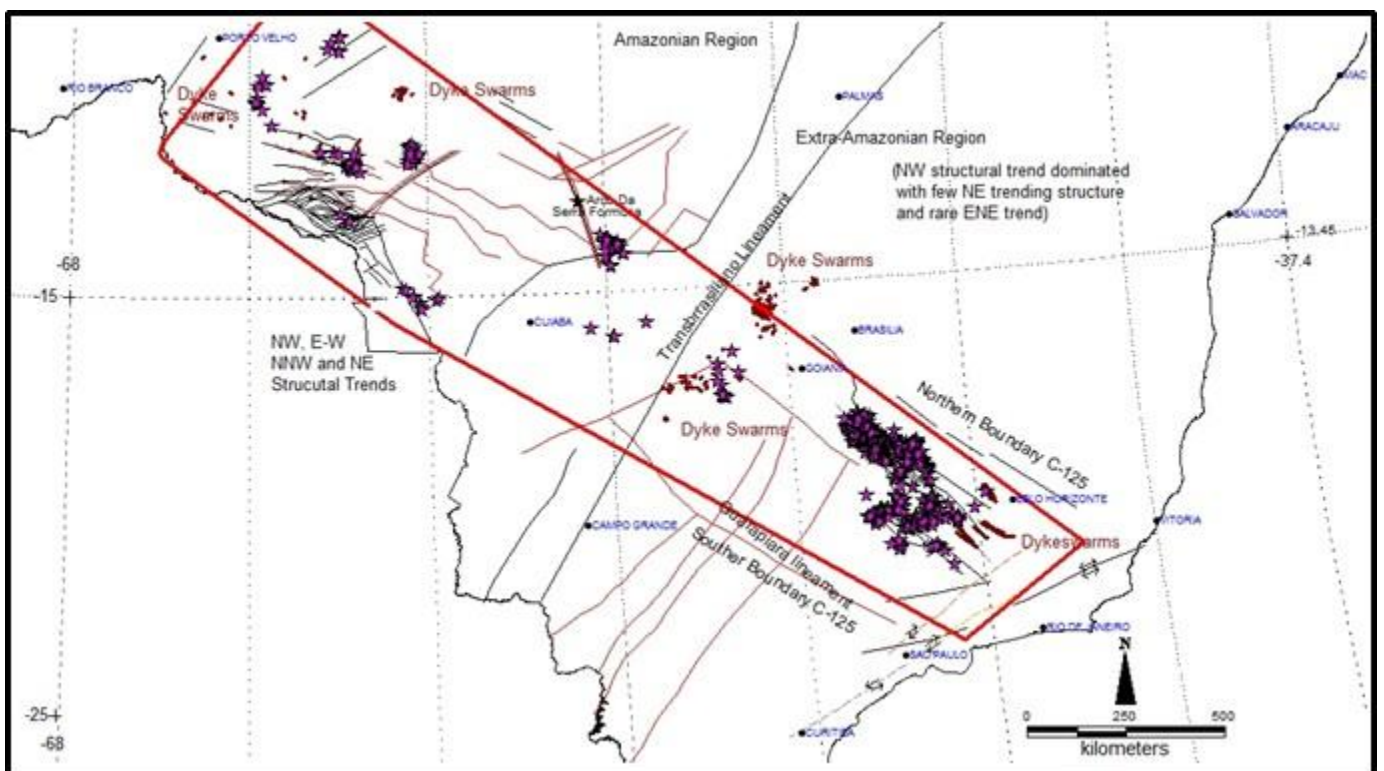


Fig. 33: Revised Structural Framework of Corridor-125 with dyke swarms, kimberlites, magnetic and mapped structures. Boundary in red represents corridor-125, Black lines, and

brown lines represents structures Thick brown lines represents dykeswarms, Pink stars represents kimberlites and related rocks and city names are in blue.

The revised structural framework of corridor-125 controlling the kimberlite emplacement is summarized in fig.33. This map is the integration map from mapped structures and the lineaments picked from the aeromagnetic signatures. The hidden basement structures are identified from the aeromagnetic map and its significance to geodynamic evolution of corridor-125 and kimberlite emplacements. The basement structural architecture of corridor-125 on Extra-Amazonian region is composed of NW-SE trending lineaments with occasional NE trending lineament intersections along the kimberlite occurrences. Thin skin tectonics is evident for the younger Brasilia belt geomorphology and tectonics. On the Amazonian region, the basement structures trending NW and NE. These structures correspond to frontal thrusting and crustal shortening events due to collision of Paraguay block to Amazonian block and Andean evolution. The older structures on both the regions are reactivated during younger rifting.

Chapter 11

Geochemistry of Brazilian Kimberlites Analysed

Review geochemical petrogenetic model on corridor-125 kimberlites.

There are many models to explain APIP kimberlite geochemical signatures. Very few initial model for Amazonian region kimberlites are available. In fact, the models for Amazonian region is not complete except for modelling their subduction derived source and group I type classification. The Brazilian kimberlites are thought to have derived from plume related geochemistry by Bizzi et al. (1995) and Carlson (1996) looking at similarity of Sr_i and Nd_i ratios of Tristan/Walvis hotspot. Later, this association of the hotspot and kimberlites was ruled out due to the large age discrepancy between the APIP magmatism (~85 Ma) and the proposed time the plume underlay the APIP (~130 Ma). Later, a model with the Trindade plume was proposed whose palae-position coincided with under the APIP cluster approximately at 85 Ma. But its distinctive Sr and Nd isotopic composition also negates the association (Gibson et al., 1995). Our current review work also rules out the link between hotspots and kimberlite magmatism in Brazil along corridor-125. A model of magma mixing between Group I and II through the same plumbing systems was the next proposal to produce transitional type kimberlites. This does not explain all the geochemical signatures. Another proposal by Felgate, 2014 research work shows the Sr_i and Nd_i of kimberlites represent derivation from a metasomatised SCLM source in all cases, with the range in isotopic values explained by heterogeneities within the source.

The younger 95Ma Juina Kimberlites of the Amazonian craton is unique, it show geochemical signatures similar to Lamproites. The diamond inclusion studies have shown that they have source region from great depths ranging from 670 to 410km (Bulanova et al, 2010).

Other kimberlites have their asthenospheric mantle source with reference to Batovi-6 (Costa, 1996) and Concorde-1(Felgate, 2014) kimberlites, due to its isotopic similarities to Group I kimberlites and OIB signatures where in Oceanic subduction along with sediments at asthenospheric depths have given rise to these kimberlites.

The transitional type signatures are formed by the adiabatic decompression melting of SCLM due to extensional tectonics (Becker et al, 2007). A SCLM source has been ascribed as the source for Brazilian kimberlites in order to characterise the isotopic and incompatible trace element signatures (Gibson et al, 1995; Guarino et al, 2013; Donatti-Filho et al, 2013b and Felgate, 2014). There is clear evidence for Extra-Amazonian region kimberlites genetic link with the South Atlantic rifting as proposed by Becker et al, 2007.

There is a need constraining a model which could accommodate kimberlite magmatism on both the regions and their associated tectonic event link. In this study an initial modelling on this line is taken up.

Geochemical Analytical Procedures

Sevenwhole rock samples with least possible weathering and contamination (without any visible country rock fragments and xenocrysts) were selected for the analysis. These samples were crushed, powdered and utilized for chemical analysis at the Institute of Geosciences of the University of Campinas after determination of Loss of ignition at 1000°C (% PF). Major elements were analysed on fusion beads by X-ray fluorescence spectrometry (XRF) - Philips PW 2404, Netherlands.

Standard analytical procedures outlined in Vendemiatto and Enzweiler (2001) were followed for the major elements Na, Mg, Al, Si, P, K, Ca, Ti, Mn and Fe; Minor and trace elements Cu, Ni, Co, Cr, V, Zn and Nb analysis by XRF using pressed powder pellets. Data quality was controlled through routine analyses of the international rock standards SARM-39 (Kimberlites), OU-6 and BPR-1 for major elements and trace elements. The relative errors are 0.4 - 1.5% for major and minor elements, while for trace elements they range within 1.5 - 10%. Rare earth elements (REE), Th, Ta, U, Hf and Nb were analysed by total digestion with HF/HNO₃ (Parr pumps, 4 days, 180 °C), followed by dissolving a mixture of nitric and hydrofluoric acids in Parr type pumps. All solutions were prepared with ultra-pure water (18.2 MΩ.cm) obtained from a Milli-Q system. The acid nitric (HNO₃) was purified by sub-boiling. The bottles used for the dilutions were previously cleaned with 5% HNO₃ and rinsed with ultra-pure water. The limit of detection (LOD) was determined as the mean (\bar{x}) plus 3 standard deviations (s) ten blank measurements ($LD = \bar{x} + 3s$).

| Sample | Forca | Collier-01 | Collier04 | Juina-23 | Tumeleiro | Indaia | Cosmos-01 |
|------------------------------------|---------|------------|-----------|----------|-----------|--------|-----------|
| Lab No. | L-571-A | L-825 | L-826 | L-827 | L-828 | L-829 | L-830 |
| Elements (%) | | | | | | | |
| SiO₂ | 31.03 | 38.00 | 49.86 | 55.98 | 36.42 | 29.56 | 45.46 |
| TiO₂ | 2.01 | 1.658 | 0.927 | 1.060 | 2.617 | 2.619 | 1.057 |
| Al₂O₃ | 1.48 | 4.36 | 7.42 | 4.86 | 4.26 | 2.17 | 4.94 |
| Fe₂O₃ | 10.42 | 9.59 | 7.59 | 5.86 | 14.46 | 12.06 | 7.44 |
| MnO | 0.182 | 0.127 | 0.112 | 0.084 | 0.490 | 0.226 | 0.131 |
| MgO | 29.56 | 22.09 | 16.19 | 13.84 | 26.40 | 28.49 | 27.60 |
| CaO | 9.40 | 9.17 | 5.94 | 5.14 | 1.33 | 11.59 | 2.88 |
| Na₂O | 0.26 | 0.05 | 0.46 | 0.09 | 0.03 | 0.09 | 1.11 |
| K₂O | 1.10 | 0.14 | 2.80 | 3.47 | 0.16 | 0.69 | 0.43 |
| P₂O₅ | 1.337 | 0.473 | 0.125 | 0.343 | 0.782 | 2.850 | 0.132 |
| BaO | 0.33 | - | - | - | - | - | - |
| Cr₂O₃ | 0.24 | - | - | - | - | - | - |
| NiO | 0.16 | - | - | - | - | - | - |
| SrO | 0.23 | - | - | - | - | - | - |
| LOI | 11.78 | 13.7 | 8.38 | 8.62 | 12.3 | 9.07 | 8.13 |
| Sum | 99.8 | 99.33 | 99.81 | 99.36 | 99.18 | 99.42 | 99.31 |
| Crustal Index (ppm) | 1.25 | 0.27 | 10.4 | 16.12 | 0.25 | 1.23 | 0.79 |
| Nd | 151 | 52 | 43 | 42 | 74 | 234 | 48 |
| Ni | 1260 | 556 | 704 | 301 | 2501 | 956 | 1177 |
| Pb | 11.8 | 9.7 | 21.0 | 15.6 | <2.5 | 10.9 | 6.1 |
| Rb | 107 | 10.1 | 123 | 123 | 15.0 | 53 | 25.9 |
| Sc | 23 | 14 | 12 | 9 | 21 | 28 | 8 |
| Sr | 1980 | 449 | 119 | 328 | 319 | 2004 | 234 |
| Th | 26.9 | 14.4 | 13.3 | 10.0 | 17.4 | 25.7 | 8.9 |
| U | 8.1 | - | - | - | - | - | - |
| V | 142 | 141 | 80 | 106 | 136 | 133 | 69 |
| Y | 27.6 | 14.5 | 42 | 13.5 | 20.1 | 39 | 23.3 |
| Zn | 72 | 61 | 64 | 53 | 97 | 98 | 49 |
| Zr | 362 | 145 | 171 | 162 | 152 | 585 | 107 |
| Nd | 151 | 52 | 43 | 42 | 74 | 234 | 48 |
| Ni | 1260 | 556 | 704 | 301 | 2501 | 956 | 1177 |
| Pb | 11.8 | 9.7 | 21.0 | 15.6 | <2.5 | 10.9 | 6.1 |
| Rb | 107 | 10.1 | 123 | 123 | 15.0 | 53 | 25.9 |
| Sc | 23 | 14 | 12 | 9 | 21 | 28 | 8 |
| Sr | 1980 | 449 | 119 | 328 | 319 | 2004 | 234 |
| Th | 26.9 | 14.4 | 13.3 | 10.0 | 17.4 | 25.7 | 8.9 |

Table 2: Major Element geochemical analysis results with crustal index values

The measurements were carried out on ICP-MS (inductively coupled plasma mass spectrometry) Xseries-II equipped with STC (Collision Cell Technology). Prior to the measurements the instrument was adjusted as recommended by the manufacturer. Instrument

calibration was performed with multielement solutions prepared gravimetrically from mono-element standard solutions of 100 mg/L (AccuStandards). The result deviation from the reference values is within 10%. The geochemical results of major and trace elements are reported in Table 2 and 3.

| Sample | Forca | Col1 | Col4 | Juina-23 | Tum | Indaia | Cosmos-1 | Sarm 39 | Sarm 39 | Detection Limit (LD) |
|----------------|-------|------|------|----------|------|--------|----------|---------|---------------|----------------------|
| Elements (ppm) | | | | | | | | Result | Reference | |
| Li | 8.35 | 9.51 | 32.6 | 15.8 | 76.2 | 8.6 | 37.8 | 9.25 | - | 0.03 |
| Be | 3.74 | 0.89 | 2.3 | 1 | 2.32 | 4.07 | 1.16 | 1.52 | - | 0.04 |
| Sc | 20.1 | 12.5 | 11.8 | 8.77 | 18.2 | 23.2 | 9.03 | 3.35 | - | 1.4 |
| V | 137 | 123 | 81 | 94.5 | 150 | 141 | 76 | 121 | 115.5 | 0.1 |
| Cr | 1481 | 547 | 539 | 277 | 2144 | 1290 | 1088 | 1278 | 1274.2 | 0.4 |
| Co | 77 | 52 | 44.1 | 28.8 | 108 | 77.2 | 60.8 | 68.5 | 69 | 0.02 |
| Ni | 1186 | 471 | 569 | 242 | 2195 | 998 | 953 | 951 | 936.8 | 0.2 |
| Cu | 56.6 | 49.7 | 17.7 | 26.4 | 80.8 | 52.9 | 19.4 | 59.4 | 59.4 | 0.2 |
| Zn | 67.9 | 72.2 | 79 | 49.2 | 95 | 98.2 | 54.1 | 71.1 | 69.5 | 3.4 |
| Ga | 5.33 | 8.09 | 10.4 | 6.98 | 8.05 | 8.85 | 7.02 | 7.51 | - | 0.009 |
| Rb | 110 | 8.07 | 113 | 116 | 10.4 | 54.8 | 21.1 | 48.3 | 50.8 | 0.2 |
| Sr | 1926 | 457 | 125 | 335 | 256 | 1929 | 241 | 1259 | 1451.4 | 0.07 |
| Y | 26.3 | 12.8 | 37.8 | 11.9 | 17 | 37.8 | 18.7 | 13.6 | 16.4 | 0.02 |
| Zr | 365 | 139 | 191 | 174 | 154 | 681 | 112 | 220 | 243.2 | 0.04 |
| Nb | 231 | 115 | 24.3 | 71.5 | 178 | 236 | 55.3 | 104 | 109.2 | 0.05 |
| Mo | 0.77 | 0.18 | 9.38 | 0.17 | 1.42 | 0.17 | 0.81 | 0.63 | - | 0.02 |
| Cd | 0.26 | 0.06 | 0.08 | 0.09 | 2.57 | 0.11 | 0.01 | 0.12 | - | 0.02 |
| Sn | 2.36 | 0.68 | 3.78 | 0.59 | 1.45 | 3.77 | 1.86 | 1.56 | - | 0.08 |
| Sb | 0.35 | 0.09 | 0.35 | 0.14 | 0.22 | 0.1 | 0.27 | 0.46 | 0.42 | 0.01 |
| Cs | 2.35 | 0.14 | 4.79 | 0.82 | 0.31 | 1.95 | 0.62 | 2.52 | 3.51 | 0.004 |
| Ba | 2640 | 966 | 536 | 1275 | 375 | 2854 | 326 | 1566 | 1683.3 | 0.08 |
| La | 256 | 73.3 | 40.9 | 49.4 | 101 | 324 | 36.6 | 86.1 | 89.2 | 0.01 |
| Ce | 480 | 134 | 85.2 | 86.1 | 181 | 630 | 71.5 | 178 | 182.9 | 0.02 |
| Pr | 52.2 | 14.2 | 9.68 | 9.29 | 20.1 | 79.6 | 8.23 | 21.4 | 21.5 | 0.006 |
| Nd | 176 | 48.1 | 35.4 | 31.9 | 70.8 | 288 | 29.7 | 79.9 | 82.2 | 0.009 |
| Sm | 23.2 | 6.51 | 6.89 | 4.59 | 10.1 | 37.9 | 5.08 | 11.7 | 12.2 | 0.007 |
| Eu | 6.09 | 1.92 | 1 | 1.49 | 2.57 | 9.99 | 0.99 | 3.12 | 3.14 | 0.003 |
| Gd | 15.7 | 5.19 | 6.56 | 3.87 | 7.58 | 27.1 | 4.39 | 8.71 | 8.58 | 0.006 |
| Tb | 1.67 | 0.59 | 1.1 | 0.47 | 0.82 | 2.73 | 0.64 | 0.9 | 0.99 | 0.003 |
| Dy | 6.8 | 2.87 | 7.11 | 2.55 | 3.7 | 11.2 | 3.68 | 3.71 | 4.23 | 0.003 |
| Ho | 1.05 | 0.49 | 1.43 | 0.46 | 0.59 | 1.61 | 0.7 | 0.56 | 0.62 | 0.003 |
| Er | 2.33 | 1.4 | 4.33 | 1.38 | 1.59 | 3.91 | 2.09 | 1.36 | 1.52 | 0.004 |
| Tm | 0.25 | 0.2 | 0.68 | 0.21 | 0.2 | 0.41 | 0.32 | 0.159 | 0.18 | 0.02 |
| Yb | 1.41 | 1.21 | 4.17 | 1.27 | 1.11 | 2.03 | 1.91 | 0.86 | 0.98 | 0.005 |
| Lu | 0.17 | 0.17 | 0.6 | 0.19 | 0.15 | 0.24 | 0.27 | 0.11 | 0.13 | 0.002 |
| Hf | 8.94 | 3.64 | 6.06 | 4.47 | 4.08 | 16.3 | 3.09 | 5.18 | 5.02 | 0.005 |
| Ta | 12.0 | 7.44 | 1.68 | 4.31 | 11.3 | 12.9 | 4.27 | 7.15 | 7.3 | 0.003 |
| W | 0.49 | 0.17 | 0.95 | 0.23 | 0.36 | 1.02 | 1.08 | 1.28 | 1.3 | 0.01 |
| Pb | 10.8 | 6.56 | 17.6 | 7.86 | 9.03 | 13.1 | 5.52 | 20.6 | - | 0.05 |
| Bi | 3.74 | 0.06 | 0.22 | 0.11 | 0.07 | 0.11 | 0.14 | 0.1 | - | 0.006 |
| Th | 30.9 | 13.9 | 17.7 | 9.17 | 17.2 | 29 | 7.91 | 6.11 | 9.75 | 0.003 |
| U | 6.88 | 2.34 | 10.5 | 2.21 | 3.21 | 6.35 | 2.29 | 2.33 | 2.52 | 0.03 |

Table 3: Trace Element Results from ICP-MS geochemical analysis.

Bulk Rock Major Element Results

The Major element signatures of the analysed samples are well in agreement with the ranges for kimberlites, though couple of samples show contamination effect. Often, major- and trace-element geochemical studies of kimberlites are hindered by the very hybrid nature due to the presence of crustal, xenolithic and xenocrystic material. Another hindrance encountered in geochemical studies is the alteration due to weathering. Brazilian kimberlites are highly weathered and very difficult to find fresh samples even from drill core samples. In order to reduce the effect of all these hindrances, several tests to arrive at control value calculations are introduced.

Contamination analysis tests proposed by Clement (1982), Mitchell (1986), Taylor et al. (1994) and Berg (1998) are used to determine the type and extent of contamination. Clement (1982) used the contamination index (C.I.) to measure the proportion of clay minerals and tectosilicates relative to olivine and phlogopite:

$$\text{C.I.} = (\text{SiO}_2 + \text{Al}_2\text{O}_3 + \text{Na}_2\text{O}) / (\text{MgO} + \text{K}_2\text{O})$$

Clement (1982) and Mitchell (1986) suggested that contamination increases the whole-rock concentrations of SiO₂, Al₂O₃ and Na₂O in kimberlite. Mitchell (1986) concluded that <35 wt. % SiO₂ and <5 wt. % Al₂O₃ are indicative of contamination-free kimberlite, and that mixing lines of various contaminants and weathering products could explain variations in kimberlite chemistry. Hence, an increased contamination will result in the sum of SiO₂, Al₂O₃, and Na₂O being much greater than the sum of MgO and K₂O, resulting in higher C.I. A sample completely devoid of alteration or crustal contamination will have a C.I. value close to 1, whereas addition of crustal material and/or alteration will result in C.I. >1. Kjarsgaard et al., (2009) proposed a C.I. = 1.5 as a useful contamination/alteration threshold. The samples with C.I. >1.5 should have entrained enough crustal material or undergone substantial alteration to compromise bulk rock geochemical signature. Hence, such analyses will not give the correct picture of the kimberlite magma composition.

The samples are rich in SiO_2 (55.98 – 29.56) and MgO (13.84 – 29.56) wt %. The samples show slightly higher range of SiO_2 than the expected range for Kimberlites which is probably due to the altered nature and presence of numerous country rock material visually seen. The aluminum oxide ranges is (1.78 – 7.42) wt %, CaO range is (2.88 – 11.59) wt %, Fe_2O_3 is (5.86 – 14.46) wt % and K_2O range is (0.14 – 3.47) wt %. The Extra-Amazonian region samples (Forca and Indaia) show lower concentration of SiO_2 compared to Amazonian region samples (Col-1, Col-4, Jun-23 and Tumeleiro). The range for these two Extra-Amazonian region samples is less than 35 wt %. The Amazonian region kimberlites are more enriched with SiO_2 , TiO_2 and Al_2O_3 in comparison to Extra-Amazonian region kimberlites. All the samples have TiO_2 range slightly higher than expected for typical uncontaminated kimberlite range.

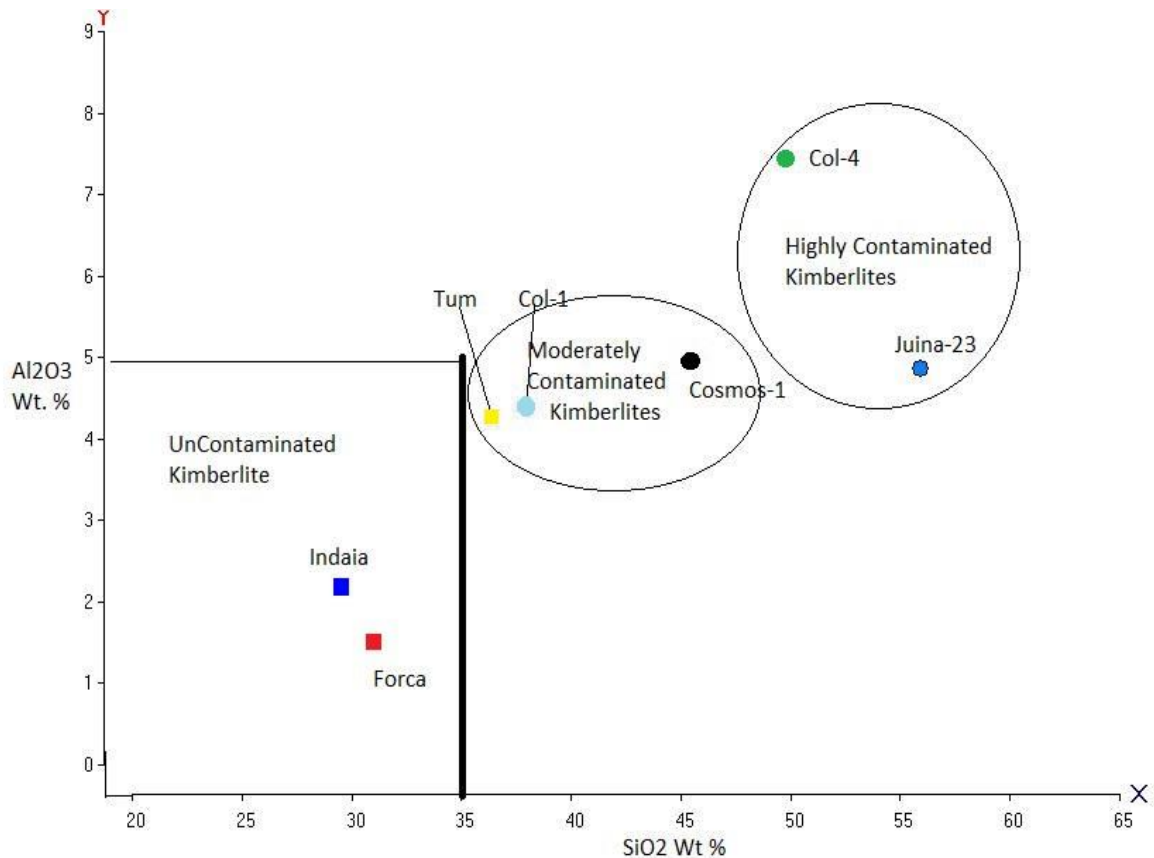


Fig. 34: Graph to distinguish the samples into fresh or altered kimberlites with Al_2O_3 Vs SiO_2 . The uncontaminated and contaminated kimberlite region is after Mitchet, 1986.

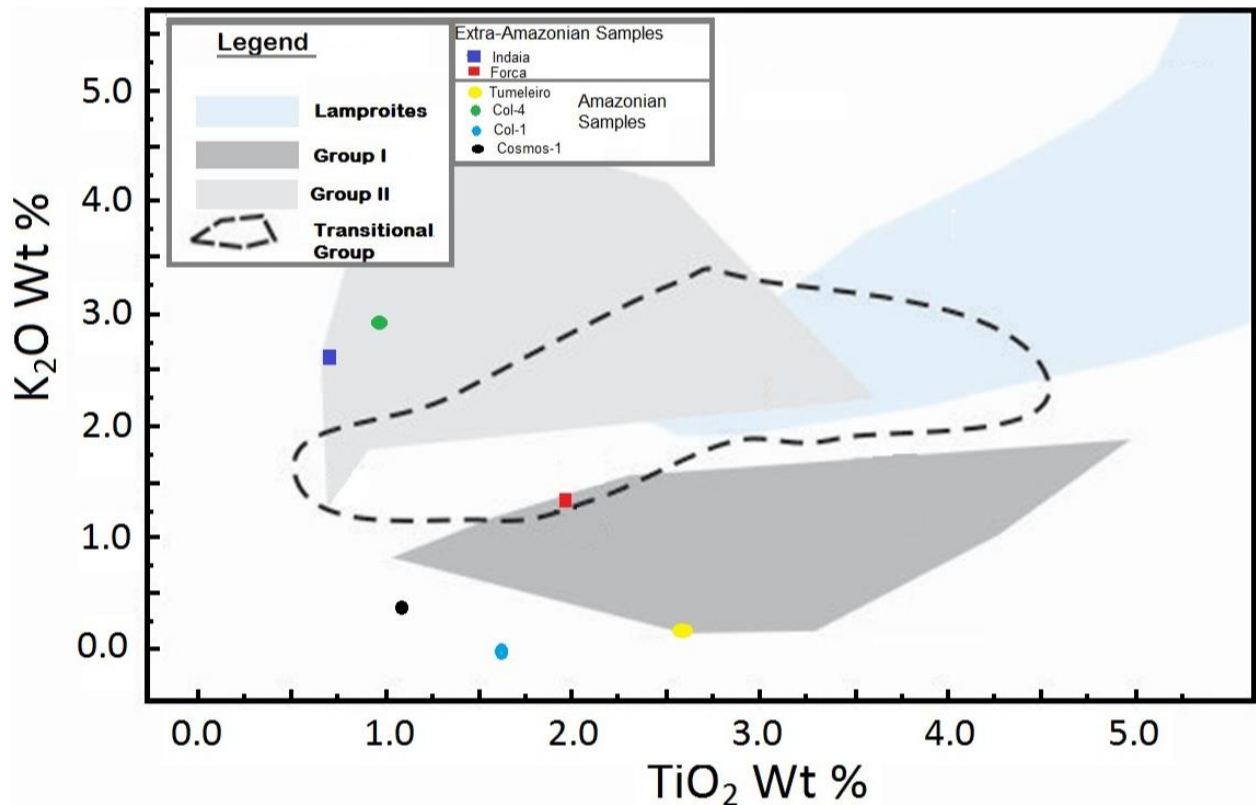


Fig.35:Major element TiO₂ Vs K₂O plot. The Kimberlite type areas pertaining to group I, II, Transition type and lamproites from Becker and le Roex, (2006); Becker,(2007) and Jaques, (1984).

The uncontaminated samples of the Extra-Amazonian kimberlites have a C.I. in the range of 1.23 to 1.25 and the Amazonian kimberlites have C.I. of 0.27 to 16.12. The samples Col-4 and Juina-23 show too high CI (10.39 and 16.12) owing to their contamination and alteration. Hence, these two samples are not taken into consideration for further interpretations.

All other samples from Amazonian region (Col-1, Tumeleiro and Cosmos-1) range are within the permissible range for uncontaminated kimberlites and hence taken into consideration for further interpretation of geochemical signatures. The Extra-Amazonian region samples (Forca and Indaia) with permissible CI range is also considered for further interpretation of geochemical signatures.

In spite of the contamination and alteration problems in the analysed samples, they plot within or slightly outside the typical kimberlite field in graph major element binary plot (Fig.34). The Extra-Amazonian region samples are less contaminated and fall within the kimberlite field on the plot. The Amazonian region kimberlites are moderate to highly contaminated. The extreme enrichment of crustal contamination has resulted in the rejection of two samples (Juina-23 and Col-4) for further interpretations. Other samples with high to moderate contamination effect are also verified if they could be used for interpretation of the geochemical signatures. They are plotted on various binary plots involving Major and trace elements as shown in figures 35 to 38. All these plots show huge variations atypical of kimberlite specific kimberlite group. This is due to the altered nature of the kimberlite sample. Hence, it is concluded that major element signatures are highly influenced by alternation and crustal contamination.

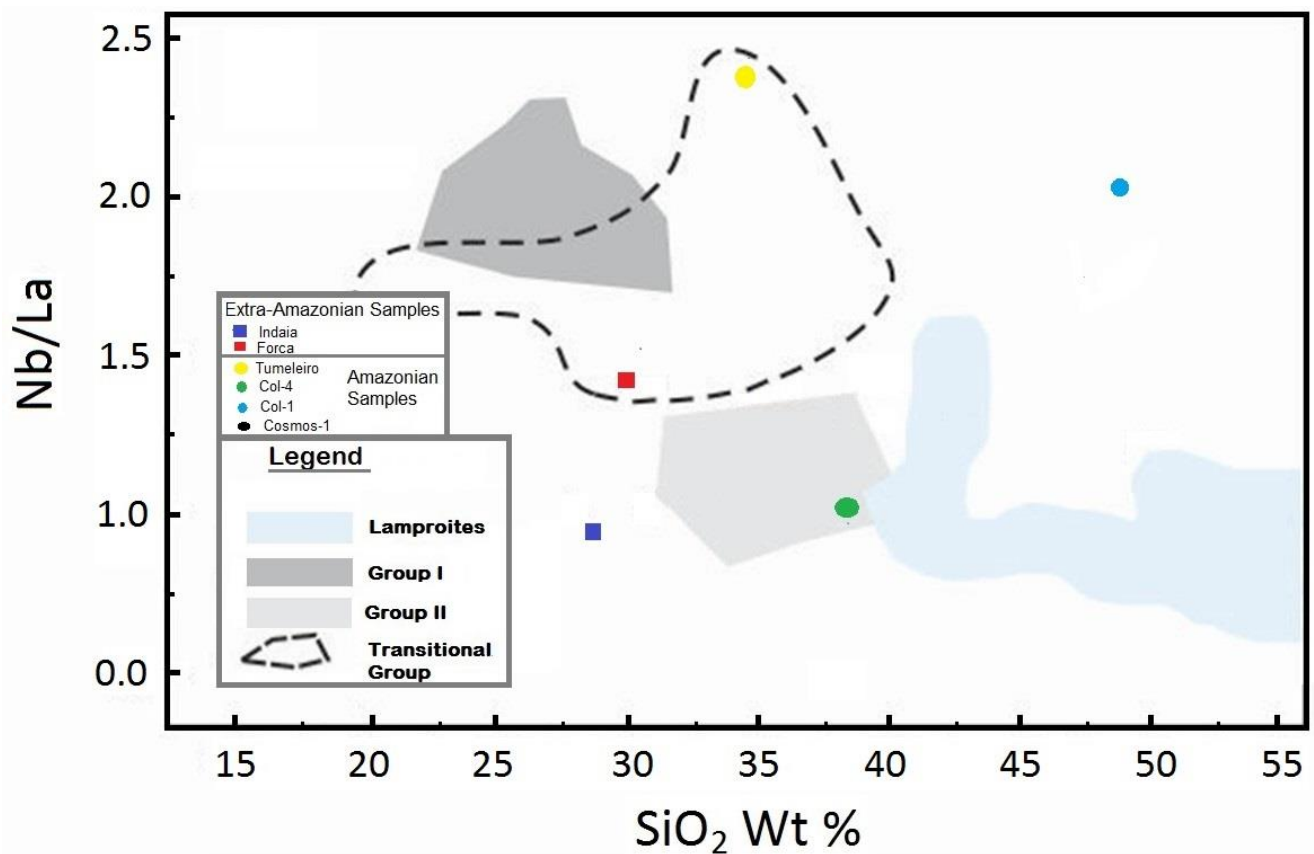


Fig 36: Major element SiO₂ Vs Nb/La plot. The Kimberlite type areas pertaining to group I, II, Transition type and lamproites from Becker and le Roex, (2006); Becker, (2007); Jaques,(1984).

Many Authors have worked on the trace-element geochemistry of kimberlites has been discussed by various authors (e.g., Dawson, 1962, 1967, 1980; Wedepohl and Muramatsu, 1979; Muramatsu, 1983; Smith et al., 1985; Mitchell, 1986, 1995; Taylor et al., 1994).

In general, kimberlites are characterized by abundances of first-period transition-compatible elements (Sc, V, Cr, Ni, Co, Cu and Zn) similar to ultramafic rocks such as dunite and peridotite, and abundances of incompatible elements (e.g., Nb, Zr, Ta, Hf, U, Th, REE) similar to alkaline rocks such as melilitite, carbonatite, and potassic lavas. Like the major elements, kimberlite trace-element geochemistry is subject to contamination problems. Incompatible trace-element abundances may be reduced by the presence of olivine macrocrysts and/or crustal contamination, but their inter element relationships remain unaffected and can be used to obtain information regarding the source regions of the magmas (Mitchell, 1986); Fesq et al. (1975) and Kable et al. (1975) concluded that elements such as

Ti, Nb, Ta, Zr, Hf, and the rare earths are insignificantly affected by crustal contamination because of their high abundance in kimberlites and related rocks. Therefore, the trace elements are significant tool in the classification of kimberlite Trace element signature of the analysed samples. Hence, the weathered samples from Amazonian region along with the Extra-Amazonian region samples are further tested with the plots for their validity to ascertain the geochemical nature of these kimberlites.

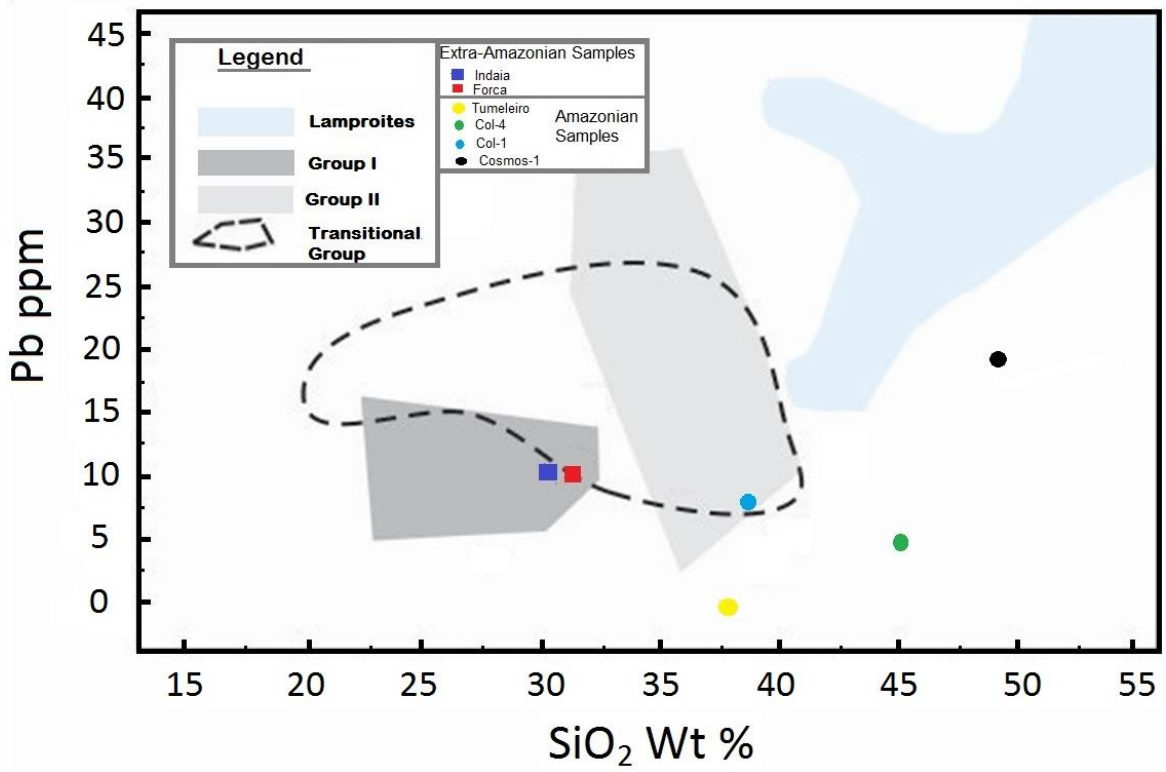


Fig.37: Major element SiO₂ Vs Pb plot. The Kimberlite type areas pertaining to group I, II, Transition type and lamproites from Becker and le Roex, (2006); Becker, (2007); Jaques, (1984).

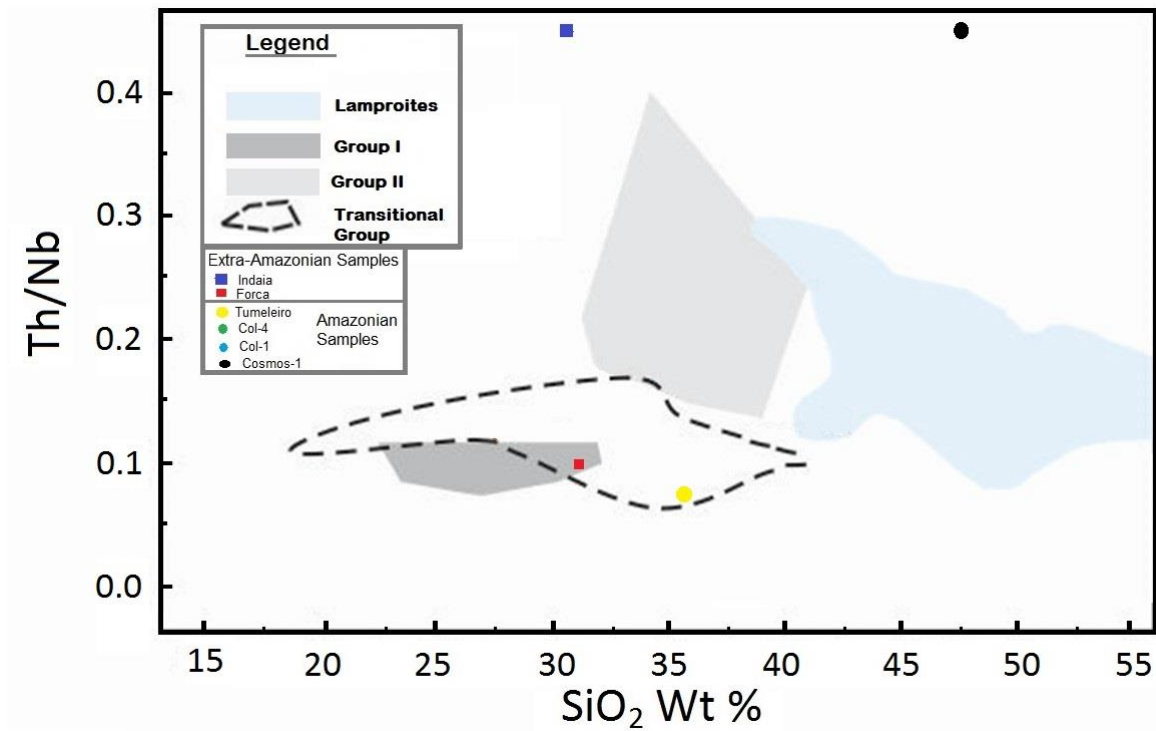


Fig.38: Major element SiO₂ Vs Th/Nb plot. The Kimberlite type areas pertaining to group I, II, Transition type and lamproites from Becker and le Roex, (2006); Becker, (2007); Jaques,(1984).

The above plots show that all samples are contaminated including the fresh looking Indaia sample. The Forca sample from Extra-Amazonian region kimberlites could be concluded to be derived of transitional group as it plots closer or within the transitional group fields. All other samples do not give a clear pictures about the group to which they belong.

The distribution of rare earth elements normalized to chondrites (Fig. 39) and the primitive mantle (Fig.40) are plotted in graphs. The La content of Extra-Amazonian region samples (Forca and Indaia) is 1000times the levels of chondrite sample and the Amazonian region samples (Cosmos-1, Col-1 and Tumeleiro) is 100 to 500 times the chondrites levels. The Lu contents are lower and are 10times the chondrites for Extra-Amazonian (Forca and Indaia) samples and less than 10 to 10 times the chondrites for the samples from Amazonian region (Cosmos-1, Col-1, Col-4 and Tumeleiro). If the extremely contaminated samples are left behind, the Lutetium content is less than 10 times the chondrite level.

In Figure 40, There is a significant Sr negative anomaly for all kimberlites and again all the samples of this research have positive anomaly for the Nd element. The Sr negative anomaly of the samples shows a parent mantle characteristics of these rocks, previously

depleted in these elements. Apart from this, there are no significant anomalies when the region is taken together. These trace element patterns, individually shows minor troughs and crests in the trend when compared to the typical South African kimberlite trends (Fig.39, 40 and 41). These individual trend needs to be further confirmed either by more sample analysis and or by mineral composition analysis for the trace elements. There might be a contamination effect that has also affected the trace element concentrations probably due to xenocrystal contamination from mantle.

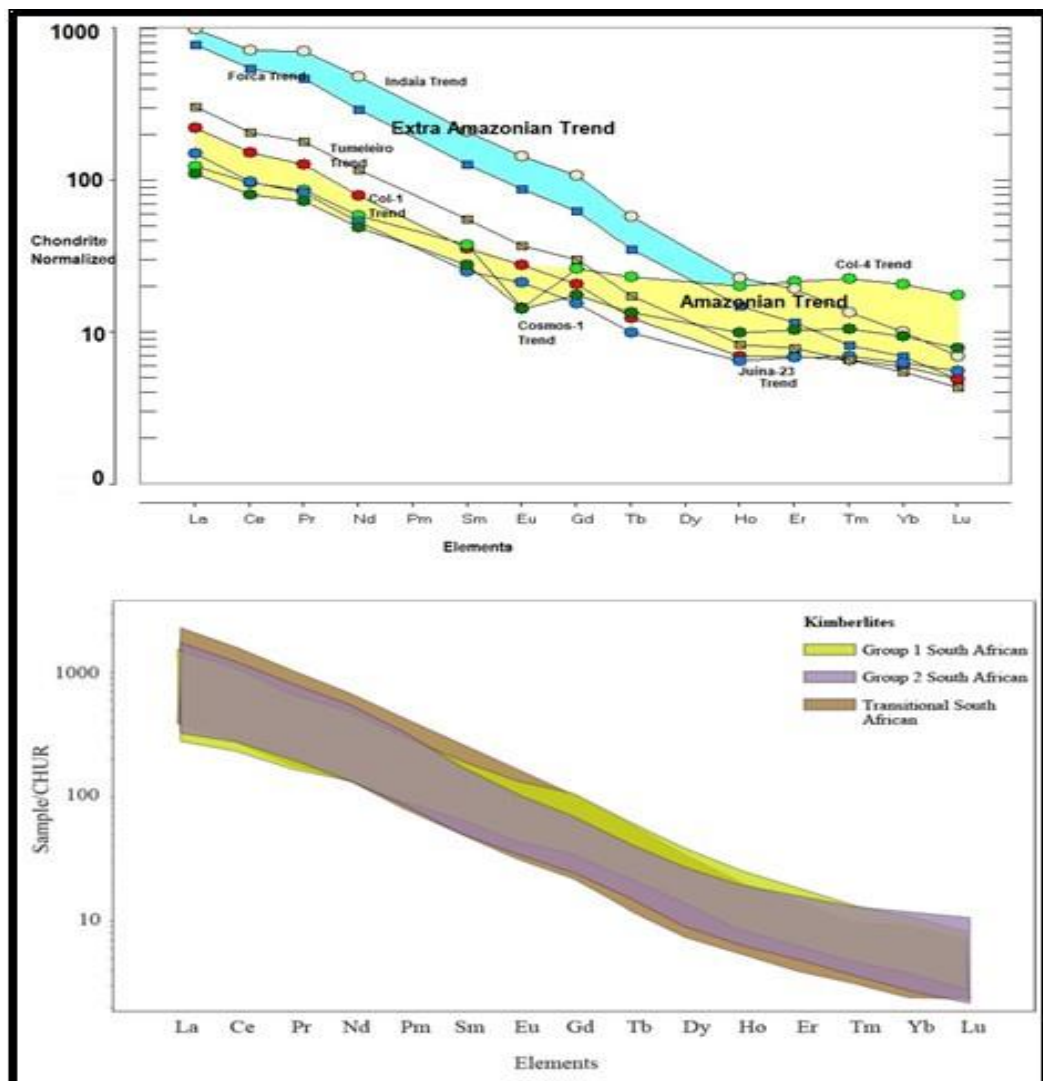


Fig. 39: Chondrite normalized REE Pattern graph for analysed samples and South African trend (Data from Becker and Le Roex 2006 and Becker et al., 2007)

From the major and trace element signatures of the analyzed samples, it is concluded that the Amazonian kimberlites are contaminated to such an extent that no precise conclusion could be drawn as far as their type is concerned and the Extra-Amazonian region kimberlite Forca could be concluded as Transitional type, which also needs further studies to support.

Indaia also poses contamination problems and could not be conclusively classified. To ascertain these characteristics further, more advanced geochemical analyses and interpretation techniques of isotopic signatures like Sr and Ni (Bizzi et al, 1994 and 1995); Hf isotope studies will provide more insight. They provide robust method for group I, II and transitional type kimberlites distinction and their associated source region characters.

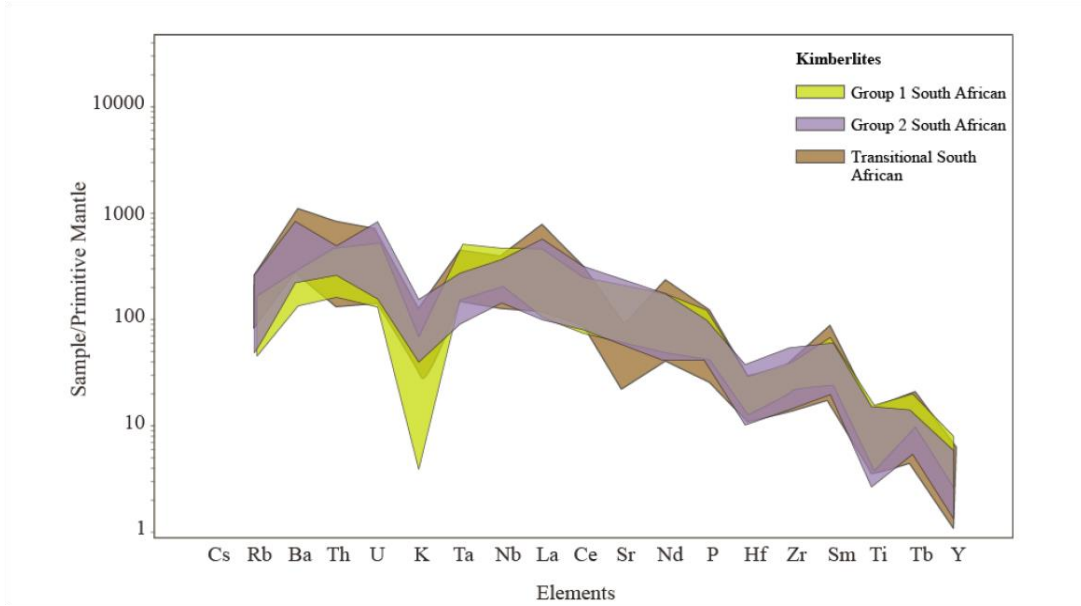


Fig. 40: Primitive mantle normalized multi-element graph (Mc Donough and Sun 1995) of South African Group I, Group II and transitional group kimberlites (Data from Becker and LeRoex 2006 and Becker et al., 2007)

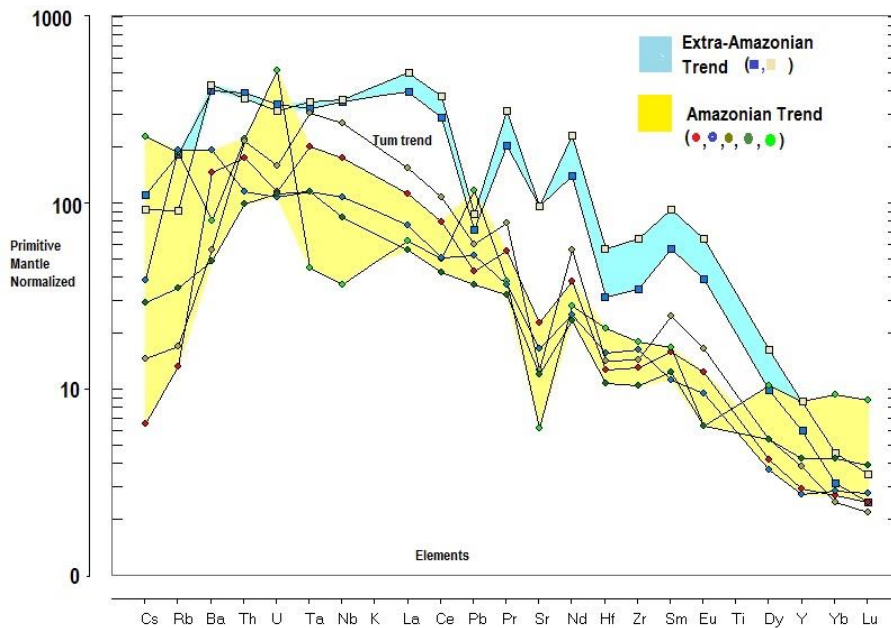


Fig. 41: Primitive mantle normalized multi-element graph for analysed samples after Mc Donough and Sun 1995.

Hence, the earlier author's conclusion as mentioned in the review section on kimberlite grouping for Brazilian corridor-125 kimberlites are followed in the final interpretation of this research.

Chapter 12

Plate Tectonic Reconstructions

The current day position of continents and ocean is the result of various paths the plates have travelled. These plate motions can be modelled and visualized with time based of scientific clues and inferences. Such modelled plate position back in time is called plate tectonic reconstruction. Reconstructions are based on calculations of the paleo-position from various geological, geophysical and mathematical data. These data can be joined to the simulated plates which will equip the researcher to trace the plate motions and further interpret the interactions of data through geological times. There are numerous softwares to model the paleo-position of plate. Gplates is state of the art software which has been of immense value to scientific community in recent times.

Gplates: this software enables interactive visualization of plate-tectonics. It is configured to handle geographic information system functionality and raster data together under the reconstructions. It is innovative software allowing the visualization and manipulation of reconstruction and associated data through geological time. This software runs on various operating systems, windows operating system compatible version is utilized in this study. Gplates is developed by an international team of scientist, professional software developers and postgraduate students like Scientists at the University of Sydney, Norwegian Geological Survey and Cal Tech have also been compiling sets of global data for plate boundaries, continental-oceanic crust boundaries, plate rotations, absolute reference frames and dynamic topography. The best part of this software is it is open-source software which is free for working. It has been licensed for distribution under GNU (general public license) version 2.

Gplates is state-of the art software as it can handle and visualize data in variety of formats geometries like raster data to link plate kinematics to geodynamic evolution models. Finally it can produce high-resolution paleo-geographic maps and animation videos for presentation.

Plate tectonic reconstructions are based on certain assumptions and principles. The motion of plates on globe is governed by Euler's fixed point theorem: "Every displacement from one position to another on the surface earth can be regarded as a rotation about a suitably

chosen axis passing through the center of the earth.”The axis of rotation is the suitably chosen axis passing through the center of the earth. The poles of rotation or the Euler’s poles are the two points where the axis of rotation cuts through the earth surface (Fig. 42).

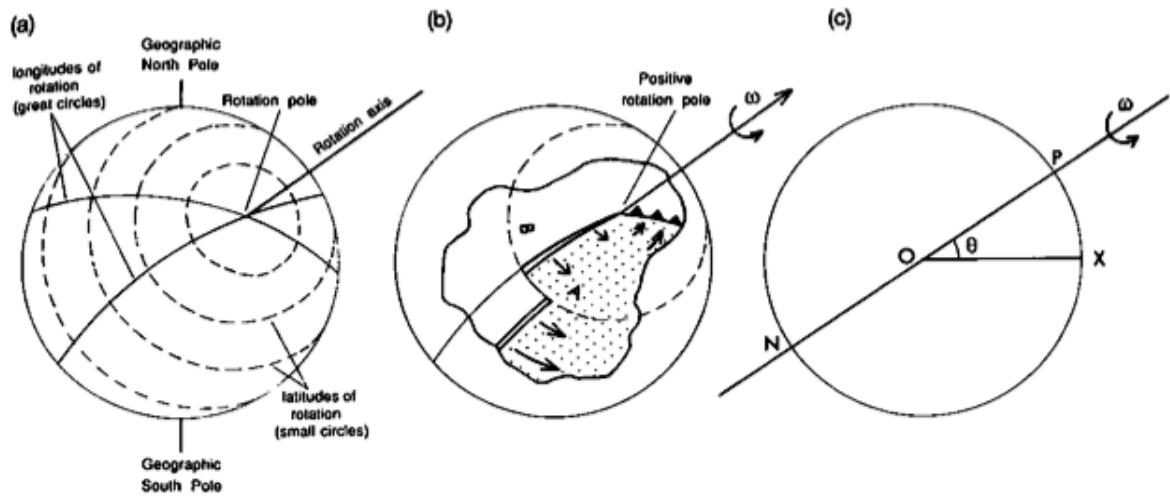


Fig.42: Diagrammatic representation of Euler pole and plate rotation relationship.

The plates behave as rigid lithospheric blocks during plate motion; whereas boundaries are dynamic. Hence, they are called rigid plates with dynamic boundaries or dynamic plate polygons. These rigid plates with dynamic boundaries moves on the globe with a rotation axis passing through the center of the Earth called Euler pole of rotation. The relative velocity ‘ v ’ of a certain point on the earth surface is a function of the angular velocity ‘ ω ’ according to:

$$v = \omega R \sin\theta$$

where R is the earth radius and θ is the angular distance between the pole of rotation and point on the plate of interest. Thus, the relative velocity is equal to zero at the poles, where $\theta=0$ degrees and is a maximum at the equator where $\theta=90$ degrees. The relative velocity is constant along small circles defined by $\theta=\text{constant}$. Note that large angular velocity does not mean large relative velocity.

Plate tectonics on a spherical earth can be defined by rotation poles and rotation axes for plates on either side of mid-ocean ridges. Transform faults are arcs of small circles about a rotation pole. The rotation pole therefore must lie somewhere on a great circle that is perpendicular to that small circle. So if two transform faults are available the intersection of the great circles marks the position of the rotation pole.

Determination of rotation poles and rotation axes for plates on either side of mid-ocean ridges: The spreading rate of mid ocean ridge changes as a function of sine the angular distance ' θ ' from the rotation pole. Thus if the spreading rates at various points along the plate boundary can be measured the rotation pole may be estimated.

Triple junctions: Triple junction is a point at which three plates meet. A triple junction is stable if the relative motion of the three plates and the azimuth of their boundaries do not change in time. An unstable triple junction exists only momentarily before evolving to a different geometry.

Practically triple junctions are the point where the plate would deform and develop into rift and move apart depending on the type of the stress and other conditions. This is the starting point along which a rigid plate breaks apart to form the dynamic plate boundary. An example is seen in the Fig.43. When one or more of the rift zones on the plate fails to develop into a rift. It remains as shear zones or trans-lithospheric structural weakness. There are many failed rifts in world which are easily recognised by the presence of mafic dyke swarms along these structures.

During plate tectonic reconstructions a reference frame is taken which remains stationary and the plate or point on the plate which is of importance is moved according to the

principles of plate tectonics. In this study, the fixed hotspot frame is utilized to all reconstructions. This hotspot fixed reference frame is also known as absolute reference frame as there is no net rotation (NNR) of each plate with respect to average of all the world's plate velocities.

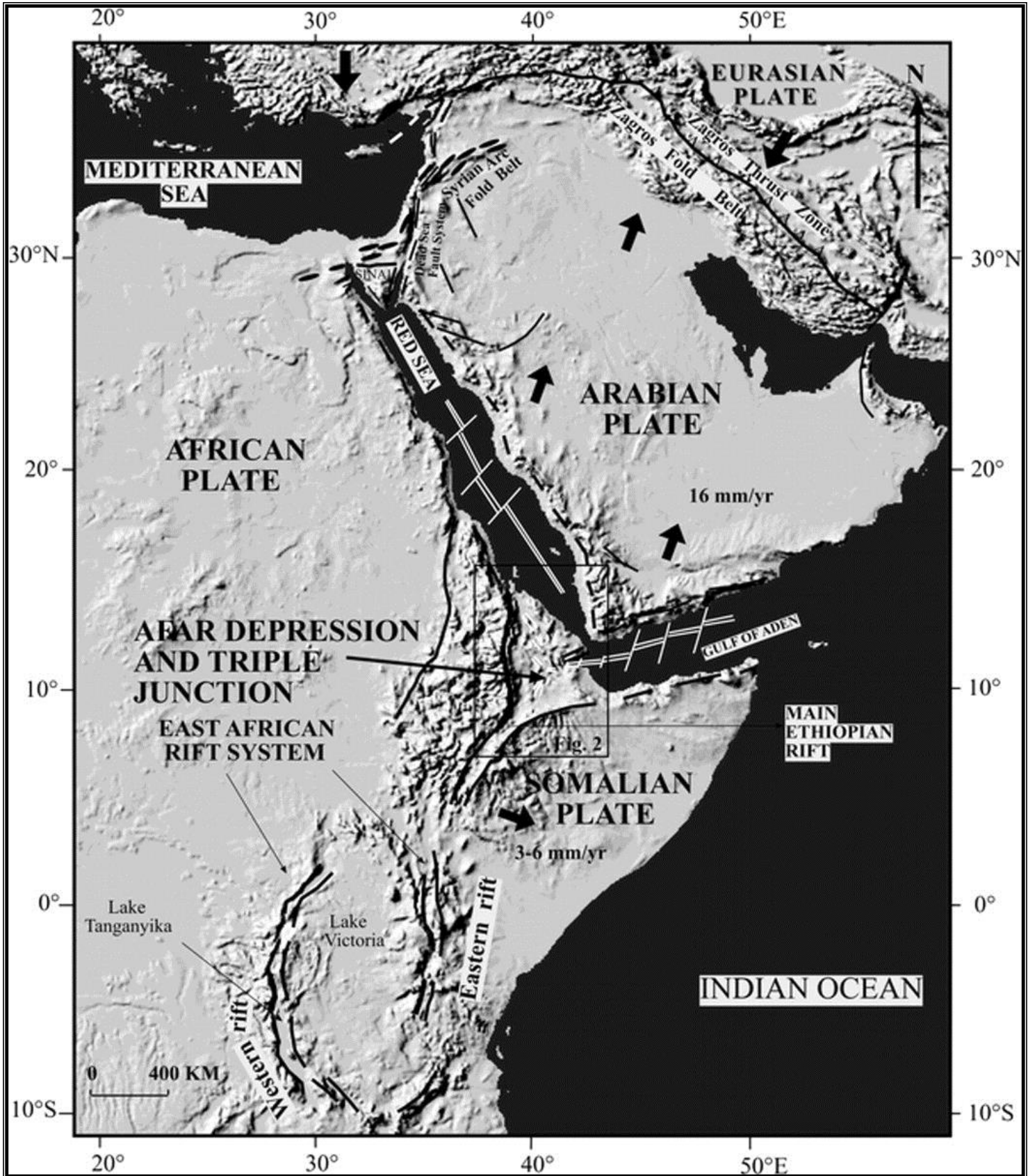


Fig. 43: An example of triple junction with African, Arabian and Somalian plates are currently rifting. Source of figure from Samson et al, 2002.

Plate Tectonic Events associated with Brazilian kimberlites Age Clusters

Kimberlite are emplaced along reactivated pre-existing zones of weakness or newly created zones of weakness during different stages of supercontinent life cycle (DeWit. 2007; Moore et al. 2008; Jelsma et al. 2009). Thus, the emplacement age of kimberlite clusters are precise time capsules in the whole history of various supercontinent life cycles. The relationship between the emplacement age and plate tectonic event can be deduced by looking at the reconstruction of the Brazilian plate back in time. The plate tectonic reconstruction is carried out up to 300 Ma. From 300 Ma to 200 Ma reconstructions is modelled based on the present day position of Brazilian plate and plate reorganisation along with African and Laurentian plates to which it was attached. The whole land mass behaved as one unit and was moving south. The motion continued even further up to 190 Ma and switched over South Atlantic rift with initial E-W followed by NE motion of South American plate.

The reconstruction of Brazilian plate form 200 Ma is taken from the Heine et al., 2013 plate model data. In this model the authors have achieved a full fit by structural restoration of the South Atlantic conjugate margins and intra-continental rift basins in Africa and South America. Heine et al (2013) have related the kinematic model of the late Jurassic/Early Cretaceous rift structures to observations from marginal and failed rift basins from the South Africa and South America conjugate margins. According to this model, the pre-rift extensions and plate kinematics are categorized into three phases:

- a) Phase I: 140 to 126.57Ma: During this phase there was intra-continental rift basin formation.
- b) Phase II: 126.57 to 120.6Ma: This phase was characterized by a change in velocity and direction of the plate motion.
- c) Phase III: 120.6 to 100Ma: this is the second phase of increased plate velocity and finally the South American and South African Plate drifted apart.

226 to 268 Ma: Amazonian craton kimberlites emplaced between 226 and 268 Ma. This episode of kimberlite magmatism is linked to the Permo-Triassic plate reorganization before the Pangea rifting at 225 Ma.

120 to 122 Ma: This is related to incipient South Atlantic rifting.

80 to 95 Ma: Tectonic trigger of kimberlite magma generation while spreading is in progress and plate motion paths are marked by cusps (variation in direction) and jogs (variation in velocity). Changes in plate motion may have caused shearing of subcontinental lithospheric mantle with strain accommodation along lithospheric discontinuities in this case in particular the continental continuation of oceanic fracture zones.

74 Ma: There is only one kimberlite named Sucesso-08 (Felgate, 2014) with this age data. This is the only emplacement age which is younger than the known kamafugites.

Thus emplacement of kimberlites magma from 74 Ma to 268 Ma along the corridor-125 with intermittent short periods of kimberlite emplacement peaks is linked to opening up of Pangea plate reorganization. South Atlantic Ocean and strain propagation with melt migration along the continental extension of the oceanic transform fault due to cusps and jogs during the Brazilian plate motion. The periods devoid of kimberlite emplacement corresponds to uniform plate motion. The phase I of Heine's model is characterized by the rift basins formation which probably also activated older structures and thus when there was cusp and jog during Phase II kinematics of South American plate motion and the 120-122 Ma kimberlites were emplacement. During phase III, there has been significant jog with respect to South American plate kinematics but this increase in velocity has not favored kimberlite emplacement. After this third phase the South American and South African plate drifted apart. This has resulted in enormous basaltic flows in the mid ocean ridge and formation of oceanic crust. With the plates continued drifting, on the continental part of South America there is another phase IV between 80 to 90 Ma corresponding to the highest kimberlite emplacement peak. The plate tectonic reconstructions carried out in gplates is presented in figures 44 to 50.

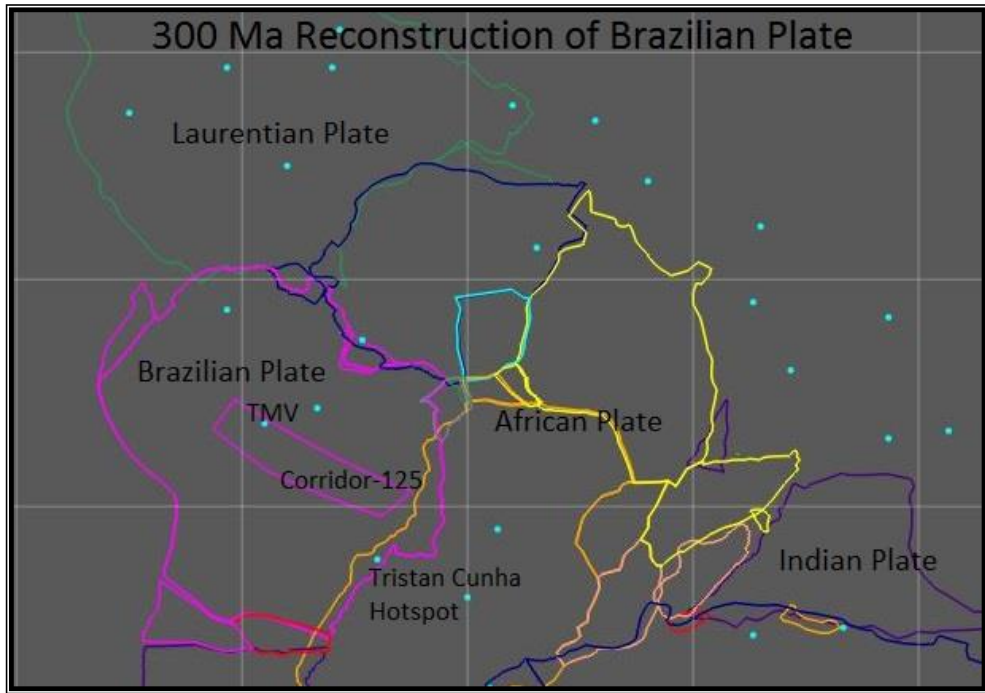


Fig.44: 300 Ma reconstructions with Brazilian plate in pink boundary, African plate with multiple blocks and Laurentian plate in green, the position of the corridor-125 is also marked.

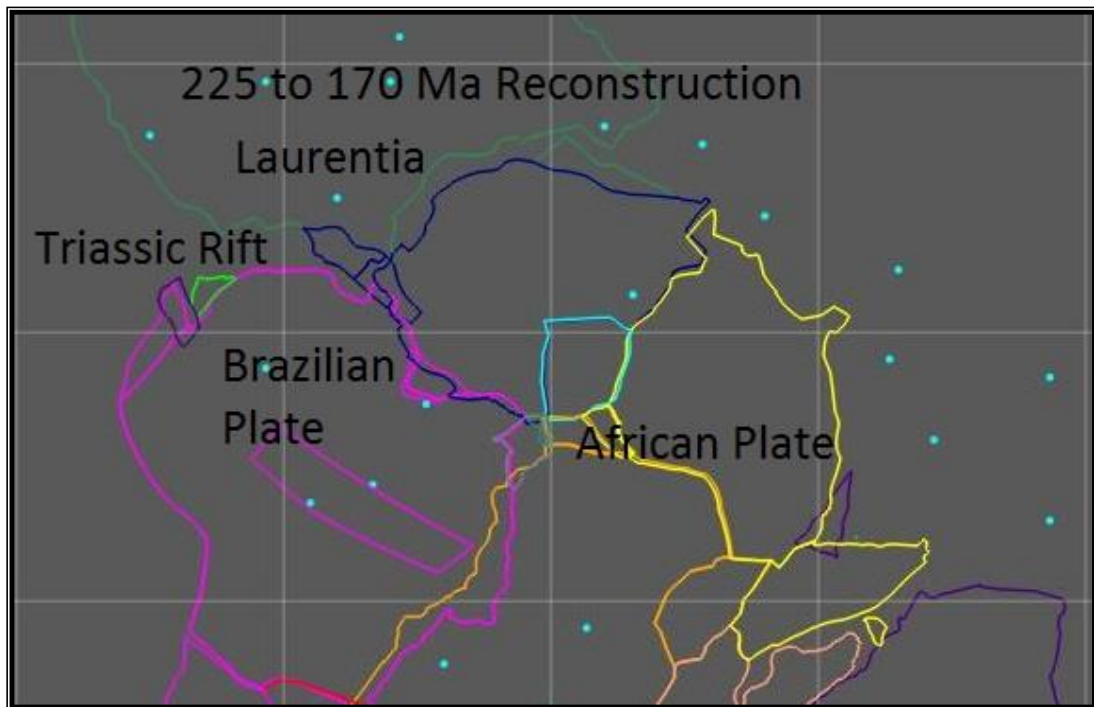


Fig.45: 225 Ma to 170 Ma reconstruction of Brazilian plate.

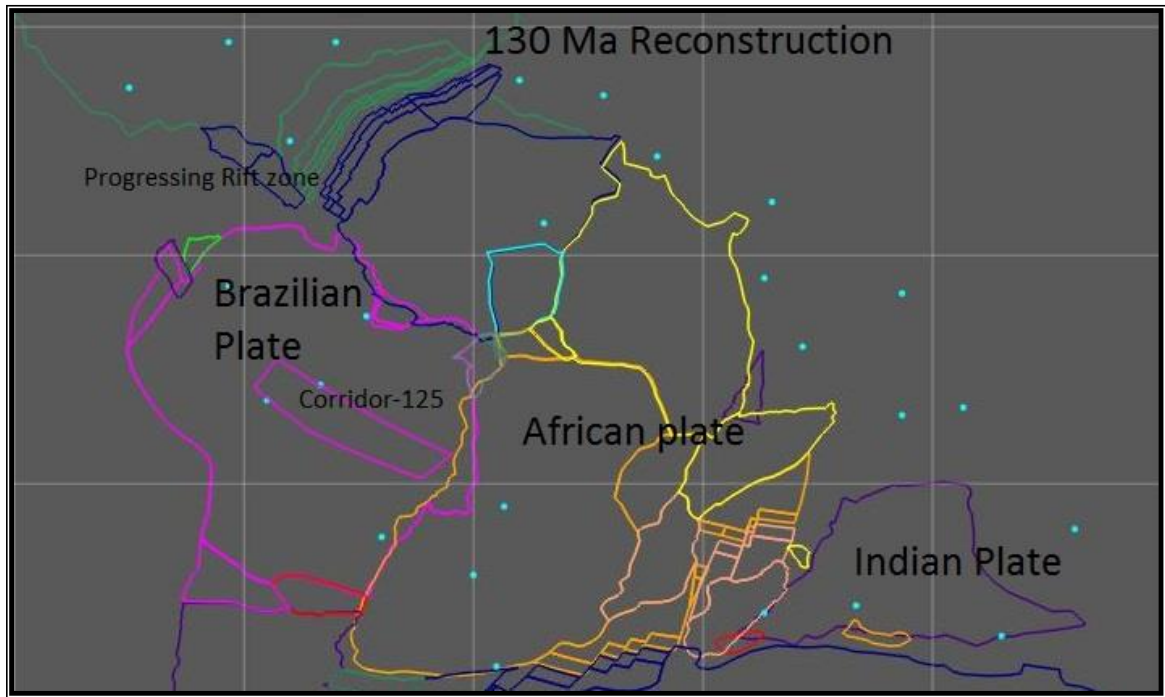


Fig.46: 130 Ma Reconstruction of Brazilian plate with progressing rift between Laurentian and Brazilian plate.

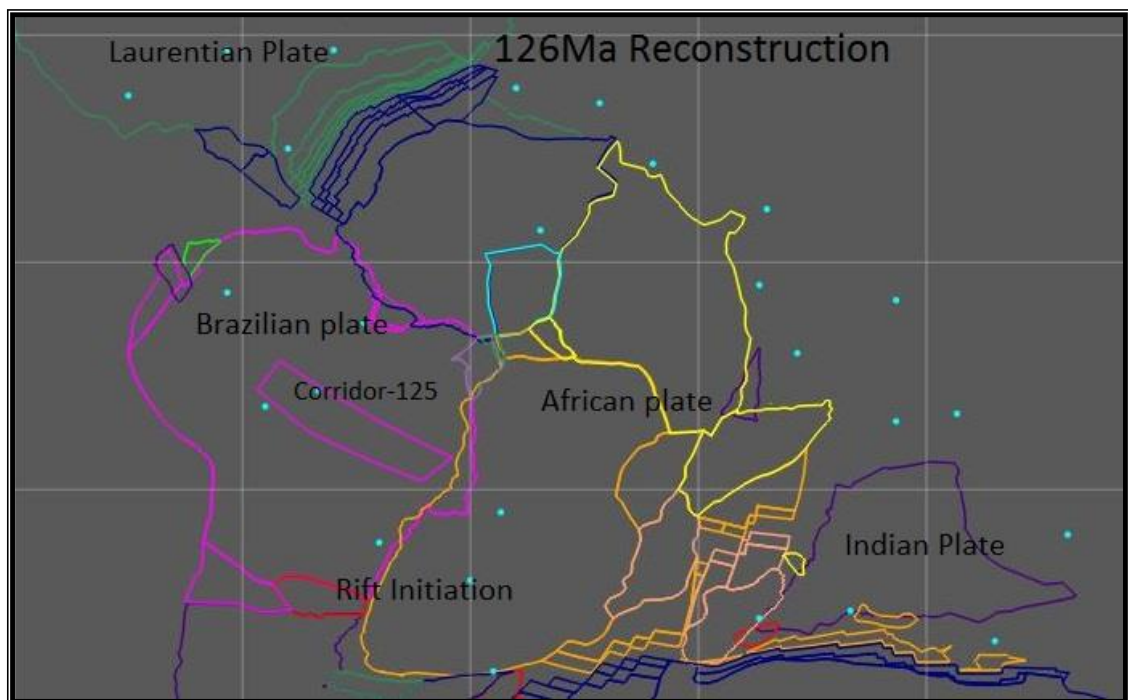


Fig.47: 126 Ma Reconstruction of Brazilian plate with South Atlantic rift initiation at the southern tip of the South American (Brazilian plate).

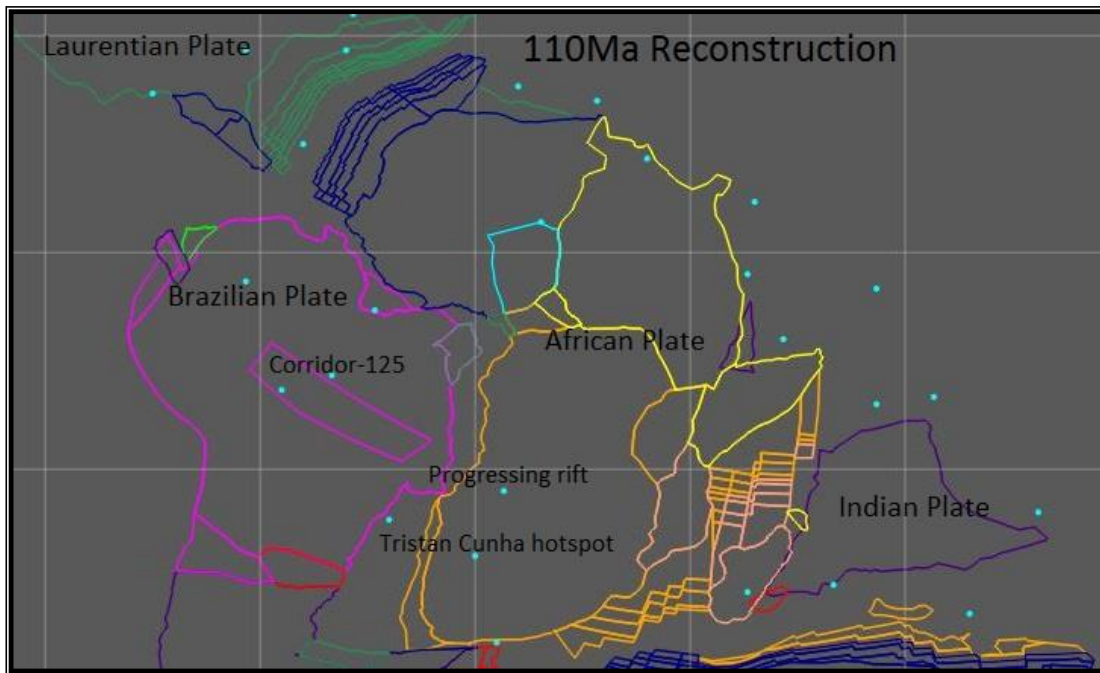


Fig.48: 110 Ma Reconstruction of Brazilian plate with progressing South Atlantic rift. Tristan Cunha hotspot is seen on the newly developing oceanic part of the Brazilian plate well below Corridor-125.

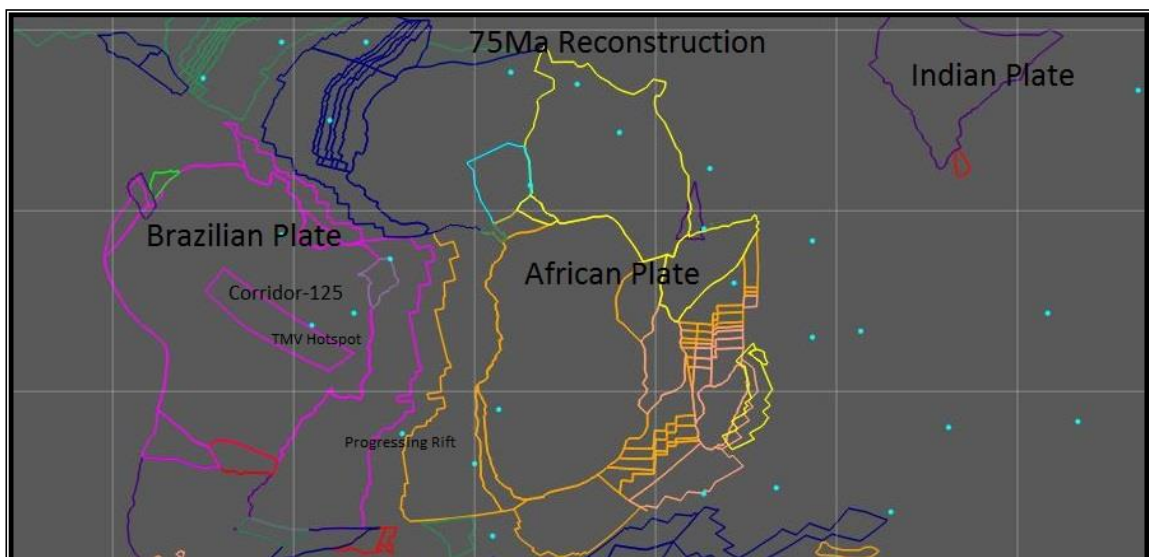


Fig.49: 75 Ma Reconstruction of Brazilian plate with progressing South Atlantic rift. Trinidad Martin Vaz (TMV) hotspot is seen under the corridor-125 of the Brazilian plate. This hotspot moves away from the corridor-125 after 75 Ma further north and finally reaches the oceanic crust on the east coast of Brazil.

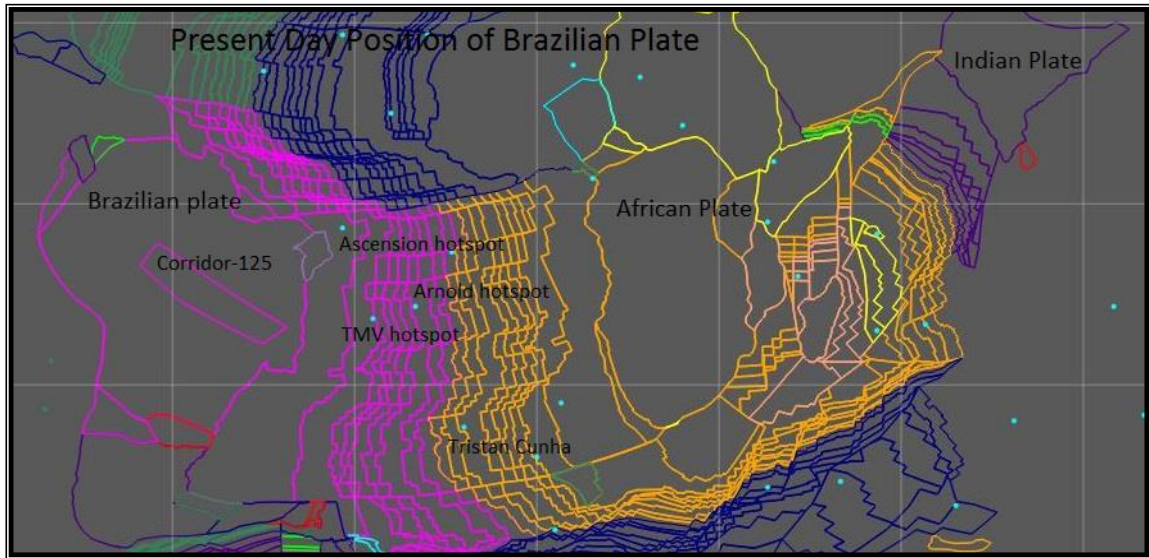


Fig.50: Present day position of Brazilian plate and east coast hotspot locations.

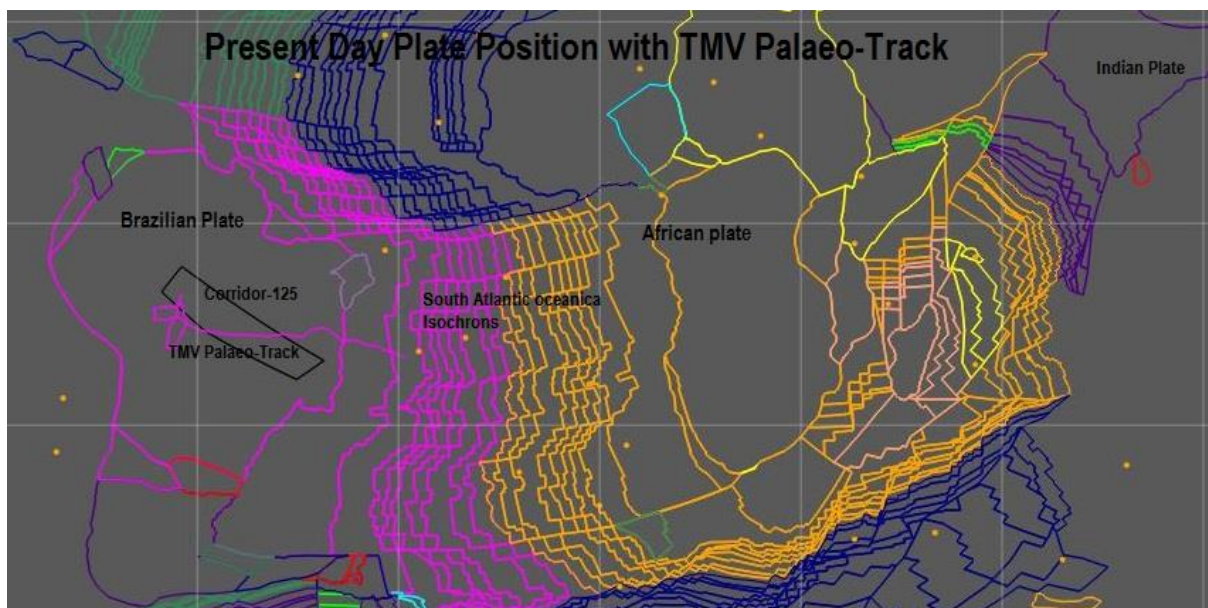


Fig.51: Trinidad Martin Vaz (TMV) Palaeo-track over Brazilian plate in relation to corridor-125 from gplates for the present day position of Brazilian plate.

Discussion on the role of Hotspot Trindade-Martin Vaz (TMV) in kimberlite emplacement

Hotspots and Kimberlite Association: The validity of influence of hotspots and kimberlite emplacement within the South American plate during South Atlantic rift is analysed by using plate reconstruction.

It has been observed that from 225 Ma to 121 Ma there has been a quiescent period with respect to kimberlite emplacement along the Corridor-125. After which the kimberlite emplacement has peaked at 122 Ma to 120 Ma followed by another short period devoid of kimberlites from 94 to 119 Ma. Again, kimberlite emplacement peak reached its maximum at 80 to 95 Ma. Lastly, a single kimberlite spike at 74 Ma is observed. In total, the kimberlite emplacement episode has lasted from 268 Ma to 74 Ma with intermittent quiescent periods of short duration along lineament Corridor-125.

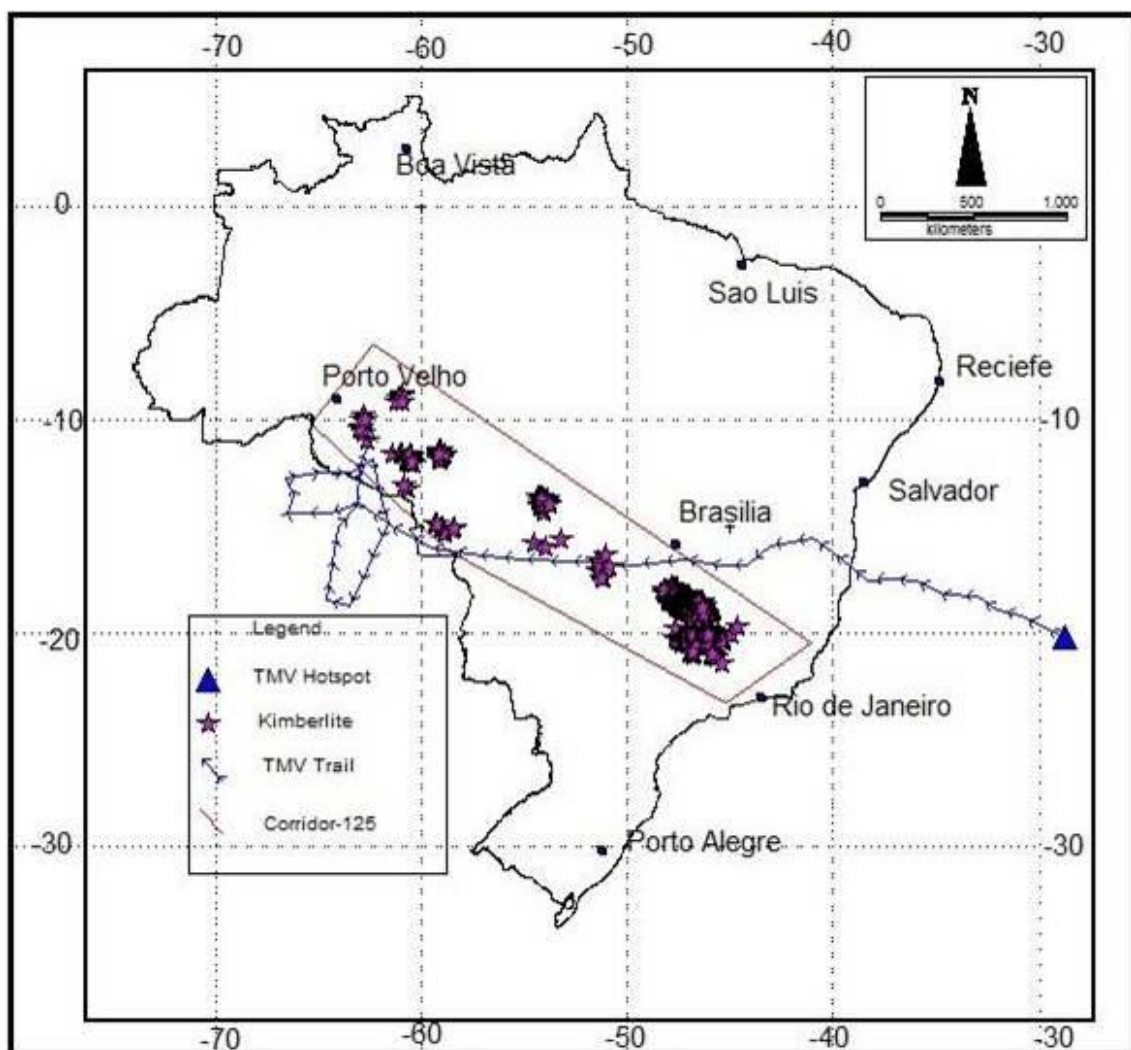


Fig.52: Georeferenced TMV (Trindade Martin Vaz) hotspot Trail up to 300 Ma with Corridor-125 and kimberlite occurrences.

Crough et al (1980) suggested age progression along the Corridor-125 due to the passage of the Trindade hotspot along the length of the lineament. With more age dating of kimberlites, the scenario has changed with respect to age progression along the Corridor-125. With a fixed hotspot reference frame, plate tectonic reconstruction depicts the passage of the South American plate along the hotspot TMV. As the South American plate moves over TMV hotspot due to Pangea plate organization and South Atlantic opening, the TMV traces a wavy path as shown in the (Figs.51 and 52). It does not coincide exactly with the corridor-125 but is found close to it. The TMV motion path has traced entire the length of Corridor-125 with initial loping around 200 Ma to 180 Ma at the North-Western end and then following the entire length as the plate as the plate motion continued. With more kimberlite age data available now, the association of the hotspots like TMV directly in the kimberlite magma generation and its emplacement is not witnessed as there is no definite age progression as suggested by Crough.

The youngest kimberlites are only present towards the south-eastern end of corridor-125 whereas the oldest is only observed along the north-western end. The intermediate age kimberlites are found mixed up all along the lineament, which does not confirm the interpretation of hotspot influence and hence this hypothesis is unsustainable. This result confirms, that, the role of paleo-track of TMV or other hotspot track is ruled out as the major cause for kimberlite emplacement along Corridor-125.

Chapter 13

Discussion

The kimberlites are found emplaced all along the corridor-125. The spatio-temporal kimberlite peaks separated by distinguished quiescence on the corridor-125 with respect to kimberlite distribution and episodicity. On local scale, structural controls for the kimberlites are due to thrusting. Fractures, faults and shear zones. All along the corridor-125, kimberlites are associated with igneous alkaline provinces. On subregional scale arches, continental rift zones and other basement structures control kimberlite emplacement. On continent wide scale, structural reactivation of older basement structures provides important emplacement loci. There is evidence of repeated reactivation of basement structures. Corridor-125 is an excellent example of continental scale structural control which is in turn composed of several mega- and giga lineaments. This forms a continuous weak zone on continent and oceanic part of the Brazilian plate. This continental weak zone being older manifests itself with newly developing oceanic crust and its signatures and evidence can be traced back to ocean floor up to the mid-ocean ridges. This emphasizes the genetic link with the rifting and the structures on continental rigid plates. This is especially much easy to find evidence from the ocean floor magnetic anomaly data and global crustal magnetic data for younger oceanic rift basins. The older ones are complicated or even masked by the overprinting of younger events. South Atlantic oceanic transform fractures can be easily traced to decipher the genetic link between the oceanic and continental structural weakness and its manifestation as lineament. Other good examples where such genetic link is easily observed are the Ponta Grossa arch and its associated fracture zones on the ocean floor. Transbrasiliano lineament and its associated oceanic transform fracture zones. Apart from kimberlites, there are other alkaline rocks found on corridor-125 proving the fact that there is switching of magma type with continued rifting.

Major kimberlite episodes found on corridor-125 are

1. 226-268 Ma
2. 120-122 Ma
3. 80-94 Ma
4. 74 Ma

These kimberlite emplacement peaks are associated with major plate kinematics with cusps and jogs in the plate motion or both. It is proposed that, the tectonic trigger of kimberlite magmatism along corridor-125 is associated with two rift events. The first tectonic trigger is Permo-Triassic rifting of North America and South America around 290-225 Ma. In this case the kimberlite emplacement is associated with the Pangea plate re-organization just prior to rifting. It is also interesting to see these kimberlites are of distinct group I type or lamproites with ultra-deep inclusions (Kaminsky et al., 2010). The presence of ultra-deep inclusions associated subduction related source quite evident from the Pacific plate subduction source. Another interesting feature of this subduction related source is that they are of short duration compared to tectonic trigger only related to rifting.

The second tectonic trigger is the Cretaceous rifting of South Atlantic rift from 125 to 74 Ma. In this case, the kimberlites are associated only with rifting plate with major cusps and jogs in plate kinematics. This magmatism has three major episodes and is a long term one compared to the subduction related one. The problem in assessing the kimberlite emplacement along corridor-125 is the presence of 120 Ma kimberlites on both the regions (Amazonian and Extra-Amazonian) and the presence of 95 Ma kimberlite related to subduction on Amazonian region which is otherwise characterized by older Permo-Triassic kimberlites.

Dual Tectonic Trigger model of Kimberlite emplacement in Brazil.

It is proposed that Dual Tectonic trigger model of kimberlite emplacement in Brazil satisfies the observed nature of kimberlites. The Initial rifting of South American plate for North American (Laurentia Plate) has triggered kimberlite emplacement along the subduction zone and has resulted in Permo-Triassic kimberlites on Amazonian craton with the reactivation of greater than 1.0 Ga basement structures. This was followed by rifting at 225 Ma at the northern border of the country. Soon the plate reorganization has reactivated structures on the East coast extending up to Upper Paraguay thrust zone (Suture zone of Amazonian and São Francisco Craton) as we see 120 Ma kimberlite in Paranatinga cluster with increased reactivation stress along the eastern coast preparing for the rift, high number of kimberlite emplacements were concentrated on to the Extra-Amazonian region. Only two peak episodes of kimberlite magmatism has affected the Amazonian region due to South Atlantic rift which needs further confirmation.

The Permo-Triassic (225 to 268 Ma) kimberlite found in Amazonian region is absent in the Extra-Amazonian region. Whereas on contrary to the above observations, similar age group younger (120Ma) kimberlite occurrences on both the regions along the corridor-125 contradicts the above observed features of non-continuation. The Amazonian craton is interpreted to have amalgamated with Extra-Amazonian region from 650 to 630 Ma (Cordani et al. 2013; Neves and Fuck. 2014). On The Amazonian region any tectono-magmatic events prior to 226 Ma is unique to the craton and does show different signatures than that of Extra-Amazonian region. Whether the younger tectono-magmatic events are genetically linked to the Extra-Amazonian region or not is an interesting area for future research. The occurrence of 95 Ma Juina magmatism and its magmatic trigger is not yet established.

Hence continuation of Corridor-125 from Extra-Amazonian region beyond Transbrasiliano lineament into the Amazonian craton is a matter of debate. Firstly, because the continuation of NW-SE structures found in the Extra-Amazonian region stops right at the Transbrasiliano lineament. The structural trend orientation also varies and lastly, significantly older age of kimberlites from Amazonian craton implies different source and trigger for kimberlite magmatism.

Hence, it is concluded that kimberlite occurrence of corridor-125 from Extra-Amazonian region and on to Amazonian region and the false appearance of continuity is merely a coincidence. Structurally, these two regions are different and the styles of kimberlite magmatism and its geochemistry clearly show that these regions are different and there is no structural continuity.

Geophysical aeromagnetic data has revealed interesting set of structural controls on kimberlite emplacement in Brazil. These structures are masked by the sedimentary cover. The integrating the mapped structures and geophysical structures from the study area has resulted in revised basement structural frame work controlling the kimberlite emplacement which is quite different from the mapped structures alone. This resulted has been observed in the geophysical magnetic lineaments map and has facilitated better understanding and constraining of the Dual tectonic trigger of the kimberlite emplacement in Brazil in study area.

Kimberlite aeromagnetic signatures are quite complicated in Brazil due to various reasons like sediment cover masking the signatures of small diameter pipes; presence of multiple intrusions also masks and complicates the signature identification. Coupled to this, the presence of other large diameter alkaline intrusions in the same area masks the kimberlite signatures completely in some cases. Another drawback is the presence of intensely packed structural lineaments again masking the signatures. In spite of all these drawbacks, there are obvious kimberlite signatures (though not clear on the anomalous magnetic field map) is clearly seen as bulls eye anomaly on the Analytical signal map. Tilt derivative and in some cases on Reduced to pole maps. There is good correlation of the obvious bull's eye signatures and Euler Structural Index-2. There are some kimberlite signatures which are very subtle. Further ground magnetic and gravity data will be a good tool to isolate better and new kimberlite signatures. It is also observed that the Anomalous magnetic field map signatures are more complicated and even the analytical signal signatures due to the fact that the study area is in the low latitude region. The presence of remanent magnetism is very clearly seen by the way the dipolar anomalies transform during transformation to reduced to pole maps.

Conclusions

There has been advances and increase in age dating of Brazilian kimberlites but still the data is limited. The following conclusions could be drawn from this study:

- The onset of the major period of kimberlite magmatism coincided with incipient breakup of Gondwana when such structures are expected to develop (before ocean crust formation).
- Subducted material gives rise to change in magma composition during short periods of kimberlite emplacements.
- The geometry including movement direction can be gleaned from studying “connected” transform faults on the adjacent oceanic crust.
- Long term episodicity is determined by periods of supercontinent breakup triggered by extension
- Short term episodicity is related to a combination of processes of Subduction, reactivation and rifting.
- The corridor-125 is a continental translithospheric lineament made of two sets of lineaments one each on Amazonian and Extra-Amazonian region.
- The Extra-Amazonian region corridor-125 is an older lineament that has a genetic link to younger South Atlantic transform fractures formed during the opening of the South Atlantic Ocean during West-Gondwana break up. It comprises of numerous mega- and giga-lineaments. Fractures, faults and minor structures which have been formed and or reactivated several times.
- The Amazonian part of corridor-125 is associated with Pangea supercontinent tectonic trigger. The Andes is the surface expression of Pacific plate subduction, the kimberlite emplacement is the continental inland expression of the Pacific plate subduction and Pangea tectonic trigger.
- Being host of few hundreds of kimberlite, major dyke swarms and other ultramafic and mafic rocks, it has no direct association to plumes that crossed the lineament; rather they are triggered due to reorganization/change in the plate motion kinematics. As there is no apparent age progression unlike what is expected from a plume-triggered kimberlite emplacement model.

- The entire episode of kimberlite magma generation and emplacement is attributed to stress propagation due to Plate reorganization, incipient rifting and tectonic trigger due to South American plate motion and its related extension and subduction on the western margin.
- It has been observed that thermal perturbations associated with tectonic events involving lithospheric faults formed or reactivated during breakup of continents resulting in strain localization and melt focusing along these reactivated/newly formed structures. Finally, the emplacement of the magmatic rocks.
- Major structural trends of kimberlite emplacement loci along the corridor-125 are associated mainly with NE and NW trends. Other structural trends of importance are along NNW-SSE. WNW and EW trends are rarely seen as kimberlite emplacement controls.
- Major dyke swarms also follow the main structural trend (NE and NW) and with kimberlites along Corridor-125. All forming part of the structural controls showing reactivation.
- Corridor-125 is an older lineament probably older than 1.8 Ga and has been reactivated several times; kimberlite emplacement is associated to one reactivation event. Neotectonic reactivation of few faults at 1.6Ma (AllaouaSaadi et al. 2002) signifies this as an ongoing process.
- Corridor-125 kimberlites are of Group I, transitional/Anomalous type and lamproitic (Juina and Facao).
- The Transitional type kimberlites are found only on Extra-Amazonian region associated with tectonic extension; the group I kimberlites are found only on Amazonian Region associated with subduction related rifts and graben. The lamproite from Amazonian Region is associated with Parecis basin horst and its associated rift. A subducted oceanic crust is attributed as the source for this lamproites.
- Kimberlite and its related magmatism in Brazil, have their source from different depths ranging from base of SCLM, SCLMasthenosphere going up to 660km as evidenced by the diamond inclusion studies.
- Kimberlite emplacement is found post-dating and partly synchronous with the emplacement of the Parana flood basalts - along the same structural.

- Kimberlite emplacement is post-dated by kamafugites again showing structural reactivation. Therefore magma composition reflects different styles of lithosphere deformation - not plume activity.
- Finally, continued rifting and the opening of the Atlantic with progressive thinning/delamination of the lithosphere beneath South America to magmatic switching from kimberlites to kamafugites are seen.

In a nutshell, Brazil has potential to find more kimberlites and its associated diamonds. A more detailed scale research around the Extra-Amazonian region sedimentary basins, Amazonian region sedimentary basins will be of worth considering for kimberlite exploration industry. On the academic grounds, Brazil is an interesting source of unique spectrum of kimberlites and related rocks probing which will provide insight into the plate tectonics of Brazilian plate, nature of lithospheric mantle, subduction related diamond source etc.

Future Research

- The occurrence of 95Ma Juina magmatism and its magmatic trigger is not yet established with respect to structural analysis from geophysical studies. Also, the Transbrasiliano cluster kimberlite dating and structural analysis from geophysical studies will thought more interesting facts about corridor-125 and its nature.
- Geophysical kimberlite signature analysis for the whole of Brazil will be an interesting study which will identify new undiscovered kimberlites in Brazil. If this research is coupled with ground geophysical studies then it will be the best tool to delineate kimberlite signatures better.
- Reminiscence magnetizations of kimberlites and alkaline rocks are evident from this study. Hence, study of the palaeo-magnetic studies will resolve the long standing problems regarding the reconstruction problems associated with various blocks of Brazilian plates.

References

1. Almeida. F. F. M., Hasui. Y., Rodrigues. E. P. & Yamamoto. J. 1978. A Faixa de Dobramentos Araçuaí na região do Rio Pardo. In: Congresso Brasileiro de Geologia, 30, Recife. SBG, Anais, v. 1, 270-283.
2. Almeida. F. F. M., Hasui. Y., Brito Neves. B. B., Fuck. R. A. 1981. Brazilian structural provinces: an introduction. *Earth Science Review*, 17: 1-29.
3. Allaudi Saadi. A., Machette. M. N., Haller. K. M., Dart. R. L., Bradley. L. A., and Souza. A. M. P. D. 2002. Map and Database of Quaternary Faults and Lineaments in Brazil. USGS open file report-02-230. A project of the International Lithosphere Program Task Group II-2. Major Active Faults of the World. 1-64.
4. Araujo. H.J.Y. 1978. Geologia. In: Brasil. MME-DNP Projecto RADAMBRASIL. Folha SB.20 Purus. Rio de Janeiro (Levantamento de Recursos Naturais. 17).
5. Aravanis. T. 1999. Legend property assessment report, BM area, Alberta; Alberta Energy and Utilities board, Alberta Geological survey, assessment file report. 20000003.
6. Assumpcao. M, An. M., Bianchi. M., Franca. G. S. L., Rocha. M., Barbosa. J. R., Berracal. J. 2004. Seismic studies of the Brasília fold belt at the western border of the São Francisco Craton, Central Brazil, using receiver function, surface-wave dispersion and teleseismic tomography
7. Barnett. W., Jelsma. H., Watkeys. M., Freeman. L., and Bloem. A. 2013. How Structure and Stress Influence Kimberlite Emplacement. *Proceedings of 10th International Kimberlite Conference. Special Issue of the Journal of the Geological Society of India. vol. 2. 51-65.*
8. Basel. M. A. S., & Teixeira. W. 1975. Geocronologia e considerações estratigráficas preliminares da região Cachimbo-Dardanelos. Belém. Projeto RADAM. 19.

9. Berg. G. W. 1998. Geochemical relations which reflect the history of kimberlites from the type area of Kimberley, South Africa. Extended Abstracts, 7th International Kimberlite Conference. Cape Town: University of Cape Town, 76–78.
10. Bizzi. L. A. 1995. Mesozoic alkaline volcanism and mantle evolution of the Southwestern São Francisco craton. Brazil. University of Cape Town. Cape Town. 205 pp.
11. Bizzi. L. A., Dewit. M. J., Smith. C. B., McDonald. I., Armstrong. R. A. 1995a. Heterogeneous enriched mantle materials and dupal-type magmatism along the SW margin of the São-Francisco Craton. Brazil. *Journal of Geodynamics*. 20(4): 469-491.
12. Bizzi. L. A., Smith. C. B., DeWit. M. J., Armstrong. R. A., Meyer. H. O. A. 1995b. Mesozoic kimberlites and related alkalic rocks in the South Western São Francisco Craton. Brazil: a case for local mantle reservoirs and their interaction. Proceedings of the fifth international kimberlite conference, Brazil. 156-171.
13. Becker. M. & Le Roex. A. P. 2006. Geochemistry of South African on- and off-craton, Group I and Group II kimberlites; petrogenesis and source region evolution. *J Petrol* 47:673-703.
14. Becker. M., Le Roex. A. P., Class. C. 2007. Geochemistry and petrogenesis of South African transitional kimberlites located on and off the Kaapvaal Craton. *South African Journal of Geology*, 110(4): 631-646.
15. Beard. A. D., Downes. H., Hegner. E., Sablukov. S. M. 2000. Geochemistry and mineralogy of kimberlites from the Arkhangelsk Region, NW Russia: evidence for transitional kimberlite magma types. *Lithos*, 51(1–2): 47-73.
16. Boyd. F. R. & Gurney. J. 1986. Diamonds and the African lithosphere. *Science* Volume 232. 472-477
17. Bulanova. G. P. 1995. The formation of diamond: *Jour. Geochem. Explor*, 53, 1–23.

18. Bulanova. G. P., Walter. M. J., Smith. C. B., Kohn. S. C., Armstrong. L. S., Blundy. J. 2010. Mineral inclusions in sublithospheric diamonds from Collier 4 kimberlite pipe. Juina. Brazil: subducted protoliths carbonated melts and primary kimberlite magmatism. *Contributions to Mineralogy and Petrology* 160 (4). 489-51.
19. Carlson. R.W., Esperanca. S., Svisero. D.P. 1996. Chemical and Os isotopic study of cretaceous potassic rocks from southern Brazil. *Contributions to Mineralogy and Petrology*, 125(4): 393-405.
20. Carlson. R. W., Araujo. A. L. N., Brod. T. C. J., Gaspar. J. C., Brod. J. A., Petrnovic. I. A., Holland. A. M. H. B., Pimentel. M. M., Schel. S. 2007. Chemical and isotopic relationships between peridotite xenoliths and mafic-ultrapotassic rocks from Southern Brazil. *Chemical Geology*, 242, 418-437.
21. Clement. C. R. 1982: A comparative geological study of some major kimberlite pipes in the Northern Cape and Orange Free State. PhD Thesis, University of Cape Town.
22. Clement. C. R., Skinner. E. M. W. 1985. A textural-genetic classification of kimberlites. *Transactions Geological Society of South Africa* 88, 403-409.
23. Clifford. T. N. 1966. Tectono-metallogenic units and metallogenic provinces of Africa. *Earth and Planetary Science Letters* 1, 421-434.
24. Cordani. U. G., Pimentel. M. M., Araújo. C. E. G., Basei. M. A. S., Fuck. R. A., Girardi. V. A. V. 2013. Was there an Ediacaran Clymene ocean in Central South America? *American Journal of Science*, 313:517-539.
25. Costa. V. S. 1996. Estudos Mineralógicos E Químicos do Kimberlito Batovi 6 (MT) em comparação com as intrusões Três Ranchos 4 (GO) e Limeira 1 (MG), Universidade Estadual de Campinas, 112.
26. Cowan, D.R., Tompkins, L.A. and Cowan, S., 2000: Screening kimberlite magnetic anomalies in magnetically active areas, *Exploration Geophysics*, v. 31,(1 & 2), 66 - 72

27. Cox. K. G., Gurney. J. J. and Harte. B. 1973. Lesotho Kimberlites. Lesotho Nat. Development Corp. Maseru, Lesotho, In Nixon (P. H.), 76-92.
28. CPRM. 2004. Carta Geológica do Brasil ao Milionésimo – Projeto GIS do Brasil.
29. Crough. S. T., Morgan. W. J. and Hargraves. R. B. 1980. Kimberlites: Their relation to mantle hot spots. *Earth Planet. Sci. Lett.* 50.260–274.
30. Davis. G.L. 1977. The ages and uranium contents of zircons from kimberlites and related rocks: *Carnegie Institution of Washington Year Book.* 76: 631-635.
31. Dawson. J. B. 1962. Basutol and kimberlites. *Bulletin Geological Society of America*, v. 73, 545-560.
32. Dawson. J. B. 1967. A review of the geology of kimberlite, In *Ultramafic and Related Rocks* (Wyllie, P.J., ed.), Wiley, New York, p. 269- 278.
33. Dawson. J. B. 1980. *Kimberlites and their xenoliths.* Berlin Spinger-Verlag, 252.
34. Dawson. J. B. 1989. Geographic and time distribution of kimberlites and lamproites: relationships to tectonic processes. In J. Ross, Ed., *Kimberlites and Related rocks*, vol.1. *Proceedings of the Fourth International Kimberlite Conference*, Perth, Geological Society of Australia Special Publication No.14, Blackwell Scientific Publications, Oxford, 489-504.
35. Dawson. J. B., & Smith. J. V. 1977. The MARID (mica-amphibole-rutile-ilmenite-diopside) suite of xenoliths in kimberlite. *Geochimica et Cosmochimica Acta*, 41(2), 309-323.
36. De. Boorder. H. 1982. Deep reaching fracture zones in the crystalline basement surrounding the West Congo system and their control of mineralization in Angola and Gabon. *Geoexploration* 20, 259-273.
37. DeWit M. 2007. The Kalahari epeirogeny and climate change: differentiating cause and effect from core to space. *S Afr J Geol.*110. 367–392

38. DeWit. M. 2010. Identification of global diamond metallogenic clusters to assist exploration. The Southern African Institute of Mining and Metallurgy. *Diamonds: Source to Use*. 1-24.
39. Donatti-Filho. J.P., Oliveira. E.P., McNaughton. N.J. 2013a. Provenance of zircon xenocrysts in the Neoproterozoic Brauna Kimberlite Field. São Francisco Craton. Brazil: Evidence for a thick Palaeoproterozoic lithosphere beneath the Serrinha block. *Journal of South American Earth Sciences*. 45. 83-96. 266
40. Donatti-Filho. J.P., Tappe. S., Oliveira. E.P., Heaman. L.M. 2013b. Age and origin of the Neoproterozoic Braunakimberlites: Melt generation within the metasomatized base of the São Francisco craton. Brazil. *Chemical Geology*.
41. Ekstrand. O. R., Sinclair. W. D., Thorpe. R. I. 1995. *Geology of Canadian mineral deposit types. The geology of North America: Boulder, Colo., Geological Society of America*, 640.
42. Evans. T., and Harris. J. W. 1989. Nitrogen aggregation, inclusion equilibrium temperatures and the age of diamonds. In *Kimberlites and Related Rocks* (ed. J. Ross), Geological Society of Australia, Spec. Publ. No. 14, Vol. 2, pp. 1001-1006. Blackwell, Oxford.
43. Felgate. M. R. 2014. The petrogenesis of Brazilian kimberlites and kamafugites intruded along the 125° lineament: improved geochemical and geochronological constraints on magmatism in Rondonia and the Alto Paranaíba Igneous Province. PhD thesis. School of Earth Science. The University of Melbourne. 1-292. Geochemistry. Geophysics. Geosystems. 10. Q08005.
44. Fesq. H. W., Bibby. D. M., Erasmus. C. S., Kable. E. J. D., Sellschop. J. P. F. 1975. A comparative trace element study of diamonds from Premier, Finsch and Jagersfontein mines, South Africa. *Phys Chem Earth* 9:817-836.
45. Fitton. J. G., Dodie. J., Quennell. A. M. 1986. Basic volcanism associated with intraplate linear features (and Discussion). *Phil. Trans. R. Soc. London. A* 317, 253-266.

46. George. R. S., Mari. J.M. 1987. Brazilian Mega faults Map, 1987. *Revista Geológica de Chile*. No. 31, p.61-75. Fig.8.
47. Gibson. S.A., Thompson. R.N., Leonardos. O. H., Dickin. A. P., Mitchell. J.G. 1995. The late Cretaceous impact of the Trindade mantle plume- evidence from large-volume mafic Potassic magmatism in SE Brazil. *Journal of Petrology*. 36(1): 189-229.
48. Gladkov. A. S., Zinchuk N. N., Bornyakov. S. A., Sherman. S. I., Manakov. A. V., Matrosov. V. A., Garat. M. N., Dzyuba. I. A. 2005. New data on the internal structure and formation mechanism of kimberlite-hosting fault zones in the Malaya Botuoba Region. Yakutian diamondiferous province. *Dokl Earth Sci* 402(4):520–523 7
49. Guarino. V., Wu. F. Y., Lustrino. M., Melluso. L., Brotzu. P., Gomes. C. D. B., Ruberti. E., Tassinari. C. C. G., Svisero. D. P. 2013. U-Pb ages. Sr-Nd- isotope geochemistry and petrogenesis of kimberlites. kamafugites and phlogopite-picrites of the Alto Paranaíba Igneous Province. Brazil. *Chemical Geology* 353. 65–82.
50. Gunn. P.J. 1975. Linear transformations of gravity and magnetic fields, *Geophysical Prospecting*, 23, 300-312.
51. Harris, M., Le Roex, A. P. and Class, C. (2004) Geochemistry of the Uintiesberg kimberlite, South Africa: Petrogenesis of an off craton, group I kimberlite. *Lithos*.74, 149 – 165.
52. Hartnady. C. J. H. 1991. About turn for supercontinents. *Nature*. 352, 476-478.
53. Hastings. D. A., Sharp. W. G. 1979. An alternative hypothesis for the origin of West African kimberlites, *Nature* 221, 152-153.
54. Heaman. L. M., Kjarsgaard. B. A. 2000. Timing of eastern North American kimberlite magmatism: continental extension of the Great Meteor hotspot track? *Earth and Planetary Science Letters* 178 (3-4), 253-268.

55. Heaman. L., Kjarsgaard. B. A., and Creaser. R. A. 2004. The temporal evolution of North American kimberlites: *Lithos*, v. 76, p. 377–397.
56. Heine. C., Zoethout. J., and Muller. R. D. 2013. Kinematics of the South Atlantic rift. *Solid Earth*. 4. 215–253.
57. Hobbs. W. H. 1904. Lineaments of Atlantic Border region. *Geological Society of America Bulletin*. 15: 483–506.
58. Hunt. L., Stachel. T., Morton. R., Grutter. H., Creaser. R.A. 2009. The Carolina kimberlite. Brazil - Insights into an unconventional diamond deposit. *Lithos*. 112: 843-851.
59. Janse. A. J. A. 2007. Global rough diamond production since 1870. *G&G*, Vol.43, No.2, 98-119.
60. Janse, A.J.A. & Sheahan, P.A. (1995): Catalogue of world wide diamond and kimberlite occurrences: a selective and annotative approach. *Journal of Geochemical Exploration*, 53, 73-111.
61. Jaques. A. L., Lewis. J. D., Smith. C. B., Gregory. G. P., Ferguson. J., Chappell. B. W., & McCulloch. M. T. 1984. The diamond-bearing ultrapotassic (lamproitic) rocks of the west Kimberley region, Western Australia. In: Kornprobst, J. (ed.) *Kimberlites I. Kimberlites and Related Rocks*. Amsterdam: Elsevier, 225–254.
62. Jelsma. H. A., Barnett. W., Watkeys., L., Watkeys, M., Freeman, L., and Bloem. A. 2004. Preferential distribution along transcontinental corridors of kimberlites and related rocks of Southern Africa. *South African Journal of Geology*. 107(1-2). 301-324.
63. Jelsma. H., Barnett. W., Richards. S., Lister. G. 2009. Tectonic setting of kimberlites.112: 155-165.
64. Jurdy. D. M., Stefanick. M., & Scotese. C. R. 1995. Paleozoic plate dynamics. *Journal of Geophysical Research* 100, 17 965-75.

65. Kaminsky. F. V., Griffin. W. L., Belousova. E. 2010. Kimberlitic sources of super-deep diamonds in the Juina area, Mato Grosso State, Brazil. *Lithos*. 114(1-2). 16-29.
66. Kable. E. J. D., Fesq. H. W., and Gurney. J. J. 1975. The significance of inter-element relationships of some minor and trace elements in South African kimberlites. *Physics and Chemistry of the Earth* 9. 709-734.
67. Keating. P., and Sailhac. P. 2004. Use of the analytic signal to identify magnetic anomalies due to kimberlite pipes: *Geophysics*, 69. 180–190.
68. Kinny. P.D., Compston. W., Bristow. J.W. and Williams. I.S. 1989. Archaean mantle xenocrysts in a Permian kimberlite: Two generations of kimberlitic zircon in Jwaneng DK2, southern Botswana. *Proc. Fourth International Kimberlite Conference. Geol. Soc. Austr., Spec. Publ. No.14*, 833-842.
69. Kong. J. M., Boucher. D. R., Scott Smith. B. H. 1999. Exploration and geology of the Attawapiskat kimberlites, James Bay Lowland, Northern Ontario, Canada. *Proceedings of the VII International Kimberlite Conference*, vol. 1. Red Roof Design, Cape Town, South Africa, 452 – 467.
70. Kushev. V.G., Sinitsyn. A.V., Mishnin. V.M. and Natapov. L.M. 1992. Kimberlite structural environments and their productivity in the East Siberian (Yakutian) Province. *Russ. Geol. Geophys*, 33: 50-60.
71. Lister. G. S., Etheridge. M. A., and Symonds. P. 1986. Detachment faulting and the evolution of continental margins. *Geology*. 14:246-250.
72. Le Roex. A. P. 1986. Geological correlation between southern African kimberlites and south Atlantic hotspots. *Nature* 324, 243-245.
73. Le Roex. A. P., Bell. D. R., Davis. P. 2003. Petrogenesis of group I kimberlites from Kimberley, South Africa: Evidence from bulk-rock geochemistry. *Journal of Petrology* 44 (12), 2261-2286.

74. Le Roex. A., Coe. N., Gurney. J., Pearson. D.G., Nowell. G. 2008. Petrogenesis of Group II kimberlites: a case study from southern Africa. 9th IKC, Extended Abstract, A-00041.
75. Lewis. H. C. 1887. On diamondiferous peridotites and genesis of the diamond. *Geol. Mag.* 4, 22-24.
76. Lewis. H. C. 1888. Matrix of diamond. *Geol. Mag.* 5, 129-131.
77. Lockhart. G., Grütter. H. and Carlson. J. 2004. Temporal, geomagnetic and related attributes of kimberlite magmatism at Ekati, Northwest Territories, Canada; *Lithos*, Volume 77, 665–682.
78. Masun. K. M., Smith. B. H. S. 2008. The Pimenta Bueno kimberlite field, Rondonia-Brazil: Tuffisitic kimberlite and transitional textures. *Journal of Volcanology and Geothermal Research.* 174(1-3). 81-89.
79. Marsh. J. S. 1973. Relationship between transform directions and alkaline igneous rock lineaments in Africa and South America. *Earth and Planetary Science letters* 18, 317-323.
80. Matthews. K. J., Müller. R. D., Wessel. P., and Whittaker. J. M. 2011. The tectonic fabric of the ocean basins. *Journal of Geophysical Research.* 116. B12109.
81. Maus. S., Barckhausen.U., Berkenbosch. H., Bournas. N., Brozena. J., Childers. V., Dostaler. F., Fairhead. J., Finn. C., Von Frese. R. 2009. EMAG2: a 2-arc min resolution Earth Magnetic Anomaly Grid compiled from satellite airborne and marine magnetic measurements.
82. McCulloch. M. T. 1984. The diamond bearing ultrapotassic (lamproitic) rocks of the west Kimberley region, Western Australia, in *Kimberlites I: Kimberlites and related rocks*, Elsevier. 225-254.

83. McDonough. W. F. and Sun. S. S. 1989. Chemical and isotopic systematics of oceanic basalts: implications for mantle composition and processes. In: Saunders, A.D., Norry, M.J. (Eds.) *Magmatism in the ocean basins*. Geological Society of London, Special Publication 42, 313-345.
84. McDonough. W. F., and Sun. S. S. 1995. Composition of the Earth. *Chemical Geology* 120: 223-253. doi: 10.1016/0009-2541(94)00140-4.
85. Mitchell. R. H. 1986. *Kimberlites: Minerology, Geochemistry and Petrology*. Plenum Press, New York.
86. Mitchell. R. 1995. The role of petrography and litho-geochemistry in exploration for diamondiferous rocks. *Journal of Geochemical Exploration* 53 (1-3), 339-350.
87. Moore. A., Blenkinsop. T., Cotterill. F. 2008. Controls on post-Gondwana alkaline volcanism in southern Africa. *Earth Planet Science Letter*. 268.151–164.
88. Morgan. W. J. 1983. Hotspot tracks and the early rifting of the Atlantic, *Tectonophysics* 94, 123-139.
89. Muramatsu. Y. 1983. Geochemical investigations of kimberlites from the Kimberley area. South Africa. *Geochem. J.* 17, 71–86.
90. Nabighian. M. N. 1972. The Analytic Signal of two-dimensional magnetic bodies with polygonal cross-section: its properties and use for automated anomaly interpretation. *Geophysics*, 37. 507-517.
91. Nabighian. M. N., Ander. R., Grauch. V.J.S., Hansen. R.O., LaFehr. T., Li. Y., Pearson. W.C., Peirce. J.W., Phillips. J.D., and Ruder. M.E. 2005. The historical development of the gravity method in exploration: *Geophysics*.
92. Nowell. G. M., Pearson. D. G., Bell. D. R., Carlson. R. W., Smith. C. B., Kempton. P. D., Noble. S. R. 2004. Hf isotope systematics of kimberlites and their megacrysts: New constraints on their source regions. *J. Petrology*, 45, 1583-1612.

93. Nance. R. D., Worsley. T. R., Moody. J. B. 1986. Post-Archean biogeochemical cycles and long-term episodicity in tectonic processes. *Geology*, 14. 514–518.
94. Neves. B. B. B., Fuck. R. A. 2014. The basement of the South American Platform: half Laurentian (N-NW) + half Gondwanan (E-SE) domains. *Precambrian Research*. 244. 75-86.
95. O'Neill. C. J., Moresi, L., Jaques, A. L. 2005. Geodynamic controls on diamond deposits: implications for Australian occurrences. *Tectonophysics* 404, 217–236.
96. Pearson. D. G., Shirey. S. B. 1999. Isotopic dating of diamonds. *Econ. Geol. Spec. Publ., SEG Reviews*, Ch. 6, 143-171.
97. Pearson. D. G., Shirey. S. B., Bulanova. G. P., Carlson. R. W., Milledge. H. J. 1999. Dating and paragenetic distinction of diamonds using the Re-Os isotope system: application to some Siberian diamonds: In Gurney, J.J., Gurney, J.L., Pascoe, M.D., & Richardson, S.H. (Eds.), *Proceedings of the 7th International Kimberlite Conference*, vol. 2, 637-643.
98. Paton. C., Hergt. J. M., Woodhead. J. D., Phillips. D., Shee. S. R. 2009. Identifying the asthenospheric component of kimberlite magmas from the Dharwar Craton, India. *Lithos*, 112: 296-310.
99. Pereira. R. S., Fuck. R. A. 2005. Archean nuclei and the distribution of kimberlite and related rocks in the São Francisco Craton, Brazil. *Revista Brasileira de Geociencias*, 35(3):93-104.
100. Pires. F.R.M. 1986. The Southern limits of São Francisco Craton. *Anais da academia Brasileira de Ciencias*. 58(1): 139-145.
101. Phillips. D., Kiviets. G.B., Barton. E.S., Smith. C.B., Viljoen. K.S. and Fourie. L.F. 1998. ⁴⁰Ar/³⁹Ar dating of kimberlites and related rocks. *Proc. Seventh International Kimberlite Conference*, Cape Town.

102. Power. M., Belcourt. G. and Rockel. E. 2004: Geophysical methods for kimberlite exploration in northern Canada; *The Leading Edge*, v.23, No. 11, 1124 – 1129.
103. Reid. A. B., Allsop. J. M., Granser. H., Millett. A . J. and Somerton. W. I. 1990. “Magnetic interpretation in three dimensions using Euler deconvolution,” *Geophysics*, vol. 55, no. 1, 80–91.
104. Ringwood. A. E., Kesson. S. E., Hibberson. W., Ware. N. 1992. Origin of Kimberlites and Related Magmas. *Earth and Planetary Science Letters* 113 (4), 521-538
105. Rocha. L. G. M., Pires. A. C. P. B., Carmelo. A. C., Araujo Filho. J. O. 2014. Geophysical characterization of Azimuth 125 lineament with aeromagnetic data: Contributions to the geology of central Brazil. *Precambrian Research* 249. 273-287.
106. Roest. W. R., and Pilkington. M. 1993. Identifying remanent magnetization effects in magnetic data: *Geophysics*, 58, 653-659.
107. Rizzotto. G.J., Hartmann. L.A. 2012. Geological and geochemical evolution of the Trincadeira Complex, a Mesoproterozoic ophiolite in the southwestern Amazon Craton, Brazil. *Lithos* 148, 277-295
108. Rizzotto. G. J., Joao Orestes. S., Santos. L., Hartmann. A., Tohver. E., Pimentel. M. M., Naughton. M. N. 2013. The Mesoproterozoic Suapore suture in the SW Amazonian Craton: Geotectonic implications based on field geology, zircon geochronology and Nd-Sr isotope geochemistry. *Journal of South American Earth Sciences*. 48. 271-295.
109. Sarma. B. S. P., Verma. B. K., Satyanarayana. S. V. 1999. Magnetic mapping of Majhgawan diamond pipe of central India: *Geophysics*, 64, 1735–1739.
110. Schmincke. H. U. 1974. Volcanological aspects of peralkaline silicic welded ash-flow tuffs. *Bulletin of Volcanology*. 38, 594–636.
111. Scotese.C. R., and McKerrow. W. S.1984. *Paleozoic World Maps* and Symposium introduction in *Paleogeography. Canadian Journal of EarthScience* (21)887-901.

112. Schnetzle. C. C., and Taylor. P. T. 1984. Evaluation of an observational method for estimation of remanent magnetization. *Geophysics*, 49: 282- 290.
113. Scott Smith. B. H., Nowicki. T. E., Russell. J. K., Webb. K. J., Mitchell. R. H., Hetman. C. M., Skinner. E. M. W., Robey. Jv. A. 2013. Kimberlite Terminology and Classification. In: Pearson, D.G.et al. (Eds.), *Proceedings of 10th International Kimberlite Conference*. Springer India.1-17.
114. Shurbet. D. H., Keller. G. R., & Friess. J. P. 1976. Remanent magnetization from comparison of gravity and magnetic anomalies. *Geophysics*, 41(1): 56–61.
115. Silva. G. G. 1974. Geologia. In: Brasil, MME-DNPM Projeto RADAM. Folhas SB.22 Araguaia e parte da SC.22 Tocantins. Rio de Janeiro (Levantamento de RecursosNaturais. 4).
116. Skinner. E., Clement. C. 1979. Mineralogical classification of southern African kimberlites.
Kimberlites, Diatremes and Diamonds: Their Geology, Petrology and Geochemistry, 129-139
117. Skinner. E. 1989. Contrasting Group I and Group II kimberlite petrology: towards a genetic model for kimberlites. *Kimberlites and related Rocks* 1, 528-544.
118. Skinner. E., Marsh. J. 2004. Distinct kimberlite pipe classes with contrasting eruption processes. *Lithos*, 76 (1-4), 183-200.
119. Skinner. E. M.W. 1986. Contrasting group 1 and group 2 kimberlite petrology, Towards a genetic model for kimberlites: 4th International Kimberlite Conference, Geological Society Australia, Extended Abstract Series16, 202–204.
120. Smith. C. B. 1983. Pb, Sr and Nd Isotopic Evidence for Sources of Southern African Cretaceous Kimberlites. *Nature* 304 (5921), 51-54.
121. Smith. C. B., Gurney. J. J., Skinner. E. M. W., Clement. C. R., and Ebrahim. N.1985. Geochemical character of the southern African kimberlites: a new approach based isotopic constraints.*Geol. Soc. S. Afr.*, 88. 267–280.

122. Smith. R.S., Annan. A.P., Lemieux. J., and Pederson. R.N. 1996. Application of a modified GEOTEM system to a reconnaissance exploration for kimberlites in the Point Lake area, NWT, Canada, *Geophysics*, Vol (61)1, 82 – 92.
123. Souza-Filho. P.W. M., Quadros. M. L. E. S., Scandolaro. J. E., Filho. E. F. S., and Reis. M.R. 1999. Compartimentação morfoestrutural e neotectônica do sistema fluvial Guaporé-Mamoré-Alto Madeira, Rondônia - Brasil. *Rev. Bras. Geo.* 29(4):469-476.
124. Stachel. T., Brey G. P., and Harris. J. W. 2005. Inclusions in sub-lithospheric diamonds; glimpses of deep earth. *Elements*, 1. 73-87.
125. Stachel. T., and Harris. J. W. 2008. The origin of cratonic diamonds-constraints from mineral inclusions. *Ore Geology Reviews* 34 (1), 5-32.
126. Svisero. D. P., Meyer. H. O. A., Haralyi. N. L. E., Hasui. Y. 1984. A Note on the Geology of Some Brazilian Kimberlites. *The Journal of Geology*. 92(3): 331-338.
127. Sykes. L. 1978. Intraplate seismicity, reactivation of pre-existing zones of weakness, alkaline magmatism and other tectonism postdating continental fragmentation-*Rev. Geophys. Space Phys.*16: 621-688.
128. Tappe. S., Pearson. D. G., Nowell. G. M., Nielsen. T. F.D., Milstead. P., and Muehlenbachs. K. 2011. A fresh isotopic look at Greenland kimberlites: cratonic mantle lithosphere imprint on deep source signal. *Earth Planet. Sci. Lett.*, 305, 235-248.
129. Tappe. S., Simonetti. A. 2012a. Combined U-Pb geochronology and Sr-Nd isotope analysis of the Ice River perovskite standard, with implications for kimberlite and alkaline rock petrogenesis. 304.
130. Tappe. S., Steinfeldt. A., Nielsen. T. 2012b. Asthenospheric source of Neoproterozoic and Mesozoic kimberlites from the North Atlantic craton, West Greenland: New highprecision U–Pb and Sr–Nd isotope data on perovskite. *Chemical Geology*, 320–321(0): 113-127.

131. Tappe, S., Pearson, G. D., Kjarsgaard, B. A., Nowell, G. And Dowall, D. 2013. Mantle transition zone input to kimberlite magmatism near a subduction zone: Origin of anomalous Nd-Hf isotope systematics at Las de Gras, Canada. *Earth Planet. Sci. Lett.*, 371–372, 235 – 251
132. Tainton. K., McKenzie. D. 1994. The generation of kimberlites, lamproites, and their source rocks. *Journal of Petrology* 35 (3). 787.
133. Thompson. D. T. 1982. EULDPH: A new technique for making computer-assisted depth estimates from magnetic data, *Geophys.* 47, 31–37.
134. Tassinari. C. C. G. 1996. O mapa geocronológico do Cráton Amazônico no Brasil: revisão dos dados isotópicos. 139p. Universidade de São Paulo, Instituto de Geociências, São Paulo. (Tese de Livre-doscência).
135. Tassinari. C. C. G., & Macambira. M. J. B. 1999. Geochronological provinces of the Amazonian Craton. *Episodes*, 22(3).174-182.
136. Taylor. L. A. 1984. Kimberlitic magmatism in the Eastern United States: Relationships to mid Atlantic tectonism, *TIKC* 1, 417-424.
137. Taylor. W. R., Tompkins. L. A. & Haggerty. S. E. 1994. Comparative geochemistry of West African kimberlites: evidence for a micaceous kimberlite end member of sublithospheric origin. *Geochimica et Cosmochimica Acta.* 58, 4017–4037.
138. Tohver. E., Van der Pluijm. B. A., Scandolara. J. E., Essene. E. J. 2005. Late Mesoproterozoic deformation of SW Amazonia (Rondônia, Brazil): geochronological and structural evidence for collision with Southern Laurentia. *J. Geol.* 113, 309-323.
139. Vasanthi. A., Mallick. K. 2005. Bouguer gravity anomalies and occurrence patterns of kimberlite pipes in Narayanpet-Maddur regions, Andhra Pradesh, India: *Geophysics*, 70, no. 1, J13–J24.

140. Vendemiatio. M. A., and Enzweiler. J. 2001. Routine control of accuracy in silicate rock analysis by X-ray fluorescence spectrometry. *Geostandards Newsletter: The Journal of Geostandards and Geoanalysis*. Vol.25. 281-291.
141. Watkins. J. M. 2009. Diamonds in South American Proexpo oral presentation. Peru.
142. Walter. M. J., Kohn. S. C., Araujo. D., Bulanova. G. P., Smith. C. B., Gaillou. E., Wang. J., Steele. A., Shirey. S. B. 2011. Deep mantle cycling of oceanic crust; evidence from diamonds and their mineral inclusions. *Science*, Vol.334, No.6052, 54–57, <http://dx.doi.org/10.1126/science.1209300>.
143. Wedepohl. K. H., and Muramatsu. Y.1979. The chemical composition of kimberlites compared with the average composition of three basaltic magma types. In F. R. Boyd and H. O. A. Meyer, Eds., *Kimberlites, Diatremes, and Diamonds: Their Geology, Petrology and Geochemistry*, 300-312.
144. Wessel. P. A., Mazzoni. R., Muller. D., Matthews., Whittaker. K. J., Myhill. R., Chandler. M. T. 2014. The Global seafloor fabric and Magnetic lineation project. *Geochemistry. Geophysics. Geosystems*. <http://www.soest.hawaii.edu/PT/GSFML/>
145. White. S.H., de Boorder. H., Smith. C.B. 1995. Structural controls of kimberlite and lamproite emplacement. *Journal of Geochemical Exploration* 53.245-264.
146. Wu. F. Y., Yang. T. H., Li. Z. L., Yang. J. H., Zhang. Y. B. 2010. In situ U-Pb age determination and Nd isotopic analysis of perovskites from kimberlites in South African and Somerset Island, Canada. *Lithos*, 115, 205-222.
147. Zonneveld. J. P., Kjarsgaard. B. A., Harvey. S. E., Heaman. L. M., McNeil. D. H., and Marcia. K. Y. 2004. Sedimentologic and Stratigraphic constraints on emplacement of the Star Kimberlite, eastcentral Saskatchewan. In: *Selected papers from the Eighth International Kimberlite Congress; Volume 1; The C. Roger Clement volume*, R. H. Mitchell, H. S. Gruetter, L. M. Heaman, B. H. Scott Smith and T. Stachel (eds), *Lithos*. 76, 115-138.

Appendix-1: Publications

Tectonic and Structural Controls on Phanerozoic-Cretaceous Kimberlite Emplacement along Corridor-125, Brazil - A Review

Authors: Manimala. M., Elson.P.Oliveira, Simon Richard

ABSTRACT

On a global scale kimberlite emplacement is controlled by pre-existing/newly formed translithospheric structures known as Continental Lineaments due to plate tectonics. These translithospheric continental lineaments are formed during plate-reorganisation prior to oceanic rift formation. These lineaments extend onto the newly developing oceanic rift and transform fractures. Finally the plates drift apart. Hence, there is a genetic link between continental translithospheric lineaments, its oceanic transform fracture counterparts and associated kimberlite emplacement. Corridor-125 in Brazil is one such continental translithospheric lineaments, which host kimberlites and other mafic/ultramafic rocks. It consists of Amazonian and Extra-Amazonian regions. These two regions of the corridor is a coincidental alignment along with its associated mafic and ultramafic magmatism. The Extra-Amazonian part of this corridor was cratonized by 2.3 Ga (Tassinari and Macambira, 1999). Later, this cratonic landmass was reactivated as there are evidences of younger mafic dyke swarms of 1.8 Ga (Sial et al., 1987), younger kimberlite clusters and other mafic rocks along its entire extent. The oldest known structural activation on the Amazonian part of the corridor is 1.8 Ga (Dyke swarms) followed by 1.4 Ga reactivation during amalgamation of SW Amazonian craton with Paraguay block (Rizzotto et al., 2012). The final basement structural reactivation at 1.0 Ga (Tohver et al, 2005) has been the control on kimberlites in this region. The kimberlite age peaks along Corridor-125 are 226 to 268 Ma, 120 to 122 Ma, 80 to 94 Ma and 74 Ma. Plate tectonic reconstruction of Brazilian plate reveals the path of Trinidad-Martin Vaz (TMV) hotspot trail does not coincide with the Corridor and there is no apparent kimberlite age progression along Corridor-125. Thus, earlier suggestions of TMV influence as possible source for kimberlite emplacement is ruled out. The kimberlite emplacement is rather related to Pangea supercontinent plate re-organization (226-268 Ma kimberlites); incipient South Atlantic rifting from 120 to 122 Ma when the South American plate movement was characterized by cusp and jog; and the last phase of kimberlite emplacement from 80 to 94 and 74 Ma is due to the second phase of increased plate velocity and continued

rifting. The quiescent periods devoid of kimberlites are stages when the South American plate was stable or experiencing a smooth plate velocity and direction.

1. Introduction

Kimberlite emplacement in time and space are related to global plate tectonics and its associated translithospheric structural controls (White et al., 1995; Barnett et al., 2013; Jelsma et al., 2009). These translithospheric structures are the Global structural controls for kimberlite emplacement (Sykes, 1978). It has been proposed that the structures contained within the corridors are repeatedly reactivated (White et al., 1995) thereby forming the pathways for kimberlite magmas. On sub-regional scale kimberlites are preferentially emplaced at the tips and shoulders of rifts, major pre-existing dyke swarms, structural bends, step-overs, and fault intersections (Jelsma et al., 2004; Gladdkov et al. 2005). Within structural corridors the brittle structures of the crust form the local structural controls for kimberlite emplacement.

Like those in Africa, the kimberlite occurrences in Brazil are clustered along major lineaments namely, Az-125, Transbrasiliano Lineament (TBL), Blumenau lineament, Rio Alonzo Lineament, Rio Grande Arch and Amazonas basin Lineaments. Of these lineaments, Az-125, here called as Corridor-125 (Fig.1) hosts the maximum number of kimberlite discoveries thereby indicating a fundamental structural control on their emplacement. As there is link with plate tectonics and structures, the key here is to understand the interplay between the structural and plate tectonic controls along with the timing and location of kimberlite emplacement along corridor-125.

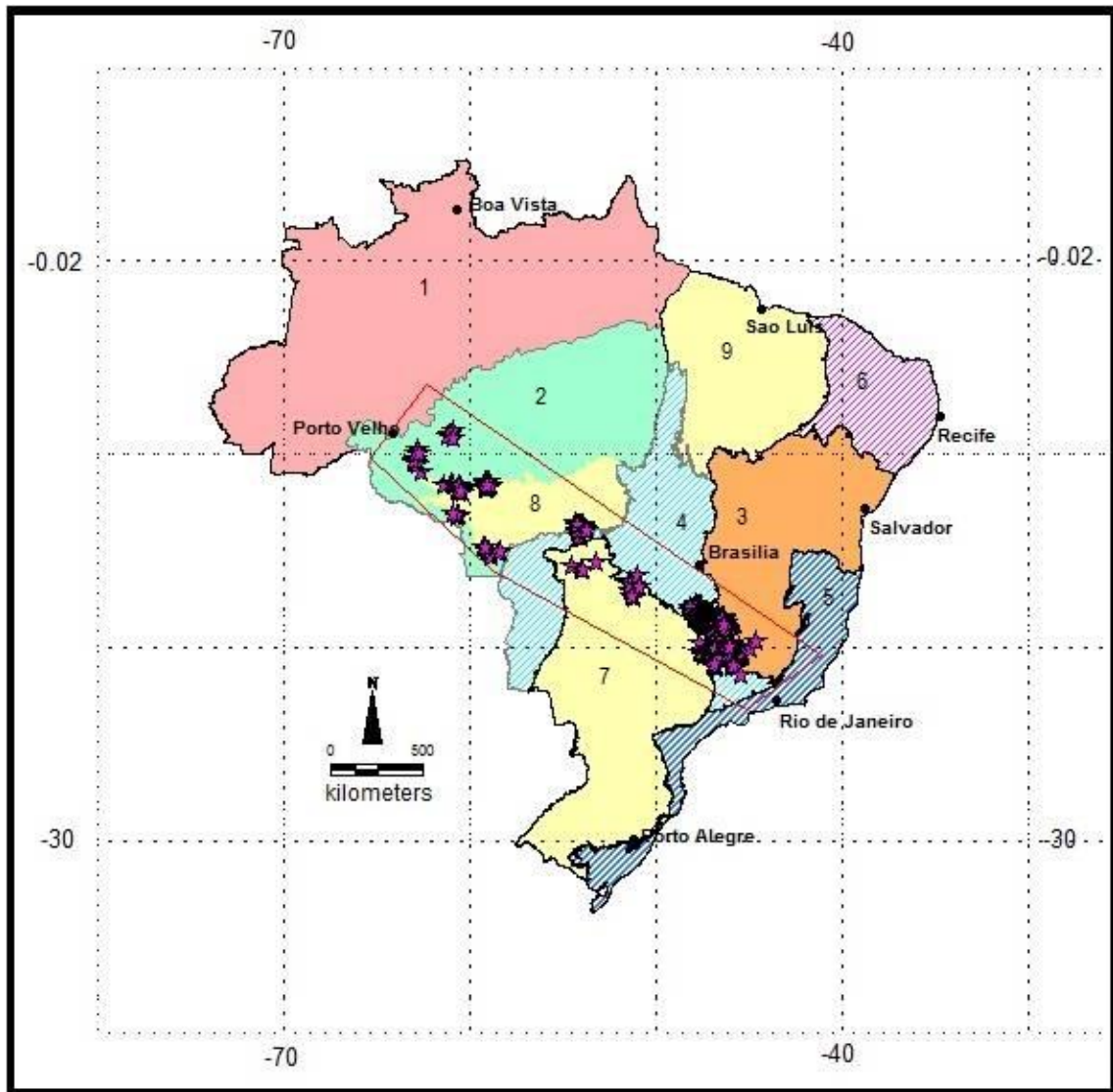


Fig.1: Corridors-125 and kimberlite occurrences in Brazil with structural provinces background. 1. Northern-Amazonian province, 2. Southern Amazonian Province (Tapajos Province), 3. São Francisco Craton, 4. Brasilia Belt, 5. Ribeira Belt, 6. Borborema province, 7. Parana Basin, 8. Parecis Basin, 9. Paraniba Basin. Pink stars are kimberlite and related rock. The boundary enclosed in red is the location of Corridor-125.

The corridor-125 is not a lineament easy to identify. Lack of signature on Landsat images and lack of geomorphic expression makes difficult to identify the existence of Corridor-125. However, analysis of aeromagnetic map, distribution of basement units, weakness zones in the form of fractures, faults along with occurrence of dyke swarms help characterise the corridor. In this paper, we present a review of aeromagnetic map signatures; structures and geology of the basement of the cratons transect by corridor-125; age, geochemistry and distribution of kimberlites; paleo-position of hot spot with plate reconstruction. From this review, we will characterize the corridor-125, its associated structural and plate tectonic controls on kimberlite emplacement.

2. Kimberlite occurrences along Corridor-125

The term corridor is described as a set of lineaments broadly parallel to each other or a single lineament on which kimberlites are preferentially oriented. Lineaments are zones of weakness or structural displacements in the crust, which can be mapped or indirectly inferred by the presence of magmatic rocks aligned in a straight or slightly curving manner when the younger geological and tectonic processes often mask its presence underneath (Hobbs et al, 1976). The length of lineament varies considerably and is typically measured in tens or hundreds of kilometres. The lineaments that are up to 100 km are termed as mega-lineament where as those that are longer than 100 km are termed as giga-lineament.

Corridor-125 trends NW-SE and is composed of several mega- and giga-lineaments from Rio de Janeiro to Porto Velho (Fig. 1). The total length of the corridor is around 2700 km and its width of c. 500 km, which is estimated with the kimberlite occurrence bordered by the dyke swarms. The width of the boundary is chosen little broader than the kimberlite occurrence to get a picture of the geology, structure and geophysical signatures of the host rocks and its structures during study.

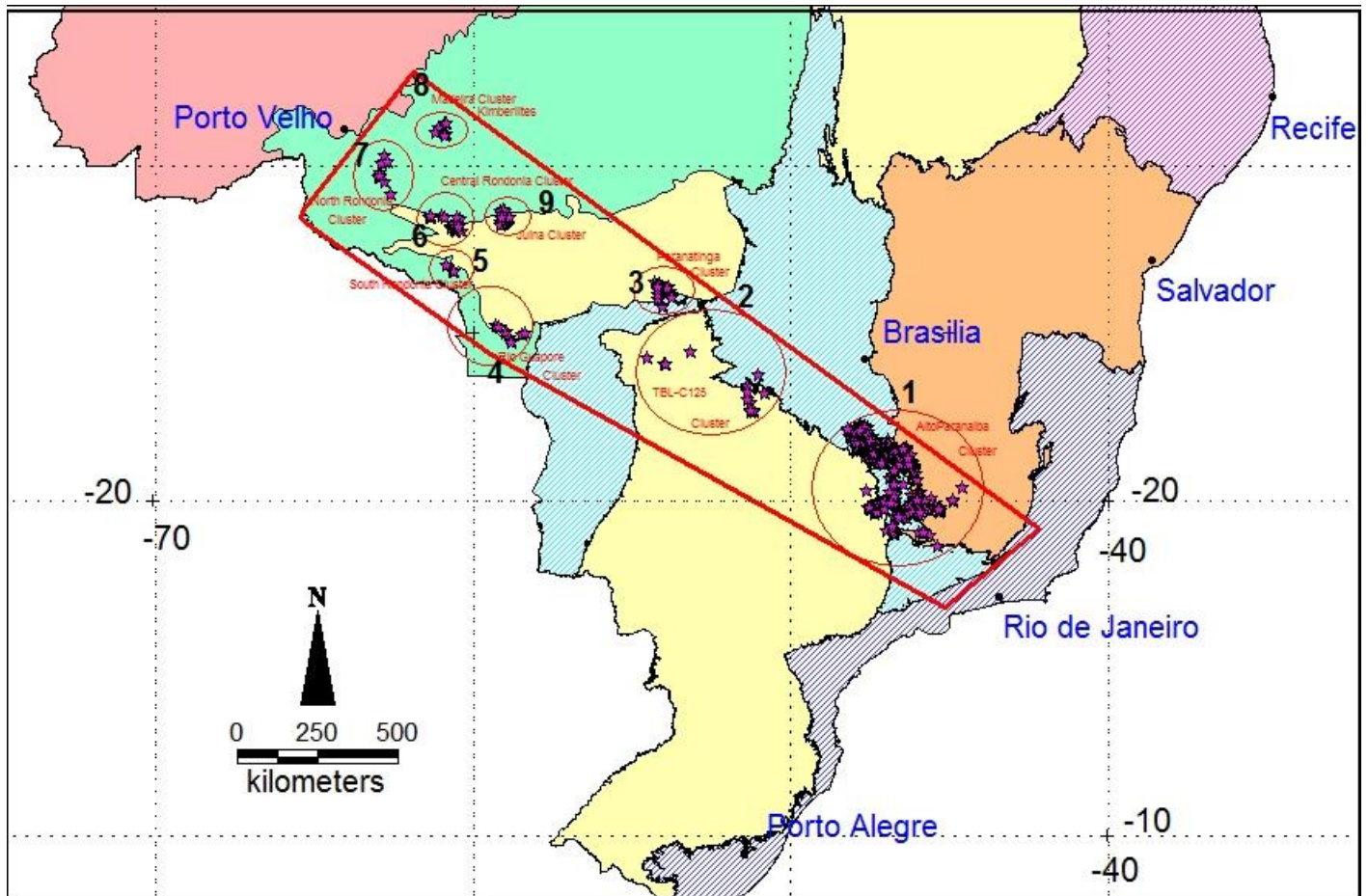


Fig.2: Kimberlite Clusters along Corridor-125 with Structural provinces background.

The kimberlite occurrences along Corridor-125 can be broadly classified into the following clusters (Fig. 2):

1. Alto Paranaíba cluster,
2. TBL-C-125 cluster,
3. Upper Paraguay cluster (Rio Guapore and Paranatinga clusters),
4. South Rondonian cluster,
5. Central Rondonian cluster,
6. North Rondonian cluster,
7. Madeira cluster and
8. Juina cluster.

3. Geological Setting of Corridor-125

Main geological units along Corridor-125 (Fig.1, 2 and 3) are the NE-trending Neoproterozoic (Brasiliano/Pan-African) Ribeira Orogen in the Southeast, São Francisco craton basement, NE-trending Neoproterozoic Brasília Orogen, Phanerozoic Parana basin, NE-trending Neoproterozoic Paraguay-Araguaia Orogen followed by Amazonian craton basement (NW-trending Mesoproterozoic Rondonian and Sunsas orogens) and Phanerozoic Parecis Basin. The NE-trending Transbrasiliano lineament cuts across Corridor-125. On the western side of Transbrasiliano lineament there occurs the Amazonian region and on the eastern side the Extra-Amazonian region.

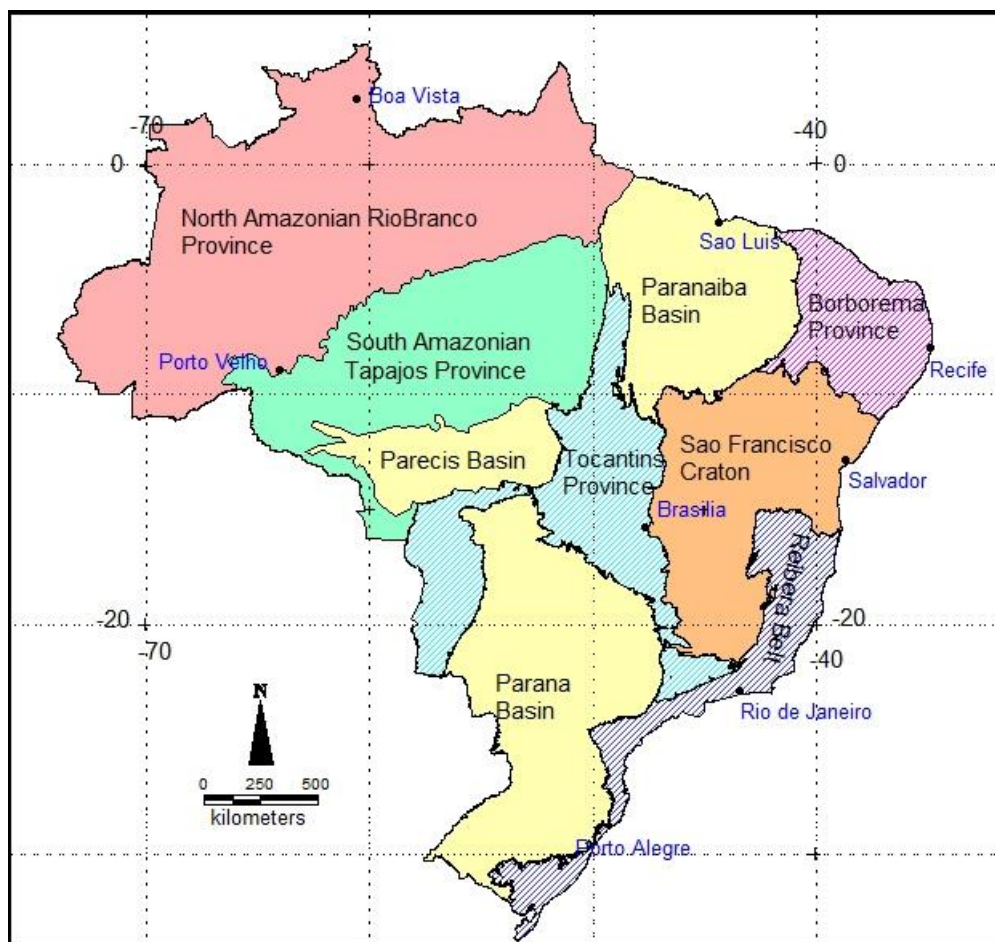


Fig.3: Simplified Brazil map with structural province after Almeida 1981.

The main structural features that characterize Corridor-125 are NW-trending Proterozoic mafic dyke swarms (Pará de Minas dyke swarm) in the Extra-Amazonian region and the Amazonian region includes NW-trending Serra Formosa, Rio Guaporé archs in the Phanerozoic Parecis Basin and its basement, Amazonian craton. In between the latter two archs another major structural feature is the Pimenta Bueno graben in the Parecis basin. In the

Extra-Amazonian region the Pará de Minas dyke swarm continues, without significant deformation, beneath the Brasilia orogen up to the Transbrasiliano Lineament as seen on aeromagnetic maps to be shown in a later section. Other lineaments at high to moderate angle to Corridor-125 are common and in several places the intersections with Corridor-125 are sites of kimberlite clustering.

4. Methods

To arrive at the objective of reviewing the available information on kimberlite occurrence along Corridor-125, we compiled data on kimberlite ages, lineaments, aeromagnetic maps, global magnetic anomaly grid, hot-spot re-location, and kimberlite geochemistry. These compiled data are analysed under the following headings:

- Lineament Analysis (taken from maps, aeromagnetic data from CPRM and global magnetic grid).
- Age of kimberlites (from the literature).
- Review on Geochemistry of kimberlites (from the literature).
- Hot spot paleo-location (from Plate tectonic reconstruction using gplates).

Lineament analysis along Corridor-125 and its potential links with oceanic transform faults

The continental structures control the position of transforms in the newly developing younger ocean (Lister et al, 1986). Thus, there exists a genetic link between the oceanic transforms and the continental Lineaments exists. Due to complex overprinting of the younger tectonic events post dating the plate rifting at global and local scales, there is masking of the older continental lineaments where as the ocean floor is tectonically less disturbed in nature. As a result they retain the structural signatures i.e. transform fractures signatures on the ocean floor and is much easily observed in comparison to landward counterparts.

The orientations of the present day oceanic and continental lineament may be different because of the change in Euler pole dynamics after the oceanic crust started to form. A single plate could have played part of different supercontinent life cycle and thus the continental lineaments are associated with more than one set of ocean floor lineaments. In such a case, the

most recent ocean floor signatures are much easier to associate with the continental lineaments while the older ones are masked by younger events. At times the relationship between older continental lineaments with its respective oceanic transforms becomes impossible to demonstrate. Kimberlite magma emplacement pathways are interpreted to be reactivated pre-existing lineaments or newly created ones due to the dynamics of plate tectonic events at different stages of supercontinent life cycle (DeWit, 2007; Moore et al, 2008; Jelsma et al, 2009). Thus, the kimberlite emplacement, continental lineaments and the oceanic transforms are all genetically related. There are several periods of kimberlite emplacement worldwide associated with plate tectonic events. It is possible to establish the link between the kimberlites and the lineaments and their associated plate tectonic events. The complexity lies in associating the older events. This is particularly true with respect to the association of older than Mesozoic kimberlites. On the other hand it is much easily accomplished with younger kimberlites.

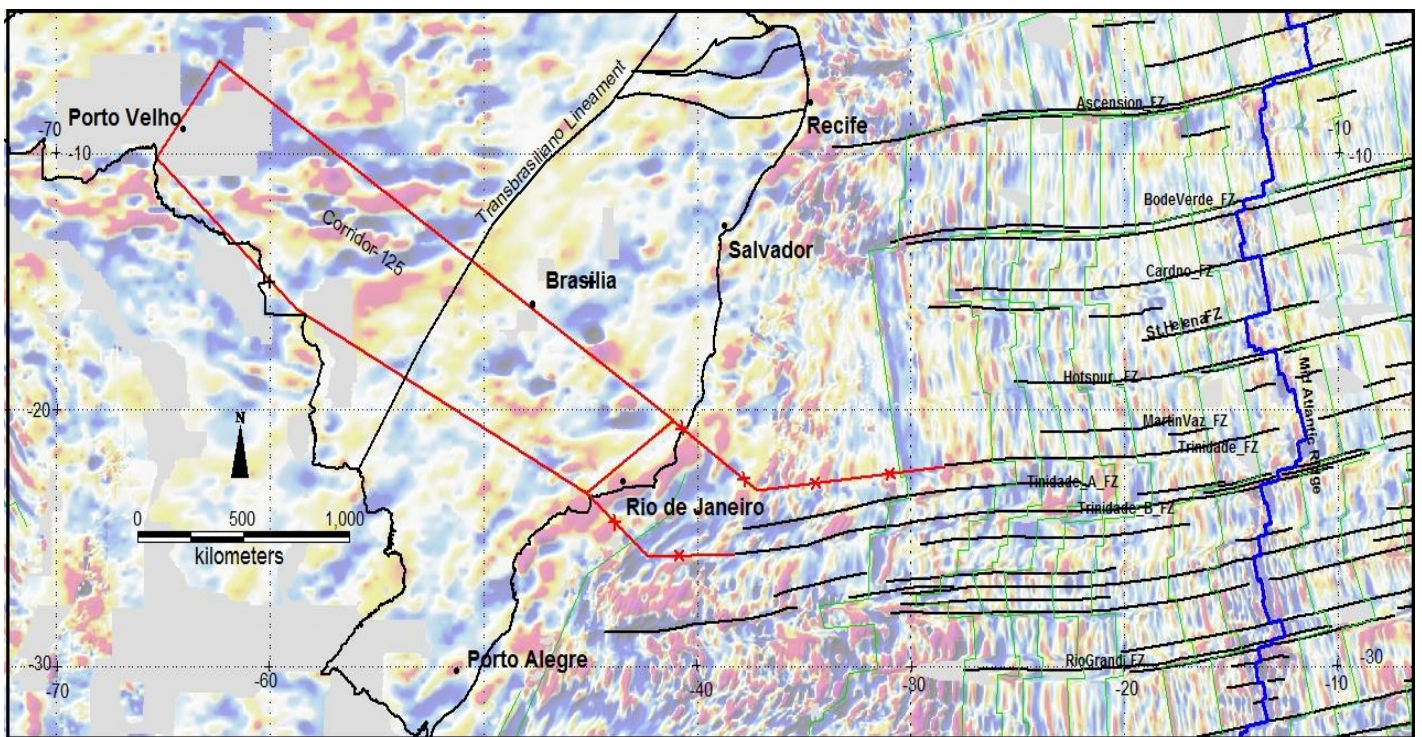


Fig.4: Oceanic extension of Continental Corridor-125 lineament in the South American plate with EMagV2 background and GFML fracture zones and mid-Atlantic ridges.

The genetic link between the oceanic transform fractures and Corridor-125 is established by using 'Global seafloor fabric and magnetic lineation' (GSFML) database by Matthews et al., (2011) and Wessel et al., (2014). The transform fractures signatures from GSFML are used in GIS platform. These fracture zones are plotted against the Earth Magnetic Anomaly Grid Version.2 (EMagV2 by Maus et al, 2009) data to trace back the fracture zones up to the Brazilian Eastern board. This result is further overlain by the global oceanic age isochron and bathymetric data. By doing so, we further refined the trace back toward higher preciseness. Once, the data trace was achieved up to the border, the total field aeromagnetic map which is reduced to IGRF, 1km square grid from the CPRM (Brazilian Geological survey) was utilized to identify the continental expression of the lineament. The work by Rocha et al., (2014) on the lineament analysis provides evidence on occurrence of lineaments within corridor-125.

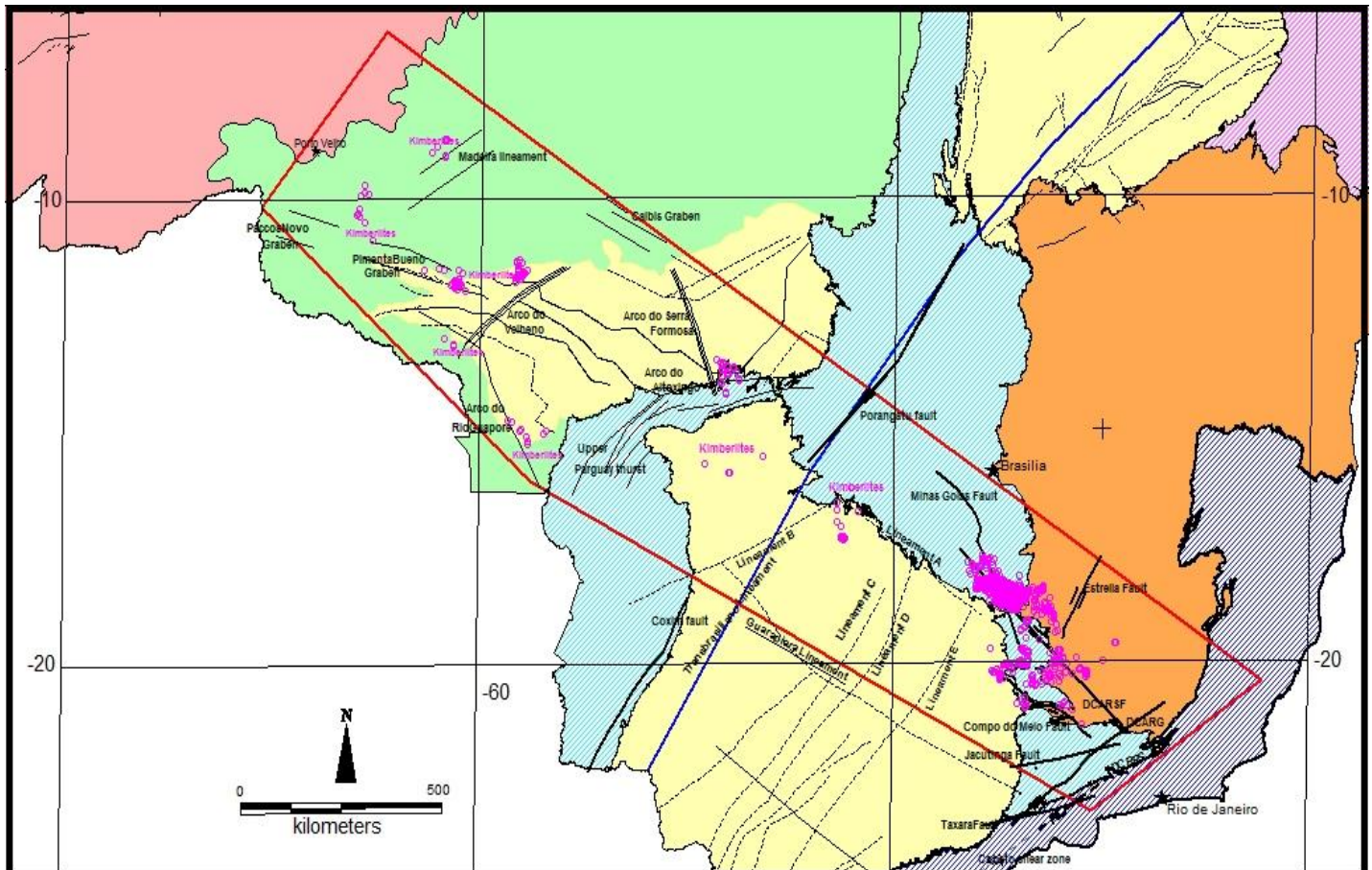


Fig.5: Structural Framework of Corridor-125 with Tectonic province background. The pink open circles represent kimberlites and related rocks, black lines represent structures. Blue line is the Giga Transbrasilino lineament.

These continental lineaments are major zones of weakness, which favours conditions necessary for the melt production, melt migration and emplacement along high strain zones of fractures and faults. Such high strain fracture/fault focused melt generation can be formed during (i) supercontinent formation, (ii) incipient rifting and onset of continental breakup and (iii) strain accommodation along the continental continuation of oceanic fracture zones during spreading (Jelsma et al 2009). The opening up of South Atlantic has a genetic link with the corridor-125 and the kimberlite occurrences along this corridor. With initiation of South Atlantic rift at 140 Ma, it manifested in the oceanic extension of the continental lineaments of South American plate. Corridor-125, Transbrasiliano lineaments are the examples of such oceanic extension associated with South Atlantic rift. This link can be traced back with the help of Earth Magnetic Anomaly Grid data as shown in fig.4. The major oceanic fractures that are associated with the landward counterpart along Corridor-125 are Trindade fracture zone, Trindade_A fracture zone and Trindade_B fracture zone.

Structural Framework of Corridor-125 and Kimberlite occurrences

A compilation (Fig.5) from the available geological, aeromagnetic map, and lineament maps of Brazil, has resulted in the identification of several Mega-and Giga-lineament systems along corridor-125 that has favoured the kimberlite emplacement while other are not. The Amazon and Extra-Amazonian region structural frameworks are dealt separately for convenience and easy analysis.

Extra-Amazonian Region Structural Framework and kimberlite occurrences

General structural framework of the Extra-Amazonian craton consists of numerous NW-SE trending parallel to subparallel lineaments running from SE end which are cross cut by NE-SW structures. The NW-SE subparallel lineaments sometimes are modified due to prevailing local tectonic regime where nappes and thrusts are seen as surface expression. The southeastern most part of the corridor is characterized by the coast parallel lineaments, which are also parallel to the corresponding orogens. TBL is the most magnificent NE-SW trending lineament cross cutting the corridor-125.

The TBL intersection with Corridor-125 has favoured two major kimberlite clusters. The lateral branching at the SW end of the TBL has also favoured two kimberlite clusters. These two sets of kimberlite occurrences on either sides of TBL are referred to as Left TBL-C-125 and Right TBL_C-125 clusters. On the southeastern end of the Corridor-125, there are no kimberlite occurrences (SE-Ribera belt); adjacent to it, the Alto Paranaiba arch is associated with the biggest kimberlite clustering in numbers. This clustering of kimberlites is referred to as Alto Paranaiba cluster. All these clusters of kimberlites and related rocks are associated with a network of NW, NE, NW/ NE intersections, WNW and WSW lineaments.

Upper Rio São Francisco Crustal Discontinuity (DCARSF): NW trending Upper Rio São Francisco Crustal discontinuity (Fig. 5 and 6)) is a major continental lineament situated at the center of the corridor. It forms one of the major kimberlite favouring lineaments in the Alto Paranaiba region. This lineament is associated with parallel to subparallel dyke swarms in the south-eastern region. There are several magnetic signatures running parallel to these dyke swarms from the SE São Francisco cratonic region up to TBL. Though we have Brasilia belt as the geomorphic feature bordering São Francisco craton, the magnetic signature lineaments

running all along the length of the corridor-125 up to TBL is a good evidence of thin skinned tectonics and a proof for intact basement. Hence, the Brazilian kimberlites are found in the mobile belts does not deviate from Clifford's rule.

Campo de Meio lineament: It starts as a NW lineament (Fig. 5 and 6) and has a characteristic bending around the São Francisco cratonic southern boundary. There are kimberlites clustering around this lineament. Beyond this lineament there is a non-kimberlite occurrence zone.

Minas-Goiás Fault system: (Fig. 5 and 6), This mega-lineament is roughly WWN trending forms part of the structures that hosts kimberlites of Alto Paranaíba Cluster.

Lineament A: this is another major mega-lineament (Fig. 5 and 6) which starts at the North-Western end of the DCARF almost subparallel to it and runs further NW and probably extends up to the Transbrasiliano Lineament. Its extension up to TBL is seen as intermittent minor linear magnetic signatures. This lineament hosts the next cluster of kimberlites, which is separated from the Alto Paranaíba cluster by a non-kimberlite zone.

Guarapiara Lineament: It is NW trending lineament (Fig. 5 and 6) which starts from the eastern Ribeira belt and runs up to the Transbrasiliano lineament. This lineament is taken as the southern limit of the Corridor-125 and is extended beyond the Transbrasiliano lineament on to the Amazonian region. Beyond this lineament there are no known kimberlites.

Estrela Fault: trends NE-SW (Fig. 5 and 6) and is a reverse strike-slip fault (Alloua Saadi et al, 2002). It also forms part of the most influential lineaments of Alto Paranaíba kimberlite cluster.

NE-SW subparallel set of lineaments: (Fig. 5 and 6) there is a set of 3 sub parallel (C, D and E) NE trending lineaments, which cut the corridor just after the Alto Paranaíba cluster of kimberlites and end at the A-lineament. These lineaments are not associated with kimberlite occurrence. There are dyke swarms occurring all along the lineament especially in the portion of Corridor-125.

Upper Paraguai Thrust: (Fig. 5 and 6) This thrust zone is found at the suture zone between Amazonian and Extra-Amazonian region. It forms the western margin of the Paraguai-Tocantins Marginal Suture zone.

Porangatu Fault Zone: (Fig. 5 and 6) This fault is also situated in the Paraguai-Tocantins Suture zone. It is a dextral fault (Saadi et al, 2002) with no kimberlite occurrence along but new clustering of kimberlites is found to the left and right of this thrust zone.

Lineament B: (Fig. 5) trending WSW-ENE intersects with NW trending lineament A and hosts the Right TBL_C125 cluster of kimberlites. Further to the east lineament A intersects with lineament- C, D and E which are NE trending and does not host any known kimberlites.

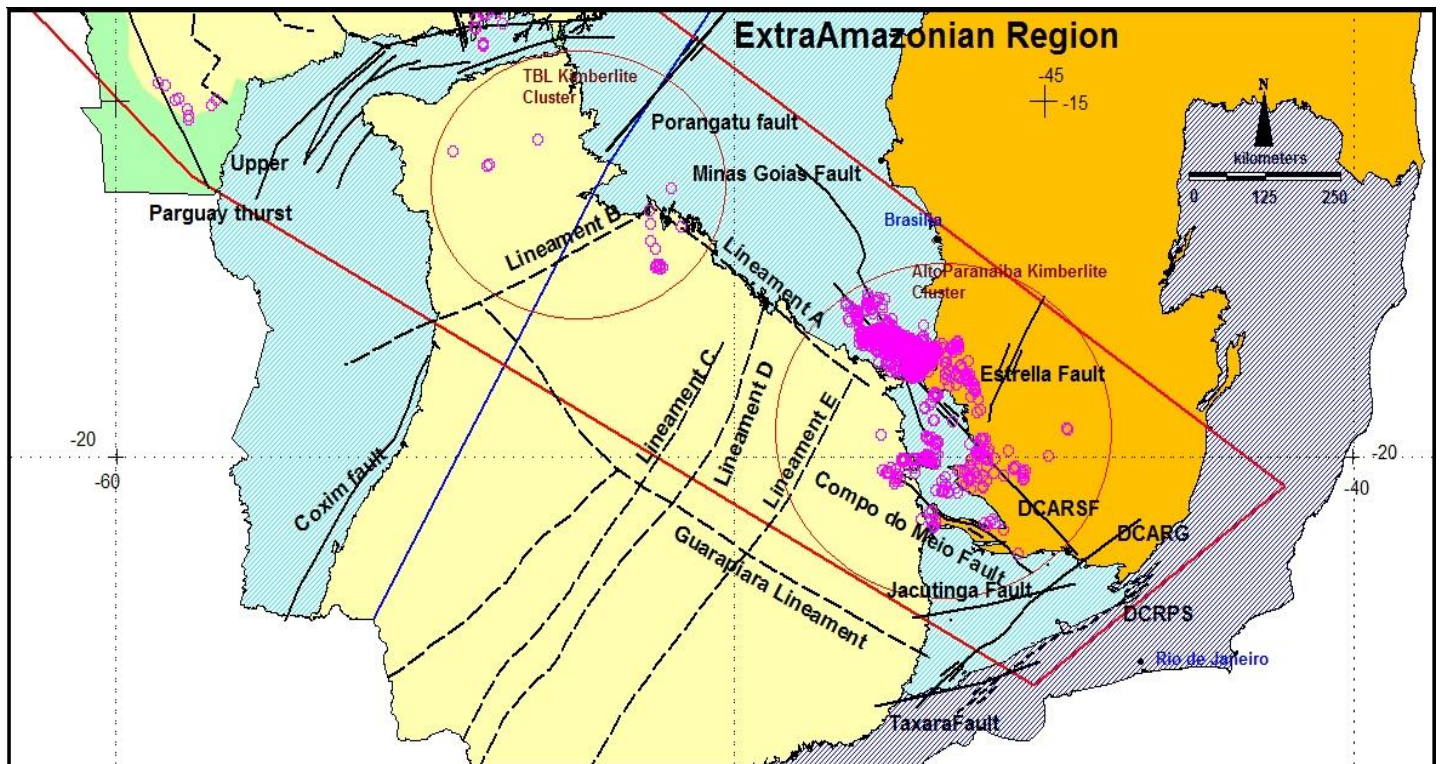


Fig6: Extra-Amazonian kimberlite Clusters and associated Structural Lineaments with Structural provinces back ground. The pink open circles represent kimberlite and related rocks.

Lineaments that are not associated with Kimberlite occurrences in Extra Amazonian Region

Rio Paraíba Do Sul Crustal discontinuity (DCRPS):(Fig. 5 and 6) It is also at the Southern end of the corridor with dextral and vertical sense of (Saadi et al, 2002). No kimberlite is associated with this lineament.

Cubatão shear zone: (Fig. 5) comprising the Serra do mar rift and Cubatão fault system is also not associated with kimberlite occurrences.

Jacutinga Fault: (Fig. 5 and 6) trends WSW-ENE fault is found towards SE portion of the Corridor-125. This fault is not associated with any kimberlite occurrence.

Local Structural Controls: Apart from these major lineaments, kimberlite occurrences in Extra-Amazonian region are associated with flexures and Arches, which forms the local or minor scale structural controls. In case of arches where there is uplifting it is interpreted as dilated mantle region. The flexures are the result of local structural regime due to the collision/compression between adjacent blocks.

The region where Alto Paranaíba kimberlite cluster occurs is known as the Alto Paranaíba high or Arch. This structural high region is geologically made up of a suture zone where the Paranaíba block from South has collided with the Northern São Francisco craton giving rise to E-W flexures and nappes which has been intruded by kimberlite magmas. This E-W flexural control on kimberlites is so evident that the whole Alto Paranaíba cluster appears as E-W flexuring in shape. As we go towards the Transbrasiliano-C125 clusters, this flexural control is absent instead is controlled by the intersection of NE and NW fractures and faults which are part of TBL south-western end offsets.

From the above study it is observed that the Extra-Amazonian sub-regional scale structural controls are NW trending, NE trending and intersection of these two trend structures have favoured kimberlite emplacements. There is one trend each of WSW-ENE and WNW-SSE structural lineament which has favoured kimberlite emplacements in this region. The east coastal region structural lineaments with mainly NE-SW trends in the Ribeira belt region of the corridor-125 is not a favourable kimberlite occurrence zone as there are no

known kimberlites in this region. On local scale, the E-W nappes are the structural controls for Alto Pranaiba cluster and lateral branches of the Transbrasiliano lineament is the structural controls for TBL-C125 cluster.

Amazonian Structural Framework and Kimberlite Clusters

General structural framework of the Amazonian craton consists of NNW, NW, NE and E-W trends which has favoured of Kimberlite occurrences in this region. The grabens, horst and rifts associated with Parecis basin forms the major loci of kimberlite emplacement along with other major lineaments, arcs, horts, flextures, structural bends and nappes. A detailed account of these structures is given in the next coming sections.

Madeira Lineament: (Fig. 7) This Lineament trends NE and forms an important structural control for Madeira cluster kimberlites.

Arco Do Rio Guapore Lineament: (Fig. 7) This lineament is found at close to the SW margin of Amazonian region and trends NW. It hosts Guapore kimberlite cluster and South Rondonia cluster. The intersection of this lineament with NE trending Arco do Velheno forms the loci of South Rondonian cluster kimberlite emplacement. The Guapore kimberlite cluster is found to the South of the lineament where it is intersect by Arco do Alto Xingu lineament. This Guapore lineament is interpreted as suture zone between the Paraguay block and the Amazonian craton (Rizzotto et al., 2013).

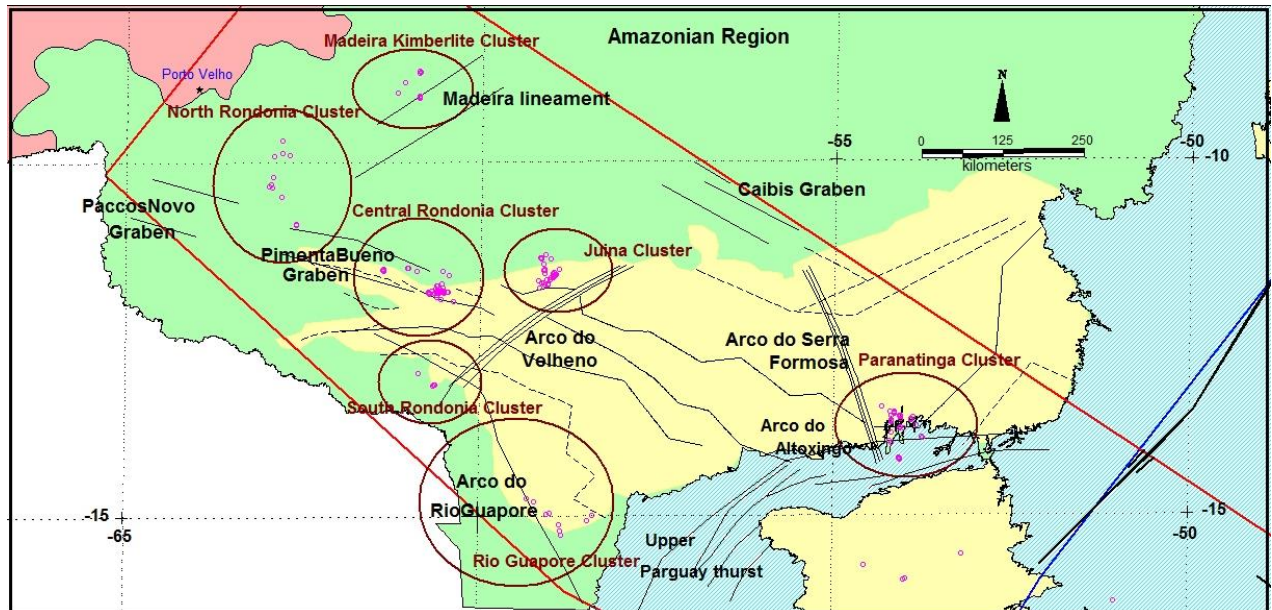


Fig.7: Amazonian Region Kimberlite clusters and associated structural lineaments.

Arco Do Alto Xingu lineament: (Fig. 7) This lineament trends NE and hosts Paranatinga kimberlites at northern end where it intersects with Arco do Serra Formosa (NNW trend); at the southern end it hosts Guapore cluster where it intersects with Acro do Rio Guapore suture zone.

Pimenta Bueno Rift (Fig. 7) is a NW trending Paleozoic rift system associated with Parecis basin. It hosts Central Rondonian cluster and Juina cluster kimberlites. It is interesting to see that the Central Rondonian cluster is in the graben region and the Juina cluster is in the horst region of the basin with cratonic basement.

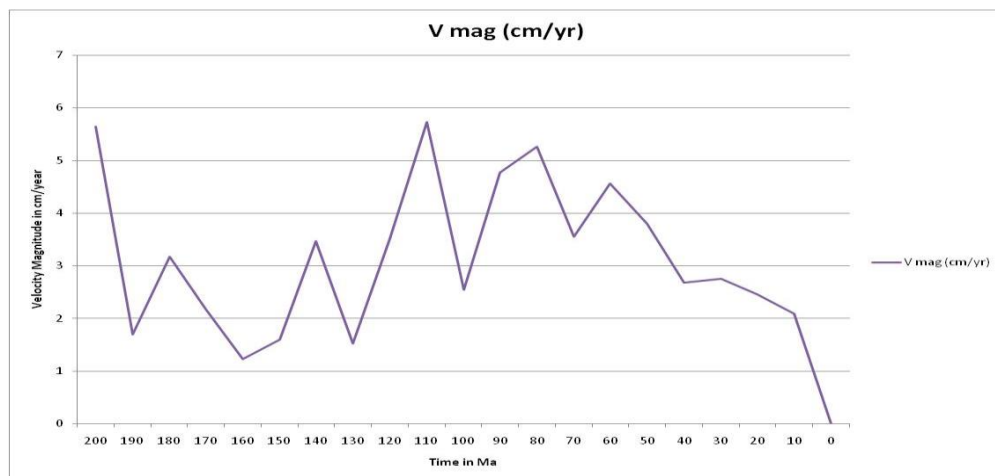
Ji Parana Shear zone (Fig.7) is regional shear zone. It consists of NNW and EW mylonite shear zones. This shear zone is interpreted as Grenvillian age (1.18 to 1.15 Ga) collisional deformation zone, which is a result of collision between North American plate and Amazonian craton (Tohver et al., 2005). Due to this collision, NNW verging nappes (Fig. 7) are formed which hosts the North Rondonian cluster kimberlites.

The Paccas Novo graben, Colorado graben, Caibis graben and Nova Brasiliandia belt found in Amazonian region do not host any kimberlites. On local scale structural bends and nappes forms the structural control for this region.

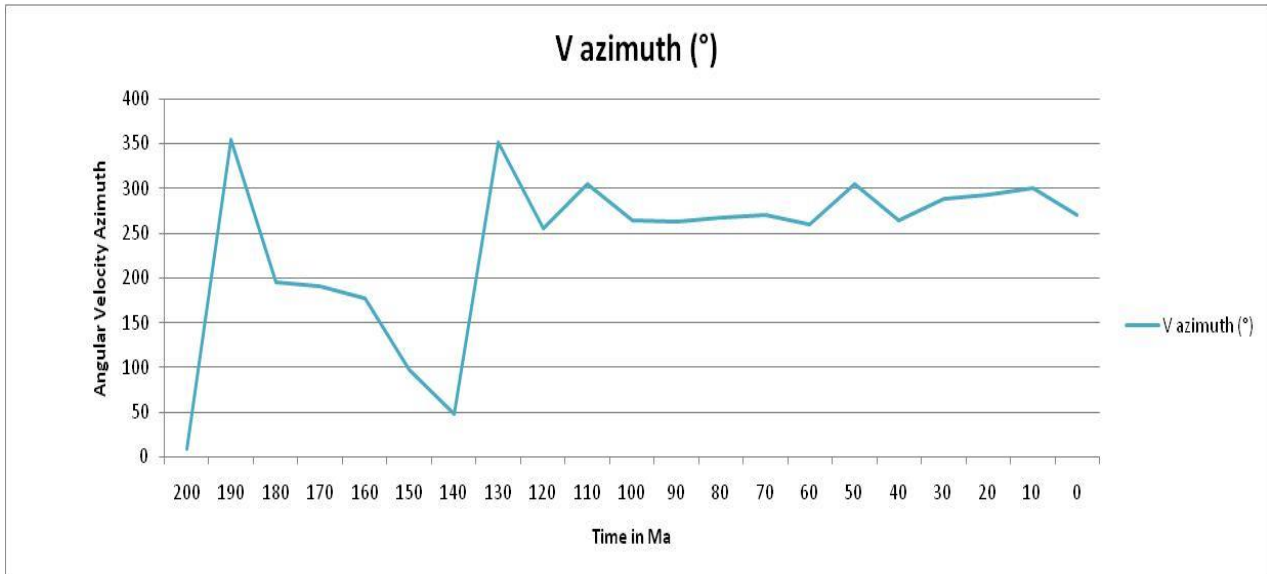
Plate Tectonic Events Associated with Brazilian kimberlites Age Clusters:

Kimberlite are emplaced along reactivated pre-existing zones of weakness or newly created zones of weakness during different stages of supercontinent life cycle (DeWit, 2007; Moore et al, 2008; Jelsma et al, 2009). Thus, the emplacement age of kimberlite clusters are precise time capsules in the whole history of various supercontinent life cycles. The relationship between the emplacement age and plate tectonic event can be deduced by looking at the reconstruction of the Brazilian plate back in time. The plate tectonic reconstruction is carried out with gplates software and the data for this work is taken from, Heine et al, 2013, plate model. In this model the authors have achieved a full fit by structural restoration of the South Atlantic conjugate margins and intra-continental rift basins in Africa and South America. Heine et al (2013) have related the kinematic model of the late Jurassic/Early Cretaceous rift structures to observations from marginal and failed rift basins from the South Africa and South America conjugate margins. According to this model, the pre-rift extensions and plate kinematics are categorized into three phases:

- d) Phase I: 140 to 126.57 Ma: During this phase, there was intra-continental rift basin formation.
- e) Phase II: 126.57 to 120.6 Ma: This phase was characterized by a change in velocity and direction of the plate motion (Graph.1).
- f) Phase III: 120.6 to 100 Ma: this is the second phase of increased plate velocity (Graph.1) and finally the South American and South African Plate drifted apart.



Graph.1: A plot of Brazilian plate velocity magnitude in cm/year Vs Time in Ma.



Graph.2: A plot of Brazilian plate Azimuth as angular velocity Vs Time in Ma.

Brazilian Kimberlite Episodicity and age peaks

The Brazilian kimberlite ages (Table.1) are of six major peaks (Fig.8) with intermittent quiescent periods. Four of these periods are associated with Corridor-125. There are two known Proterozoic kimberlites in Brazil, namely the Salvador kimberlite, which are dated as 1150 Ma (Watkins et al, 2009; Dewit, 2010) and the Brauna kimberlites, which are dated at 640 Ma (Donatti-Filho et al., 2013). All other kimberlites are Triassic and Mesozoic in age. The Proterozoic kimberlites are absent along corridor-125. Only Triassic and Cretaceous kimberlite clusters are found along the corridor-125. These kimberlites are grouped into the following clusters:

1. 226-268 Ma,
2. 120-122 Ma
3. 80-94 Ma,
4. 74 Ma

5.

| Sl_No | Name_Unit | Age in Ma | Method_Dating | Year_Dating/Ref |
|-------|-----------------|-----------|--|---|
| 1 | Collier 04 | 93 | U/Pb on Zircon | Heaman et al 1998 |
| 2 | Batovi 07 | 120 | U/Pb on Zircon | Heaman et al 1998 |
| 3 | P-01 | 120 | U/Pb on Zircon | Heaman et al 1998 |
| 4 | Brauna 03 | 642 | U/Pb on Zircon, Perovskite | Donatti-Filho et al. 2013 |
| 5 | Brauna 07 | 642 | U/Pb on Zircon, Perovskite | Donatti-Filho et al. 2013 |
| 6 | Canastra 01 | 120 | K/Ar on Phlogophite | Pereira & Fuck, 2005 |
| 7 | Pandrea-01 | 93 | U/Pb on Zircon | Andrezza et al, 2008 |
| 8 | Pandrea-06 | 93 | U/Pb on Zircon | Andrezza et al, 2008 |
| 9 | Pandrea-07 | 93 | U/Pb on Zircon | Andrezza et al, 2008 |
| 10 | Tres Ranchos 04 | 81 | U/Pb on Perovskite, Rb/Sr on Phlogophite | Bizzi, 1995; Felgate, 2014 |
| 11 | Tres Ranchos 78 | 87 | Rb/Sr on Phlogophite | Felgate, 2014 |
| 12 | Tres Ranchos 27 | 82 | U/Pb on Perovskite | Felgate, 2014 |
| 13 | Tres Ranchos 14 | 87 | U/Pb on Perovskite | V. Guariano et al, 2013 |
| 14 | Carolina | 232 | Rb/Sr on Phlogophite | Hunt et al, 2009 |
| 15 | Cosmos 01 | 226 | Rb/Sr on Phlogophite | Masum et al., 2008 |
| 16 | Cosmos 03 | 240 | Rb/Sr on Phlogophite | Felgate, 2014 |
| 17 | Concordo 01 | 267 | U/Pb on Perovskite | Felgate, 2014 |
| 18 | Jacare 01 | 242 | U/Pb on Perovskite | Felgate, 2014 |
| 19 | Perdizes 02 | 88 | Rb/Sr on Phlogophite | Felgate, 2014 |
| 20 | Perdizes 04 | 94 | U/Pb on Perovskite | Felgate, 2014 |
| 21 | Limpeza 18 | 80 | U/Pb on Perovskite | Felgate, 2014 |
| 22 | Limeira 01 | 91 | U/Pb on Perovskite | Guariano et al, 2013 |
| 23 | Pantano 01 | 84 | U/Pb on Perovskite | Guariano et al, 2013 |
| 24 | Pantano 02 | 82 | U/Pb on Perovskite | Guariano et al, 2013 |
| 25 | Lemes | 84 | U/Pb on Perovskite | Guariano et al, 2013 |
| 26 | Indiana 01 | 80 | U/Pb on Perovskite | Guariano et al, 2013 |
| 27 | Esperanca | 76 | K/Ar on Mica (80Ma) | Davis 1977 |
| 28 | Pepper 13 | 237 | U-Pb on Perovskite | Masum et al, 2008 |
| 29 | Poco Verde | 85 | Rb/Sr on Phlogophite | Felgate, 2014 |
| 30 | Santa Rosa 04 | 83 | Rb/Sr on Mica, Rb/Sr on Phlogophite | Pereira & Fuck, 2005; Felgate, 2014 |
| 31 | Successo 08 | 74 | Rb/Sr on Phlogophite | Felgate, 2014 |
| 32 | X270 | 89 | U/Pb on Perovskite | Pereira & Fuck, 2005 |
| 33 | Botavi-09 | 122 | U/Pb on Zircon | Davis 1977 |
| 34 | Salvador 01 | 1150 | Rb/Sr on Phlogophite | Williamson and Pereira 1991, Dewit, 2010. |

Table.1: Brazilian kimberlite ages from literature.

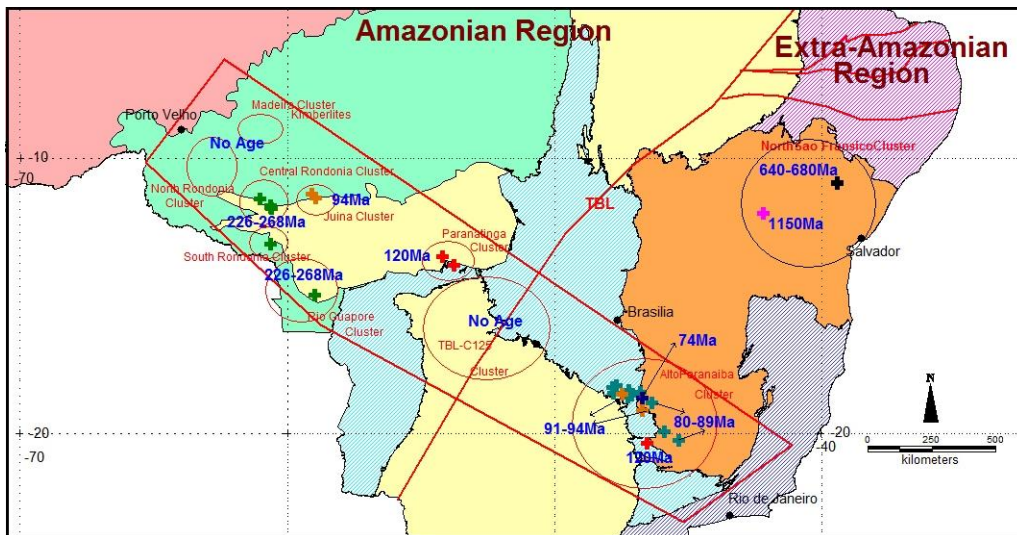


Fig.8: Brazilian Kimberlite age map. The age data are taken from literature.

Amazonian craton kimberlites emplaced between 226 Ma and 268 Ma: This episode of kimberlite magmatism is probably linked to the Permo-Triassic Alto Paraguay magmatism, which is in turn related to Pangea plate reorganization.

120 to 122 Ma: This is related to incipient South Atlantic rifting.

80 to 95 Ma: Tectonic trigger of kimberlite magma generation while spreading is in progress and plate motion paths are marked by cusps (variation in direction) and jogs (variation in velocity). Changes in plate motion may have caused shearing of subcontinental lithospheric mantle with strain accommodation along lithospheric discontinuities, in this case in particular the continental continuation of oceanic fracture zones.

74 Ma: There is only one kimberlite named Sucesso-08 (Felgate, 2014) with this age.

Thus emplacement of kimberlites magma from 74 Ma to 268 Ma with intermittent quiescent periods is observed along the corridor-125. A short period of kimberlite emplacement peaks from 268 Ma to 226 Ma is linked to Pangea plate reorganization. The younger Cretaceous kimberlite peaks from 120 to 74 Ma is related to opening up of South Atlantic Ocean and strain propagation with melt migration along the continental extension of the oceanic transform fault due to cusps and jogs during the Brazilian plate motion. The periods devoid of kimberlite emplacement (225 to 120 Ma and 73 to 0 Ma) corresponds to uniform plate motion or stabilization of plate. The phase I of Heine's model is characterized by the rift basins formation there by activating older structures. During phase II kinematics the South American plate experienced cusp and jog and the emplacement of 120-122 Ma

kimberlites. During phase III, there has been significant jog with respect to South American plate kinematics but this increase in velocity has not favored kimberlite emplacement. After this third phase the South American and South African plate drifted apart. This has resulted in enormous basaltic flows in the mid ocean ridge and formation of oceanic crust. Further, the plates continued to drift apart and the continental part of South American plate has witnessed another phase of kimberlite emplacement peak between 80 to 90 Ma corresponding to phase IV. Lastly, a single kimberlite spike at 74 Ma is observed corresponding to continued rifting of South American plate.

Geochemistry of Kimberlites

In this review work, a summary of various kimberlite types on both Amazonian and Extra-Amazonian region is presented from available literatures. Kimberlites are classified into three main groups namely Group I, Group II (Smith et al., 1985) and the Transitional groups based on the mineralogy and geochemistry. The general composition range for kimberlites can be made in spite of its wide compositional ranges. It is typically low in SiO₂ (25–30 wt. %), low in Al₂O₃ (usually <5 wt. %) and very low in Na₂O (usually < 1 wt. %). Group I kimberlite is generally non-micaceous and the radiogenic isotopic signature is similar to many ocean island basalts (OIB). In contrast, micaceous Group II kimberlite is derived from ancient (>1 Ga) cratons with enriched trace-element signature originating from within the subcontinental lithospheric source. In order to interpret geochemistry of any kimberlite one has to resolve the contamination effect due to pre/post/syn emplacement alteration xenoliths entrapment and weathering.

The nature of Brazilian kimberlites (APIP Cluster) was initially thought to be of Group II by many authors (Bizzi et al 1995b, Gibson et al., 1995; Carlson et al. 1996; Araujo et al., 2001; Carlson et al. 2007; Guarino et al. 2013). But they show an overlapping signature between Group I and II. Felgate (2014) thesis work on the isotopic signatures shows that these APIP kimberlites are transitional type. They show similarities to South African, Brauna kimberlites (Donatti-Filho et al, 2013) from north east of Brazil and Guaniamo kimberlite (Kaminsky et al., 2004) from Venezuela with elemental and isotopic values corresponding to transitional group kimberlites. The Amazonian craton kimberlites are Group I type (Felgate, 2014). The Juina kimberlites of Amazonian craton show lamproitic affinities (geochemistry data from Costa, 2013).

To summarize, the Brazilian kimberlites are of three types known so far namely, transitional type, group I type and lamproitic type. These kimberlites are less documented in literature with respect to its source and paragenesis. These different groups of rocks show subtle differences in major element concentrations, the trace element composition along with isotopic signature provides a better understanding. The Sr, Nd, Hf- isotopic range is the best indicator to classify the kimberlite into its corresponding type. The transitional type kimberlites plot below mantle array, the group II kimberlites plot well within the mantle array and show negative epsilon Ndi values compared with group I and transitional type.

Petrogenesis of Kimberlites from Corridor-125

Bizzi et al. (1995a) and Carlson (1996) proposed a hotspot triggered kimberlite magma source based on Sr and Nd ratios similarity with that of the Tristan/Walvis ridge hotspot. This association could not sustain with new kimberlite age data results and later, Trindade plume triggered model was due to the paleo-location of this plume under the kimberlite occurrence region. But, this was also abandoned as its distinctive Sr and Nd isotopic composition also precludes it from being the source of the APIP magmatism (Gibson et al., 1995). The next model proposed (Becker et al., 2007) was that of magma mixing between Group I and II though the same plumbing systems to produce transitional type kimberlites does not explain all the geochemical signatures. Donatti et al., 2013b; Beard et al., 2000) have proposed that transitional kimberlites are sourced from the base of the SCLM, where asthenospheric fluids/melts have interacted with the SCLM and subsequently melted. The Sr and Nd of all three rock types are thought to represent derivation from a metasomatised SCLM source in all cases, with the range in isotopic values explained by heterogeneities within the source.

On Amazonian region, an asthenospheric mantle has been proposed for Batovi-6 (Costa, 1996) and Concorde-1 (Felgate, 2014) kimberlites, due to its isotopic similarities to Group I kimberlites and OIB signatures. These kimberlites show signatures of Oceanic subduction along with sediments at asthenospheric depths. The younger 93 Ma Juina Kimberlites of the Amazonian craton is unique, it show geochemical signatures similar to Lamproites. The super deep diamond inclusion studies (Kaminsky et al, 2010; Bulanova et al 2010) have shown that they have source region from great depths ranging from 670 to 410km.

The transitional type signatures are thought to have formed by the adiabatic decompression melting of SCLM due to extensional tectonics (Becker et al, 2007). A SCLM source has been ascribed as the source for Brazilian kimberlites in order to characterise the isotopic and incompatible trace element signatures (Gibson et al, 1995; Guarino et al, 2013; Donatti-Filho et al, 2013b). In this model, it is proposed that asthenospheric fluids/melts have interacted with SCLM and subsequently melted. As proposed by Becker et al, the cretaceous APIP kimberlite magmatism is related to the continental extension due to South Atlantic rifting.

The role of Hotspot Trindade-Martin Vaz (TMV) in kimberlite emplacement

Crough et al (1980) suggested age progression along the Corridor-125 due to the passage of the Trindade hotspot below the Brazilian plate along corridor-125. The validity of hotspots influence with kimberlite emplacement within the Brazilian plate during South Atlantic rift is analyzed in this section. It is carried out by using plate reconstruction with the help of Gplates open source software {<http://www.gplates.org>} and the Heine's plate kinematic model is used along with data from gplates hotspot data.

Gplates: this open source software enables interactive visualization of plate-tectonics open source. It is configured to handle geographic information system functionality and raster data together under the reconstructions. It is innovative software allowing the visualization and manipulation of reconstruction and associated data through geological time. This software runs on various operating systems, windows operating system compatible version is utilized in this study. Gplates is developed by an international team of scientist, professional software developers and postgraduate students at School of Geosciences at the University of Sydney, the Division of Geological and Planetary Sciences at CalTech and The Centre for Geodynamics at the Norwegian Geological Survey (NGU).

Scientists at the University of Sydney, Norwegian Geological Survey and Cal Tech have also been compiling sets of global data for plate boundaries, continental-oceanic crust boundaries, plate rotations, absolute reference frames and dynamic topography. It has been licensed for distribution under GNU (general public license) version 2. Gplates being state-of the art software, it can handle and visualize data in variety of formats geometries like raster data to link plate kinematics to geodynamic evolution models. Finally it can produce high-resolution paleo-geographic maps and animation videos for presentation.

As mentioned in the earlier paragraph, Crough related kimberlite occurrence age along corriod-125 with Trinidad Martin Vaz hotspot paleo-track based on the kimberlite age data that was available at that time. With more available robust age dating techniques and age of kimberlites, the scenario has changed with respect to age progression along the Corridor-125. There is no precise age progression along entire length of the corridor-125 as proposed by Crough. Though oldest kimberlites are only found on the NW end of the corridor and youngest kimberlites are found in the SE end, the intermediate age kimberlites are found

mixed up all along the lineament, which makes the interpretation of hotspot influence unsustainable. Example of such intermittent age group kimberlite is the 120 Ma kimberlite found in the Extra-Amazonian and Amazonian region. To arrive at a conclusion, the reconstruction of the Brazilian plate with hotspot fixed frame is taken up. The Trinidad Martin Vaz paleo track is traced on Brazilian plate and checked with respect to kimberlite age and location along corridor-125. This reconstruction depicts the passage of the Brazilian plate over fixed the hotspot TMV. As the Brazilian plate moves over TMV hotspot due to Pangea plate organization and South Atlantic opening, the TMV traces a wavy path as shown in the fig.9a &b. The TMV path is not exactly coincident with the Corridor-125 but it has been to in close proximity to the Corridor.

The TMV motion path has traced the close proximity of Corridor-125 with initial loping around 300 Ma to 180 Ma at the North-Western end and then following the entire length close proximity of the plate as the plate motion continued. If the kimberlite emplacement is influenced by this hotspot paleo-track, then the position of corridor-125 should have been slightly lower than the currently considered location and more kimberlite occurrences should have been found in this slightly lower corridor region. This is not observed. Also, in the previous section on geochemistry of Brazilian kimberlites, we have seen there are no geochemical similarities with the TMV rock and kimberlite geochemistry from Corridor-125. Sequential age progression along the corridor is also not seen. Thus, the association of the hotspots like TMV directly in the kimberlite magma generation and its emplacement is ruled out.

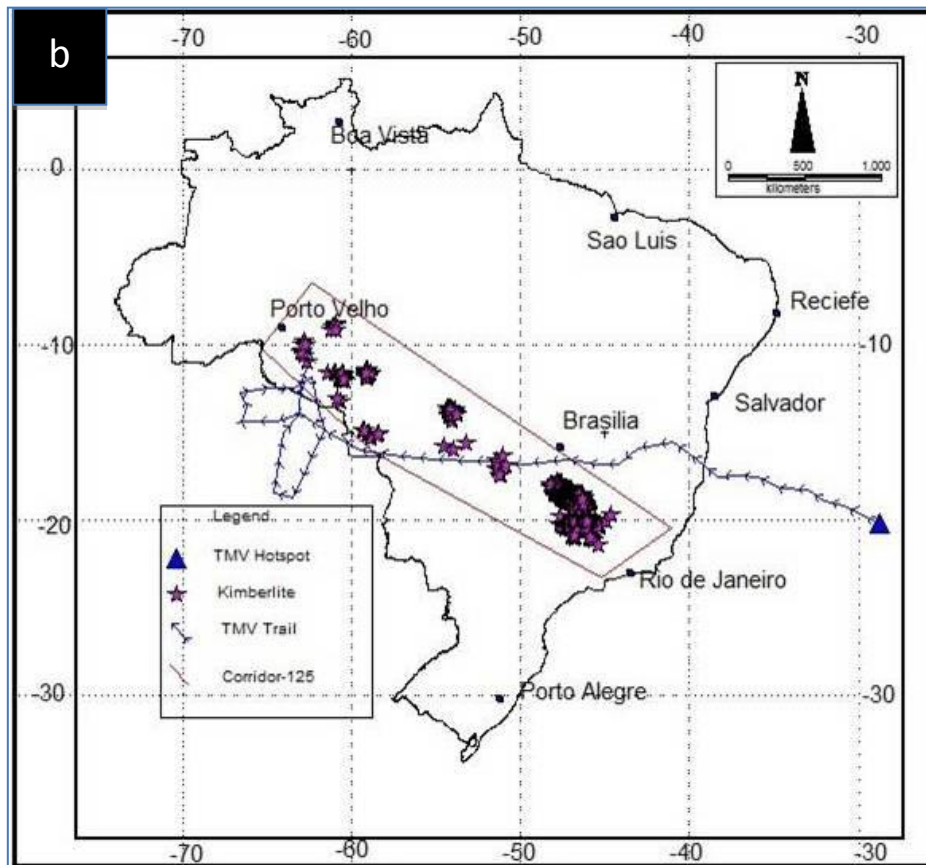
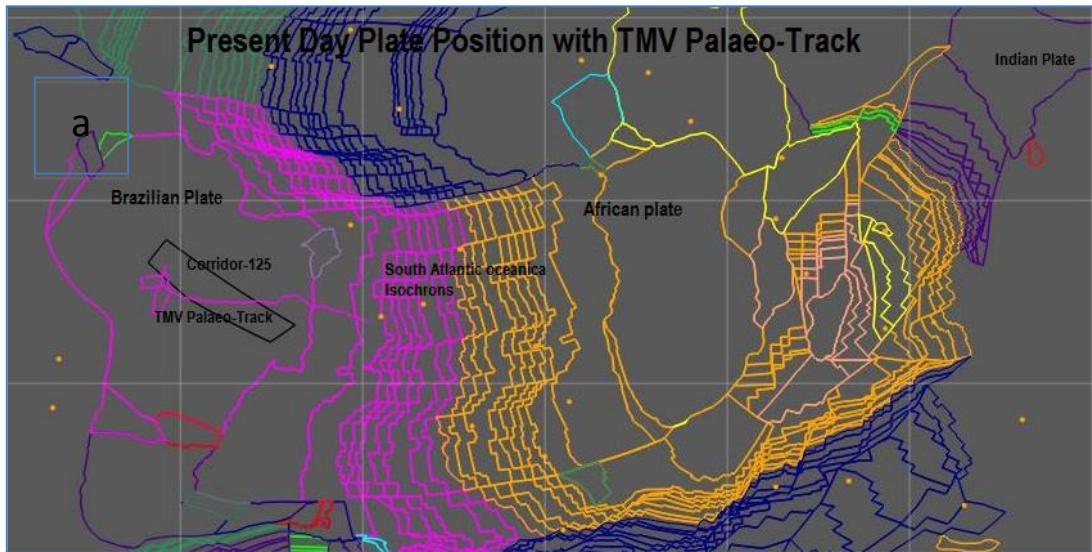


Fig.9a &b: TMV hotspot Trail along the Corridor-125 with kimberlite occurrences.

5. DISCUSSION

The continuation of Corridor-125 from Extra-Amazonian region beyond Transbrasiliano lineament into the Amazonian craton is a matter of debate. Firstly, because the continuation of dykes found in the Extra-Amazonian region stops right at the Transbrasiliano lineament. Secondly, basement structural trend orientation also varies, and lastly, age of kimberlites from Amazonian craton is different from the Extra-Amazonian craton Cretaceous kimberlites. The Permo-Triassic (225 to 268 Ma) kimberlite found in Amazonian region and is absent in the Extra-Amazonian region. Whereas on contrary to the above observations, similar age group younger (120 Ma, 91 to 93 Ma) kimberlites on both the regions along the corridor-125 contradicts the above observed features of non-continuation. The Amazonian craton is interpreted to have amalgamated with Extra-Amazonian region from 650 to 630 Ma (Cordani et al, 2013; Neves and Fuck, 2014). On The Amazonian region any tectono-magmatic events prior to 225 Ma is unique to the craton and does show different geochemical signatures than that of Extra-Amazonian region. The 93 Ma kimberlites of Juina show subduction related magmatic signatures and magma generation trigger related to South Atlantic opening. There is a genetic link between the Extra-Amazonian part of the corridor-125 with that of the oceanic transforms namely Trinidad fracture zone, Trinidad_A fracture zone and Trinidad_B fracture zone. This link is clearly visible on global magnetic anomaly map. These transforms are related to South Atlantic opening and hence, a clear association with the continental lineaments, its associated kimberlites and the newly developed oceanic transforms are genetically related to one another and the tectonic event associated with them.

Dual Tectonic Trigger model of Kimberlite emplacements in Brazil.

It is proposed that Dual Tectonic trigger model of kimberlite emplacement has affected corridor-125. The Initial rifting of South American plate from North American (Laurentia Plate) has triggered kimberlite emplacement in the Amazonian region along the western boarder subduction zone and has resulted in Permo-Triassic kimberlites on Amazonian craton. The older basement structures have been reactivated and the kimberlites of Permo-Triassic age are emplaced during the Pangea plate reorganization. This is soon followed by Pangea rifting at 225Ma at the northern border of the country. The Permo-Triassic kimberlite occurrence region is characterized by suture zone where subduction of the Pacific plate due to east-ward directed motion has been in place since 300 Ma to 130 Ma. Probably, the group I signature of these kimberlites is due to its associated with this

subduction derived material. This fact needs confirmation from geochemical signatures. This magmatism has been switched over to another plate reorganization and reactivation of structures due second tectonic rifting – The South Atlantic Rifting, along the eastern margin of the lineament. This rifting has favoured kimberlite emplacements extending up to Upper Paraguay thrust zone (Suture zone between Amazonian and São Francisco Craton) as we see 120 Ma kimberlite in Paranatinga cluster. With maturing rift on the east coast, increased incidence of kimberlite emplacements with younger age are found concentrated on the Extra-Amazonian region. Only two peak episodes of kimberlite magmatism has affected the Amazonian region due to South Atlantic rift. The occurrence of 95Ma Juina magmatism with ultra-deep diamond inclusions have been attributed to subduction derived source magma generated during plate reorganization related to South Atlantic rifting.

6. Conclusions

From this review the following conclusions could be drawn:

- Detailed analysis of kimberlite and related magmatism in time and space has allowed us to pinpoint lithosphere-scale transfers as important structural controls for emplacement. Corridor-125 is one such lithosphere-scale lineament controlling kimberlites emplacements.
- The onset of the major period of kimberlite magmatism coincided with incipient breakup of Gondwana when such structures are expected to develop/reactivation of old continental structures (before ocean crust formation).
- Subducted material gives rise to change in magma composition during short periods of kimberlite emplacements. This is seen in the 226-268 Ma short episode kimberlite magmatism in Amazonian region. Short term episodicity is related to a combination of processes of subduction, reactivation and rifting in Brazil.
- The geometry including movement direction can be gleaned from studying “connected” transform faults on the adjacent oceanic crust. As we seen there is a link between the South Atlantic transforms with the corridor-125.
- Long term episodicity is determined by periods of supercontinent breakup triggered by extension. The Cretaceous and younger kimberlites in Brazil is an evidence for this long term episodicity.
- The corridor-125 is a continental translithospheric lineament made of two sets of lineaments. These two sets correspond to The Amazonian and Extra-Amazonian region lineaments. The Extra-Amazonian region corridor-125 is an older lineament that has a genetic link to younger South Atlantic transform fractures formed during the opening of the South Atlantic Ocean and West-Gondwana break up. It comprises of numerous mega- and giga-lineaments. Fractures, faults and minor structures which

have been formed and or reactivated several times. The Amazonian part of corridor-125 is associated with Pangea supercontinent tectonic trigger. The Andes is the surface expression of Pacific plate subduction, the kimberlite emplacement is the continental inland expression of the Pacific plate subduction and Pangea tectonic trigger. This tectonic trigger has reactivated older than 1.0 Ga basement structures.

- The emplacement of Kimberlites is not related to plumes that crossed the lineament; rather they are triggered due to reorganization/change in the plate motion kinematics. As there is no apparent age progression unlike what is expected from a plume-triggered kimberlite emplacement model.
- The entire episode of kimberlite magma generation and emplacement is attributed to stress propagation due to Plate reorganization, incipient rifting and tectonic trigger due to South American plate motion and its related extension and subduction on the western margin.
- It has been observed that thermal perturbations associated with tectonic events involving lithospheric faults reactivated during breakup of continents resulting in strain localization and melt focusing along these reactivated structures. Finally, the emplacement of the magmatic rocks.
- Major structural trends of kimberlite emplacement loci along the corridor-125 are associated mainly with NE and NW trends. Other structural trends of importance are along NNW-SSE. WNW and EW trends are rarely seen as kimberlite emplacement controls.
- Major dyke swarms also follow the main structural trend (NE and NW) and with kimberlites along Corridor-125. All forming part of the structural controls showing reactivation.
- Corridor-125 is an older lineament probably older than 1.8 Ga and has been reactivated several times; kimberlite emplacement is associated to one reactivation

event. Neotectonic reactivation of few faults at 1.6 Ma (Saadi et al. 2002) signifies this as an ongoing process.

- Corridor-125 kimberlites are of Group I, transitional type and Juina is a lamproite.
- The transitional type kimberlites are found only on Extra-Amazonian region associated with tectonic extension; the group I kimberlites are found only on Amazonian Region associated with subduction related rifts and grabens. The lamproite is associated with Parecis basin horst and its associated rift and a subducted oceanic crust is attributed as the source for these lamproites.
- Kimberlite emplacement is post-dated by kamafugites of shallow depth origin than kimberlites (Felgate, 2014) again showing structural reactivation. Therefore magma composition reflects different styles of lithosphere deformation - not plume activity.
- Finally, continued rifting and the opening of the Atlantic with progressive thinning/delamination of the lithosphere beneath South America where magmatic switching from kimberlites to kamafugites are seen.

ACKNOWLEDGEMENTS

This research article was funded by CNPq-TWAS funding as part of PhD funding (Grant No. 3240240127) at the Unicamp University. We greatly acknowledge the comments by Prof. Darcy Pedro, Prof. Ricardo Weska, Prof. Emilson and Dr. Jose Paulo Donatti Filho in improving this article.

References

Andreazza, P., Kaminsky, F.V., Sergei M. Sablukov, S. M., Belousova, E. A., Mousseau Tremblay, M., Griffin, W.L. 2008. Kimberlitic sources of super-deep diamonds in the Juina area, Mato Grosso State, Brazil. 9th International Kimberlite Conference Extended Abstract No. 9IKC-A-00004.

Araujo, A.L.N., Carlson, R.W., Gaspar, J.C., Bizzi, L.A., 2001. Petrology of kamafugites and kimberlites from the Alto Paranaíba Alkaline Province, Minas Gerais, Brazil. *Contributions to Mineralogy and Petrology*, 142(2): 163-177.

Barnett, W., Jelsma, H., Watkeys, M., Freeman, L., and Bloem, A., 2013. How Structure and Stress Influence Kimberlite Emplacement. *Proceedings of 10th International Kimberlite Conference, Special Issue of the Journal of the Geological Society of India*, vol. 2, 51-65.

Beard, A. D., Downes, H., Hegner, E., Sablukov, S. M. 2000. Geochemistry and mineralogy of kimberlites from the Arkhangelsk Region, NW Russia: evidence for transitional kimberlite magma types. *Lithos*, 51(1-2): 47-73.

Becker, M., Le Roex, A. P., Class, C. 2007. Geochemistry and petrogenesis of South African transitional kimberlites located on and off the Kaapvaal Craton. *South African Journal of Geology*, 110(4): 631-646.

Bizzi, L.A., 1995. Mesozoic alkaline volcanism and mantle evolution of the Southwestern São Francisco craton, Brazil, University of Cape Town, Cape Town, 205 pp.

Bizzi, L.A., Dewit, M.J., Smith, C.B., McDonald, I., Armstrong, R.A., 1995a. Heterogeneous enriched mantle materials and dupal-type magmatism along the SW margin of the São-Francisco Craton, Brazil. *Journal of Geodynamics*, 20(4): 469-491.

Bizzi, L.A., Smith, C.B., de Wit, M.J., Armstrong, R.A., Meyer, H.O.A., 1995b. Mesozoic kimberlites and related alkalic rocks in the South Western São Francisco Craton, Brazil: a case for local mantle reservoirs and their interaction, *Proceedings of the fifth international kimberlite conference, Brazil*, pp. 156-171.

Bulanova. G. P., Walter. M. J., Smith. C. B., Kohn. S. C., Armstrong. L. S., Blundy. J. 2010. Mineral inclusions in sublithospheric diamonds from Collier 4 kimberlite pipe. Juína. Brazil: subducted protoliths carbonated melts and primary kimberlite magmatism. *Contributions to Mineralogy and Petrology* 160 (4). 489-51.

Carlson, R.W., Esperanca, S., Svisero, D.P., 1996. Chemical and Os isotopic study of Cretaceous potassic rocks from southern Brazil. *Contributions to Mineralogy and Petrology*, 125(4): 393-405.

Carlson, R.W. et al., 2007. Chemical and isotopic relationships between peridotite xenoliths and mafic-ultrapotassic rocks from Southern Brazil. *Chemical Geology*, 242(3-4): 415-434.

Cordani, U. G., Pimentel, M. M., Araújo, C. E. G., Basei, M. A. S., Fuck, R. A. and Girardi, V. A. V. 2013. Was there an EdiacaranClymene Ocean in central South America, *Am. J. Sci.*, 313(6), 517–539, doi:10.2475/06.2013.01.

Costa, V. S. 1996. Estudos Mineralógicos E Químicos do Kimberlito Batovi 6 (MT) em comparação com as intrusões Três Ranchos 4 (GO) e Limeira 1 (MG), Universidade Estadual de Campinas, 112.

Costa, V. S. 2013. Mineralogia e Petrologia de xenólitos mantélicos da Província Kimberlítica de Juína, MT. Doctoral Thesis, Instituto de Geociências, University of São Paulo, São Paulo.

Crough, S. T., W. J. Morgan, and R. B. Hargraves (1980), Kimberlites: Their relation to mantle hot spots, *Earth Planet. Sci. Lett.*, 50, 260–274.

Davis, G.L., 1977. The ages and uranium contents of zircons from kimberlites and related rocks: *Carnegie Institution of Washington Year Book*. 76: 631-635.

De Wit M, 2007. The Kalahari epeirogeny and climate change: differentiating cause and effect from core to space. *S Afr J Geol*.110, 367–392.

De Wit, M., 2010. Identification of global diamond metallogenic clusters to assist exploration. *The Southern African Institute of Mining and Metallurgy. Diamonds: Source to Use*. P 1-24.

Donatti-Filho, J.P., Oliveira, E.P., McNaughton, N.J., 2013a. Provenance of zircon xenocrysts in the Neoproterozoic Brauna Kimberlite Field, São Francisco Craton, Brazil: Evidence for a thick Palaeoproterozoic lithosphere beneath the Serrinha block. *Journal of South American Earth Sciences*, 45(0): 83-96. 266.

Donatti-Filho, J.P., Tappe, S., Oliveira, E.P., Heaman, L.M., 2013b. Age and origin of the Neoproterozoic Brauna kimberlites: Melt generation within the metasomatized base of the São Francisco craton, Brazil. *Chemical Geology*.

Felgate, Matthew Richard, 2014. The petrogenesis of Brazilian kimberlites and kamafugites intruded along the 125° lineament: improved geochemical and geochronological constraints on magmatism in Rondonia and the Alto Paranaíba Igneous Province. PhD thesis, School of Earth Science, The University of Melbourne. 1-292. *Geochemistry, Geophysics, Geosystems*, 10. Q08005.

Gibson, S.A., Thompson, R.N., Leonardos, O.H., Dickin, A.P., Mitchell, J.G., 1995. The late Cretaceous impact of the Trindade mantle plume- evidence from large-volume, mafic, potassic magmatism in SE Brazil. *Journal of Petrology*, 36(1): 189-229.

Guarino, V., Wu, F.-Y., Lustrino, M., Melluso, L., Brotzu, P., Gomes, C.d.B., Ruberti, E., Tassinari, C.C.G., Svisero, D.P., 2013. U-Pb ages, Sr-Nd isotope geochemistry, and

petrogenesis of kimberlites, kamafugites and phlogopite-picrites of the Alto Paranaíba Igneous Province, Brazil. *Chemical Geology* 353, 65–82.

Rizzotto, G.J., Hartmann, L.A. 2012. Geological and geochemical evolution of the Trincheira Complex, a Mesoproterozoic ophiolite in the southwestern Amazon Craton, Brazil. *Lithos* 148, 277-295.

Rizzotto, G. J., Joao Orestes, S., Santos, L., Hartmann, A., Tohver, E., Pimentel, M. M., Naughton, M. N. 2013. The Mesoproterozoic Suapore suture in the SW Amazonian Craton: Geotectonic implications based on field geology, zircon geochronology and Nd-Sr isotope geochemistry. *Journal of South American Earth Sciences*. 48. 271-295.

Heaman, L., Teixeira, N. A., Gobbo, L., Gaspar, J.C. 1998. U-Pb mantle zircon ages for kimberlites from the Juina and Paranatinga provinces, Brazil. In: VIIth International Kimberlite Conference, Extended abstracts, Cape Town, pp 322–324

Heine, C., J. Zoethout, and R. D. Muller, 2013, Kinematics of the South Atlantic rift. *Solid Earth*, 4, 215–253, 2013.

Herz, N., 1977. Timing of spreading in the South Atlantic: Information from Brazilian alkalic rocks. *Geological Society of America Bulletin*, 88(1): 101-112.

Hobbs, W.H., (1904), Lineaments of Atlantic Border region, *Geological Society of America Bulletin*, 15: 483–506. Hobbs, H., Means, W., Williams, P. (1982). *An outline of Structural Geology*. Text book by New York: Wiley and Sons, inc.

Hunt, L., Stachel, T., Morton, R., Grutter, H., Creaser, R.A., 2009. The Carolina kimberlite, Brazil - Insights into an unconventional diamond deposit. *Lithos*, 112: 843-851.

Jelsma, H., Barnett, W., Richards, S., Lister, G., 2009. Tectonic setting of kimberlites. *Lithos*, 112: 165.

Jelsma, H.A. et al., 2004. Preferential distribution along transcontinental corridors of kimberlites and related rocks of Southern Africa. *South African Journal of Geology*, 107(1-2): 301-324.

Kaminsky, F.V., Sablukov, S. A., Sablukova, L. I., Channer, D. 2004. Neoproterozoic 'anomalous' kimberlites of Guaniamo, Venezuela: mica kimberlites of 'isotopic transitional' type. *Lithos*, 76(1-4): 565-590.

Kaminsky, F.V. et al., 2010. Kimberlitic sources of super-deep diamonds in the Juina area, Mato Grosso State, Brazil. *Lithos*, 114(1-2): 16-29.

Lister, G.S. Etheridge, M.A. and Symonds, P., 1986. Detachment faulting and the evolution of continental margins. *Geology*, 14:246-250.

Masun, K.M., Smith, B.H.S., 2008. The Pimenta Buena kimberlite field, Rondonia, Brazil: Tuffisitickimberlite and transitional textures. *Journal of Volcanology and Geothermal Research*, 174(1-3): 81-89.

Matthews, K.J., Müller, R.D., Wessel, P. and Whittaker, J.M., 2011, The tectonic fabric of the ocean basins, *Journal of Geophysical Research*, 116, B12109.

Maus, S., Barckhausen, U., Berkenbosch, H., Bournas, N., Brozena, J., Childers, V., Dostaler, F., Fairhead, J., Finn, C., Von Frese, R., 2009. EMAG2: a 2-arc min resolution Earth Magnetic Anomaly Grid compiled from satellite, airborne, and marine magnetic measurements.

Meyer, H.O.A., Garwood, B.L., Svisero, D.P., Smith, C.B., 1995. Alkaline ultrabasic intrusions in Western Minas Gerais, Brazil, *Proceedings of the 5th international kimberlite conference, Brazil*, pp. 140-156.

Moore A, Blenkinsop T, Cotterill F (2008) Controls on post-Gondwana alkaline volcanism in southern Africa. *Earth Planet Science Letter*, 268, 151–164.

Neill, W.M., 1973. Possible continental rifting in Brazil and Angola related to opening of South-Atlantic. *Nature-Physical Science*, 245(146): 104-107.

Neves, B. B. B., Fuck, R. A., 2014. The basement of the South American Platform: half Laurentian (N-NW) + half Gondwanan (E-SE) domains. *Precambrian Research*, 244, 75-86.

Pereira, R.S., Fuck, R.A., 2005. Archeannucleii and the distribution of kimberlite and related rocks in the São Francisco Craton, Brazil. *Revista Brasileira de Geociencias*, 35(3): 93-104.

Read, G. et al., 2004. Stratigraphic relations, kimberlite emplacement and lithospheric thermal evolution, Quirico basin, Minas Gerais state, Brazil. *Lithos*, 77(1-4): 803-818.

Rocha.L.G.M.,Pires, A.C.P.B, Carmelo.A.C., AraujoFilho. J.O., 2014.Geophysical characterization of Azimuth 125 lineament with aeromagnetic data: Contributions to the geology of central Brazil. *Precambrian Research* 249, 273-287.

Saadi, A., Machette, M.N., Haller, K.M., Dart, R.L., Bradley, L.A., and Souza, A.M.P.D., 2002. Map and Database of Quaternary Faults and Lineaments in Brazil. USGS open file report-02-230. A project of the International Lithosphere Program Task Group II-2, Major Active Faults of the World. 1-64.

Sial, A., N., Oliveira, E.P. and Choudhuri, A. 1987. Mafic dyke swarms of Brazil; In Mafic dyke swarms, editors Halls, H. C. And Fahrig, W. F., Geological association of Canada special paper 34. 467-481.

Sykes, L., 1978. Intraplate seismicity, reactivation of pre-existing zones of weakness, alkaline magmatism, and other tectonism postdating continental fragmentation. *Rev. Geophys. Space Phys.*, 16: 621-688.

Tassinari, C. C. G., & Macambira, M. J. B. 1999. Geochronological provinces of the Amazonian Craton. *Episodes*, 22(3).174-182.

Tohver, E., Van der Pluijm, B. A., Scandolaro, J. E., Essene, E. J. 2005. Late Mesoproterozoic deformation of SW Amazonia (Rondônia, Brazil): geochronological and structural evidence for collision with Southern Laurentia. *J. Geol.* 113, 309-323.

Watkins, J.M., 2009. Diamonds in South America. Proexpo oral presentation. Peru.

Wessel, P., A. Mazzoni, R., Muller, D., Matthews.,Whittaker,K. J. , Myhill, R., Chandler, M. T., 2014. The Global seafloor fabric and Magnetic lineation project, Geochemistry, Geophysics, Geosystems. <http://www.soest.hawaii.edu/PT/GSFML/>

White, S.H., de Boorder, H., Smith, C.B., 1995. Structural controls of kimberlite and lamproite emplacement. *Journal of Geochemical Exploration* 53, 245-264.

Williamson P.A. & Pereira R.S. 1991. The Salvador 01 Kimberlite, Bahia, Brazil: its regional and local geological setting with comments on the sequence of prospecting activities leading to its discovery. Strategic Services Unit, Internal Report, De Beers Brasil, Brasilia, 27p.